Coupling the entropy scaling concept with SAFT or cubic equations of state to model the transport properties of fluids

Aghilas Dehlouz

Thèse

présentée et soutenue publiquement pour l'obtention du titre de

DOCTEUR DE l'UNIVERSITE DE LORRAINE

Mention : Génie des procédés, des produits et des molécules

par **Aghilas DEHLOUZ**

Couplage du concept d'entropy scaling et des équations d'état de types SAFT ou cubique pour modéliser les propriétés de transport des fluides

le 7 juin 2022

Composition du jury :

Rapporteurs :

Christophe COQUELET	Professeur à l'école nationale supérieure des Mines d'Albi (Président du jury)
Jean-Luc DARIDON	Professeur à l'université de Pau et des pays de l'Adour

Examinateurs :

Véronique LACHET	Docteur-ingénieur (HDR) à l'IFPEN
Jean-Noël JAUBERT	Professeur à l'université de Lorraine, Nancy, France (directeur de thèse)
Romain PRIVAT	Maître de conférences à l'université de Lorraine, Nancy, France (co-directeur de thèse)

Invités :

Saifuddin AHMED	Ingénieur modélisation thermodynamique chez GTT
Marc BONNISSEL	Responsable modélisation et analyse thermique chez GTT
Guillaume GALLIERO	Professeur à l'université de Pau et des pays de l'Adour
Honggang ZHOU	Spécialiste thermodynamique et comportement des phases chez TotalEnergies

Table des matières :

Remerciements :

Cette thèse a été financée par la compagnie GazTransport & Technigaz (GTT). Elle s'est d'abord déroulée au sein de l'entreprise GTT puis au sein du Laboratoire Réactions et Génie des Procédés (LRGP) rattaché à l'École Nationale Supérieure des Industries Chimiques (ENSIC). Je remercie ces deux parties pour tous les moyens mis à ma disposition et les efforts fournis pour m'avoir accueilli et intégré.

Je souhaite exprimer ma plus grande gratitude à monsieur le professeur Jean-Noël JAUBERT qui a dirigé ce travail. Plus qu'un directeur de thèse exemplaire, j'ai trouvé en toi un mentor et un ami. Tu as ma profonde reconnaissance pour ton soutien indéfectible tant sur le plan scientifique qu'humain, pour toutes les connaissances que tu as partagées avec moi, pour ta pédagogie, tes avis éclairés et ta disponibilité tout au long de ces années.

Je remercie sincèrement monsieur Romain PRIVAT, qui a co-dirigé ce travail, pour son encadrement irréprochable. Tes conseils avisés, ta maîtrise et ton expertise scientifiques ont été au cours de cette thèse d'une aide inestimable.

Jean-Noël, Romain, j'ai pour vous le plus grand respect et la plus sincère sympathie. Travailler à vos côtés a été une expérience exceptionnelle et enrichissante tant sur le plan professionnel que personnel et je vous en remercie. Je n'aurais pu espérer meilleurs encadrants que vous.

Je tiens à remercier particulièrement monsieur Marc BONNISSEL qui a supervisé ce travail du côté de l'entreprise GTT et qui a participé au jury de cette thèse en qualité de membre invité. Son implication continue ainsi que ses nombreux conseils scientifiques et techniques ont grandement contribué au bon déroulement de cette thèse.

Je remercie monsieur le professeur Guillaume GALLIERO pour toutes les discussions scientifiques enrichissantes que nous avons partagées et pour avoir contribué scientifiquement à ce travail. Je le remercie également d'avoir participé à ma soutenance en tant que membre invité.

Je remercie messieurs les professeurs Christophe COQUELET et Jean-Luc DARIDON d'avoir accepté de juger mon travail en tant que rapporteurs. Leur présence dans le jury m'honore.

Que madame Véronique LACHET trouve ici l'expression de ma gratitude pour avoir accepté de participer à mon jury de thèse en qualité d'examinatrice.

Je remercie également messieurs Saifuddin AHMED et Honggang ZHOU pour avoir fait partie de mon jury de thèse en qualité de membres invités.

Je remercie l'équipe Process & Instrumentation de l'entreprise GTT pour les moments chaleureux que j'ai passé à leur cotés.

Je remercie toute l'équipe ThermE du LRGP et notamment Silvia, Andrés et Nicolás pour tous les bons moments qu'on a pu partager ensemble.

Enfin, je souhaite adresser ma sincère gratitude et toute ma reconnaissance à mes parents, mon frère Salem et à toi Aya pour votre soutien et votre amour inestimables à mes yeux. À vous, je dédie ce travail.

Nancy, le 10 septembre 2022

Aghilas DEHLOUZ

I- Introduction

I-A) Contexte :

A l'heure où les besoins énergétiques sont en constante augmentation et où les questions climatiques poussent la société à être plus responsable en matière de pollution et de préservation de l'environnement, le GNL s'est imposé comme un bon compromis entre efficacité énergétique et réduction des émissions polluantes en comparaison à d'autres hydrocarbures conventionnels. Il constitue l'une des solutions pouvant assurer une transition sereine vers des sources renouvelables et durables.

Contrairement aux autres hydrocarbures comme le pétrole qui est liquide à l'ambiante, les mélanges de type gaz naturel sont quant à eux à l'état gazeux dans ces conditions. Au-delà des enjeux géopolitiques, cette caractéristique l'a, dans un premier temps, restreint à une distribution locale entre pays frontaliers via des pipelines, puis l'a amené à être transporté par voie navale vers les grands marchés de consommation.

Son transport par bateau à l'état gazeux étant beaucoup moins pratique comparé à son transport à l'état liquide où il occupe un volume environ 600 fois plus petit, le GNL est produit par refroidissement jusqu'à -160 °C environ, à la pression atmosphérique, pour être ensuite chargé dans des cuves de méthanier spécialement conçues à cet effet (Figure I-1).

Développées par la société Gaz Transport et Technigaz (GTT), les technologies dites « à membranes » sont nées de l'idée de réduire les coûts du transport maritime du gaz naturel liquéfié (GNL). Le terme « membrane » signifie que les cuves sont dotées d'un revêtement cryogénique, capable de conserver le GNL à une température de - 163 °C, en assurant une parfaite étanchéité entre la cargaison et la coque du navire, une bonne isolation thermique mais aussi une bonne résistance aux fortes sollicitations mécaniques du méthane liquide balloté par les mouvements des vagues marines (phénomène dit de « sloshing »).

Malgré une efficacité d'isolation continuellement améliorée, le fluide transporté à très basse température reçoit de la chaleur de son environnement ce qui entraîne des vaporisations partielles. L'une des répercussions majeures de cette évaporation est l'augmentation de pression qui, si elle dépasse un certain seuil, peut conduire à la déformation des cuves. De ce fait, une attention particulière doit lui être portée.

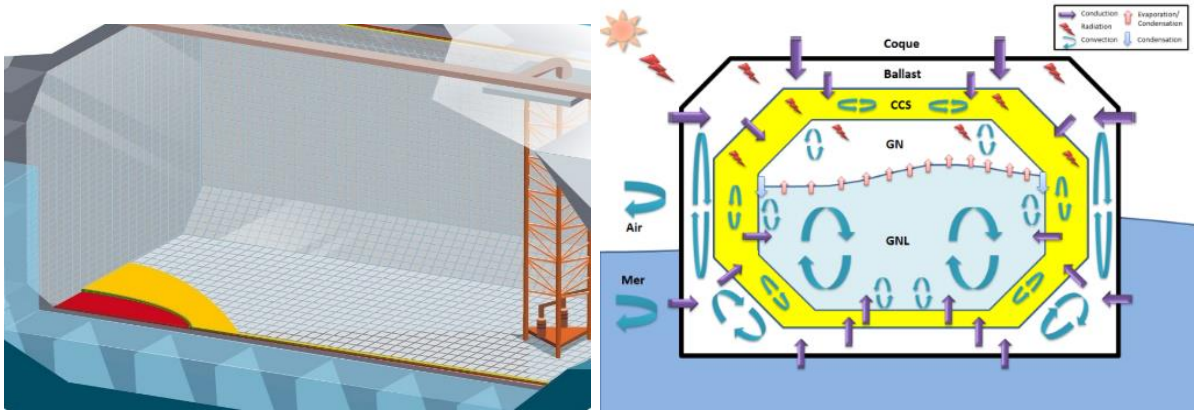

Figure I-1- Système de transport de GNL et schéma simplifié du transfert thermique associé

Ce gaz produit par évaporation partielle du GNL est appelé « Boil-off gas » (BOG) en anglais, soit « gaz d'évaporation », en français. S'il n'est pas évacué, le BOG s'accumule, dans la cuve de volume constant, entraînant ainsi une montée en pression. Sur les méthaniers, en exploitation normale, des systèmes adaptés permettent de maintenir la pression stable dans les cuves : en évacuant le BOG vers les moteurs ou vers des torchères (lorsque le BOG disponible dépasse les besoins moteurs). Le taux journalier d'évaporation sur un méthanier est généralement de 0,05 à 0,15 %. La maîtrise et la gestion du taux d'évaporation représentent donc un enjeu majeur pour les armateurs et affréteurs.

De plus, le GNL étant constitué de plusieurs espèces, son changement d'état conduit à l'évolution de sa composition et donc de ses propriétés physiques, que l'on dénomme sous le terme *vieillissement du fluide*. Une description fine du comportement global du système diphasique GN/GNL est primordiale pour une meilleure sécurité et une gestion optimale de la cargaison. Ce comportement dépend de plusieurs paramètres, parmi lesquels :

- Le flux de chaleur transmis de l'extérieur vers l'intérieur des cuves,
- La composition et les propriétés thermo-physiques des fluides,
- La géométrie de la cuve,
- Les mouvements de ballotement des navires.

Les cuves cryogéniques commercialisées par GTT possèdent des géométries variables et peuvent être utilisées dans diverses conditions de niveaux de remplissage et de composition du gaz liquéfié ; elles peuvent être totalement fermées ou échanger de la matière avec le milieu extérieur ; elles sont placées sur des bateaux soumis à des conditions météorologiques variables. Ainsi, on se retrouve en présence de systèmes complexes où de nombreux phénomènes prennent place simultanément, et parmi eux :

- Un transfert de chaleur provoqué par des gradients de température importants au sein des cuves contenant le liquide et le gaz
- Une stratification thermique ayant un impact direct sur le taux d'évaporation qui prend place au sein de la phase liquide d'une cuve fermée (ne subissant pas d'opération de soutirage ou de remplissage).

- Une forte évaporation qui refroidit l'interface liquide/vapeur et engendre un phénomène de mélange dans le cas d'une cuve ouverte (subissant un soutirage de gaz),
- L'évolution de la composition (dans le cas de fluides multiconstituants) et des propriétés de la cargaison (vieillissement).

Comme première étape des travaux menés au cours de cette thèse et afin de simuler ces phénomènes de façon rigoureuse, un modèle numérique de mécanique des fluides a été développé sous OpenFOAM afin de répondre au cahier des charges suivant :

- Simuler un système diphasique compressible en utilisant une formulation à un fluide (Volume Of Fluid),
- Considérer des fluides purs ou des mélanges pour lesquels des phénomènes de transport/diffusion d'espèces sont pris en compte (voir la Figure I-2),
- Affiner la modélisation des conditions aux limites grâce à la possibilité de dupliquer ou coupler des zones solides (où le transfert de chaleur par conduction est pris en compte) et des zones fluides diphasiques,
- Tenir compte de la vaporisation à l'interface LV grâce à un modèle de type Scharge utilisant la pression de saturation du fluide
- Pouvoir appliquer des mouvements d'ensemble au fluide (translation, rotation …) grâce aux librairies disponibles dans OpenFOAM (voir Figure I-3)

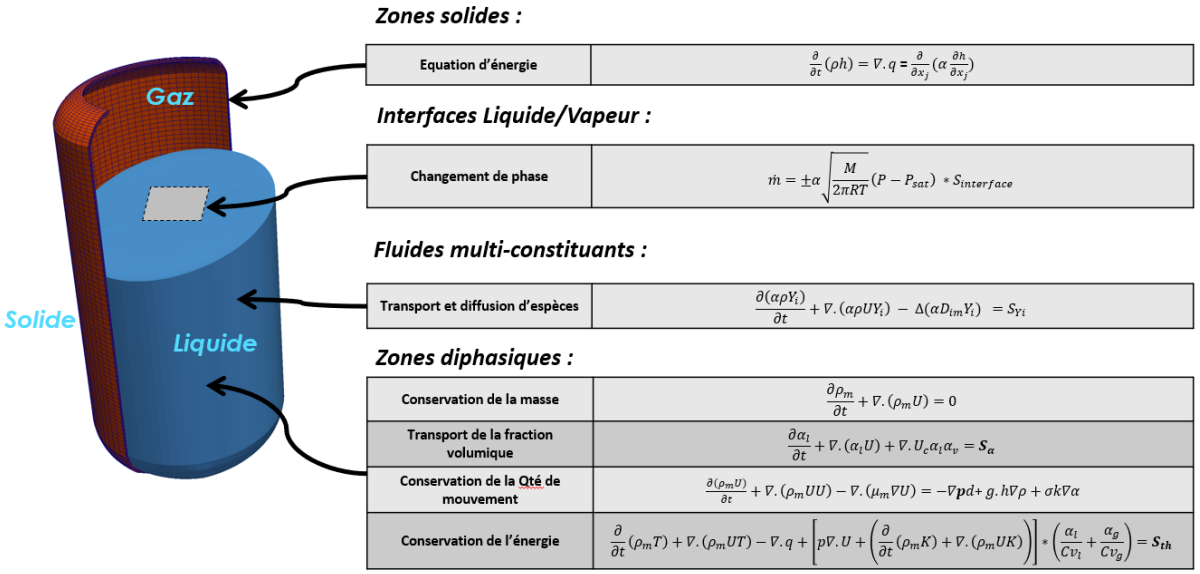

Figure I-2 - Système d'équations du modèle CFD

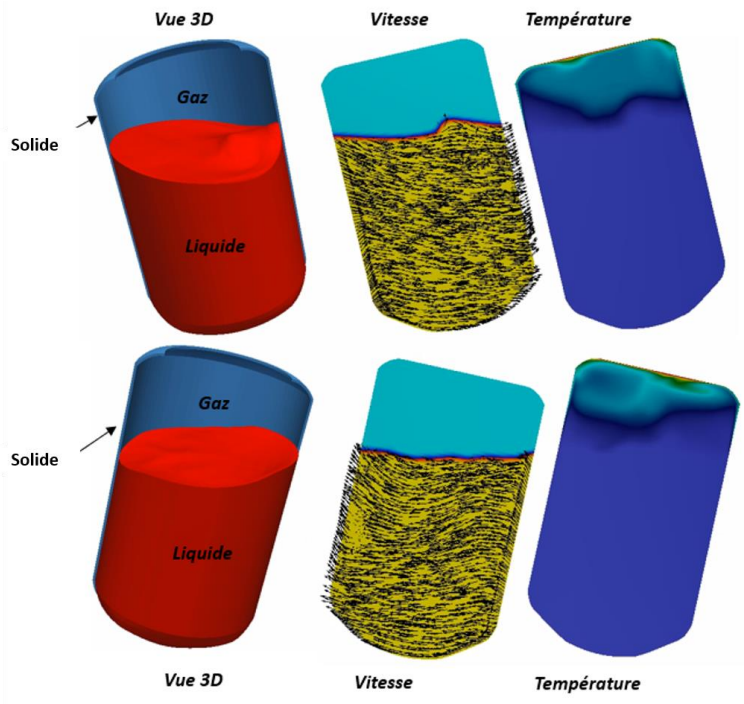

Figure I-3 - Exemple de simulation effectuée avec le modèle numérique développé sous OpenFOAM

Le développement de ce code de calcul ainsi que la réflexion sur les perspectives de son amélioration, afin qu'il soit apte à reproduire de façon rigoureuse des essais expérimentaux ou des situations réelles de transport/stockage du GNL, ont mis en évidence plusieurs éléments auxquels il fallait apporter une solution. Parmi ces éléments, les plus importants sont :

- Le changement de phase se produisant à l'interface GNL/GN qui a un impact direct sur la composition, la pression et le comportement global de la cargaison. Il fallait donc trouver un model adapté à un code de calcul CFD, permettrant de le reproduire numériquement de façon satisfaisante,
- L'évolution des propriétés de transport des fluides en fonction de la pression, de la température et de la composition et ce, avec un rapport temps de calcul/précision optimal.

Une modélisation précise du comportement dynamique du GNL et du GN, qui induit une caractérisation adéquate de l'état de l'interface GN/GNL, s'impose comme prioritaire à la prospection des modèles de changement de phase. Le comportement du système GN/GNL est régi par le transfert de masse, de chaleur et de quantité de mouvement s'y produisant lesquels, à leur tour, dépendent respectivement du coefficient de diffusion de la matière, de la conductivité thermique et de la viscosité (présents dans les équations de conservation résolues dans notre modèle numérique). Ces trois grandeurs représentent les principales propriétés de transport d'un fluide. Leur prédiction/estimation a été et est toujours une question fondamentale impactant la majorité des applications et procédés industriels et elle constitue le sujet principal de cette thèse.

I-B) Les propriétés de transport :

Un ensemble de molécules peut être considéré à l'état fluide lorsque ces dernières se trouvent sous forme liquide, gazeuse ou supercritique. Ces états sont une directe conséquence des conditions environnantes de température, pression et composition lorsqu'il s'agit d'un mélange, dans lequel se trouve le fluide.

Sujet à une force motrice (gradients de vitesse, de température ou de concentration), un fluide transporte de la quantité de mouvement, de l'énergie et/ou de la matière en son sein avant d'atteindre un état d'équilibre. Ce transport se fait grâce à des phénomènes microscopiques tels que des translations ou des collisions entre molécules. Pour un gradient donné, l'habilité d'un fluide à atteindre un état d'équilibre après une sollicitation extérieure (par exemple, à homogénéiser sa température après avoir subi un apport de chaleur) est caractérisée par ses propriétés de transport.

Les propriétés de transport peuvent être vues comme une simplification du comportement microscopique d'un fluide permettant de lier, à l'échelle macroscopique, une densité de flux $\boldsymbol{J}$ d'une propriété $\boldsymbol{\alpha}$ à la force motrice f qui lui correspond à travers une loi linéaire de la forme $\boldsymbol{J_\alpha} = -k\boldsymbol{\nabla} f$. Ainsi, selon le gradient $\boldsymbol{\nabla} f$ considéré, on aboutit à :

- La loi de **Newton** lorsqu'il s'agit du transfert de la quantité de mouvement : $\boldsymbol{J_{mvt}} = -\eta \boldsymbol{\nabla} v$ où η est la viscosité dynamique et où v est la vitesse
- La loi de **Fick** lorsqu'il s'agit du transfert d'une quantité de matière par diffusion : $\boldsymbol{J_m} = -D\ \boldsymbol{\nabla} c$ où D est le coefficient de diffusion massique et c la concentration massique
- La loi de **Fourier** lorsqu'il s'agit du transfert d'une quantité de chaleur par conduction : $\boldsymbol{J_q} = -\lambda \boldsymbol{\nabla} T$ où λ est la conductivité thermique et T est la température

De nos jours, la connaissance des propriétés de transport d'un fluide est un élément essentiel dans la majorité des domaines industriels. Par exemple, elles influencent le choix des fluides dans un procédé et sont nécessaires au dimensionnement des équipements.

Différentes techniques peuvent être suivies afin d'estimer les propriétés de transport. On peut notamment citer :

- **Mesures expérimentales :** elles constituent la source la plus fiable pour l'obtention des propriétés de transport. Cependant, c'est généralement le moyen le plus couteux qui nécessite l'utilisation de dispositifs expérimentaux plus ou moins élaborés, la disponibilité de la matière première et qui requiert un temps important.
- **Simulations de dynamique moléculaire :** rendues de plus en plus accessibles grâce à l'évolution de la puissance de calcul des ordinateurs, elles nécessitent l'utilisation de modèles moléculaires adaptés afin de décrire les interactions intermoléculaires. Elles permettent une estimation rigoureuse des propriétés de transport et ont permis une meilleure compréhension de l'évolution complexe de ces dernières en fonction de la température, de la pression et de la composition.
- **Corrélations empiriques :** basées sur des observations expérimentales, elles constituent des relations simples (souvent polynômiales) entre une propriété de

transport donnée et la température et la densité du fluide. Si elles représentent des alternatives abordables et sont largement utilisées en industrie et plus spécifiquement dans les logiciels de simulation, elles sont le plus souvent restreintes à un état de fluide donné (e.g. liquide, gaz, état saturé) ou à des conditions expérimentales spécifiques (e.g. un intervalle de température donné).

- **Modèles théoriques :** Ayant une forme prédictive et étant basés sur des lois physiques, ils représentent le moyen le plus rigoureux de décrire les propriétés de transport. Malgré les efforts et les avancées considérables effectués en ce sens, la complexité des phénomènes microscopiques intervenant (collisions, translations, vibrations, rotations des molécules), la variété des fluides (monoatomiques ou polyatomiques), leur état (gaz, liquide ou supercritique) et leurs spécificités chimiques (polaires, associatifs …) fait qu'il n'existe pas encore de théorie unificatrice pouvant rassembler les trois états fluides, toutes les familles chimiques et les trois propriétés de transport dans un même modèle.
- **Modèles semi-théoriques :** à ce jour, ils représentent le meilleur compromis précision/coût et sont une solution adaptée à la majorité des cas (simulations de procédé, validations de mesures expérimentales, etc.). Ils sont basés sur des principes et/ou des lois fondamentales mais font intervenir des paramètres ajustables déterminés grâce à des données expérimentales. Quand ces dernières sont disponibles en quantité suffisante (e.g. pour plusieurs composés chimiques) et complètes (c-à-d recouvrant la majorité des conditions en température et en pression), elles permettent d'aboutir à des approches prédictives (s'affranchissant des données expérimentales) en utilisant par exemple une méthode de contribution de groupes ou un algorithme de ''machine learning''.

L'approche dont fait l'objet cette thèse s'inscrit dans cette dernière catégorie et est communément appelée l'« Entropy Scaling ».

I-C) L'Entropy Scaling:

L'entropie résiduelle à volume et à température fixés, notée $s_{\mathrm{Tv-res}}$ exprimant la différence entre l'entropie d'un fluide réel et celle du gaz parfait à la même température et au même volume molaire, est la pierre angulaire du concept de l'Entropy Scaling. Cette quantité peut être interprétée comme une quantification du désordre du système, par rapport à celui du gaz parfait, et peut être estimée à l'aide d'une équation d'état de manière simple. D'un point de vue microscopique, $s_{\mathrm{Tv-res}}$ renseigne sur la structure du fluide réel et quantifie le nombre de micro-états accessibles par rapport au gaz parfait.

Les propriétés de transport et l'entropie résiduelle sont les deux étroitement liées à la structure moléculaire des fluides. Dans cette optique, l'entropy scaling mis en évidence par Rosenfeld[1] en 1977 est un concept qui repose sur le raisonnement suivant : pour un système de sphères dures (communément noté HS pour « Hard Spheres » et représentant une bonne approximation d'un liquide simple), l'entropie résiduelle est une fonction qui dépend uniquement de sa compacité (taux d'occupation de l'espace). D'un autre côté, ses propriété dynamiques, i.e. les

propriétés de transport du système de sphères dures, sont-elles aussi des fonctions uniques de cette compacité. Alors qu'il existe différentes possibilités et voies d'obtenir la compacité d'un système simple, son estimation ainsi que la caractérisation de sa relation avec les propriétés de transport peut s'avérer être une tâche ardue voire inatteignable pour des fluides réels.

Afin de contourner ce problème et pour proposer une méthode simple et accessible, Rosenfeld[1,2] a proposé de faire directement référence à l'entropie résiduelle pour la description des propriétés de transport.

Concernant le coefficient d'autodiffusion qui caractérise l'habilité de la matière à se mouvoir dans elle-même en l'absence de gradient de concentration ou de mouvements induits de l'extérieur, l'hypothèse de Dzugutov[3] est telle que « *La dynamique atomique dans les phases condensées est régie par les effets dits de cage, dans lesquels la diffusion est couplée à des relaxations structurelles. En raison des corrélations structurelles prononcées, chaque atome se retrouve dans une cage formée par ses voisins immédiats, et son mouvement diffusif est affecté par une fluctuation locale de densité transformant la configuration atomique environnante* ».

Afin de conceptualiser sommairement le point de vue de Dzugotov[3] et plus généralement, la dépendance des propriétés de transport à l'entropie résiduelle (en particulier aux états denses), la représentation schématique proposée par McLaughlin[4] dans son examen approfondi de la conductivité thermique des fluides denses est ici utilisée pour illustrer les mécanismes de transport dans les systèmes de sphères dures (voir figure I-4). Tout d'abord, rappelons que pour les systèmes de fluides réels avec une faible densité, une telle distribution (en cage ou en réseau comme représenté dans la figure I-4) n'est pas une hypothèse adéquate du fait des distances intermoléculaires plus importantes et des plus amples libertés de mouvement des molécules, non-entravées par des forces intermoléculaires. Néanmoins, un système de sphères dures fournit une visualisation pratique et constitue une hypothèse valable pour des systèmes simples à l'état dense (c'est-à-dire un état dense modélisé avec des sphères dures).

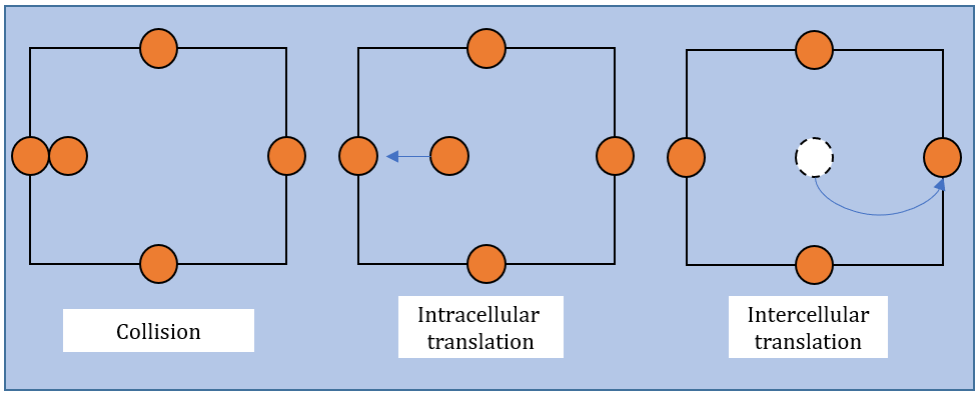

Figure I-4 – Représentation schématique des mécanismes de transport pour un système de sphères dures, selon McLaughlin[4]

Comme le souligne McLaughlin[4], qui a supposé que les molécules à l'état liquide obéissent à un modèle de réseau, les translations intercellulaires (voir Figure I-4), définies comme le mouvement de la sphère centrale d'une cellule donnée vers un site vacant, conduit au phénomène de diffusion. Notons que ce phénomène contribue également à la viscosité et à la conductivité thermique. Les autres phénomènes illustrés par la figure I-4, c'est-à-dire les collisions et les translations intracellulaires, contribuent à la viscosité et à la conductivité thermique mais que dans une moindre mesure, à la diffusion de la matière. Comme l'a souligné Dzugutov[3], l'existence de sites vacants, qui peuvent être assimilées à des relaxations structurelles, est une condition nécessaire à la migration des particules d'un site à un autre (translation intercellulaire). Ce nombre de sites vacants est proportionnel au nombre de configurations accessibles par atome, c'est à dire à l'entropie selon la définition de Boltzmann ($s = \mathrm{k_b} ln(\Omega)$ où Ω est le nombre de configurations microscopiques accessibles au système).

A forte densité où les translations intercellulaires sont le mécanisme prépondérant dans les phénomènes de transport, la forte dépendance des propriétés de transport aux relaxations structurelles fait que ces propriétés peuvent être directement liées à l'entropie résiduelle sans avoir recourt à l'introduction d'autres informations dans la fonction qui les lie à cette dernière. Cependant, avec l'augmentation des distances intermoléculaires et lorsque l'hypothèse d'une distribution par réseau n'est plus valide, d'autres mécanismes de transfert voient leur impact devenir non-négligeable.

Ainsi, dans diverses conditions de fluide, les collisions entre molécules jouent un rôle primordial (e.g. dans le transfert de la quantité de mouvement ou de l'énergie thermique). Aussi, les translations intermoléculaires et intramoléculaires deviennent indiscernables avec la diminution de la densité. Dans ces conditions, il devient indispensable d'apporter des éléments supplémentaires pour décrire l'évolution des propriétés de transport en plus de l'information transmise par l'entropie sur l'état structurel du fluide.

A partir d'un raisonnement basé sur la théorie cinétique, Rosenfeld a introduit une réduction dite macroscopique où les propriétés de transport sont divisées par un terme dépendant de la température T et de la densité moléculaire ρ_N, ici appelée « propriété de référence », ayant la même dimension que le coefficient de transport (voir le tableau I-1 pour les trois propriétés de transport). Rosenfeld a montré que les propriétés de référence dépendant de T et ρ_N sont prédisposées à bien corréler les propriétés de transport réduites à l'entropie résiduelle.

En réalité, une telle propriété de référence a le potentiel de mimer qualitativement le comportement dynamique de molécules/particules animées de translations rectilignes sur une distance maximale $l = \rho_\mathrm{N}^{-1/3}$, à la vitesse thermique moyenne $v = \sqrt{\mathrm{k_b}T/\mathrm{m_0}}$ des molécules (où k_b est la constante de Boltzmann et m_0 la masse moléculaire), avant qu'une collision ne se produise.

Tableau I-1 - Récapitulatif des propriétés de référence macroscopiques proposées par Rosenfeld pour la réduction des propriétés de transport

Propriété de transport	**Viscosité dynamique**	**Coefficient d'auto-diffusion**	**Conductivité thermique**
Expression de la propriété de référence proposée par Rosenfeld	$\eta_{\mathrm{ref}} = \rho_{\mathrm{N}}^{2/3}\sqrt{\mathrm{m_0 k_b} T}$	$D_{\mathrm{self,ref}} = \rho_{\mathrm{N}}^{-1/3}\sqrt{\mathrm{k}_b T / \mathrm{m}_0}$	$\lambda_{\mathrm{ref}} = \rho_{\mathrm{N}}^{2/3}\mathrm{k_b}\sqrt{\mathrm{k_b} T / \mathrm{m}_0}$

De ce fait, ces propriétés de référence qui permettent de corréler (voir Figure I-5) de façon satisfaisante une forme réduite des propriétés de transport à l'entropie résiduelle, véhiculent de façon qualitative l'information sur le transfert qui se fait par collision et/ou par translation intramoléculaire faisant défaut dans la relation propriété de transport / entropie résiduelle.

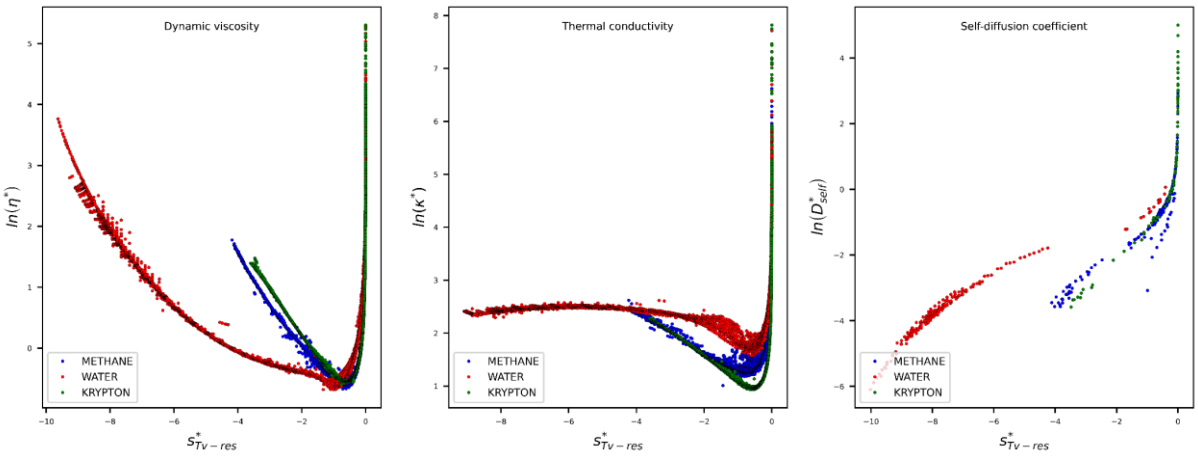

Figure I-5 – Illustration du concept d'Entropy Scaling sur les trois propriétés de transport comme postulé initialement par Rosenfeld. Dans cette figure, chaque point représente une mesure expérimentale et chaque couleur un composé (rouge : eau, bleu : méthane, vert : krypton)

Par rapport aux méthodes de réduction reposant sur une propriété de référence constante pour réduire le coefficient de transport, la technique de Rosenfeld a l'avantage d'introduire des variables révélant le changement de structure du fluide dans la définition de la propriété de référence. Par conséquent, la propriété de transport réduite résultante peut être interprétée comme un rapport révélant à quel point le système réel s'écarte d'une représentation de systèmes liquides simples (fictifs) déduite de la théorie cinétique en raison de la structure locale. Des écarts par rapport à ces représentations simples sont observés lorsque :

- Des voies de transfert supplémentaires, accessibles aux molécules du système, existent (ex. degrés de liberté vibrationnels pour les fluides polyatomiques à faible densité),
- Des effets de forme, des forces intermoléculaires, une association par liaison hydrogène, etc. se produisent dans le fluide.

Lorsque des écarts importants par rapport aux comportements des systèmes simples cités au-dessus sont observés, les courbes d'Entropy Scaling s'écartent de l'universalité, limitant ainsi le champ de son application. Ce problème peut être partiellement contrecarré par l'introduction de paramètres empiriques ajustés aux données expérimentales et/ou en modifiant l'expression de la propriété de référence utilisée pour la réduction.

Comme on peut l'observer dans la figure I-5, différents comportements contraignants subsistent lorsque l'approche initialement proposée par Rosenfeld est appliquée à des substances réelles. Parmi ces défaillances, on peut noter :

- L'entropie résiduelle n'étant pas une grandeur mesurable expérimentalement, la variété des équations d'état permettant son estimation donne lieu à des modèles spécifiques à chaque équation considérée.
- Un comportement divergeant systématique à faible densité (quand $s_{Tv\text{-}res}$ tend vers 0) pour les trois propriétés de transport
- Des paramètres caractérisant les courbes d'Entropy Scaling propres à chaque composé chimique (pas d'universalité)
- Une dispersion des points expérimentaux dans le cas des conductivités thermiques à partir des densités modérées jusqu'aux faibles densités.

Afin d'améliorer le concept d'un point de vue applicatif, différentes méthodes de réduction des propriétés de transport dont celles proposées dans la littérature ont été étudiées. Plusieurs modifications concernant l'expression de la propriété de référence ont été testées et malgré des améliorations conséquentes sur certaines gammes de températures et de pressions, une perte du comportement affine aux faibles densités et l'absence d'existence de paramètres universels (i.e., identiques pour tous les corps purs) restent des problèmes persistants.

Ce constat nous a conduit à remettre en cause la relation entre l'entropie résiduelle et la viscosité telle que Rosenfeld la postula. Nous avons alors introduit une modification de la variable adimensionnelle contenant l'entropie résiduelle (autrement dit, un changement d'abscisse sur le graphe de la figure I-5). Celle-ci a entraîné un comportement plus régulier et plus facilement modélisable des propriétés réduites sur l'ensemble du domaine fluide. Ce changement d'abscisse a consisté à apporter deux modifications à la variable initiale ($s_{Tv\text{-}res}/R$) :

- Normer l'entropie résiduelle avec l'entropie résiduelle $s_{\mathrm{Tv-res}}$ par sa valeur au point critique afin de tendre vers un comportement indépendant du composé chimique mais aussi indépendant de l'équation d'état considérée et ainsi approcher l'universalité.
- Ajouter un terme décrivant le comportement des fluides à faible densité.

En outre, des modifications supplémentaires au concept de base ont été mises en évidence et ont été proposées afin d'aboutir à une forme fonctionnelle simple pour chacune des propriétés de transport. Ces dernières sont détaillées dans les chapitres suivants pour chacune des propriétés de transport. Parmi elles :

- La proposition d'une version corrigée pour l'expression de la conductivité thermique de référence qui tient compte des degrés de liberté internes relatif aux molécules polyatomiques permettant le transfert de l'énergie par vibration et par rotation.
- La proposition d'une formulation polyvalente, utilisant un formalisme similaire aux trois propriétés de transport, pour la prédiction des courbes d'Entropy Scaling permettant la reproduction de façon continue de l'évolution de ces dernières dans les états gaz, liquide et supercritique.

Dans la suite de ce manuscrit (chapitres 1, 2 et 3), le concept d'Entropy Scaling est discuté et revisité pour les trois propriétés de transport (viscosité dynamique, coefficient d'auto-diffusion et conductivité thermique respectivement) en vue de son application aux substances pures en utilisant deux types d'équations d'état (respectivement *I*-PC-SAFT qui appartient à la famille d'équation d'état de type SAFT et *translated-consistent* Peng-Robinson (*tc*-PR) qui est une version revisitée de la fameuse équation d'état cubique de Peng-Robinson). Différentes versions de modèles sont proposées, utilisant des paramètres spécifiques aux composés chimiques, à la famille chimique ou universels, et sont validées sur de larges bases de données expérimentales. Au terme des différents résultats satisfaisants obtenus, le chapitre 4 détaille certaines perspectives très prometteuses et les résultats préliminaires qui en découlent (comme par exemple, l'extension des modèles aux propriétés de transport des mélanges). Ce manuscrit se termine par une conclusion globale sur les résultats obtenus et leurs débouchés.

II- Chapitre 1 : La viscosité dynamique des corps purs

Ce chapitre a donné lieu à la publication suivante :

Revisiting the entropy-scaling concept for shear-viscosity estimation from cubic and SAFT equations of state: application to pure fluids in gas, liquid and super-critical states.

Aghilas Dehlouz[1,2], Romain Privat[1(*)], Guillaume Galliero[3], Marc Bonnissel[2], Jean-Noël Jaubert[1(*)]

[1] *Université de Lorraine, École Nationale Supérieure des Industries Chimiques, Laboratoire Réactions et Génie des Procédés (UMR CNRS 7274), 1 rue Grandville, 54000, Nancy, France*

[2] *Gaztransport & Technigaz (GTT), 1 route de Versailles, 78470 Saint-Rémy-lès-Chevreuse, France*

[3] *Université de Pau et des Pays de l'Adour, E2S UPPA, CNRS TotalEnergies, LFCR UMR 5150, Pau, France*

Abstract :

The entropy scaling concept postulates that reduced transport properties of fluids are related to the residual entropy, a property that reveals intermolecular interactions and can be estimated from equations of state (EoS) in a straightforward way. In that framework, two models for dynamic viscosity are presented in this paper: in both models, similar expressions inspired from Rosenfeld's seminal idea are used to reduce transport properties and are related to a carefully-selected function of the Tv-residual entropy. This latter is estimated from the PC-SAFT EoS for one model or the *tc*-PR cubic EoS for the other. The two models are able to predict the viscosities in the whole fluid region (liquid, gas and supercritical states), which is a great advantage in comparison to most of the correlations available in the open literature that are specific to a physical state. Model parameters were fitted over a large database containing more than 100 000 pure-fluid experimental data associated with 142 chemical species. For each model, different sets of parameters are provided, each of them being likely to be used in specific situations: firstly, component-specific parameters were estimated for 142 pure compounds; secondly, chemical-family specific parameters were proposed for describing components not included in our database but belonging to one of the chemical families we considered. Eventually, for compounds present neither in the original database, nor in the considered chemical families, universal parameters (leading to lower accuracy but applicable to any species) are proposed. The accuracy of the models is obviously maximal when using component-specific parameters and minimal with universal parameters.

Thus, the entropy-scaling formulation presented in this work can be used for routinely modelling the dynamic viscosity of any pure fluid. As main advantages, it can be applied to any pure species without restriction and is valid for all fluid states, from the dilute gas to the liquid and even the supercritical state.

II-A) Introduction:

The dynamic viscosity of a fluid (liquid, gas or supercritical), sometimes called *absolute viscosity*, characterizes the rate of fluid resistance to gradual deformation induced by shear stress. Depending on temperature and pressure conditions (and composition as well, for mixtures), viscosity like other transport properties (thermal conductivity and mass diffusion coefficient) is a consequence of molecule displacement, collisions and interactions. Being observed when fluid is in motion, this property is of crucial relevance for pressure-drop calculation, fluid-flow modelling, heat-transfer coefficient estimation, etc. Consequently, the design of a wide variety of industrial-process unit operations (pipes, heat exchangers etc.) and products (working fluid for power or refrigeration cycles, lubricants etc.) strongly depends on viscosity.

From experimental measurements to molecular-simulation tools, various techniques[6,7] enable to estimate the viscosity of a fluid. To make the property available in a reasonable time (compatible with simulation times classically expected by users of chemical-engineering software) and with an acceptable accuracy (suitable for an industrial use), the viscosity (and the transport properties in general) are commonly estimated either from empirical correlations depending on temperature and/or density applicable in specific conditions, or from semi-theoretical models, e.g.:

- Cubic equations for viscosity[8,9] taking advantage of the similitudes between the density behaviour in the (temperature T, pressure P, density) space and the dynamic-viscosity behaviour in the (temperature T, pressure P, viscosity) space,
- The kinetic theory of gases[10] and derived versions[11–15] based on the hard-sphere assumption,
- Corresponding-state models[16–19] deducing a reduced (dimensionless) viscosity from the one of a reference fluid under the same reduced conditions,
- The Free-Volume Theory[20,21] relating the viscosity to the available free space or free volume between molecules,
- The Friction Theory[22,23] postulating that the residual viscosity (a departure property defined as the difference between the real-fluid property and the dilute-gas contribution) can be expressed as a function of the repulsive- and attractive-pressure terms of an Equation of State (EoS),
- The expanded-fluid Theory[24,25] providing a correlation between residual viscosity and density based on the observation that the fluidity (inverse of viscosity) increases as the fluid expands (i.e., with increasing inter-molecular distance),
- Scaling approaches encompassing both the thermodynamic scaling[26,27] which relates a reduced viscosity to a temperature-density ratio and the entropy scaling[1,28] which relates reduced transport properties to the so-called *residual entropy* (sometimes called "excess entropy").

Despite a keen interest in transport-property prediction over past decades and although efficient methods were proposed in the literature (Friction theory, Free Volume, Entropy scaling …), researchers are still searching for a unifying theory, valid in all fluid conditions (i.e., for

subcritical gases and liquids as well as supercritical fluids), applicable to any substance, modelled and real, capable to predict these properties with an excellent accuracy. To start addressing the modelling of viscosity coefficients, one needs to clearly identify the nature of the variables influencing this property. The kinetic theory of gases provides fundamental temperature-dependent expressions for the three transport coefficients at the zero-density limit; they can thus be used in low-pressure (dilute) condition, whenever real fluids can be considered as an assembly of molecules subject to collisions but not to intermolecular forces. When a fluid deviates significantly from the dilute-gas behaviour, the temperature variable becomes insufficient to describe entirely the dynamic behaviour for the simple reason that in addition to kinetic effects, intermolecular effects must be considered.

From the majority of the above-mentioned approaches that could be used to describe the viscosity at dense states, recurrent observations can be made:

(a) the more specific the model is (in terms of substances, temperature and pressure conditions), the more accurate are predictions,
(b) to be able to describe both liquid and gaseous states, semi-theoretical models introduce additional variables to the temperature such as the density for the Free Volume Theory, attractive and repulsive pressures for the Friction Theory and the residual entropy for the Entropy Scaling approach. Note that all these quantities are interrelated. When an EoS is used to express these quantities, the final viscosity models depend on the temperature and density state variables.

The nature of the variable(s) to be used in addition to the temperature in viscosity models remains thus an issue and does not make consensus currently. However, in the perspective of including variables accounting for deviations from the dilute-gas behaviour, residual properties can be considered legitimately as promising candidates. Among these ones, the residual entropy deserves attention as it is the cornerstone variable of the entropy-scaling concept and therefore, shows predispositions to describe the behaviour of transport coefficients.

At this step, let us recall precisely what *residual entropy* means. Sometimes called "excess entropy", the residual entropy is a departure function expressing the difference between the entropy of a real fluid and the one of a perfect gas having the same temperature T and molar volume v as the real fluid. For the sake of clarity, we will name this quantity "Tv-residual entropy" thereafter. Note that it is always a negative quantity since the entropy of the perfect gas (maximum-disorder state) is always larger than the one of a real fluid. From a microscopic viewpoint, the Tv-residual entropy provides information about fluid structure and quantifies the number of accessible microstates relative to the perfect gas. It can be commonly estimated from an EoS as follows.

$$\text{For a pure fluid: } s_{\mathrm{Tv-res}} = s_{\mathrm{real}}(T,v) - s_{\text{perfect gas}}(T,v) = -\left(\frac{\partial a_{\mathrm{Tv-res}}}{\partial T}\right)_v \qquad \text{(II-1)}$$

Where $s_{\mathrm{Tv-res}}$ is the Tv-residual entropy, s_{real} is the molar entropy of the real fluid (liquid, gas, supercritical), $s_{\text{perfect gas}}$ the perfect-gas entropy, R the gas constant and a_{Tv-res}, the Tv-residual molar Helmholtz energy. While SAFT EoS are provided classically as Helmholtz

energy expressions, cubic EoS are written generally as pressure expressions. In such a case, $a_{\mathrm{Tv-res}}$ can be deduced from the following integral: $a_{\mathrm{Tv-res}} = -\int_{+\infty}^{v}\left[P(T,v) - \frac{RT}{v}\right]dv$.

The entropy scaling concept, originally proposed by Rosenfeld in 1977[1] postulates that a reduced function $\tilde{\eta}$ of the viscosity (or any other transport property) depends on the reduced Tv-residual entropy ($\tilde{s}_{\mathrm{Tv-res}} = s_{\mathrm{Tv-res}}/R$):

$$\ln(\tilde{\eta}) = \ln\left(\frac{\eta_{\mathrm{real}}}{\eta_{\mathrm{ref}}}\right) = f(\tilde{s}_{\mathrm{Tv-res}}) \tag{II-2}$$

Where η_{real} is the dynamic viscosity of a real fluid and η_{ref} is a scaling term proposed by Rosenfeld, arriving naturally from a consideration of the natural length, time, and energy scales in a liquid:

$$\eta_{\mathrm{ref}} = \rho_{\mathrm{N}}^{2/3}\sqrt{\mathrm{m_0 k}_b T} \tag{II-3}$$

In Eq. (II-3), ρ_{N} is the molecular density (number of molecules per unit of volume), m_0 is the molecular mass, k_b is the Boltzmann constant.

Consequently, the dynamic viscosity η_{real} depends not only on T, but also on the Tv-residual entropy and the density as well:

$$\eta_{\mathrm{real}} = f(T, \rho_{\mathrm{N}}, \tilde{s}_{\mathrm{Tv-res}}) \tag{II-4}$$

Since this approach can be applied to the three transport coefficients and covers the entire fluid region, it appears as a solid basis for viscosity-model developments[29–46].

Since Rosenfeld's seminal work[1], the introduction of the Tv-residual entropy in viscosity laws has shown surprising strengths but also some important deficiencies. First, it can be said that the apparent success of this approach should probably be ascribed to the use of the reduced Tv-residual entropy variable ($\tilde{s}_{\mathrm{Tv-res}}$) which reflects the internal structure of a fluid and has thus, a prominent influence on its dynamic behaviour[47].

As illustrated in Figure II-1, plotting the logarithm of the reduced viscosity (as defined by Rosenfeld) as a function of the reduced residual entropy for a series of n-alkanes, from low to high temperatures and pressures, results in continuous curves showing the same shape. Unfortunately, instead of following a unique master/universal line as initially expected, it is observed that the application of the entropy-scaling concept to the reduced viscosity leads to:

(a) non-universal (i.e., component-specific) behaviours,

(b) the systematic presence of a diverging behaviour at low density which is difficult to describe and cannot be captured by some current literature models.

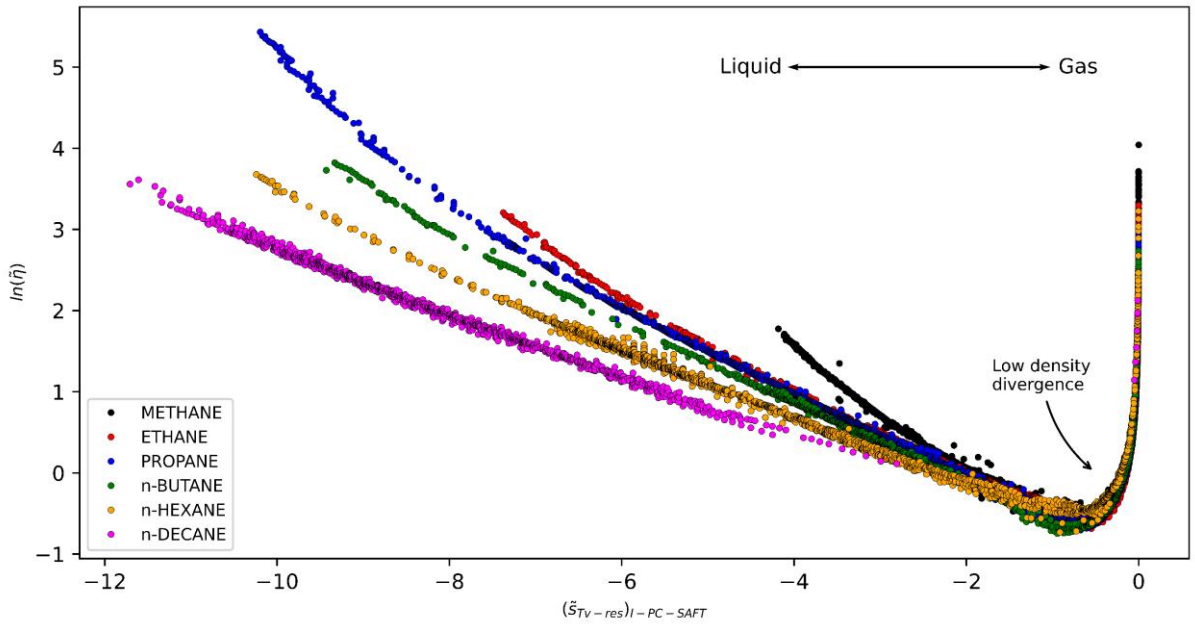

Figure II-1 – Plot of the reduced viscosity (as defined by Rosenfeld) as a function of the reduced residual entropy for 6 n-alkanes with carbon number ranging between 1 and 10. Circles: experimental data. Values ($\tilde{s}_{\mathrm{Tv-res}} = s_{\mathrm{Tv-res}}/R$) estimated from the I-PC-SAFT EoS (source: Dortmund Data Bank; the data selection procedure is described in section II-C).

To improve models derived from the entropy-scaling concept, some authors[28,33–41] revisited the formulation of this approach by using different reduction functions for the viscosity (this point is further discussed in the next section).

With the aim of deriving a universal model (applicable to any pure substance) enabling the prediction of pure-component transport properties, and dynamic viscosity especially, some key questions remain unanswered, such as:

- The residual entropy being a non-measurable thermodynamic property, EoS cannot be selected following their ability to provide accurate estimations of residual entropy; in that regard, which EoS is likely to ensure the best applicability of the concept, in the widest range of chemical species, and of temperature and pressure conditions?
- Which reference viscosity should be used in the definition of the reduced viscosity present in Eq. (II-2)?

In this work, two models aimed at predicting the dynamic viscosity of pure species and based on two different EoS are proposed and compared. EoS are used to generate Tv-residual entropy and density estimations. They have been selected for their accuracy, their applicability to a high number of pure species, in large temperature and pressure conditions. These are:

- a translated and re-parametrized version of the Perturbed-Chain SAFT EoS called *I*-PC-SAFT [48] (where "*I*" stands for "*Industrialized*"),
- and the *translated*[49,50] and *consistent*[51,52] Peng-Robinson EoS[53] (denoted *tc*-PR).

In our study, several expressions were tested out for the reference viscosity, involving microscopic and / or macroscopic variables and the relationship between the dynamic viscosity and the Tv-residual entropy was reformulated. This unique formulation encompasses all fluid states, from liquid to gas, from subcritical to supercritical states, and improves the predictive capability at low and high densities of other models based on the entropy-scaling concept[1].

For each model (i.e., cubic based or SAFT based), different parameter sets are proposed:

- a component-specific set (model parameters are component specific; for each pure compound, they were fitted to experimental viscosity data); this is the parametrization offering the highest accuracy.
- a chemical-family specific set: in that case, model parameters can be used with any compound belonging to a specific chemical family (e.g., n-alkanes, n-alcohols etc.)
- or a universal parameter set (i.e., applicable to any species without restriction) with a high predictive potential but showing the lowest accuracy.

The quality of the proposed models (and parameter sets) was evaluated by calculating deviations with respect to experimental data taken in a specifically-dedicated database of experimental dynamic viscosities spanning 14 chemical families, 142 molecules and containing more than 100 000 experimental data points.

II-B) Theoretical background:

II-B-1) Understanding the viscosity phenomenology through the entropy-scaling concept:

As illustrated in Figure II-1 showing the curves of various n-alkanes in the ln $\tilde{\eta}$ vs. $\tilde{s}_{\mathrm{Tv-res}}$ plane, the Entropy Scaling concept, as formulated by Rosenfeld, is a quasi-universal law[54–62] since each pure compound is characterized by:

- the same general (or component-independent) law (all the curves shown in Figure II-1 exhibit a quasi-universal shape and thus, could be modelled from the same physical law),
- component-specific law parameters (since in the ln $\tilde{\eta}$ vs. $\tilde{s}_{\mathrm{Tv-res}}$ plane, the various curves could not be superimposed).

However, these curves exhibit all an intriguing feature revealing the presence of small-scale physical phenomena: the presence of a common minimum approximately located around $\tilde{s}_{\mathrm{Tv-res}} \approx -0.5$, whatever the compound (see Figure II-1). Rosenfeld explained the presence of this singular point as the transition between a weak-coupling regime (low densities), "*where the viscosity is determined by the kinetics of pair collisions*", and a strong coupling regime (high densities) where the viscosity "*is determined mainly by interaction effects*"[28]. Following this analysis, Bell et al. have proposed recently to define a line separating gas-like and liquid-like fluid behaviours from the standpoint of shear viscosity which "*corresponds to points in the*

thermodynamic phase diagram for which the kinetic contribution to viscosity is approximately half of the total viscosity" [63]. For hard-spheres, the line is given by the simple equation $\tilde{s}_{\mathrm{Tv-res}} = -\frac{2}{3}$.

Following a similar idea, Galliero et al.[64] noticed that the transfer of shear stress results (i) from particle displacement (translation) and (ii) from interactions by collision between particles. This led them to claim that the total viscosity can be written as:

$$\eta = \eta_{\mathrm{translation}} + \eta_{\mathrm{collision}} \tag{II-5}$$

Where $\eta_{\mathrm{translation}}$ denotes a translational viscosity and $\eta_{\mathrm{collision}}$, a viscosity resulting from particle collisions.

Both contributions exist from low to high density and are influenced increasingly by intermolecular forces as density grows.

In the vicinity of a fluid critical point, the viscosity increases dramatically and becomes infinite at the critical point, even if this divergence is weak compared to other transport properties[65]. This phenomenon called "*critical enhancement*" (or "*viscosity enhancement*" sometimes) is induced by the large fluctuations in thermodynamic properties (and density in particular) in this region. For deriving models capable of evaluating the viscosity in the complete fluid region including the critical domain, one needs then to add a specific contribution (η_{cp}) accounting for critical fluctuations:

$$\eta = \eta_{\mathrm{translation}} + \eta_{\mathrm{collision}} + \eta_{\mathrm{cp}} \tag{II-6}$$

The previous approaches are well adapted to models stemming from molecular simulations which provide direct access to translational and collisional contributions to viscosity. When such information is not accessible, as for real fluids, viscosity models are usually based on a similar decomposition in which the translational viscosity is replaced by the zero-density viscosity (or dilute-gas) η_0, both quantities sharing common features at low density[64]. The zero-density limit of the viscosity depends on the temperature, only. In the absence of intramolecular forces, the expression for this function is generally derived from the kinetic theory of gases[66,67]. Thus, by using η_{res} as the residual viscosity defined as a complementary quantity to the total viscosity in non-critical regions[66–68], the total viscosity can be written:

$$\eta = \eta_0 + \eta_{\mathrm{res}} + \eta_{\mathrm{cp}} \tag{II-7}$$

Various methodologies exist to express the residual viscosity. While some authors used series expansion in density powers involving temperature-dependent coefficients (similarly to the virial equation),

$$\eta_{\mathrm{res}} = \eta_1(T) \cdot \rho + \eta_2(T) \cdot \rho^2 + \cdots \tag{II-8}$$

(where η_1 is the so-called "initial density" term), some others attempted to express the residual viscosity as a whole.

In the present study, although the approach considered is different from all the previous ones, a gas-like term and a liquid-like term were nevertheless introduced in the viscosity expression.

Because the critical enhancement is not taken into account, the models proposed here can be applied to the whole fluid domain except in the very close vicinity of the critical point. Limitations in terms of application domains will be discussed more precisely in the conclusion.

II-B-2) Review of the key advances in the modelling of shear viscosities from the entropy scaling concept:

Originally, Rosenfeld deduced the entropy scaling approach from a reasoning on dense systems, and hard spheres in particular[1]. As explained recently by Dyre, "*Rosenfeld's explanation of excess-entropy scaling was based on the fact that simple liquids have virtually the same physics as the hard-sphere system*"[69]. While for hard-sphere systems, "*the packing fraction determines quantities like the reduced diffusion constant, viscosity, and thermal conductivity*", Rosenfeld avoided the determination of the effective hard-sphere packing fraction "*by referring instead to the system's excess entropy, a purely thermodynamic quantity that for the hard-sphere system is in a one-to-one correspondence with the packing fraction. This is how excess-entropy scaling was arrived at*"[69]. As previously mentioned, note that *excess entropy* is called here *Tv-residual entropy*.

In his approach, Rosenfeld introduced macroscopically reduced (dimensionless) transport properties. Alternatively to a classical scaling which consists in forming the ratio of the property of interest over a constant having the same dimension, he used state-dependent variables to make the viscosity, the self-diffusion coefficient and the thermal conductivity dimensionless. These temperature- and density-dependent variables were issued from a dimensional analysis based on the kinetic theory of gases. In particular, in the case of viscosity:

- $\rho_{\mathrm{N}}^{-1/3}$ represents the mean intermolecular distance l (where ρ_{N} denotes the molecular density) and $\sqrt{\mathrm{k_b}T/\mathrm{m_0}}$, the mean thermal velocity v,
- The product $\mathrm{m_0}\rho_{\mathrm{N}}vl$ having the dimension of a viscosity, Rosenfeld defined a reduced viscosity as:

$$\begin{cases} \tilde{\eta} = \frac{\eta_{real}}{\eta_{ref}} \\ \eta_{\mathrm{ref}} = \rho_{\mathrm{N}}^{\frac{2}{3}}\sqrt{\mathrm{m_0 k_b}T} \end{cases} \qquad \text{(II-9)}$$

Note that the variable η_{ref} is called "reference viscosity" in the rest of the paper. Later, he proposed the following universal relationship for the viscosity of dense media[2]:

$$\tilde{\eta} \approx 0.2\, e^{0.8\, s}, \text{ with } s = -\tilde{s}_{\mathrm{Tv-res}} \text{ and } s \geq 1 \qquad \text{(II-10)}$$

In parallel, he showed the possibility to extend the method over the entire fluid region but highlighted a sensibly different behaviour at low densities[2,28]. Indeed, a steep increase of the reduced viscosity was observed with decreasing density in this region. Rosenfeld proposed to correlate the reduced viscosity of dilute gas and the Tv-residual entropy by using a power law dependence, inspired from Enskog's theory[10,40]:

$$\tilde{\eta} \approx 0.27\, s^{-\frac{2}{3}}, \quad \text{with: } s = -\tilde{s}_{\mathrm{Tv-res}} \tag{II-11}$$

With the aim to extend Rosenfeld's theory to dilute gases, Novak[34] proposed to replace the reference viscosity proposed by Rosenfeld by the one stemming from the Chapman-Enskog (CE) theory[6,10,70]. He used the following expression for η_{ref}.

$$\eta_{ref} = \eta_{CE} = \frac{5}{16}\frac{\sqrt{\mathrm{m_0 k_b} T}}{\sigma^2 \Omega^{(2,2)*}} \tag{II-12}$$

Where σ is the Lennard-Jones characteristic collision diameter and $\Omega^{(2,2)*}$ is the Lennard-Jones collision integral. Novak claimed that his reduction model "*was found to have the following advantages over the Rosenfeld model for correlating […] viscosity: (1) well-defined ideal-gas mathematical limit, (2) relatively simple dimensionless transport coefficient - dimensionless residual entropy component correlations over the entire fluid region, and not just the dense fluid region*"[34].

To be used, Eq. (II-12) requires the knowledge of molecular parameters (m and σ). Novak noted that "*the applicability of the component-based transport scaling approach is limited by the existence of component Lennard-Jones parameters*" and that "*the use of a spherical component LJ model becomes physically unrealistic for larger alkanes*". To circumvent these issues, he proposed to use a segment-based viscosity scaling combined to PC-SAFT segment parameters[33]. In a subsequent study, he replaced segments by entities[35] (where entities are smaller than segments) with the aim to derive a corresponding state-like model. He explained that "*The entity size, based on viscosity data, appears to more realistically represent n-alkane viscosities in the ideal gas state compared to the segment size*"[35,36]. Beyond this slight improvement of the entropy-scaling concept at low densities, Novak's work has opened the way to the derivation of predictive models for the viscosity of pure fluids[38,39] through the use of parameters that could be estimated from group-contribution methods.

Attempting to improve Rosenfeld's theory, Galliero[37] applied Rosenfeld's scaling method to the residual viscosity (i.e., the difference between the total viscosity and the low-density viscosity) and tried to correlate this reduced property to the reduced Tv-residual entropy. Although promising, the reduction shows as main drawback an undefined limit of the reduced viscosity at low density. Indeed, while the residual viscosity tends to zero when $\rho_{\mathrm{N}} \to 0$, Rosenfeld's reference viscosity tends to zero too ($\eta_{\mathrm{ref}} \to 0$) and their ratio shows an undefined limit at low density.

To fix the low-density divergence issue of this scaling method, Bell[40] proposed to multiply the reduced viscosity $\frac{\eta_{\mathrm{real}}}{\eta_{\mathrm{ref}}}$ by an empirical correction factor $(-\tilde{s}_{\mathrm{Tv-res}})^{2/3}$. He observed that this new quantity "[is] no longer a monovariate function of [the reduced entropy], but [has] a well characterized limit at zero density". Although having positive effects on Rosenfeld's method, a consequent dispersion of the data remains observed at low density (i.e., at low absolute values of the Tv-residual entropy). Bell[40,41] reduced this dispersion by subtracting the dilute-gas term to the real viscosity to form the reduced viscosity term: $\frac{\eta_{\mathrm{real}}-\eta_0}{\eta_{\mathrm{ref}}} \cdot (-\tilde{s}_{\mathrm{Tv-res}})^{2/3}$. Table II-1 summarizes the formalism of the various entropy-scaling versions presented above and highlights their advantages and limitations.

Table II-1: Overview of the main entropy-scaling models for viscosity discussed in section II-B-2. As entropy scaling (ES) is primarily based upon a graphical representation of a function of the viscosity (y-coordinate) with respect to a function of the Tv-residual entropy (x-coordinate), the corresponding functions are denoted Y_{ES} and X_{ES}.

Authors	X_{ES}	η_{ref}	Y_{ES}	Advantages	Limitations
Rosenfeld[1,28]	$\tilde{S}_{\mathrm{Tv-res}}$	$\rho_{\mathrm{N}}^{2/3}\sqrt{\mathrm{m_0 k_b} T}$	$\ln\left(\frac{\eta_{real}}{\eta_{ref}}\right)$	Simplicity and broad applicability (quasi-universality)	divergence of the reduced viscosity at low density
Galliero et al.[37]	$\tilde{S}_{\mathrm{Tv-res}}$	$\rho_{N}^{2/3}\sqrt{\mathrm{m_0 k_b} T}$	$\ln\left(\frac{\eta_{res}}{\eta_{ref}}\right) = \ln\left(\frac{\eta_{real}-\eta_0}{\eta_{ref}}\right)$	Gain of linearity	- Necessity of a reliable estimation of η_0 - divergence of the reduced viscosity at low density
Novak[33]	$\frac{\tilde{S}_{\mathrm{Tv-res}}}{\mathrm{m}}$ (m denotes the chain length = the segment number)	$(\eta_{\mathrm{seg}})_{\mathrm{CE}} = \frac{5}{16}\frac{\sqrt{\mathrm{m_{0,seg}k_b}T}}{\sigma_{\mathrm{seg}}^2\Omega^{(2,2)*}}$ Where CE means "Chapman-Enskog"	$\ln\left[\frac{\eta_{real}}{m\times(\eta_{seg})_{CE}}\right]$	- Improved low-density limit - introduction of molecular parameters (collision diameter) made available through the use of a molecular EoS (PC-SAFT)	Dispersion is observed at low density
Bell et al.[40,41]	$\tilde{S}_{Tv-res}$	$\rho_{\mathrm{N}}^{2/3}\sqrt{\mathrm{m_0 k_b} T}$	$\ln\left[\frac{\eta_{\mathrm{real}}}{\eta_{\mathrm{ref}}}\times(-\tilde{S}_{\mathrm{Tv-res}})^{\frac{2}{3}}\right]$ Or $\ln\left[\frac{\eta_{\mathrm{res}}}{\eta_{\mathrm{ref}}}\times(-\tilde{S}_{\mathrm{Tv-res}})^{\frac{2}{3}}\right]$	- Simplicity and broad applicability - Improved low-density limit	- Introduction of an empirical correction to define Y_{ES} - Dispersion at low density (reduced when switching from η_{real} to η_{res} in variable Y_{ES})

To compare the performances of the approaches mentioned in Table II-1 on a fair basis, results obtained from each of them are represented in Figure II-2 for 4 different substances (argon, nitrogen, water, n-hexane). Note that in the approaches by Galliero et al.[37] and Bell et al.[40,41] (where residual viscosity is used instead of total viscosity in the definition of quantity Y_{ES}):

- Tv-residual viscosities may exhibit negative values because of the initial density dependence of viscosity that could be negative[71]; when such a case arises, data cannot be plotted in semi log coordinates and are thus disregarded. Note that Bell identified this problem and in return, proposed to add an offset value of 1 to the reduced viscosity "to ensure that the data can still be plotted in semi log coordinates"[41,72].
- The Chapman-Enskog relation (see Eq. (II-12)) was used for the estimation of the dilute-gas viscosity (η_0) used to estimate residual viscosity from total viscosity.
- More fundamentally, these approaches postulate that only the residual reduced viscosity $\frac{\eta_{\mathrm{real}}-\eta_0}{\eta_{\mathrm{ref}}}$ (or equivalent quantity) depends on $\tilde{s}_{\mathrm{Tv-res}}$ while other approaches assume that the total reduced viscosity $\frac{\eta_{\mathrm{real}}}{\eta_{\mathrm{ref}}}$ can be related to $\tilde{s}_{\mathrm{Tv-res}}$. It is shown in this article that it is possible to describe the total reduced viscosity (including the dilute-gas term) as a function of $\tilde{s}_{\mathrm{Tv-res}}$. As a pragmatic advantage, the correlation of the total viscosity (instead of the residual property) enables to avoid the use of a dilute-gas viscosity correlation to apply the viscosity model.

For Novak's approach, Neufeld's empirical relation[73] was used for the estimation of collision integrals while collision diameters σ and attraction energies ε were obtained from reference [74].

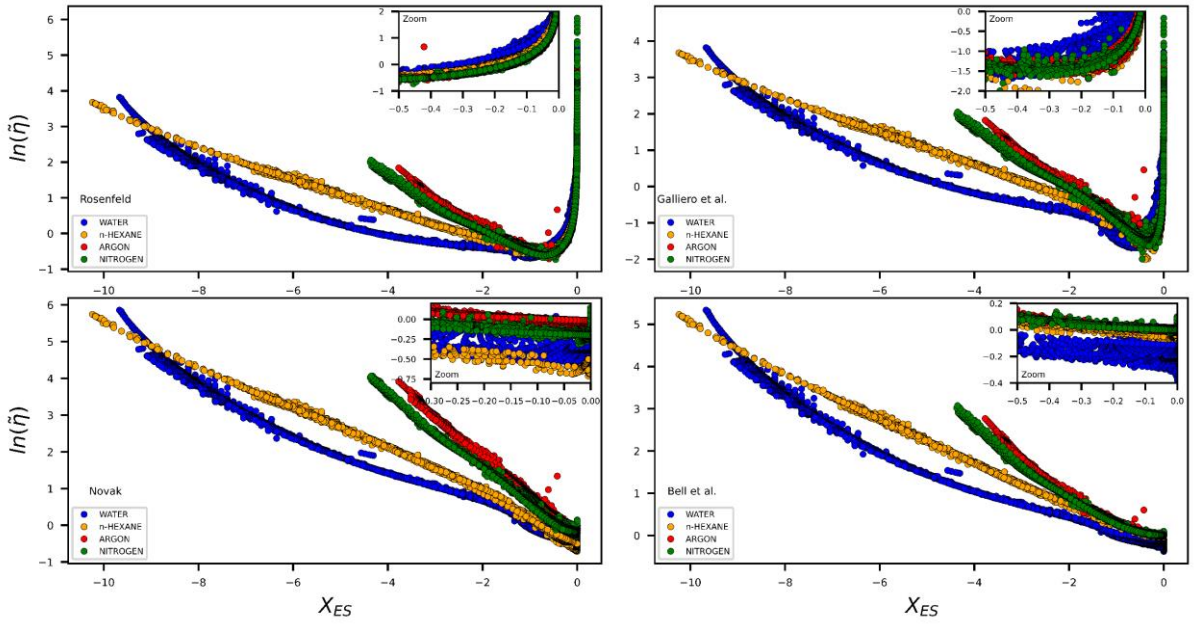

Figure II-2 – Illustration of results obtained from the methods listed in table 1 for 4 compounds: argon, nitrogen, n-hexane and water. Properties X_{ES} and Y_{ES} are the ones defined in Table 1 for each approach. Circles: gas data, squares: liquid data, diamonds: supercritical data (source: Dortmund Data Bank; the data selection procedure is described in section II-C).

As illustrated in Figure II-2, a diverging behaviour of the reduced viscosity in the low-density region (i.e., for $\tilde{s}_{\mathrm{Tv-res}} \to 0$) is systematically observed but varies in magnitude depending on the approach considered. In that regard, the best versions are the ones by Novak and Bell et al.

In addition, while viscosity data seem to align along component-specific curves regardless of the chosen approach, a scatter of deviation is always observed at low density.

Regarding the linearity of the curves, it can be noticed that:

- All models predict a quasi-linear behaviour in dense fluid regions for argon, nitrogen and n-hexane but not for water,
- Water curves are all characterized by the presence of convex and concave parts and thus, seem to exhibit an irregular behaviour with respect to other compounds, in accordance with previous observations: Chopra et al. noticed that the departure from linear law using Rosenfeld scaling "is particularly noticeable in the case of water"[58] while Dyre explained that "water exhibits a multitude of anomalies" and "does not obey excess-entropy scaling"[69].

II-B-3) A new formulation of the entropy-scaling approach for viscosity estimation

According to the previous section, it can be observed that literature models were developed with the aim of increasing the domain of linearity, in particular from the dense to the low-to-moderate regions. To do so, new reduction methods were proposed. Unfortunately, although improvements were obtained with respect to Rosenfeld's proposal, the modelling of the viscosity in the low-density region remained an issue. In addition, it can be said that some of these modifications are made at the expense of the predictability of model parameters. In light of these observations, a new formulation of the entropy-scaling approach for viscosity should:

- Ensure, for a given species, a continuous representation of the reduced viscosity along a single and well-defined curve, over the entire fluid domain (in the gas, liquid and supercritical regions), with special attention paid to the low-density region,
- Be applicable to the largest set of substances (from monoatomic to chain molecules, from non-associating to associating species),
- Rely on a mathematical formulation independent of the EoS used to generate density or entropy values.

II-B-3.1) Step1: new scaling for the Tv-residual entropy variable

The reduced Tv-residual entropy $\tilde{s}_{\mathrm{Tv-res}}$ is not a measurable quantity. EoS are able to estimate this property at any temperature and pressure. Selecting the best EoS among the multiplicity of existing models remains a key issue for developing an entropy-scaling based method. In order to illustrate the qualitative and quantitative differences in terms of residual entropy predictions from one model to another, Figure II-3 compares the reduced residual entropy of Argon calculated from two EoS, i.e., the *tc*-PR EoS[53,75] and the reference model by

Tegeler et al.[76] (present in NIST-REFPROP[77] software), to the reduced residual entropy calculated from the *I*-PC-SAFT EoS[48]. As a first insight, the multiparameter Tegeler EoS could be considered potentially as an accurate model from which pseudo-experimental data could be generated and was considered for this reason. To generate Figure II-3, a high number of (temperature, pressure) sets taken in the subcritical liquid, subcritical gas and supercritical regions were selected and for each of them, reduced residual entropy data were calculated for the three EoS considered (*tc*-PR, *I*-PC-SAFT and Tegeler). Figure II-3 shows that the *I*-PC-SAFT and Tegeler EoS exhibit a rather similar behaviour while significant deviations appear between the cubic *tc*-PR EoS and the 2 remaining EoS (note however that at low density, important differences between predictions from EoS present in the NIST-REFPROP software on one side and *tc*-PR and *I*-PC-SAFT EoS predictions on the other side were observed; see section III-A-4).

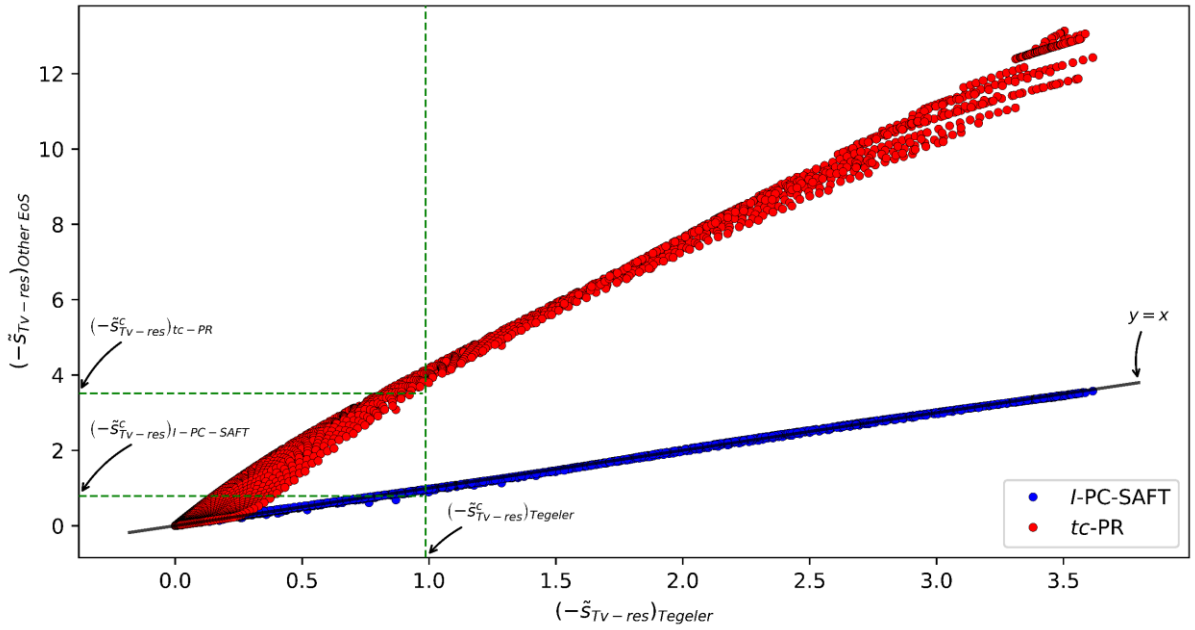

Figure II-3 – Comparison between reduced Tv-residual entropy values of Argon ($\tilde{s}_{\mathrm{Tv-res}} = s_{\mathrm{Tv-res}}/R$) estimated from the *tc*-PR, Tegeler and *I*-PC-SAFT EoS.

While this study is aimed at proposing a scaling method applicable to any EoS, this difference of behaviour appears as an important obstacle to achieving this goal. In order to limit the effect of the EoS choice on the prediction of entropy (and recalling that it is hard, if not impossible, to benchmark EoS according to their capacity to reproduce residual entropies), it is proposed to explore an alternative way by identifying a dimensionless function of the entropy which is (nearly) independent of the considered EoS. In other words, the solution lies probably in the way the entropy-related property is reduced.

In a number of entropy-scaling applications using SAFT-type EoS for density and entropy estimation, authors used as reduced entropy variable the ratio of the residual entropy and the number of molecular segments[30,32–34,38,39] enabling to obtain a similar range of variation of the entropy variable, regardless of the compound. Similarly, in a recent study[45], authors introduced a component-specific adjustable parameter in the denominator of the reduced-entropy variable

to get a universal behaviour of refrigerant viscosities in the dense-fluid region. Although these reduction techniques are inspiring, the properties these authors used to reduce the residual entropy were not kept as (1) they cannot be applied in a systematic way to any species and (2), parameters specific to SAFT models are not well suited to cubic EoS.

In this study, following Van der Waals' idea for reducing EoS variables when he proposed the corresponding-states theorem, it has been decided to scale the residual entropy using the corresponding critical value (denoted $s^{c}_{\mathrm{Tv-res}}$):

$$X_{\text{step 1}} = -\left(\frac{s_{\mathrm{Tv-res}}}{s^{c}_{\mathrm{Tv-res}}}\right) = -\left(\frac{\tilde{s}_{\mathrm{Tv-res}}}{\tilde{s}^{c}_{\mathrm{Tv-res}}}\right) \tag{II-13}$$

As illustrated in Figure II-4(a), doing so makes it possible to reduce dramatically the difference between quantitative predictions of Tv-residual entropy from one model to another (see Figure II-4(a)). This is thus a step forward in the search for an EoS-independent formulation of the entropy-scaling concept. It was observed indeed that this reduction entails the standardization of the reduced-entropy range for most of the compounds (whatever the species being, the liquid and gas-phase regions are found in similar reduced-entropy ranges, respectively). To summarize, considering $\frac{s_{\mathrm{Tv-res}}}{s^{c}_{\mathrm{Tv-res}}}$ instead of $s_{\mathrm{Tv-res}}$ as entropy variable in the entropy-scaling concept provides 2 important advantages: it reduces (i) the sensitivity of the entropy variable to the selected EoS and (ii) the sensitivity of the entropy variable to the considered species. We consider this result as an important basis for the formulation of a revised entropy scaling.

Figure II-4(b) shows that the application of the entropy-scaling concept with entropy variable X_{ES} produces curves that are comparable to the ones obtained using classical Rosenfeld's reduction technique (see Figure II-2). At this step, a vertical asymptote persists at low density; to address this issue, a second modification of the Tv-residual entropy variable is now proposed.

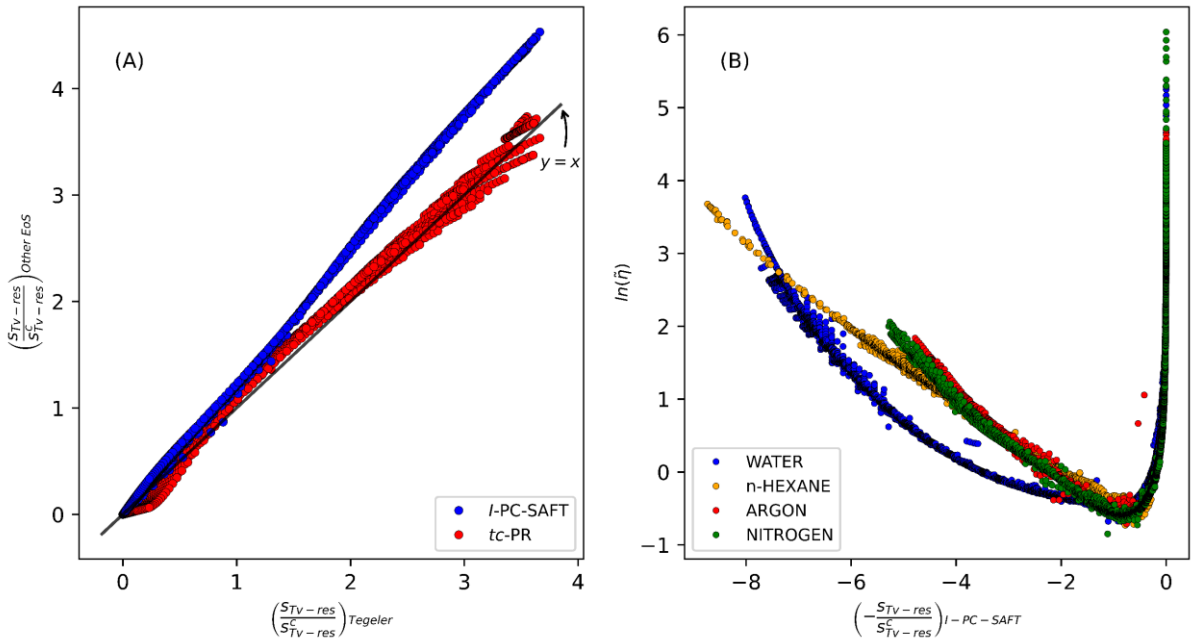

Figure II-4 – (a) Comparison between reduced Tv-residual entropy values ($s_{\mathrm{Tv-res}}/s^{c}_{\mathrm{Tv-res}}$) estimated from the *tc*-PR, Tegeler and *I*-PC-SAFT EoS for Argon. (b) Application of the entropy scaling concept using $s_{\mathrm{Tv-res}}/s^{c}_{\mathrm{Tv-res}}$ as reduced entropy variable.

II-B-3.2) Step 2: second modification of the entropy variable to fix the low-density divergence issue

The exponential form of the relation between reduced viscosity and reduced entropy, postulated by Rosenfeld to describe dense fluids (see Eq. (II-10)) is purely empirical [1,28] and cannot be extrapolated to the low-density domain (see Figure II-1). For dilute gases, Rosenfeld used a power-law dependence[28] derived from Enskog's theory[10] (see Eq. (II-11)). Therefore, at low density, the X-coordinate is the logarithm of the reduced residual entropy while at high density, it is the reduced residual entropy itself. This variety of scaling laws depending on the considered density domain is an obstacle to the description of the whole fluid domain from a unique approach. To combine both scales (i.e., the low-density and dense regions), it is proposed to gather the quantity $\frac{s_{\mathrm{Tv-res}}}{s^{c}_{\mathrm{Tv-res}}}$ and its logarithm in the same expression. Doing so, the entropy variable definition proposed in this work is:

$$X_{ES} = -\left(\frac{s_{\mathrm{Tv-res}}}{s^{c}_{\mathrm{Tv-res}}}\right) - \ln\left(\frac{s_{\mathrm{Tv-res}}}{s^{c}_{\mathrm{Tv-res}}}\right) = -\left(\frac{\tilde{s}_{\mathrm{Tv-res}}}{\tilde{s}^{c}_{\mathrm{Tv-res}}}\right) - \ln\left(\frac{\tilde{s}_{\mathrm{Tv-res}}}{\tilde{s}^{c}_{\mathrm{Tv-res}}}\right) \qquad \text{(II-14)}$$

In Eq. (II-14), the term $-\left(\frac{s_{\mathrm{Tv-res}}}{s^{c}_{\mathrm{Tv-res}}}\right)$ dominates at high density while $-\ln\left(\frac{s_{\mathrm{Tv-res}}}{s^{c}_{\mathrm{Tv-res}}}\right)$ is preponderant in dilute-gas conditions. Eventually, the revisited version of Rosenfeld's entropy scaling concept becomes:

$$\ln(\tilde{\eta}) = \ln\left(\frac{\eta_{\text{real}}}{\eta_{\text{ref}}}\right) = f(X_{\text{ES}}) \tag{II-15}$$

Figure II-5 illustrates the application of the entropy-scaling approach defined by Eqs. (II-14) and (II-15) using the same experimental data as the ones reported in Figure II-2. As expected, a straight line is obtained in dilute-gas conditions ($X_{\text{ES}} > 0$). Remarkably, the assumption of quasi-universality postulated by Rosenfeld for dense fluids is actually more robust at low densities using this new formulation of entropy scaling.

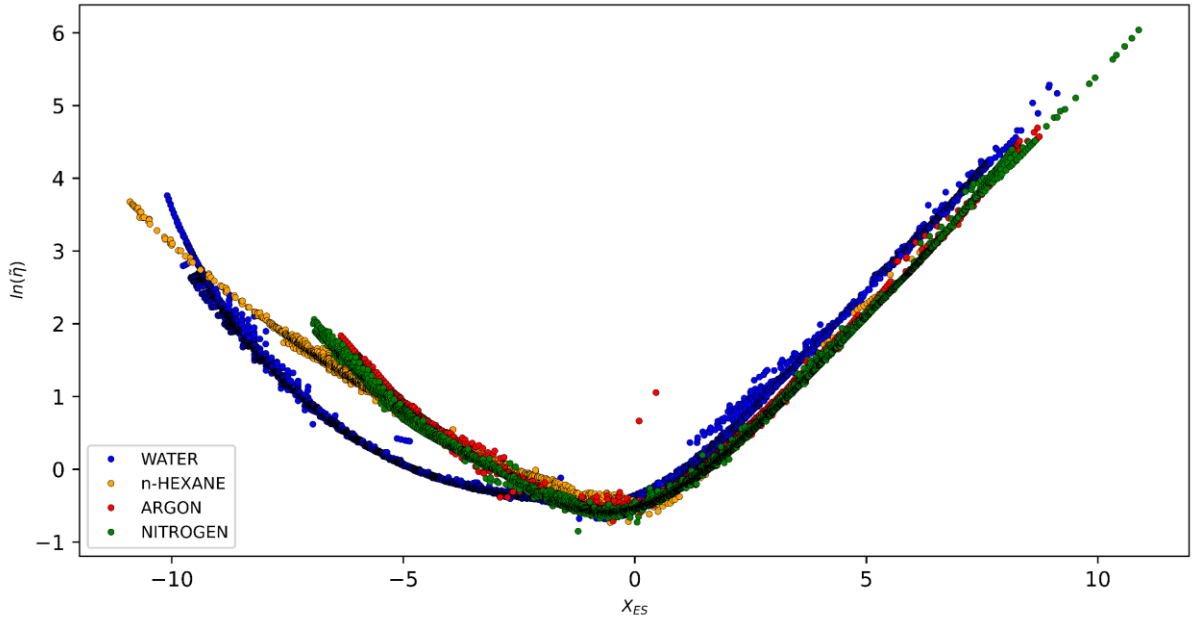

Figure II-5 – Application of the new entropy scaling for viscosity proposed in this study (see Eqs. (II-14) and (II-15)) to argon, nitrogen, n-hexane and water. Symbols: circle = gas state, square = liquid state, diamond = supercritical state.

As can be observed from Figure II-5, the second modification of the entropy variable induces the appearance of a perfectly-defined oblique asymptote in the $\ln(\tilde{\eta})$ versus X_{ES} graph at the low-density limit (i.e., for positive X_{ES} values). As discussed later, the entropy-scaling version proposed here highlights a quasi-universal behaviour in the dilute-gas region that could be substituted to any dilute-gas model of the literature. In section III-A-2 of the Supporting Information file, proof is given that this simple behaviour could be expected.

As a final remark, noticing that anomalies arose in the $\ln(\tilde{\eta})$ versus X_{ES} plane when applying the proposed entropy scaling version to light fluids modelled with the *tc*-PR EoS and undergoing high temperature conditions, it was decided to slightly modify the X_{ES} definition by adding a correction term that becomes non-negligible far from the critical point:

$$\begin{cases} X_{\text{ES}}^{\text{corrected}} = -\left(\frac{s_{\text{Tv-res}}}{s^{\text{c}}_{\text{Tv-res}}}\right) - \ln\left(\frac{s_{\text{Tv-res}}}{s^{\text{c}}_{\text{Tv-res}}} \times f_{\text{corr}}(T)\right) \\ f_{\text{corr}}(T) = 1 + \alpha\left(\frac{T - T_c}{T_c}\right)^3 \end{cases} \tag{II-16}$$

Such a modification is a *tc*-PR specific patch that makes it possible to delay the appearance of the undesirable phenomenon. More details about this last modification are provided in Appendix II-A.

II-B-3.3) Selection of a reference viscosity and discussion around the construction of the reduced viscosity variable

On the selection of a reference viscosity term. As previously mentioned, entropy scaling is a semi-theoretical concept that fixes neither the expression of the entropy variable, nor the viscosity function. That said, one should mention nevertheless that the isomorph theory is a general framework from which the entropy scaling concept can be derived and discussed[69]. According to Dyre, *Isomorph theory provides insights into why excess-entropy scaling may apply also for molecular systems quite different from the quasi-universal simple point-particle liquids traditionally studied in liquid-state theory. [...] if the phase diagram has lines of the invariant structure and dynamics, these lines must be the configurational adiabats, i.e., excess-entropy scaling must apply*"[69]". In a subsequent paper, Bell, Dyre et al.[40] mention that "*for the 'ordinary' condensed liquid phase […] the isomorph theory explains entropy scaling […] Excess-entropy scaling is a consequence of 'hidden scale invariance' [….] Hidden scale invariance applies to a good approximation for the condensed liquid phase […] of most or all metals and van der Waals bonded systems, whereas it is not expected to work for […] hydrogen-bonded or covalently bonded systems*". As an important argument for the selection of a proper reference-viscosity, "*hidden scale invariance and the isomorph theory refer to so-called reduced quantities, which are defined by reference to the following unit system:* $e = \mathrm{k_b}T$" (energy unit), "$l = \rho_{\mathrm{N}}^{-1/3}$" (length unit) and "$t = \rho_{\mathrm{N}}^{-1/3}\sqrt{\mathrm{m_0}/\mathrm{k_b}T}$" (time unit)[78,79]. It appears that the isomorph theory, that can be seen as a partial justification of the entropy scaling concept, leads exactly to the state-point dependent macroscopic units used by Rosenfeld and thus, to the same expression of the reference viscosity. Though the aforementioned theories are imperfect ("*It must be emphasized that not all observations in this intriguing field of research are explained by the isomorph theory*"[69]), their capacity to partially support some entropy-scaling successes led us to select the same reference viscosity as Rosenfeld.

From a pragmatic viewpoint, Novak's formulation (see Table II-1) could have been used for expressing the viscosity reference term. However, this option was not retained for the following reasons:

- Contrary to the reduction proposed by Novak, Rosenfeld's definition of η_{ref} introduces a density dependent intermolecular distance. It has been observed that using a density dependence of the reference viscosity is essential to describe moderately-dense fluids; working on dense fluids that exhibit nearly constant density does not allow to highlight this necessary dependence.

- According to our personal observations and in relation with the previous comment, Novak's reduction is efficient for dense fluids but not fully satisfactory to model moderate- to low-density fluids.

On the construction of the reduced viscosity variable. Once a reference viscosity was selected, different options could be considered to form the reduced viscosity variable. As a first possibility, a residual viscosity $\eta_{\mathrm{real}} - \eta_0$ term could be used in the numerator of the ratio defining this variable. Implicitly, this choice would presuppose that the entropy scaling concept does not apply efficiently in the dilute-gas region. The use of a viscosity model built in this way would thus require the prior knowledge of a viscosity model for dilute gases. Following our observations (see Figure II-5) and according to the results shown subsequently, the dilute-gas region can be kept and therefore, instead of a residual viscosity, a total viscosity was considered.

As another option, a factor $(\tilde{s}_{\mathrm{Tv-res}})^{\frac{2}{3}}$ could be introduced as proposed by Bell[41,72]. As mentioned above, this option is of clear interest to avoid divergence at low density when using Rosenfeld scaling. In the present case, we solved this issue by modifying the entropy variable of the entropy scaling. Applying this factor was thus unnecessary and the reduced viscosity variable considered here was strictly the same as the one Rosenfeld considered, i.e.:

$$Y_{\mathrm{ES}} = \ln(\tilde{\eta}) = \ln\left[\eta_{\mathrm{real}} / \left(\rho_{\mathrm{N}}^{\frac{2}{3}}\sqrt{m_0 \mathrm{k_b} T}\right)\right] \qquad \text{(II-17)}$$

II-B-3.4) Graphical interpretation of the entropy-scaling formulation proposed in this study and identification of matter states in the $(Y_{\mathrm{ES}}, X_{\mathrm{ES}})$ plane

Through the example of pure methane modelled with the *I*-PC-SAFT EoS, Figure II-6 shows characteristic vapor-liquid saturation curves as well as series of liquid, subcritical and supercritical gas branches of various isotherms. These curves are represented in the $(P_{\mathrm{r}}, Y_{\mathrm{ES}}, X_{\mathrm{ES}})$ space (see panel A) - where $P_{\mathrm{r}} = P/P_{\mathrm{c}}$ denotes the reduced pressure, in the $(P_{\mathrm{r}}, X_{\mathrm{ES}})$ plane (see panel B) and in the $(Y_{\mathrm{ES}}, X_{\mathrm{ES}},)$ plane (see panel C). Definitions of variables X_{ES} and Y_{ES} are provided by Eqs. (II-14) and (II-17). Remarkably and in accordance with the entropy-scaling concept, liquid and gas-like states align along a single curve when working in the $(Y_{\mathrm{ES}}, X_{\mathrm{ES}},)$ plane. In particular, note that according to Eq. (II-14), the critical point is obtained for: $X_{\mathrm{ES}}^{\mathrm{c}} = -1 - \ln(1) = -1$. Liquid states are all found for $X_{\mathrm{ES}} \leq -1$ while subcritical gas states are found at $X_{\mathrm{ES}} \geq -1$. Supercritical gases may be found at any value of X_{ES}.

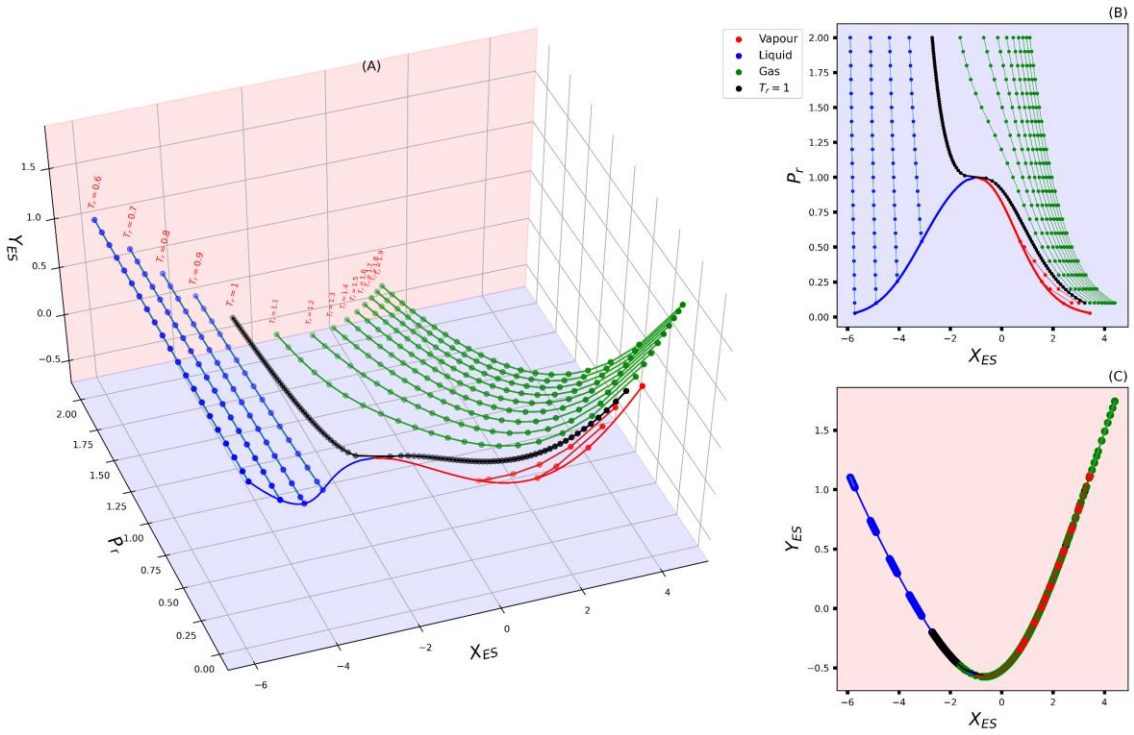

Figure II-6 – Illustration of the entropy-scaling formulation proposed here through the representation of isotherms and saturation curves of pure methane. Reduced temperatures of isotherms range from 0.6 to 1.9 while reduced pressures range from 0.1 to 2. Panel (A): representation in the (P_r, Y_{ES}, X_{ES}) space. Panel (B): representation in the (P_r, X_{ES}) plane. Panel (C): representation in the (Y_{ES}, X_{ES}) plane.

II-B-4) Final functional form proposed for the entropy-scaling law

The modified entropy-scaling approach defined by Equations (II-3), (II-14), (II- 15), and (II-16), for light molecules modelled with the *tc*-PR EoS) leads to component specific curves in the $\ln(\tilde{\eta})$ versus X_{ES} plane sharing all a series of common features and in particular, the same V shape. In addition, all curves exhibit:

- A nearly universal common minimum located at $X_{ES} \approx 0$ (a deeper discussion is proposed thereafter),
- A quasi-universal behaviour for positive values of X_{ES} characterizing dilute gases subcritical gases and several supercritical fluids as well,
- Almost superimposed curves at dense states (as discussed later, a more detailed look at component-specific curves highlights their great similarity when all molecules stem from the same chemical family).

The functional form selected here is given by Eq. (II-18). It is expected to have the capacity to exhibit a minimum and to reproduce the behaviour of the liquid- and gas-like branches framing this minimum.

$$\ln\left(\frac{\eta}{\eta_{\mathrm{ref}}}\right)_{\mathrm{calc}} = f_{\mathrm{dense}}(\tilde{s}_{\mathrm{Tv-res}}) \times g_{\mathrm{dense}} + f_{\mathrm{gas}}(\tilde{s}_{\mathrm{Tv-res}}) \times g_{\mathrm{gas}} + k \qquad \text{(II-18)}$$

Where f_{dense} and f_{gas} are functions describing the dense-state behaviour ($X_{\mathrm{ES}} < 0$; by "dense", it is meant subcritical liquid and supercritical fluids) and gas-state behaviour ($X_{\mathrm{ES}} > 0$; by "gas", it is meant subcritical gas and supercritical fluids), respectively; g_{dense} and g_{gas} are damping factors making f_{dense} dominating in the dense region, and conversely, f_{gas} dominating in the gas region; k is a component-specific constant. The following expressions are proposed for these quantities:

$$\begin{cases} f_{\mathrm{dense}}(\tilde{s}_{\mathrm{Tv-res}}) = (a_1 + a_2\tilde{s}_{\mathrm{Tv-res}})X_{\mathrm{ES}} \\ f_{\mathrm{gas}}(\tilde{s}_{\mathrm{Tv-res}}) = (b_1 + b_2\tilde{s}_{\mathrm{Tv-res}})X_{\mathrm{ES}} \\ g_{\mathrm{dense}} = \frac{1}{1+e^{cX_{\mathrm{ES}}}} \\ g_{\mathrm{gas}} = \frac{1}{1+e^{-cX_{\mathrm{ES}}}} \\ k = \frac{d}{\tilde{s}^{\mathrm{c}}_{\mathrm{Tv-res}}} \end{cases} \qquad \text{(II-19)}$$

In Eq. (II-19), (a_1,a_2), (b_1,b_2), c and k are 6 adjustable parameters that can be chosen either component-specific or chemical-family specific. The final functional form proposed in this article is thus:

$$\begin{cases} \ln\left(\frac{\eta}{\eta_{\mathrm{ref}}}\right)_{\mathrm{calc}} = \left[\left(\frac{a_1+a_2\tilde{s}_{\mathrm{Tv-res}}}{1+e^{cX_{\mathrm{ES}}}}\right) + \left(\frac{b_1+b_2\tilde{s}_{\mathrm{Tv-res}}}{1+e^{-cX_{\mathrm{ES}}}}\right)\right]X_{\mathrm{ES}} + \frac{d}{\tilde{s}^{\mathrm{c}}_{\mathrm{Tv-res}}} \\ \text{with: } \eta_{\mathrm{ref}} = \rho_{\mathrm{N}}^{2/3}\sqrt{\mathrm{m_0 k_b} T} \\ X_{\mathrm{ES}} = -\left(\frac{s_{\mathrm{Tv-res}}}{s^{\mathrm{c}}_{\mathrm{Tv-res}}}\right) - \ln\left(\frac{s_{\mathrm{Tv-res}}}{s^{\mathrm{c}}_{\mathrm{Tv-res}}}\right) \text{ for the } \textit{I}\text{-PC-SAFT EoS} \\ X_{\mathrm{ES}} = -\left(\frac{s_{\mathrm{Tv-res}}}{s^{\mathrm{c}}_{\mathrm{Tv-res}}}\right) - \ln\left(\frac{s_{\mathrm{Tv-res}}}{s^{\mathrm{c}}_{\mathrm{Tv-res}}}\left[1 + \alpha\left(\frac{T-T_{\mathrm{c}}}{T_{\mathrm{c}}}\right)^3\right]\right) \text{ for the } \textit{tc}\text{-PR EoS} \end{cases} \qquad \text{(II-20)}$$

The α coefficient is an optional component-specific parameter to be used with the *tc*-PR EoS only and with light components. It enables to improve viscosity predictions for $4 < T_r < 8$.

At a first view, Eq. (II-20) may appear surprising since it involves not only the entropy-scaling variable X_{ES} presented and discussed above but also the $\tilde{s}_{\mathrm{Tv-res}}$and $\tilde{s}^{\mathrm{c}}_{\mathrm{Tv-res}}$ variables, independently of X_{ES}. Although the simultaneous involvement of X_{ES}, $\tilde{s}_{\mathrm{Tv-res}}$ and $\tilde{s}^{\mathrm{c}}_{\mathrm{Tv-res}}$ in the functional form does not change the spirit of the approach, it must be noted that this expression was deduced from an empirical trial and error procedure in order to better correlate experimental viscosities when chemical-family specific or universal parameters are used. As a noticeable feature, this expression leads to component-specific curves in the $\ln\left(\frac{\eta}{\eta_{\mathrm{ref}}}\right)$ versus

X_{ES}, even if chemical-family specific or universal parameters are used (thanks to the introduction of $\tilde{s}_{\mathrm{Tv-res}}$ and $\tilde{s}^{\mathrm{c}}_{\mathrm{Tv-res}}$).

Before closing this section, let us address a specific phenomenon recently identified in the dense-state region: as can be observed on some curves shown in Figure II-5, the logarithm of the reduced viscosity does not change linearly with negative values of X_{ES} but exhibits both linear and convex behaviours. At this step, it is mentioned that following the definition of X_{ES} (see Eq. (II-20)), $X_{\mathrm{ES}} \approx \frac{s_{\mathrm{Tv-res}}}{s^{\mathrm{c}}_{\mathrm{Tv-res}}}$ for $X_{\mathrm{ES}} \ll 0$ (X_{ES} is thus proportional to the $s_{\mathrm{Tv-res}}$ property). This behaviour was recently justified by Bell[41] as the existence of a transition point, approximately located at $\tilde{s}_{\mathrm{Tv-res}} = \left(\frac{\tilde{s}^{\mathrm{critical}}_{\mathrm{Tv-res}} + \tilde{s}^{\mathrm{triple}}_{\mathrm{Tv-res}}}{2}\right)$, where the dynamic regime changes and where the reduced viscosity increases much faster than the exponential of absolute $s_{\mathrm{Tv-res}}$. However, if this hypothesis is convenient to propose an adapted scaling law for dense states, it is still under debate since the transition point was only highlighted for a few molecules and its location seems to be component-dependent (according to our observations). In addition, it could be thought that this irregular behaviour could result from a decreasing accuracy of EoS in this region. Eventually, it was decided not to take this phenomenon into account specifically in the functional form of the entropy-scaling law. Nevertheless, Eq. (II-20) is flexible enough to reproduce convex behaviors in the dense region.

II-C) Results and discussion:

To determine the 3 sets of parameters (component-specific, chemical-family specific and universal) for the two entropy-scaling models proposed here (i.e., combination of Eq. (II-20) with the *tc*-PR and *I*-PC-SAFT EoS), a large database of experimental shear viscosity data was built. All the data were extracted from the commercial Dortmund Data Bank (DDB: http://www.ddbst.com). Our database contained liquid, subcritical and supercritical gas data, involves 142 pure compounds spanning 14 different chemical families (including alkanes, alcohols, amines, esters, ethers, refrigerants …) and more than 100 000 data points. Temperatures covered the range [14 K , 2150 K], pressures were within [10^{-3} MPa ; 10^{2} MPa] while dynamic viscosities spread from $7.4 \cdot 10^{-7}$ Pa · s to $0.47 \cdot$ Pa · s). All the data are reported in Figure II-7, in the ($\ln \tilde{\eta}$, X_{ES}) plane, which highlights the existence of V-shape curves for any compound, as expected. A detailed description of experimental data is provided in section III. Note that some experimental data points were removed from the database after application of the following filters:

- Data associated with pressures out of the range [10^{-3} MPa ; 10^{2} MPa] were considered as potentially inaccurate and disregarded,
- Because the present model does not account for *viscosity enhancement*, data in the close critical region ($0.95 < T_{\mathrm{r}} < 1.05$ and $0.95 < P_{\mathrm{r}} < 1.05$) were removed. In addition, data such that $T_{\mathrm{r}} > 8$ were removed when using the *tc*-PR EoS, deemed as non-capable of modelling these data.

- To eliminate out-of-chart data, the absolute deviation $\Delta Y^i = |Y^i_{\text{calc}} - Y^i_{\text{exp}}|$ was calculated for each data and compared to the average deviation $\overline{\Delta Y}$ estimated for the species under consideration. If it was decided to disregard data such that: $\Delta Y^i > \overline{\Delta Y} + 3\sigma$ (where σ denotes the standard deviation). As a double check, it was verified graphically that each datum eliminated by the test was deviating strongly from the general trend and could be considered as an outlier.

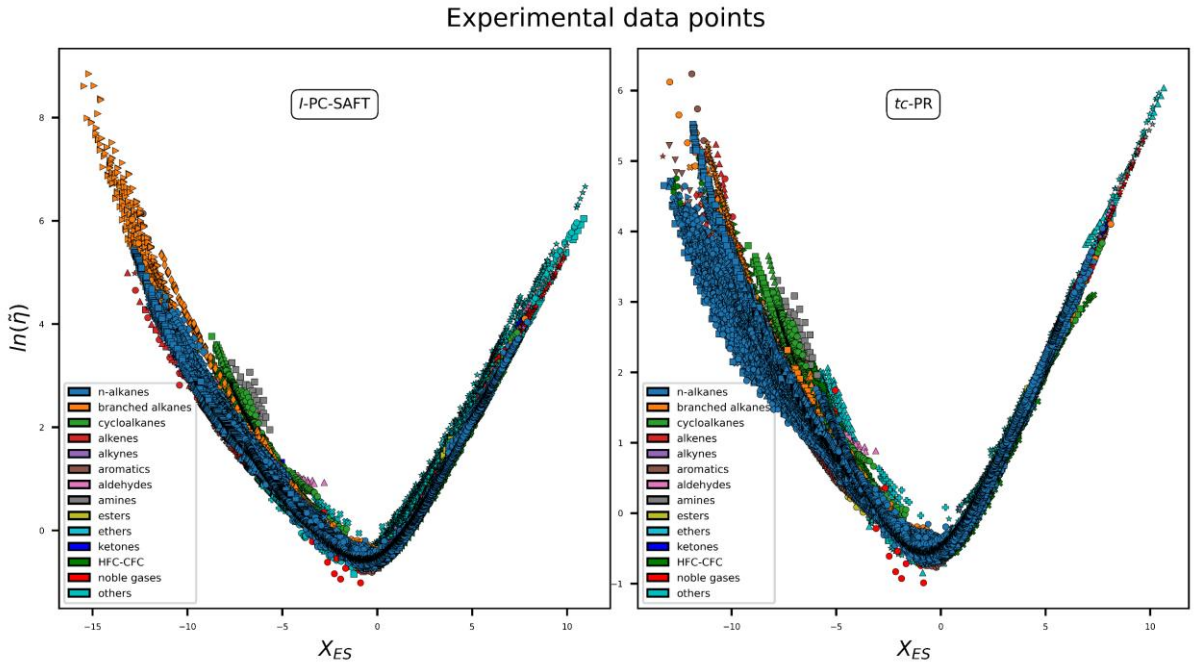

Figure II-7 - Overview of all experimental data in the $ln(\tilde{\eta})$ *versus* X_{ES} plane. Thermodynamic properties involved in the definition of $\tilde{\eta}$ and X_{ES} were estimated using the *I*-PC-SAFT EoS (left panel) and the *tc*-PR EoS (right panel). Each color corresponds to a chemical family and each symbol to specific compound.

To determine the values of the 6 parameters defined in Equation (II-20) (a_1, a_2, b_1, b_2, c and d) as well as the α coefficient when necessary (i.e., for light molecules modelled with the *tc*-PR EoS), the following objective function $\Delta\eta$ was minimized with respect to the 6 (or 7, with α) coefficients:

$$\Delta\eta = \frac{100}{Nb_{data}} \sum_{i=1}^{Nb_{data}} \frac{|\eta_{\text{calc},i} - \eta_{\text{exp},i}|}{\eta_{\text{exp},i}} \qquad \text{(II-21)}$$

Where Nb_{data} denotes the total number of experimental data considered.

Note that for some compounds, viscosity data did not allow to describe both the dense part (left side of the V-shape curve) and the gas part (right side of the V-shape curve) but only one of them. In such cases, component-specific parameters (a_1, a_2, b_1, b_2, c and d) could not be determined accurately and were replaced by chemical-family specific and universal parameters.

The minimization of Equation (II-21) was performed using the Broyden-Fletcher-Goldfarb-Shanno (BFGS) algorithm, a quasi-Newton optimization method. To ensure the robustness of the optimized parameter sets by avoiding dependence on initial estimates and convergence to local minima, multiple initialization sets were systematically generated using a random process for each compound. Parameter bounds generally used as constraints of the optimization routine are reported in Table II-2.

Table II-2 – Parameter bounds used in the optimization routine

Coefficient	Min. value	Max. value	Comments
a_1	-0.50	0.90	Strongly influences the modelling of the dense region. Generally negative for non-polar and non-associating species, generally positive for associating species.
a_2	10^{-6}	0.15	Strongly influences the modelling of the very-dense region
b_1	10^{-6}	5	Influences the modelling of the low-density region
b_2	-0.50	5	Influences the modelling of the moderately-dense region
c	10^{-6}	5	Characterizes the transition between the gas-like and the dense region
d	10^{-6}	5	Defines the vertical position at the origin

Among all the parameter sets returned by the routine, the optimal one was identified as follows:

- At least half of the initial guesses led to the same optimal parameter set,
- This parameter set was associated with the lowest objective function value and a nearly-zero gradient norm.

II-C-1) Component-specific parameters

As previously explained, component-specific parameters were obtained by fitting all viscosity experimental data available for each chemical species providing enough experimental data exist to describe both the liquid and gas states. For illustrative purpose, results obtained with 4 molecules of significantly different chemical natures are shown in Figure II-8. Parameter values for 142 molecules are provided in Tables III.2 and III-28 of the Supporting Information file.

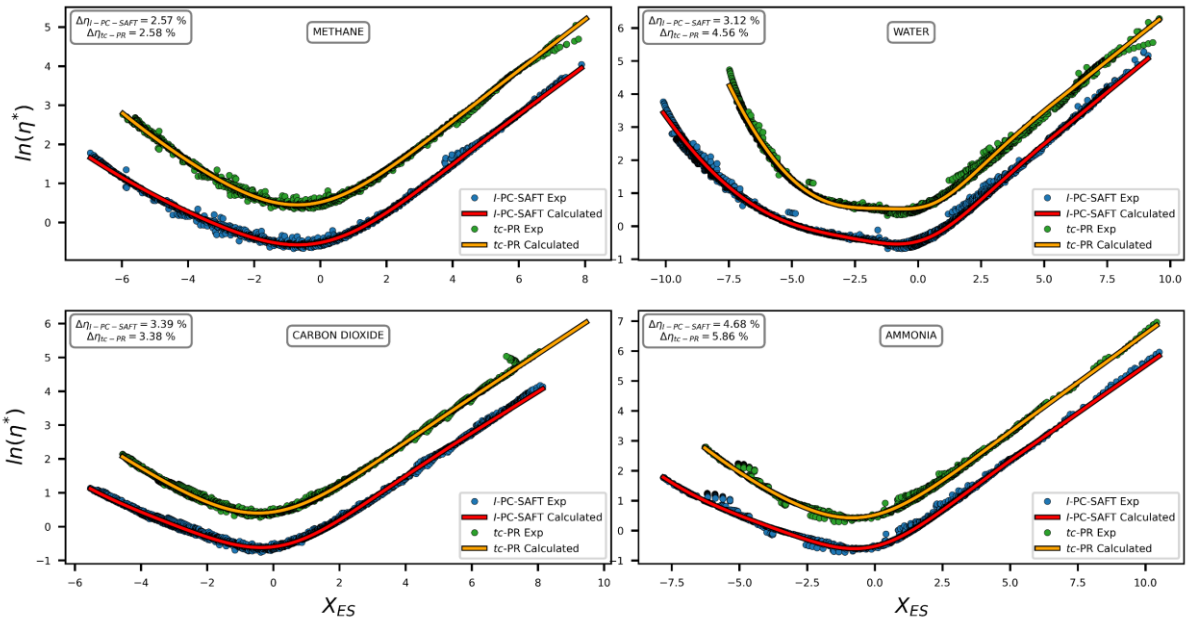

Figure II-8 - Comparison between experimental data and their modelling using component-specific parameters in entropy-scaling laws. Results are obtained with the *tc*-PR and *I*-PC-SAFT EoS for four different components deemed as well illustrative. For *tc*-PR, Y coordinates were offseted by 1 unit in the vertical direction to differentiate both EoS results. Deviations are expressed as MAPE (mean absolute percent error).

Figure II-8 highlights the flexibility of the proposed approach that enables to describe species of different chemical natures and multiple shapes of V-curves. For non-associating and non-polar molecules, one observes close-packed curves sharing a quasi-common minimum and a universal behaviour at low-density. Although component-specific behaviours (i.e., non-universal behaviours) may arise when density increases, the entropy-scaling models developed here appear capable of catching these behaviours using component-specific parameters. These statements are illustrated in Figures II-9, II-10, II-11 and II-12 showing results obtained with linear alkanes, branched alkanes, aromatics and refrigerants.

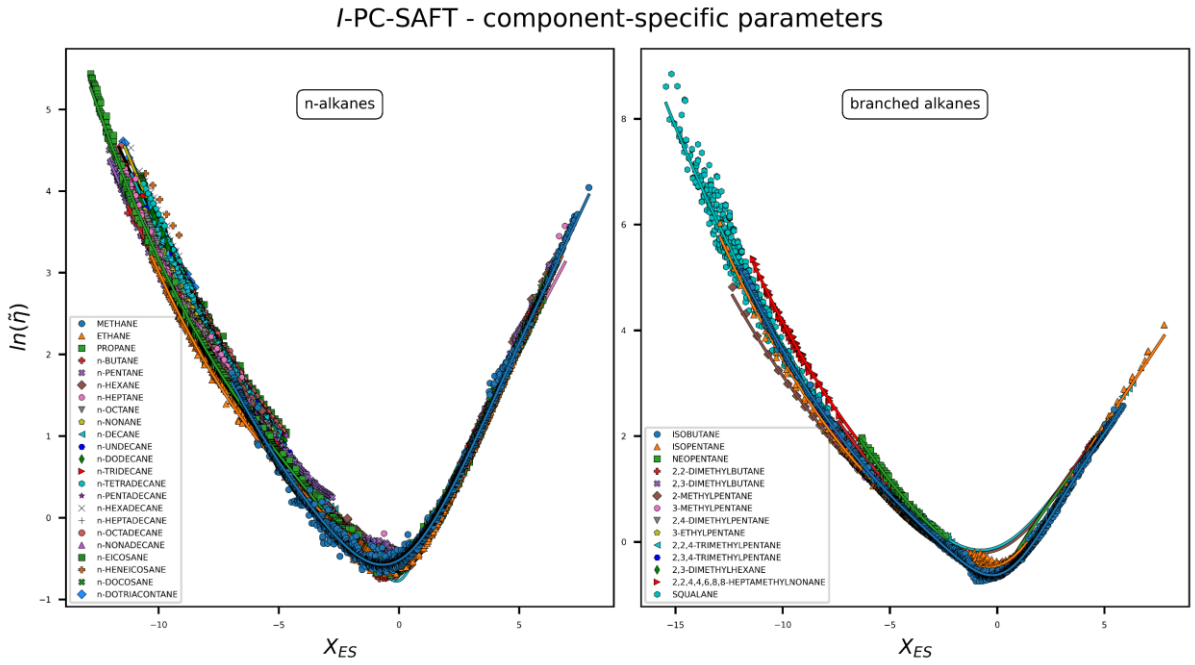

Figure II-9 – Combination of component-specific parameters and the *I*-PC-SAFT EoS for modelling the viscosity of linear alkanes and branched alkanes components. Symbols: experimental data points. Solid lines: calculated values.

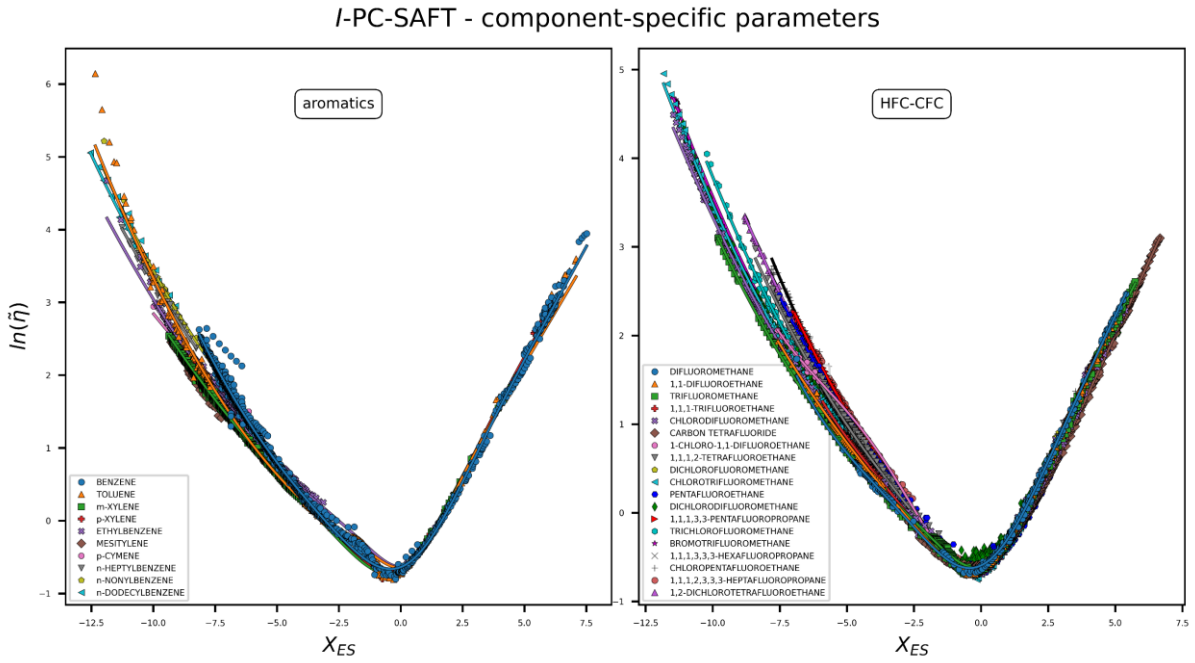

Figure II-10 – Combination of component-specific parameters and the *I*-PC-SAFT EoS for modelling the viscosity of aromatics and HFC-CFC components. Symbols: experimental data points. Solid lines: calculated values.

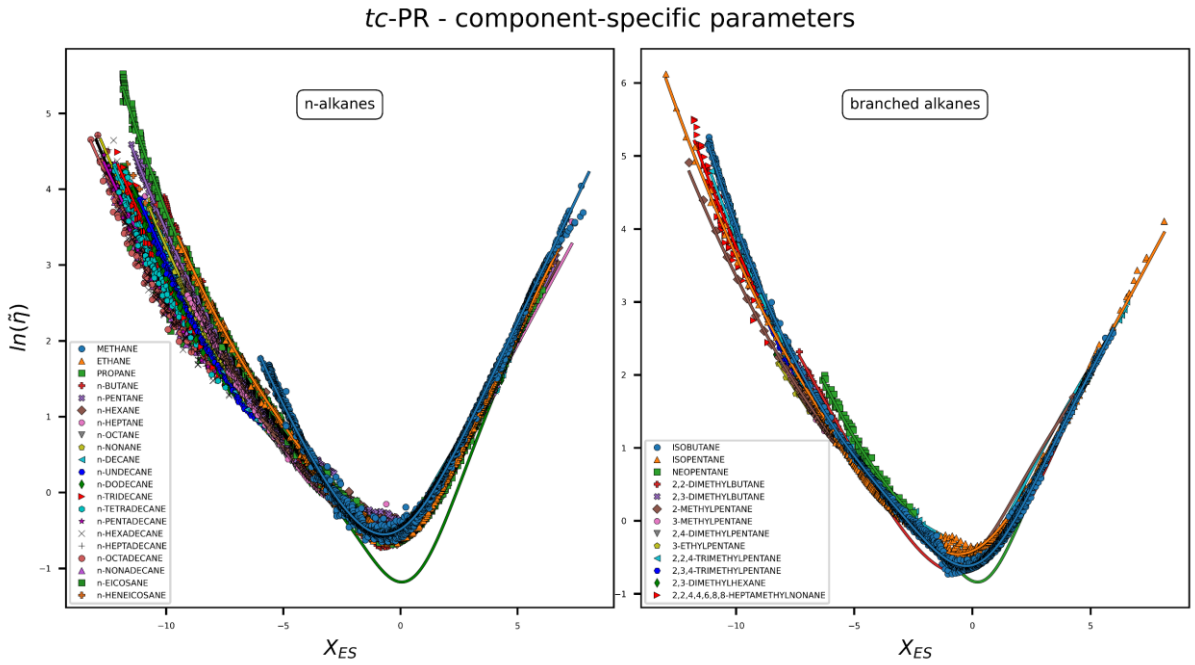

Figure II-11 - Combination of component-specific parameters and the *tc*-PR EoS for modelling the viscosity of linear alkanes and branched alkanes components. Symbols: experimental data points. Solid lines: calculated values.

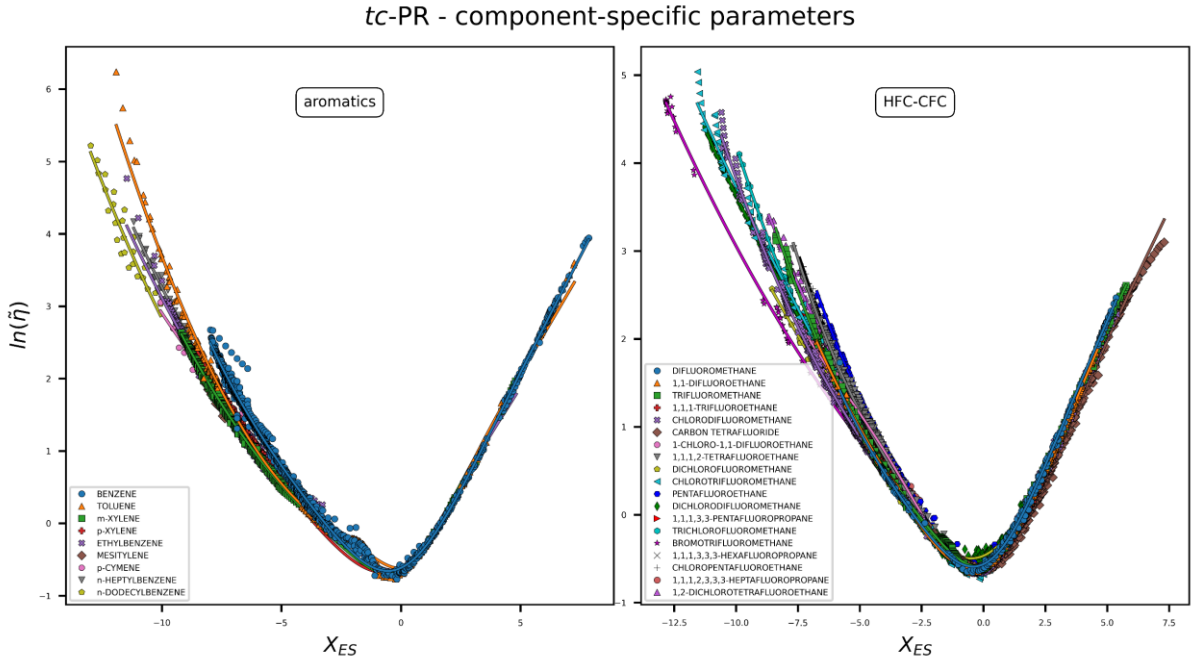

Figure II-12 - Combination of component-specific parameters and the *tc*-PR EoS for modelling the viscosity of aromatics and HFC-CFC components. Symbols: experimental data points. Solid lines: calculated values.

Self-associating and highly-polar substances are more difficult to describe. While the universal behaviour at low density still holds (see Figures II-13 and II-14), curves slopes at high densities vary more consequently when the chain length increases. Remarkably, for these compounds, the curvatures of the liquid branch are significantly higher with the *tc*-PR EoS than with *I*-PC-SAFT (see Figure II-14).

As previous, the use of component-specific parameters enables an accurate representation of the data.

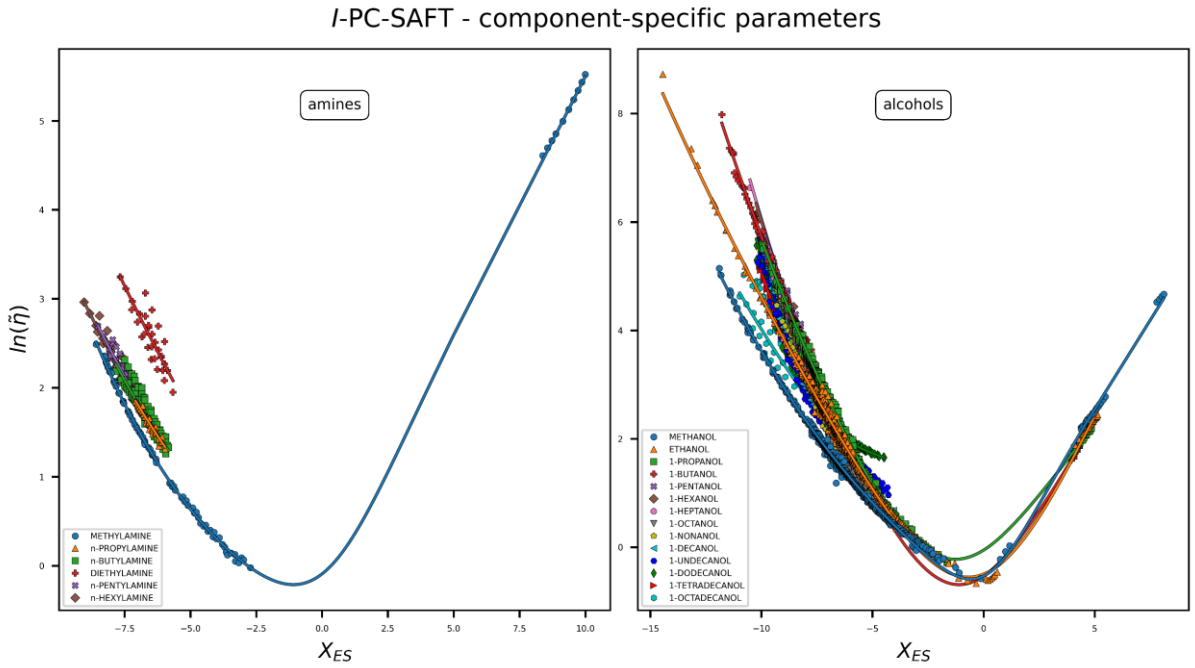

Figure II-13 - Combination of component-specific parameters and the *I*-PC-SAFT EoS for modelling the viscosity of linear alcohols and amines. Symbols: experimental data points. Solid lines: calculated values.

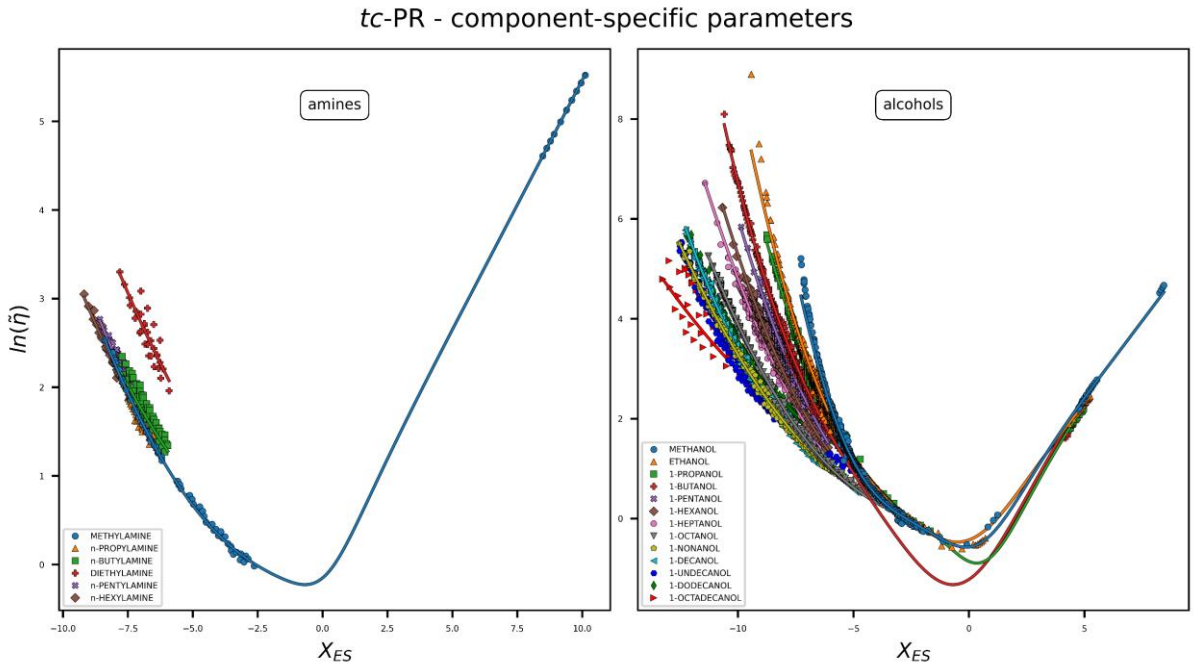

Figure 14 - Combination of component-specific parameters and the *tc*-PR EoS for modelling the viscosity of linear alcohols and amines. Symbols: experimental data points. Solid lines: calculated values.

To conclude this section, the *tc*-PR and *I*-PC-SAFT based models enable to describe viscosity data with a high accuracy in all fluid conditions. The overall MAPE (mean absolute percent error), calculated over the complete data base, is lower than 3.6% with the *tc*-PR EoS and 3.5% with the *I*-PC-SAFT EoS thus pointing out the similarity between both EoS. The detailed MAPEs for each chemical family (calculated by averaging the MAPEs of all the compounds present in a given chemical family) is represented in Figure II-15 showing that nearly all the deviations are below 5 %, regardless of the chemical family considered. Note that aldehydes exhibit MAPEs equal to 6.4% and 7%. These high values can be explained by the limited number of experimental data available and a strong data scatter.

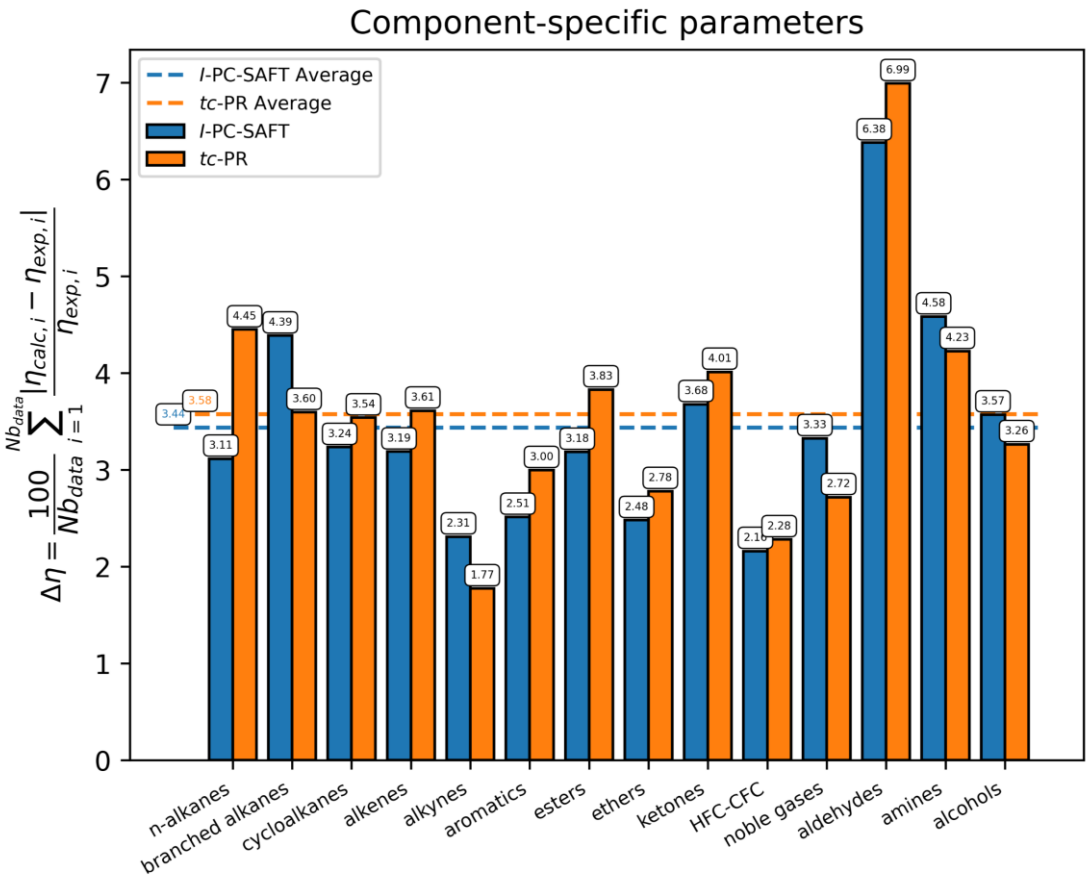

Figure II-15 – Summary of MAPEs obtained with the *I*-PC-SAFT and the *tc*-PR models combined with component-specific parameters

The reliability of the component-specific parameter sets depends obviously on the availability of experimental data. Thus, extrapolations of entropy-scaling laws beyond temperature and pressure domains covered by the data used for fitting may lead to high deviations. When few data are available for determining component-specific parameters, chemical-family specific and universal parameters are certainly a better option.

To conclude this section, a comparison is proposed between the results obtained in the study and the ones recently reported by Lötgering-Lin et al.[80] with an PC-SAFT-based entropy-scaling model (see Table II-3). Although databases used to benchmark both models are different, it is believed that the comparison of these overall deviations, calculated in both cases using component-specific model parameters and over large datasets, makes sense.

Table II-3 – Comparison between the model proposed by Lötgering-Lin et al.[80] and this work (both models rely on the PC-SAFT EoS)

Chemical family	This work (PC-SAFT based model)		Lötgering-Lin et al.[80]	
	Data number	MAPE (%)	Data number	MAPE (%)
n-alkanes	28105	3.11	17115	3.91
Branched alkanes	4778	4.39	2456	9.55
Cycloalkanes	2142	3.24	1359	4.50
Alkenes	3178	3.19	1546	4.18
Aromatics	5660	2.51	5295	4.81
Aldehydes	348	6.38	370	8.82
HFC-CFC	9771	2.16	7833	5.13
Ketones	1101	4.01	885	5.66
Esters	1013	3.18	584	3.26
Amines	496	4.58	310	4.69
Alcohols	9023	3.57	5361	6.38

II-C-2) On the universal minimum arising in $(\ln \tilde{\eta}, X_{ES})$ planes

As a remarkable feature, entropy-scaling curves exhibit all a minimum in the $\ln(\tilde{\eta})$ versus X_{ES} plane that is systematically located around $X_{ES} = 0$. To characterize this minimum with more precision, it was decided to calculate accurately its coordinates $(X_{ES}, \ln \tilde{\eta},)$ from Eq. (II-20) for several species associated with reliable model parameters, i.e., for species presenting enough experimental data to offering a complete description of the V-shape curves. Results are reported in Figure II-16; the 3 coordinates considered were plotted against molecular weight.

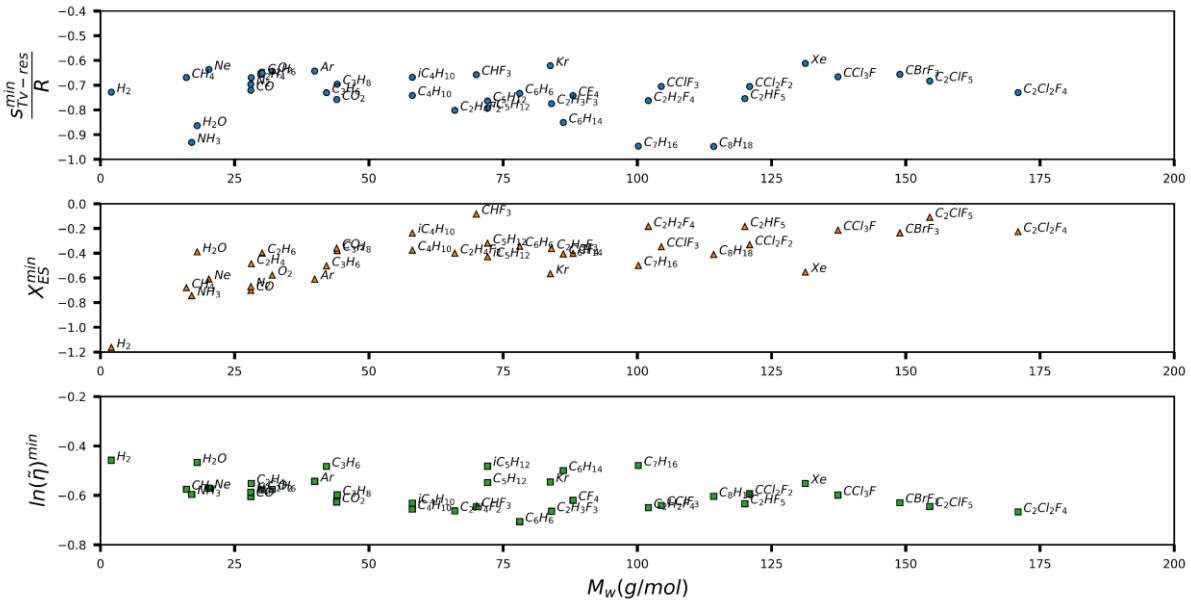

Figure II-16 – Coordinates of the minimum of V-shape curves for a series of pure species plotted against molecular weight.

This figure highlights that quasi-universality is achieved (e.g. gas states), it appears from Figure II-16 that $\left(\tilde{s}_{\mathrm{Tv-res}}^{\mathrm{min}}\right)$ and $\left(X_{\mathrm{ES}}^{\mathrm{min}}\right)$ are rather similar for most of species revealing that at the minimum, these fluids show similar microstructural states; in addition, because $(\ln\tilde{\eta}_{\mathrm{min}})$ is nearly identical for all the species, it can be claimed that they are characterized by the same dynamical state at this minimum. At this particular point, it is thus presumed that the viscosity regime changes. More specifically, it is thought that dynamic properties pass from intermolecular-interaction driven to kinetic driven regimes when decreasing the fluid density.

This observation is in perfect agreement with Bell et al.[63] who identified a viscosity regime transition at $\tilde{s}_{\mathrm{Tv-res}} = -0.7$ which is highly similar to the average $\left(\tilde{s}_{\mathrm{Tv-res}}^{\mathrm{min}}\right)$ value of the compounds represented in Figure II-16.

II-C-3) Chemical-family specific parameters

Chemical-family specific parameters were determined for 11 different chemical families (alkanes, alkenes, refrigerants, amines, esters etc.). Parameter values are reported in the Supporting Information file (see section III-C-2 for the *I*-PC-SAFT based model and section III-D-2 for the *tc*-PR based model). Prediction capacities of the *I*-PC-SAFT and *tc*-PR based models using this approach are illustrated in Figures II-17 and II-18.

As mentioned previously, these parameters lead to less-accurate predictions than component-specific values but can be used to describe molecules for which component-specific parameters cannot be determined due to a lack of experimental information.

In the case of the *I*-PC-SAFT EoS, a satisfactory fitting is achieved for regular chemical families such as n-alkanes or refrigerants (see Figure II-17). It can be observed a loss of extrapolation capacity at highly negative residual entropies ($X_{\mathrm{ES}} < -10$) for some chemical species (visible with n-alkanes in Figure II-17).

Predictions are similar but slightly less accurate when considering the *tc*-PR based model (see Figure II-18).

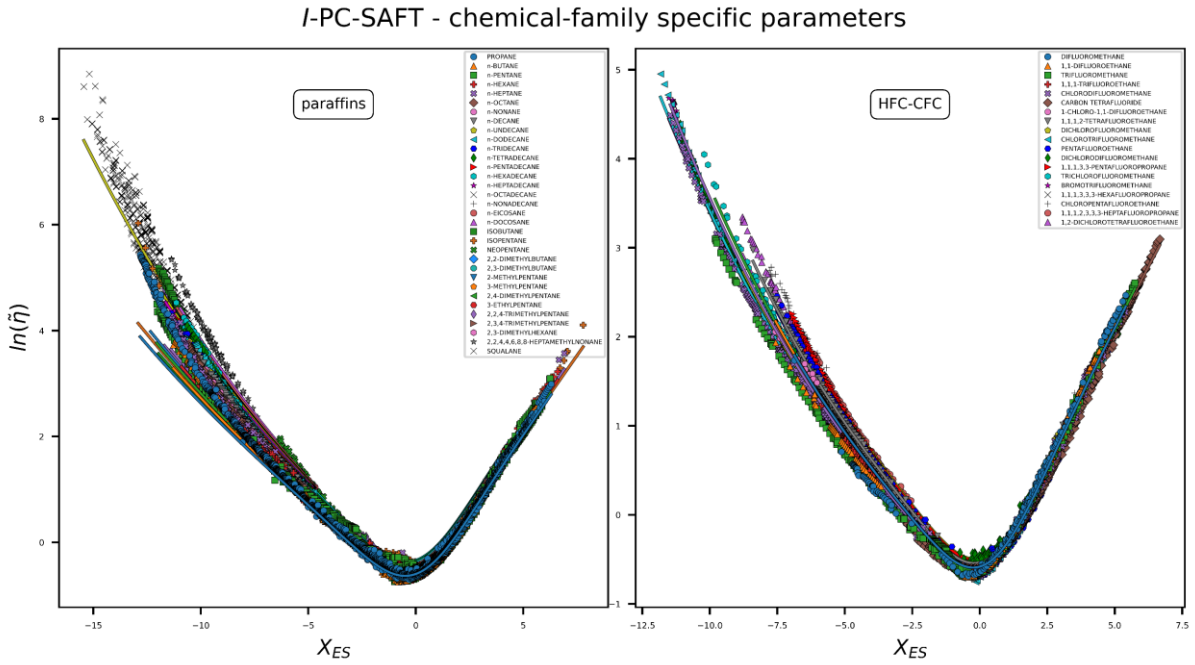

Figure II-17 - Combination of chemical-family specific parameters and the *I*-PC-SAFT EoS for modelling the viscosity of linear alkanes and HFC-CFC components. Symbols: experimental data points. Solid lines: calculated values.

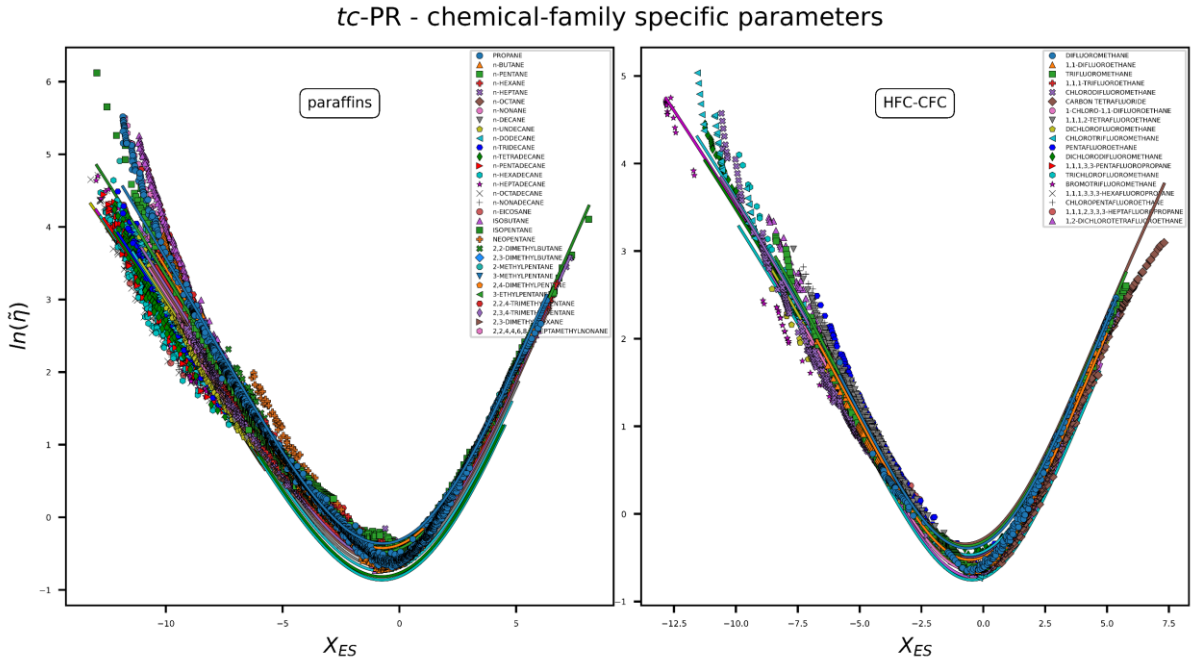

Figure II-18 - Combination of chemical-family specific parameters and the *tc*-PR EoS for modelling the viscosity of linear alkanes and HFC-CFC components. Symbols: experimental data points. Solid lines: calculated values.

For highly self-associating substances (and alcohols in particular), the definition of chemical-family specific parameters does not allow accurate predictions (mean error is found around 30%

with alcohols). This inaccuracy is possibly due to an absence of an association term in both EoS and the scarcity of experimental data for estimating alcohol parameters.

Overall statistics on the chemical-family approach are reported in Figure II-19. The mean errors are around 8% and 10% for the *I*-PC-SAFT and *tc*-PR based models respectively.

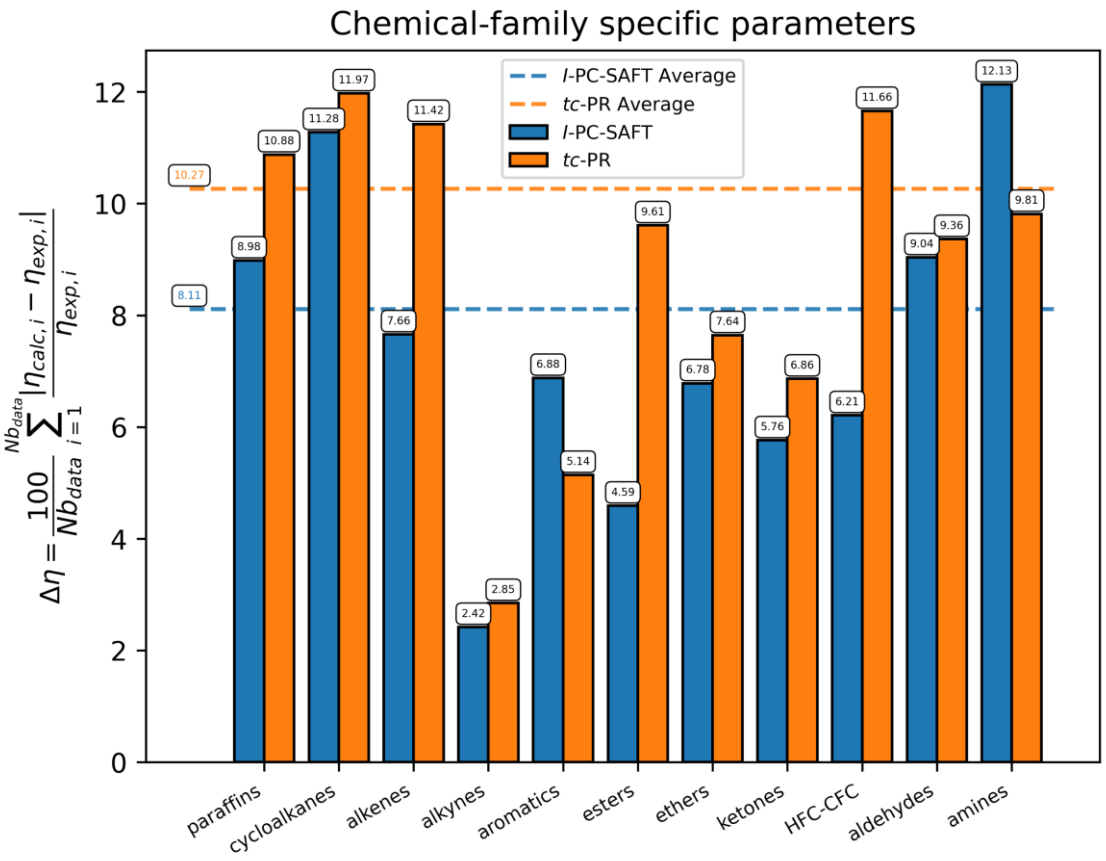

Figure II-19 - Summary of MAPEs obtained with the *I*-PC-SAFT and the *tc*-PR models combined with chemical-family specific parameters

II-C-4) Universal parameters

This approach can be used for any molecule the viscosity of which cannot be estimated from the chemical-family based or component-specific methods.

Universal coefficients were fitted over the quasi-totality of data contained in the complete database. Because of their specific behaviour, water and alcohols were excluded in order not to bias the determination of universal parameters. In the *tc*-PR model, experimental data associated with $T_r > 4$ were voluntary removed from the fitting procedure, as discussed above.

Therefore, using this approach makes it possible to guestimate the shear viscosity of any pure fluid by only providing the critical temperature T_c, critical pressure P_c, acentric factor ω and volume translation c for the *I*-PC-SAFT EoS or T_c, P_c, c and the three component-specific alpha-function parameters (L, M, N) for the *tc*-PR EoS. The corresponding predictions enable:

- A correct reproduction of pressure and temperature effects on shear viscosity,
- Quantitatively efficient predictions for a large number of pure substances, regardless of the temperature or pressure domain considered, regardless of the chemical nature of the component.

To evaluate model performances, results are graphically reported in Figures II-20 and II-21.

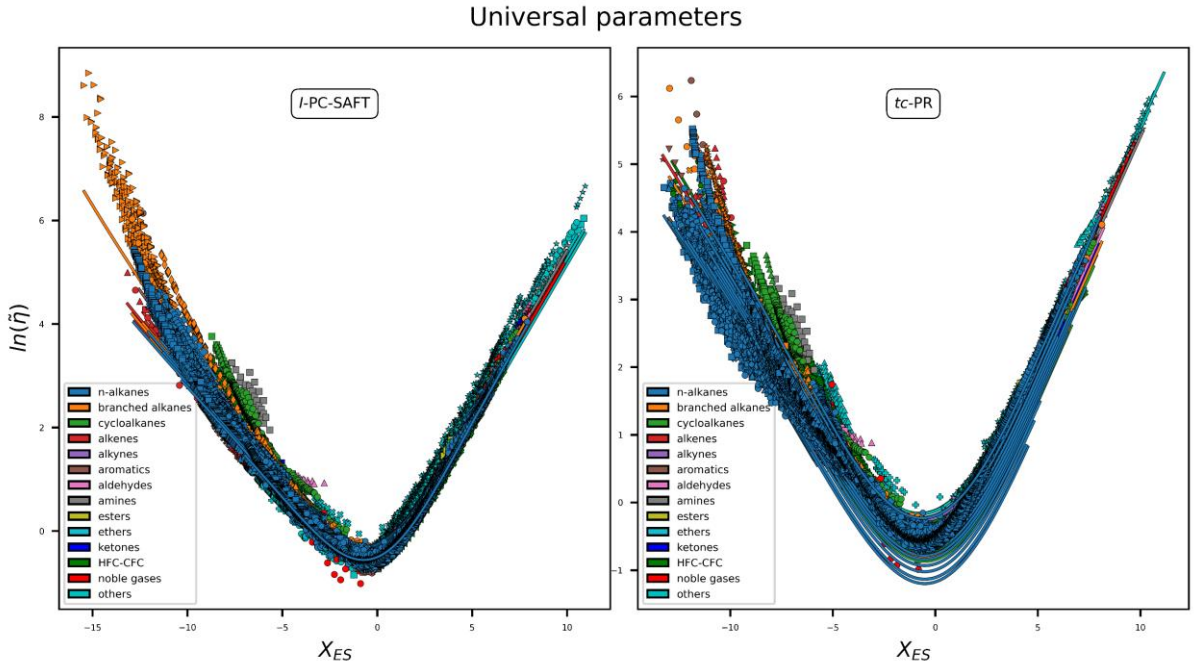

Figure II-20 - Use of universal parameters in the *I*-PC-SAFT (left panel) and *tc*-PR (right panel) EoS for modelling the viscosity of pure species. Symbols: experimental data points. Solid lines: calculated values.

Mean deviations are around 12% and 16% for the *I*-PC-SAFT and *tc*-PR based models, respectively, as highlighted by Figure II-21.

These deviations are higher than those obtained from the group contribution method by Lötgering-Lin and Gross[38] who reported an overall deviation around 5%. Compared to the universal correlation proposed by Bell[72] who predicted the viscosity of n-alkanes with an overall error of 18%, it appears that the combination of the proposed model with either chemical-family specific or universal parameter sets enable a more accurate description of viscosity data.

It is worth noting that the universal approach presented here is neither constrained by the affectation of a compound to a given chemical family or by group decomposition issues.

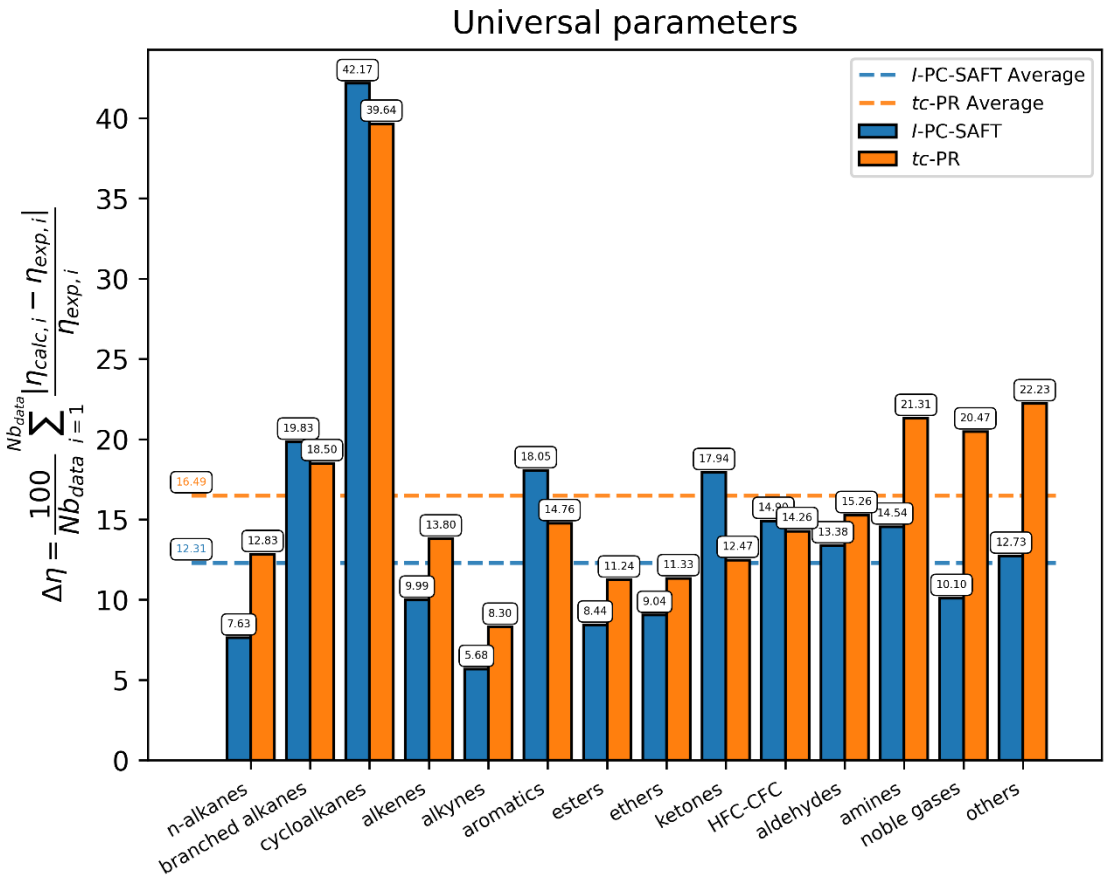

Figure II-21 - Summary of Mean Absolute Percentage Errors of both the *I*-PC-SAFT and the *tc*-PR models with universal parameters

Universal parameters are reported in Table II-4 for both EoS based methods.

Table II-4 - Universal parameters of the *tc*-PR and the *I*-PC-SAFT based models

EoS	*I*-PC-SAFT	*tc*-PR
a_1	-0.28758348	-0.4075878
a_2	0.00593637	0.0025349
b_1	0.58243502	0.593408
b_2	-0.03017106	-0.03077821
c	0.50190584	0.38279452
d	0.39946247	0.45826483
Component number	131	126
Data number	82379	75866
MAPE on viscosity (%)	12.31	16.49

II-D) Conclusion

In this paper, a new formulation of entropy scaling was proposed. As an extension of Rosenfeld's original idea, the present approach highlighted:

- That the original entropy scaling variables proposed by Rosenfeld, that are $Y_{\mathrm{ES}} = \ln\left(\frac{\eta_{\mathrm{real}}}{\rho_{\mathrm{N}}^{2/3}\sqrt{\mathrm{m_0 k_b} T}}\right)$ and $-s_{\mathrm{Tv-res}}/R$ can be advantageously replaced by Y_{ES} and $X_{\mathrm{ES}} = -\left(\frac{s_{\mathrm{Tv-res}}}{s^{\mathrm{c}}_{\mathrm{Tv-res}}}\right) - \ln\left(\frac{s_{\mathrm{Tv-res}}}{s^{\mathrm{c}}_{\mathrm{Tv-res}}}\right)$.
- Similar V shape curves are obtained for any chemical species in the $(Y_{\mathrm{ES}}, X_{\mathrm{ES}})$ space, regardless of the EoS used to estimate residual entropy and density,
- A quasi-universal and linear behaviour of reduced viscosity at low density is obtained systematically in the $(Y_{\mathrm{ES}}, X_{\mathrm{ES}})$ space,
- All fluids exhibit a quasi-universal minimum in the $(Y_{\mathrm{ES}}, X_{\mathrm{ES}})$ space that can be considered as transition point between interaction-driven and kinetic-driven dynamic regimes.

Based on these observations, two new models for predicting shear viscosity were proposed. These models rely on the use of a SAFT-like and a cubic-like EoS, respectively, for the calculation of thermodynamic properties (that are the Tv-residual entropy and density).

When parameters are component specific, it can be claimed in the light of the low deviations on viscosity observed (around 3.5%) that both models offer a high accuracy for nearly all pure components, including self-associating and polar substances, independently of the used EoS.

As an alternative for species for which it was not possible to estimate component-specific model parameters (because of a lack of data), chemical-family specific or universal parameter can be used and provide reasonable estimation of shear viscosity along with temperature and pressure. When using chemical-family specific parameters, deviations on viscosity are around 8.1% and 10.3% when using the *I*-PC-SAFT and *tc*-PR EoS, respectively. Moving to universal models, deviations reach 12.3% and 16.5%, respectively. It could be pointed out that the accuracy of both models is rather similar with a slight advantage to the *I*-PC-SAFT based model, when using the chemical-family and universal versions of the viscosity models proposed here.

More generally, this conclusion reinforces a conclusion we reached previously in the article dealing with the development of the *I*-PC-SAFT EoS[48]: SAFT-type and cubic-type models offer predictions of similar accuracy when they are parametrized in the same way. This is today confirmed with the viscosity models relying on both these EoS.

Overall, the proposed entropy scaling approach introduced in this article seems very promising and opens the way to correlate other transport properties such as self-diffusion coefficients and thermal conductivities. The multiple common features shared by all the studied substances in the entropy-scaling reduced space defined through this work opens the way to the extension of this methodology to the modelling of mixtures transport properties. This key development will be the topic of a next study.

II-E) Appendix A - Minor modification of the entropy variable applying to the *tc*-PR model only

As mentioned above, two EoS are considered here for estimating thermodynamic properties involved in the definition of entropy-scaling properties: the *I*-PC-SAFT and the *tc*-PR models. To illustrate the influence EoS selection may have, the formulation of entropy-scaling approach proposed here was applied to argon by considering successively the two EoS mentioned above. Results are reported in Figure II-A1.

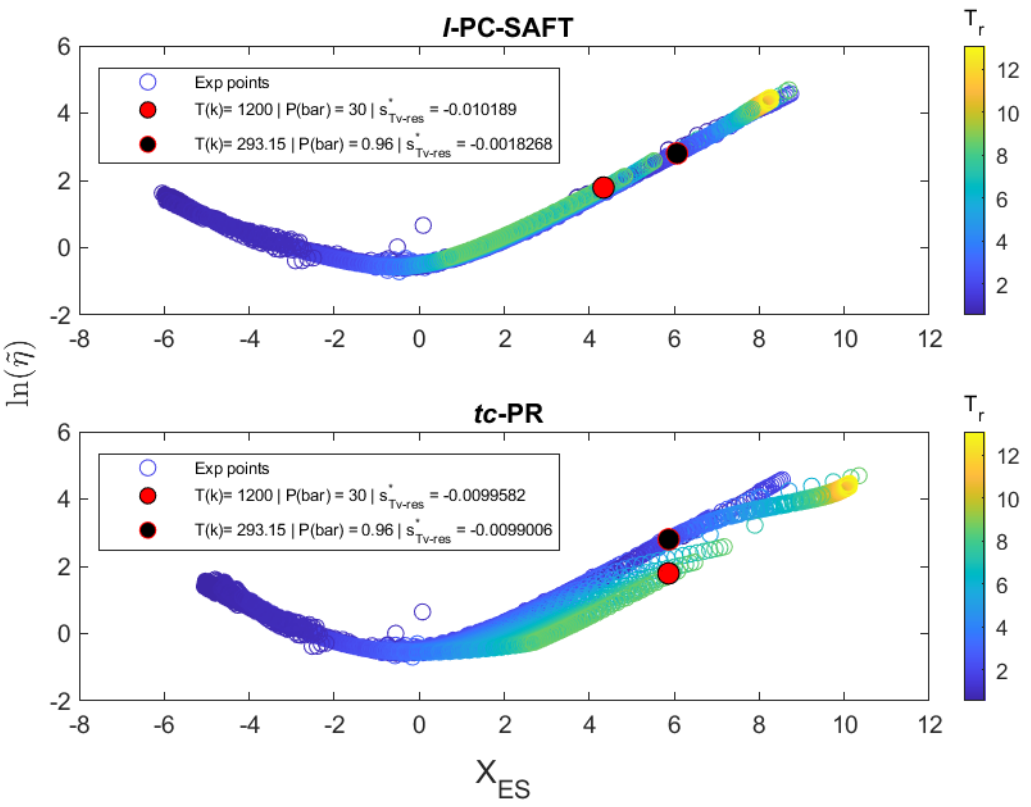

Figure II-A1 – Application of the entropy scaling concept to argon by considering two different EoS for residual entropy and density estimations. $T_r = T/T_c$ is the reduced temperature.

While argon seems to obeys the entropy-scaling law (at least qualitatively) when using the *I*-PC-SAFT model (i.e., a single curve is observed in the reduced $(\ln(\tilde{\eta}),\ X_{ES})$ plane), a scatter of deviation appears at high X_{ES} values with the *tc*-PR model. It is worth noting that for any reduced temperature lower than 4, both EoS predict similar X_{ES} values at fixed temperature and pressure which makes both experimental curves looking similar. At reduced temperatures (T_r) above 4, the estimated Tv-residual entropies are particularly low and considerably differ when switching from the *I*-PC-SAFT to the *tc*-PR EoS, thus causing the irregular behaviour observed with the *tc*-PR EoS in Figure II-A1. Because density estimations from both EoS are in agreement, and therefore, the quantity $\ln(\eta^*)$ is nearly unaffected by the EoS choice.

To overcome this undesired behaviour observed with the *tc*-PR model, the X_{ES} expression was corrected by applying an empirical patch:

$$\begin{cases} X_{\mathrm{ES}}^{\mathrm{corrected}} = -\left(\frac{s_{\mathrm{Tv-res}}}{s^{\mathrm{c}}_{\mathrm{Tv-res}}}\right) - \ln\left(\frac{s_{\mathrm{Tv-res}}}{s^{\mathrm{c}}_{\mathrm{Tv-res}}} \times f_{\mathrm{corr}}(T)\right) \\ f_{\mathrm{corr}}(T) = 1 + \alpha\left(\frac{T-T_{\mathrm{c}}}{T_{\mathrm{c}}}\right)^3 \end{cases} \quad \text{(II-22)}$$

Doing so makes it possible to extend the validity of the *tc*-PR model from $T_{\mathrm{r}} < 4$ to $T_{\mathrm{r}} < 8$. The effect of the proposed correction is illustrated in Figure II-A2. Note that by setting $\alpha = 0$, the correction vanishes and $X_{\mathrm{ES}}^{\mathrm{corrected}}$ becomes identical to X_{ES}. The left panel of Figure II-A2 highlights the important reduction of the undesirable effects in the $(\ln\tilde{\eta},\ X_{\mathrm{ES}})$ plane when replacing X_{ES} by $X_{\mathrm{ES}}^{\mathrm{corrected}}$ with the *tc*-PR model. The right panel is a kind of parity plot showing that the corrected $X_{\mathrm{ES}}^{tc-\mathrm{PR}}$ quantity is very similar to $X_{\mathrm{ES}}^{I-\mathrm{PC-SAFT}}$; a slight linear divergence appears for $X_{ES}^{I-\mathrm{PC-SAFT}} < -2$ while a stronger divergence is observed for high $X_{ES}^{I-\mathrm{PC-SAFT}}$ values (associated with $T_{\mathrm{r}} > 8$).

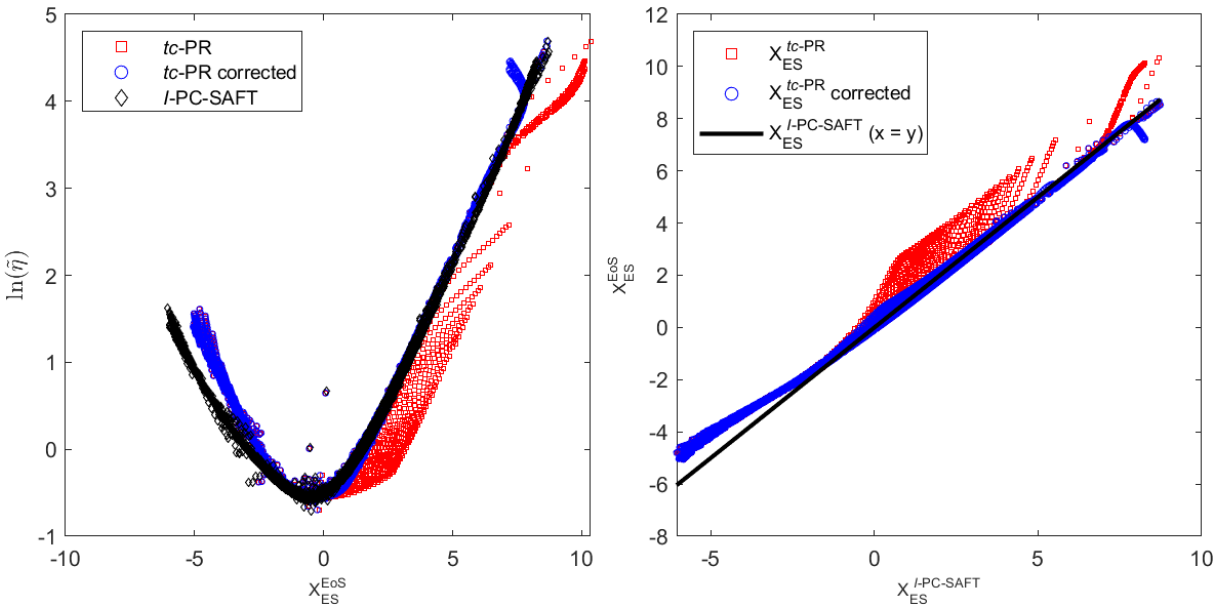

Figure II-A2 – Effect of the correction of the X_{ES} quantity on the modelling of argon viscosity. Left side: representation of $\ln(\tilde{\eta})$ *versus* X_{ES} by using 2 different expressions for X_{ES} (the non-corrected expression is used for *I*-PC-SAFT; non-corrected and corrected expressions are both used with the *tc*-PR EoS). Right side: representation of non-corrected and corrected expressions of $X_{\mathrm{ES}}^{tc-\mathrm{PR}}$ versus $X_{\mathrm{ES}}^{I-\mathrm{PC-SAFT}}$. The alpha parameter (involved in the corrected $X_{\mathrm{ES}}^{tc-\mathrm{PR}}$ term) was set to 0.01.

To sum up:

- At T_{r} lower than 4, both EoS (*tc*-PR and *I*-PC-SAFT) exhibit a similar behaviour. Above this limit, divergence may appear between both model predictions.

- Deviations from the entropy-scaling concept were only observed for the *tc*-PR based model. Adding a correction to the X_{ES} quantity enables to recover an entropy-scaling compatible behaviour with the *tc*-PR model. This correction involved a flexible α parameter.
- When considering the *I*-PC-SAFT, a null α value was selected systematically.
- Regarding the *tc*-PR EoS: for heavy molecules, the temperature domain $T_{\mathrm{r}} > 4$ is not of practical interest. For all of them, a null α value was selected. However, for light molecules (having a low critical temperature) such as argon, nitrogen, oxygen, neon, krypton … applications operating in this domain may exist. In such a case, a non-zero α coefficient was selected.

III- Complément d'information du chapitre 1

Supporting information:

Revisiting the entropy-scaling concept for shear-viscosity estimation from cubic and SAFT equations of state: application to pure fluids in gas, liquid and super-critical states.

Aghilas Dehlouz[1,2], Romain Privat[1(*)], Guillaume Galliero[3], Marc Bonnissel[2], Jean-Noël Jaubert[1(*)]

[1] *Université de Lorraine, École Nationale Supérieure des Industries Chimiques, Laboratoire Réactions et Génie des Procédés (UMR CNRS 7274), 1 rue Grandville, 54000, Nancy, France*

[2] *Gaztransport & Technigaz (GTT), 1 route de Versailles, 78470 Saint-Rémy-lès-Chevreuse, France*

[3] *Université de Pau et des Pays de l'Adour, E2S UPPA, CNRS TotalEnergies, LFCR UMR 5150, Pau, France*

III-A) The revisited entropy scaling (ES) approach:

III-A-1) Brief presentation of the proposed approach:

In the previous chapter, the ES approach proposed by Rosenfeld was reformulated in order to remove the classical low-density divergence and to make it less sensitive to the EoS used for density and residual entropy estimations. As a result, it was shown that the representation of viscosity data of a given species in the reduced space (Y_{ES}, X_{ES}) such that:

$$\begin{cases} X_{\mathrm{ES}} = -\left(\dfrac{s_{\mathrm{Tv-res}}}{s^{\mathrm{c}}_{\mathrm{Tv-res}}}\right) - \ln\left(\dfrac{s_{\mathrm{Tv-res}}}{s^{\mathrm{c}}_{\mathrm{Tv-res}}}\right) \\ Y_{\mathrm{ES}} = \ln\left(\dfrac{\eta}{\rho_{\mathrm{N}}^{2/3}\sqrt{\mathrm{m_0 k_b} T}}\right) \end{cases} \quad \text{(III– 1)}$$

align along a unique V-shape curve.

III-A-2) The zero-density limit

In the original Rosenfeld's approach[2], the reduced viscosity:

$$\tilde{\eta} = \eta \rho_{\mathrm{N}}^{-2/3} (\mathrm{m_0 k_b} T)^{-1/2} \quad \text{(III– 2)}$$

is considered as a simple function of the reduced residual entropy $\left({}^{-s_{\mathrm{Tv-res}}}/_{R}\right)$. Due to the presence of the factor $\rho_{\mathrm{N}}^{-2/3}$, $\tilde{\eta}$ diverges when $\rho_N \to 0$ resulting in the presence of a vertical asymptote in the ($\tilde{\eta}$, ${}^{-s_{\mathrm{Tv-res}}}/_{R}$) plane when $\left({}^{-s_{\mathrm{Tv-res}}}/_{R}\right) \to 0$ (i.e., for dilute gases).

The use of the modified entropy variable X_{ES} (see Eq. (III-1)) instead of $\left({}^{s_{\mathrm{Tv-res}}}/_{R}\right)$ fixes this issue. This transformation converts the vertical asymptote observed in Rosenfeld reduced space by an oblique asymptote along which, all viscosity data align universally. A proof of this statement is now given.

Proof: using a virial-type approach, the viscosity can be written as a power expansion in density involving temperature- dependent coefficients[66,67]:

$$\eta = \eta_0(T) + b(T)\rho_{\mathrm{N}} + b(T)\rho_{\mathrm{N}}^2 + \cdots \quad \text{(III– 3)}$$

Where ρ_{N} denotes the molecular density (in molecule/m^3).

Therefore, the reduced viscosity (defined by Eq. (III-2)) can be expressed as:

$$\tilde{\eta} = \frac{\eta_0}{\sqrt{\mathrm{m_0 k_b} T}} (\rho_N)^{-2/3} + \frac{b}{\sqrt{m_0 \mathrm{k_b} T}} (\rho_\mathrm{N})^{1/3} + \cdots \qquad \text{(III– 4)}$$

Similarly, for low to moderate density, the residual entropy can be expressed from the virial equation of state[6]:

$$\frac{-s_{Tv-res}}{R} = \left[B_N(T) + T \frac{dB_N}{dT} \right] \rho_N + \cdots - \ln(z) \qquad \text{(III– 5)}$$

Where B_N denotes the molecular second viral coefficient (in $\mathrm{m^3}$ per molecule) and $z = P/(\rho_\mathrm{N} \mathrm{k_b} T)$, the compressibility factor expressed from the virial equation of state:

$$z = 1 + B_\mathrm{N}(T)\rho_\mathrm{N} + C_\mathrm{N}(T)\rho_\mathrm{N}^2 + \cdots \qquad \text{(III– 6)}$$

The X_ES variable, defined by Eq. (III-1), is the sum of 2 terms: $\left(-\frac{s_{\mathrm{Tv-res}}}{s^{\mathrm{c}}_{\mathrm{Tv-res}}} \right)$ and $-\ln\left(\frac{s_{\mathrm{Tv-res}}}{s^{\mathrm{c}}_{\mathrm{Tv-res}}} \right)$. At low density, the residual entropy of the fluid vanishes and consequently, the logarithmic term becomes dominant:

$$X_\mathrm{ES} \underset{\rho_\mathrm{N} \to 0}{\backsim} -\ln\left(\frac{s_{\mathrm{Tv-res}}}{s^{\mathrm{c}}_{\mathrm{Tv-res}}} \right) \underset{\rho_\mathrm{N} \to 0}{\backsim} -\ln\left(\frac{s_{\mathrm{Tv-res}}/R}{s^{\mathrm{c}}_{\mathrm{Tv-res}}/R} \right) \underset{\rho_\mathrm{N} \to 0}{\backsim} -\ln\left(-\frac{s_{\mathrm{Tv-res}}}{R} \right) \qquad \text{(III– 7)}$$

Combining Eqs. (III-5) and (III-7) and noticing that the $\ln(z)$ term is negligible (when $\rho_\mathrm{N} \to 0$, $z \to 1$), one obtains:

$$X_\mathrm{ES} \underset{\rho_\mathrm{N} \to 0}{\backsim} -\ln\left[\left(B_\mathrm{N}(T) + T \frac{dB_\mathrm{N}}{dT} \right) \rho_\mathrm{N} \right] \qquad \text{(III– 8)}$$

Consequently, in the zero-density domain, the above expression can be reversed and the density can be then expressed as a function of the modified entropy scaling variable:

$$\rho_\mathrm{N} \underset{\rho_\mathrm{N} \to 0}{\backsim} \frac{1}{\left[B_\mathrm{N}(T) + T \frac{dB_\mathrm{N}}{dT} \right] e^{X_\mathrm{ES}}} \qquad \text{(III– 9)}$$

Combining (III-4) and (III-9) leads to:

$$\tilde{\eta} \underset{\rho_N \to 0}{\backsim} \frac{\eta_0}{\sqrt{\mathrm{m_0 k_b} T}} \left(\left[B_\mathrm{N}(T) + T \frac{dB_\mathrm{N}}{dT} \right] e^{X_\mathrm{ES}} \right)^{2/3} + \frac{b}{\sqrt{m_0 \mathrm{k_b} T}} \left(\left[B_\mathrm{N}(T) + T \frac{dB_\mathrm{N}}{dT} \right] e^{X_\mathrm{ES}} \right)^{-1/3} + \cdots \text{(III– 10)}$$

Keeping the dominant term only and applying a logarithmic transformation, one has:

$$\ln(\tilde{\eta}) \underset{\rho_\mathrm{N} \to 0}{\backsim} \ln\left[\frac{\eta_0}{\sqrt{\mathrm{m_0 k_b} T}} \left(B_\mathrm{N}(T) + T \frac{dB_\mathrm{N}}{dT} \right)^{2/3} \right] + \frac{2}{3} X_\mathrm{ES} \qquad \text{(III– 11)}$$

The first term of the right-hand side of the above equation is a temperature-dependent function denoted $K(T)$. Eventually:

$$\ln(\tilde{\eta}) \underset{\rho_\mathrm{N} \to 0}{\backsim} K(T) + \frac{2}{3} X_\mathrm{ES} \qquad \text{(III– 12)}$$

This limiting law is partially similar to the one derived by Bell et al. in a recent article[81] where it is proved that the reduced viscosity variable η^+(which has a different formulation from the one defined here: $\eta^+ = \tilde{\eta} \times \left({}^{-S_{\mathrm{Tv-res}}}/_{R}\right)^{2/3}$ tends to $e^{K(T)}$ when $\rho_{\mathrm{N}} \to 0$. Bell et al. studied extensively this term and observed that η^+ is a decreasing function of the temperature that becomes constant at high temperature. To ensure a correct limit at low density, they decided to use as reduced residual viscosity variable $\eta^+ - \eta^+_{\rho_{\mathrm{N}} \to 0}$ [72]. This choice requires the preliminary knowledge of a dilute-gas model for the viscosity which appears as an additional constraint for the implementation of this approach. As explained below, this practice appears unnecessary in the present case.

Sharing the concern that a viscosity model should reproduce the correct low-density limit, we decided to verify empirically the consistence of the proposed model. To do so, pure water and pure methane were selected as reference molecules for illustrating the different low-density behaviours observed. Low-density gas viscosity data were extracted from the DDB (only data of pure gases at P < 10 bar were considered) and were reported in a ($ln(\tilde{\eta})$, $X_{I-\mathrm{PC-SAFT}}$). The *I*-PC-SAFT model was used to estimate residual entropy and density. Data calculated from the component- specific version of our model were compared to experimental data and to data obtained from the Chapman-Enskog (CE) model which is a well-acknowledged viscosity model for dilute gas. Results, reported in Figures III-1 and III-2, highlight the noticeable capacity of our model to reproduce experimental data with an accuracy generally higher than the CE model.

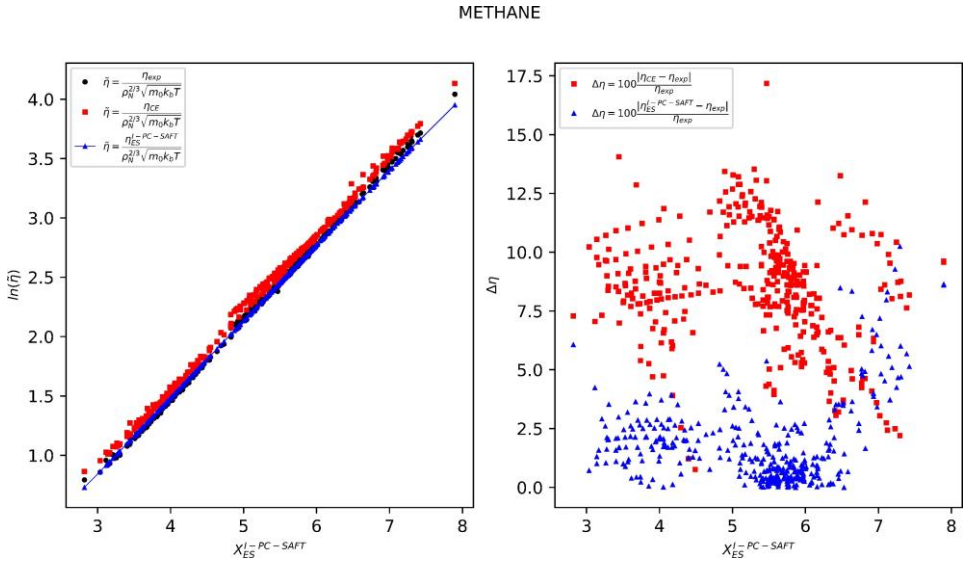

Figure III-1 - Study of the viscosity behaviour of pure methane at low density in the ($ln(\tilde{\eta})$, $X_{I-\mathrm{PC-SAFT}}$) plane: comparison between experimental data (●), issued from the DDB, and predictions from two viscosity models. (▲): component-specific version of the model proposed here; (■): prediction from the Chapman-Enskog model.

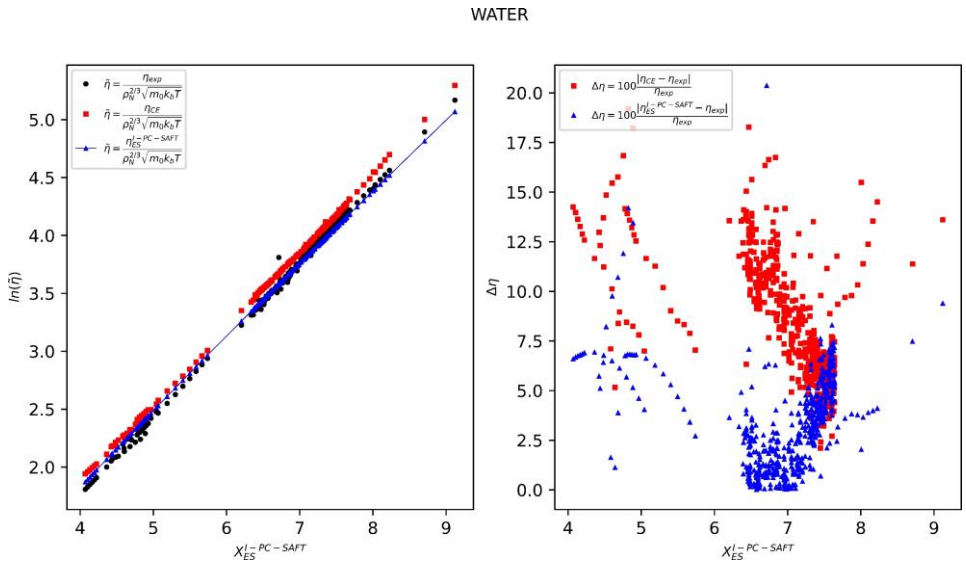

Figure III-2 - Study of the viscosity behaviour of water at low density in the $(ln(\tilde{\eta}), X_{I-\mathrm{PC-SAFT}})$ plane: comparison between experimental data (●), issued from the DDB, and predictions from two viscosity models. (▲): component-specific version of the model proposed here; (■): prediction from the Chapman-Enskog model.

To reinforce this conclusion, the $K(T)$ function was plotted against the X_{ES} variable. Results are reported in Figure III-3 and show that $K(T)$ is a monotonic function of X_{ES}. This result applies regardless of the molecule considered. As an immediate consequence, the reduced-viscosity law $K(T) + \frac{2}{3}X_{\mathrm{ES}}$, introduced in Eq. (III-12), defines a unique function of X_{ES} and thus, is perfectly compatible with the entropy-scaling concept. In addition, Figure III-3 highlights the small variation of the $K(T)$ function (K values remain in a narrow range). Once again, this result was observed for all the studied molecules. In most of the cases, the $K(T)$ versus X_{ES} behaviour can be modelled by a straight line. More interesting, $K(T) + \frac{2}{3}X_{\mathrm{ES}}$ can be systematically represented by a unique and well-defined straight line.

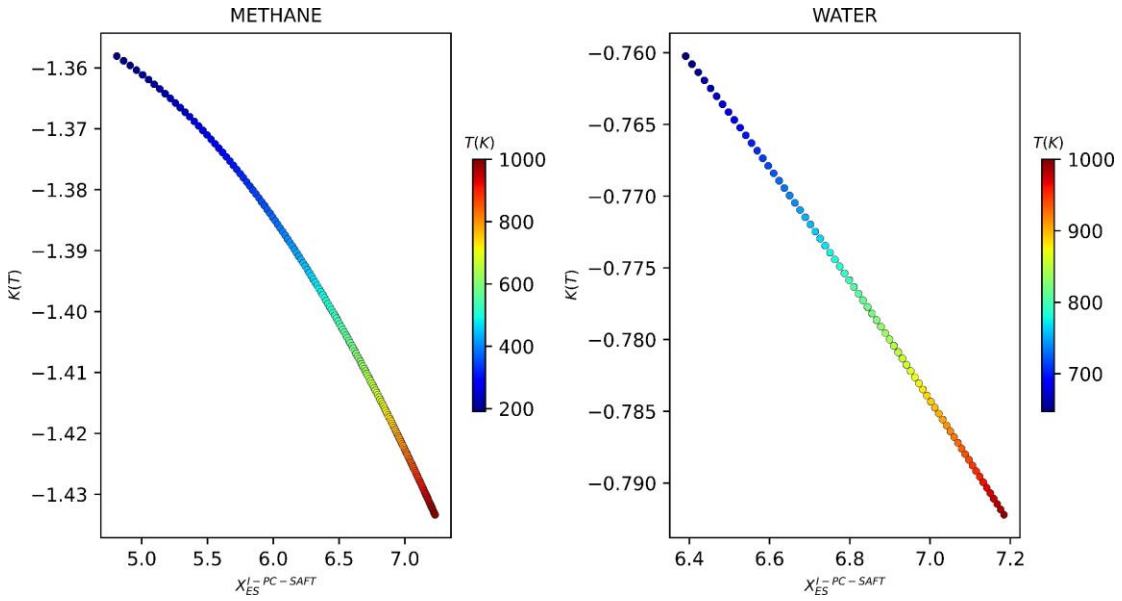

Figure III-3 - Evolution of the $K(T)$ function with respect to X_{ES} in the cases of pure methane and pure water.

To conclude this section, it can be claimed that the low-density law stemming from the revised entropy-scaling concept proposed here can be represented systematically by a unique straight line in the $ln(\tilde{\eta})$ versus X_{ES} plane. This result applies to any compound, at any temperature *T*.

III-A-3) On the selection of a proper reference entropy

As mentioned in chapter 1, a reduced viscosity can be defined by:

$$\tilde{\eta} = \frac{\eta_{\mathrm{real}}}{\eta_{\mathrm{ref}}} \qquad (\mathrm{III}-13)$$

There are essentially two options to define η_{ref} : either Rosenfeld's reference term ($\eta_{\mathrm{ref}} = \rho_{\mathrm{N}}^{2/3}\sqrt{\mathrm{m_0 k_b} T}\eta$) or Chapman- Enskog's reference term ($\eta_{\mathrm{ref}} = \eta_0$, an estimation of the dilute-gas viscosity). Obviously, using η_0 leads to the appearence of a horizontal asymptote in the (η_{ref}, X_{ES}) plane when $X_{\mathrm{ES}} \to +\infty$, characterizing the dilute-gas region. This behaviour is illustrated in Figures III-4 to III-7. For comparison, the curves associated with Rosenfeld's reference term are also reported in these figures.

It is recalled that using Chapman-Enskog reference term requires the preliminary knowledge of additional parameters (σ, $\Omega^{(2,2)*}$) to estimate $\tilde{\eta}$ while Rosenfeld's method does not involve other properties than those used for residual entropy estimation. In our proposed approach, Rosenfeld's reference viscosity was selected because: (i) as mentioned, it only involves temperature and density (as discussed above) and (ii) this choice is theoretically justified by the isomorph theory.

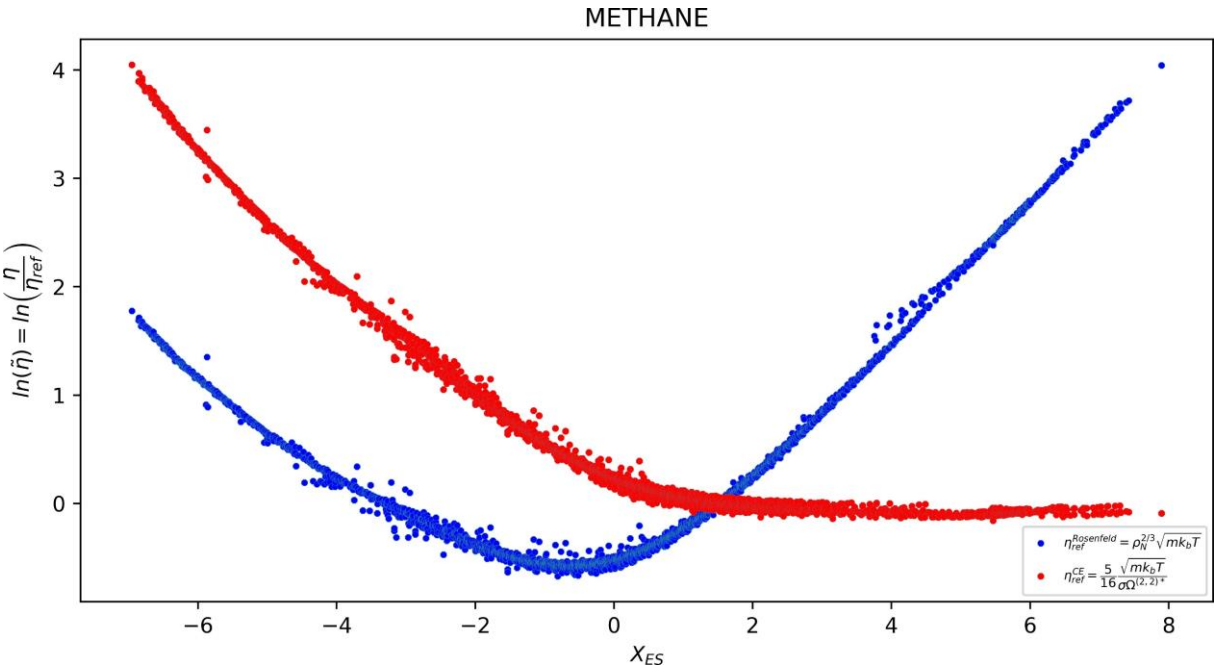

Figure III-4 - Illustration of the effect of the reference viscosity selection on the shape of pure-methane curves in the $(ln(\tilde{\eta}),\ X_{I-\mathrm{PC-SAFT}})$ plane: comparison between the definition of a reduced viscosity from Chapman-Enskog's expression[10] and from Rosenfeld's expression. Thermodynamic properties were estimated with *I*-PC-SAFT EoS. Parameters σ and used in the Chapman-Enskog relation and in Neufeld's[73] empirical relation for the collision integrals were taken from Ref[74]

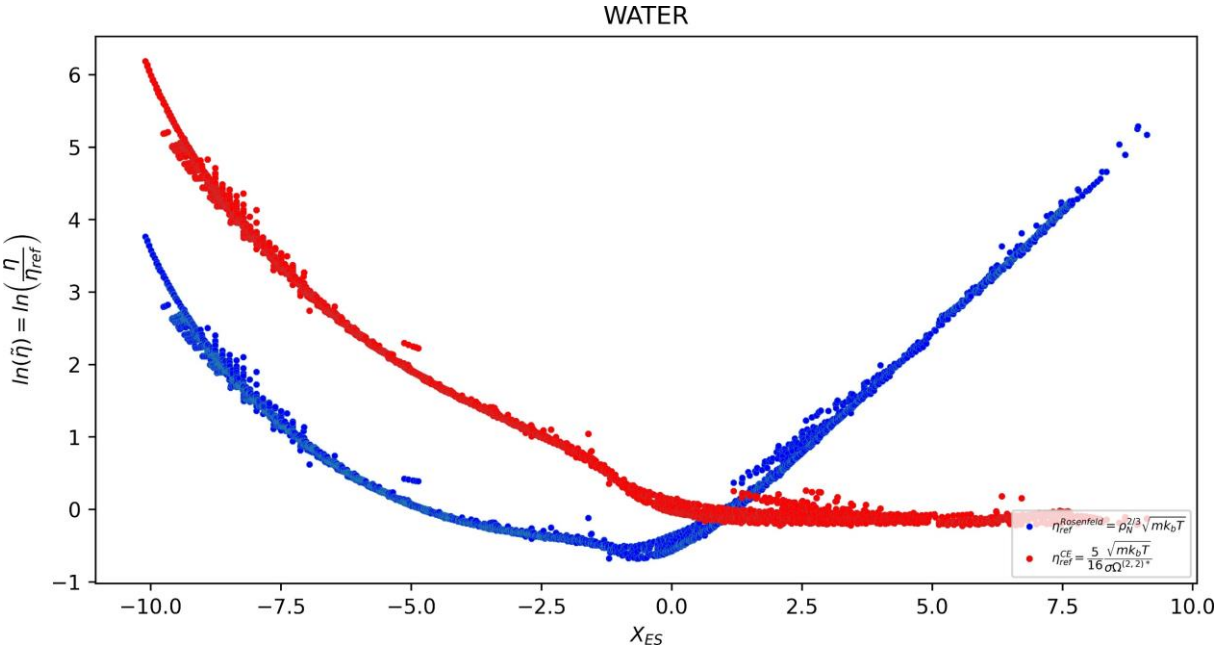

Figure III-5 - Illustration of the effect of the reference viscosity selection on the shape of pure-water curves in the $(ln(\tilde{\eta}),\ X_{I-\mathrm{PC-SAFT}})$ plane: comparison between the definition of a reduced viscosity from Chapman-Enskog's expression[10] and from Rosenfeld's expression. Thermodynamic properties were estimated with *I*-PC-SAFT

EoS. Parameters σ and used in the Chapman-Enskog relation and in Neufeld's[73] empirical relation for the collision integrals were taken from Ref[74]

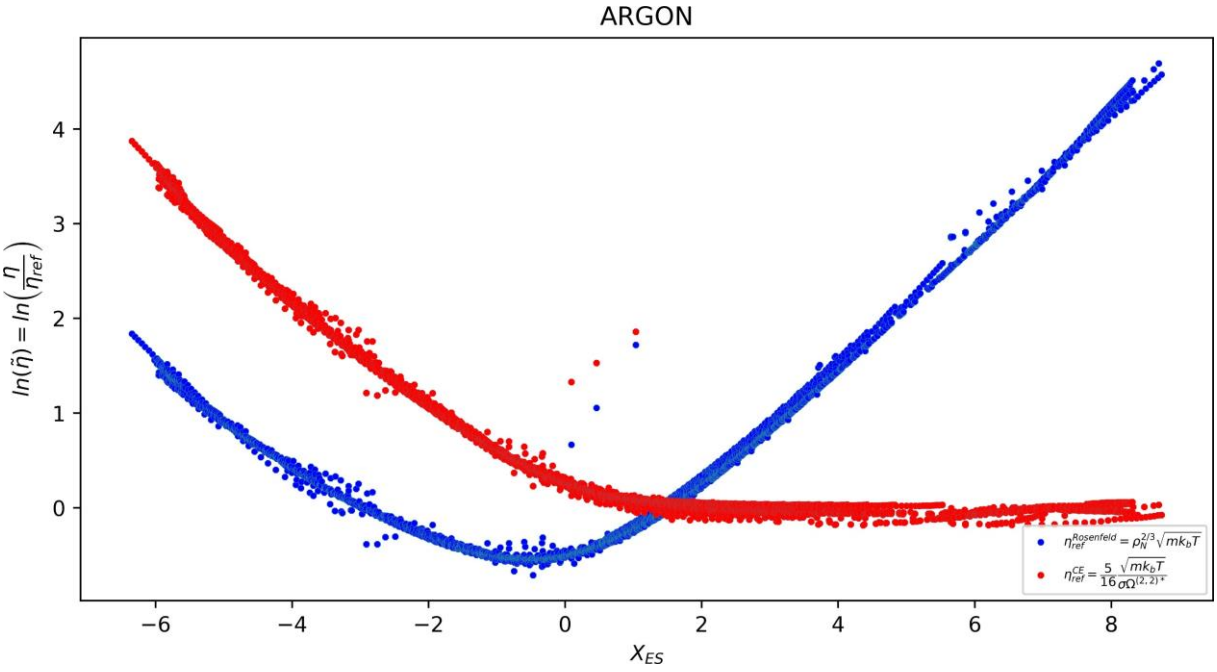

Figure III-6 - Illustration of the effect of the reference viscosity selection on the shape of pure-argon curves in the $(ln(\tilde{\eta}),\ X_{I-\mathrm{PC-SAFT}})$ plane: comparison between the definition of a reduced viscosity from Chapman-Enskog's expression[10] and from Rosenfeld's expression. Thermodynamic properties were estimated with *I*-PC-SAFT EoS. Parameters σ and used in the Chapman-Enskog relation and in Neufeld's[73] empirical relation for the collision integrals were taken from Ref[74]

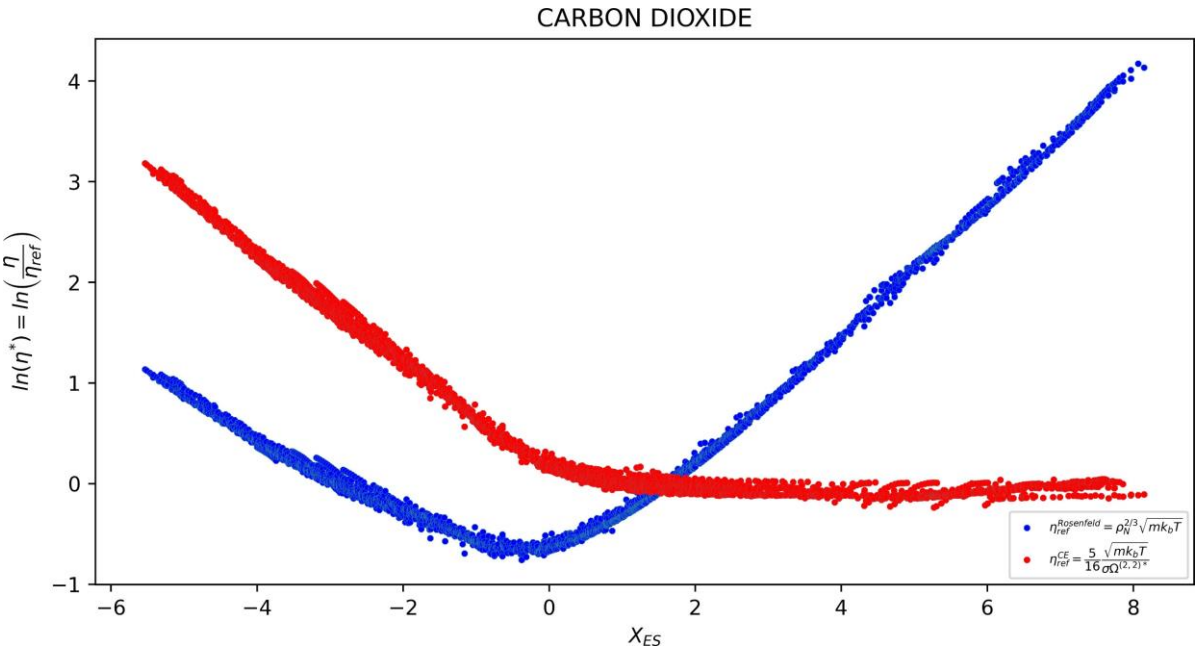

Figure III-7 - Illustration of the effect of the reference viscosity selection on the shape of pure-CO_2 curves in the $(ln(\tilde{\eta}), X_{I-\mathrm{PC-SAFT}})$ plane: comparison between the definition of a reduced viscosity from Chapman-Enskog's expression[10] and from Rosenfeld's expression. Thermodynamic properties were estimated with *I*-PC-SAFT EoS. Parameters σ and used in the Chapman-Enskog relation and in Neufeld's[73] empirical relation for the collision integrals were taken from Ref[74]

III-A-4) Influence of EoS selection on the calculated residual entropy variable

The definition of variable X_{ES} is recalled in Eq. (III-1). It can be noticed that residual entropy was scaled using the critical value of the residual entropy value with the aim to reduce the difference of behavior from one EoS to another. Doing so, X_{ES} values calculated in the same conditions, for the same fluid, with two different EoS become more similar. Important differences may however persist. As an illustration, 2 compounds were considered (methane and water) as well as, 2 different EoS (Tegeler and *I*-PC-SAFT).

With methane, important differences between both EoS can be observed at very low (i.e., high X_{ES} values) or very high density ($X_{\mathrm{ES}} \ll 0$), as shown in Figure III-8. Behaviors are very similar otherwise.

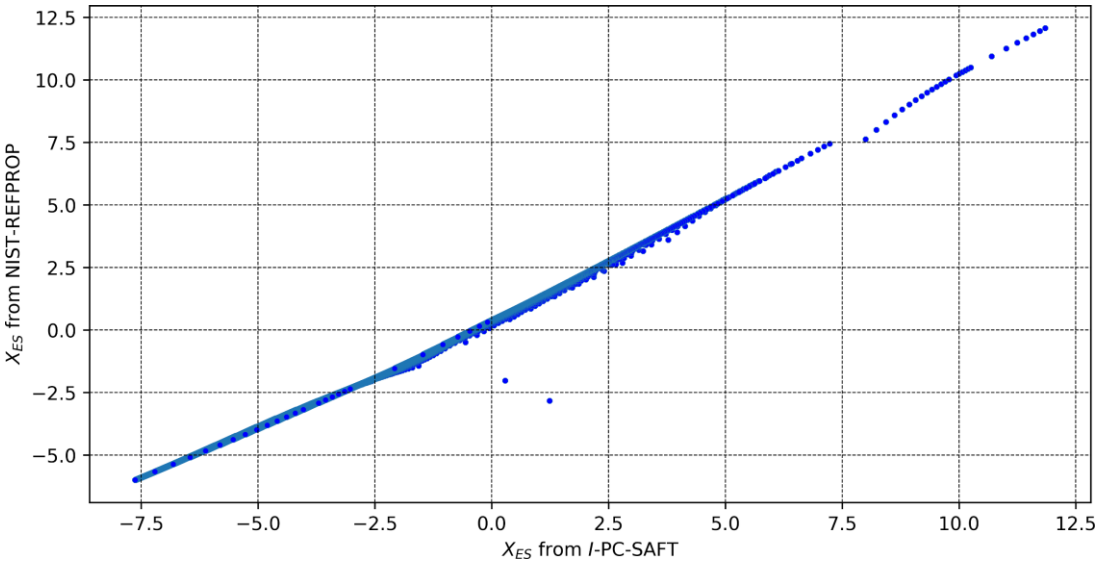

Figure III-8 - Comparison between X_{ES} values of pure methane estimated from the *I*-PC-SAFT and Tegeler EoS (EoS used in the NIST-REFPROP software for methane).

With water, important differences arose systematically, as illustrated in Figure III-9. They can be assigned quasi certainly to the absence of association term in the *I*-PC-SAFT EoS. Because it was intended to propose entropy- scaling models both accurate and simple, it has been decided to avoid the use of association terms in the EoS leading to the necessity to dispose of additional association parameters to estimate residual entropy and the loose of generality for the estimation of the *I*-PC-SAFT input parameters.

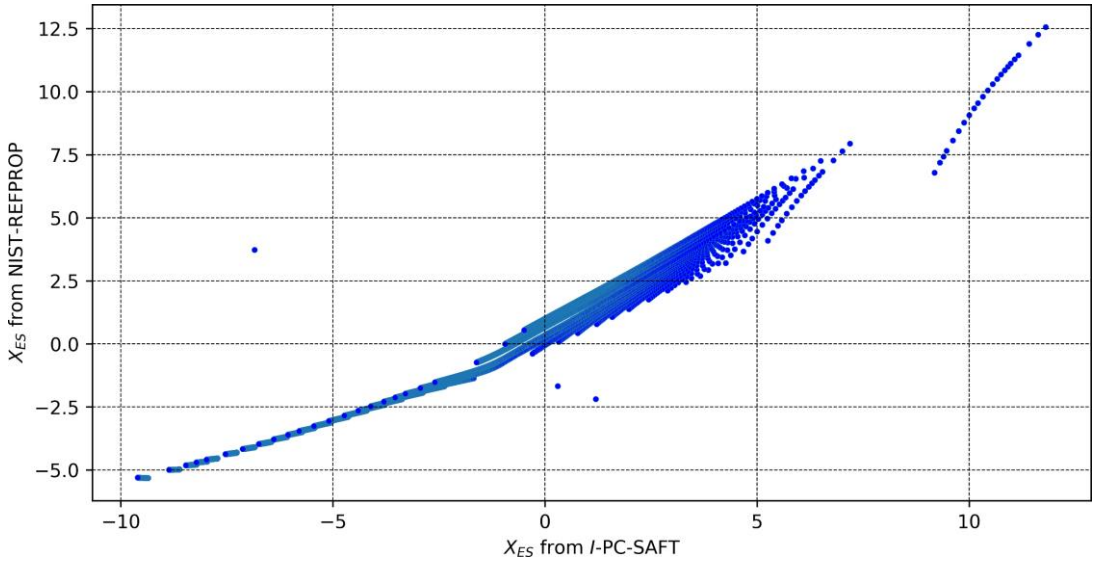

Figure III-9 - Comparison between X_{ES} values of pure water estimated from the *I*-PC-SAFT and Wagner EoS (EoS used in the NIST-REFPROP software for water).

III-B) Limitation of the proposed models:

In this study, the experimental data used to estimate the model coefficients were collected from the Dortmund Data Bank (DDB). Care was taken to limit the processing of these raw data. The only filters applied to these experimental data are those mentioned the previous chapter.

This strategy was selected to ensure that the optimised coefficients are as significant as possible in the temperature and pressure ranges of data existence. Consequently, data ranges little or not experimentally explored are usually reproduced less accurately by the fitted model coefficients.

In figures III-10 to III-15, series of experimental isotherms are reported both in the (X_{ES},$ln(\tilde{\eta})$) and (P, η) planes for pure methane and pure water. They can be compared with their prediction using our I-PC-SAFT based entropy-scaling model. To assess the model accuracy, relative deviations on viscosity were reported as a function of X_{ES}. Data were taken from the DDB.

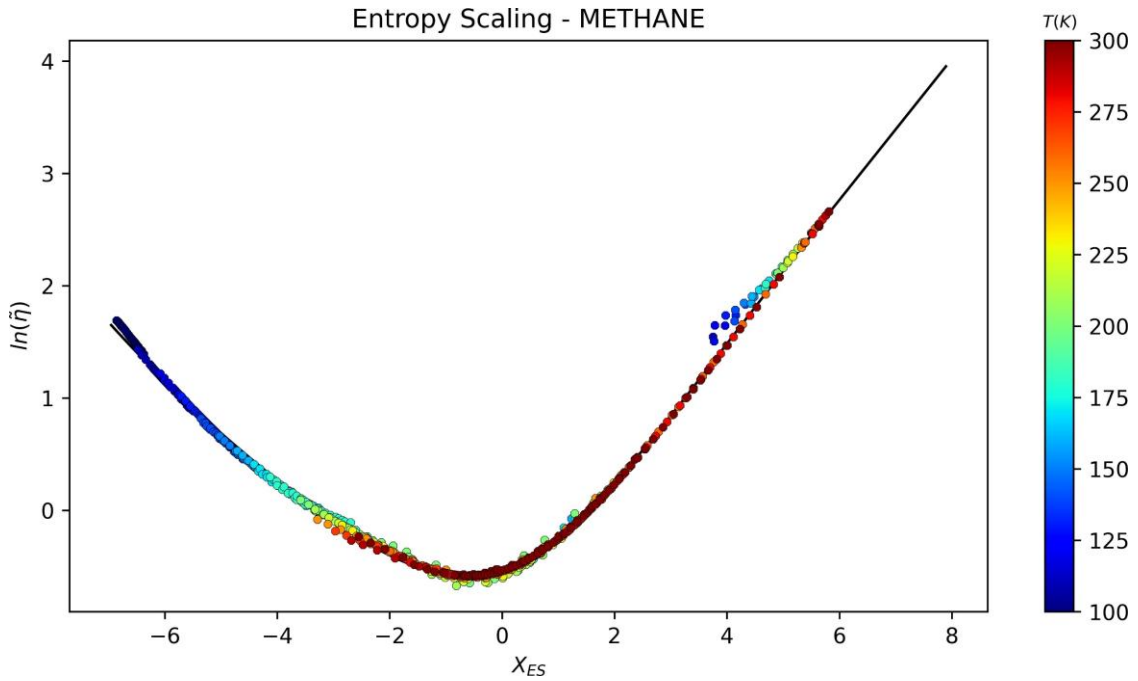

Figure III-10 - Superimposition of pure-methane isotherms in the (X_{ES},$ln(\tilde{\eta})$) plane. (●): experimental data; solid line: predictions using the *I*-PC-SAFT entropy-scaling based model developed in chapter 1.

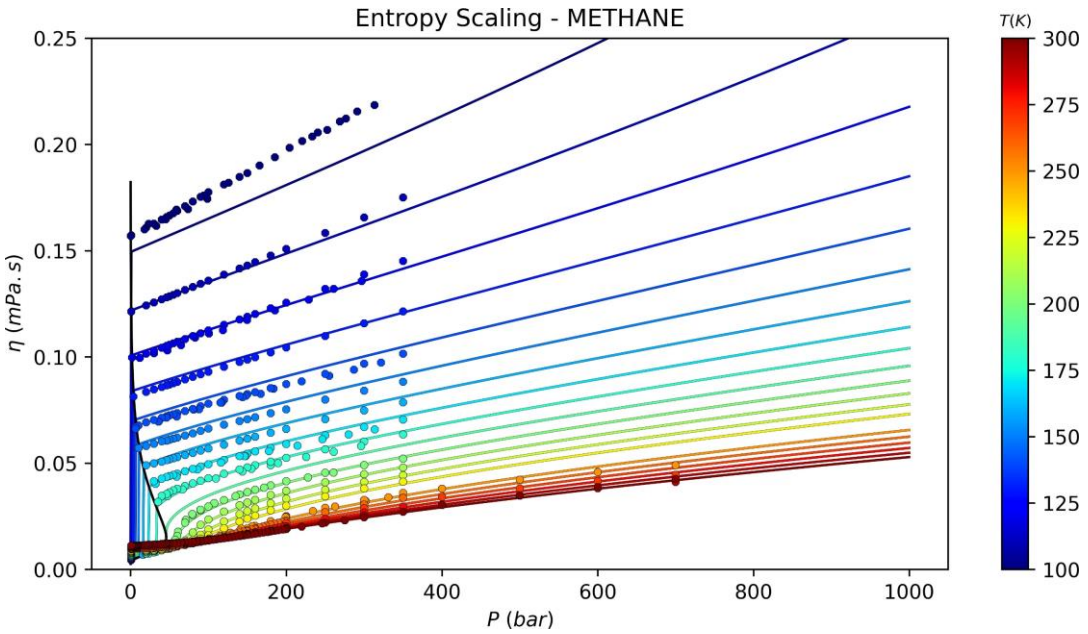

Figure III-11 - Pure-methane isotherms in the (pressure, viscosity) plane. (●): experimental data; solid line: predictions using the *I*-PC-SAFT entropy-scaling based model developed in chapter 1.

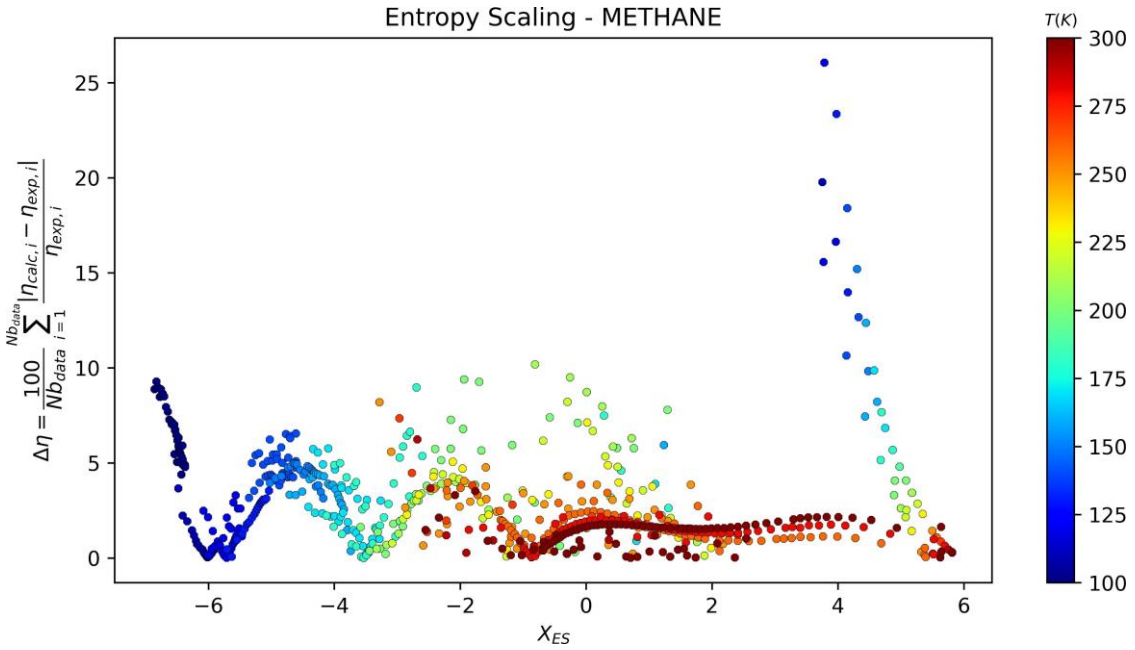

Figure III-12 - Deviations between experimental viscosity data and their prediction from I-PC-SAFT entropy- scaling based model. The experimental data considered are those reported in figures III-10 and III-11.

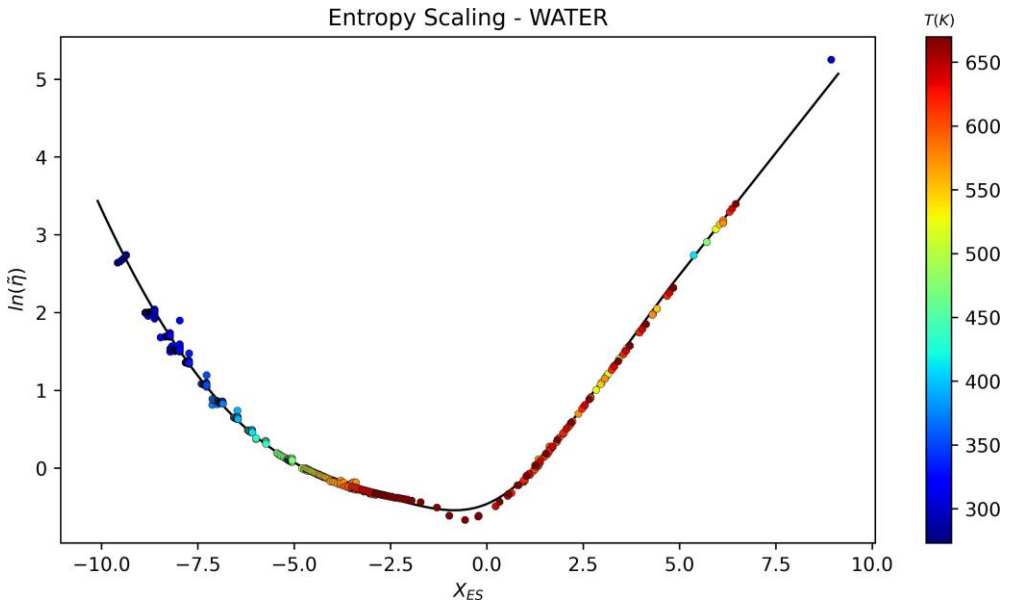

Figure III-13 - Superimposition of pure-water isotherms in the (X_{ES},$ln(\tilde{\eta})$) plane. (●): experimental data; solid line: predictions using the *I*-PC-SAFT entropy-scaling based model developed in chapter 1.

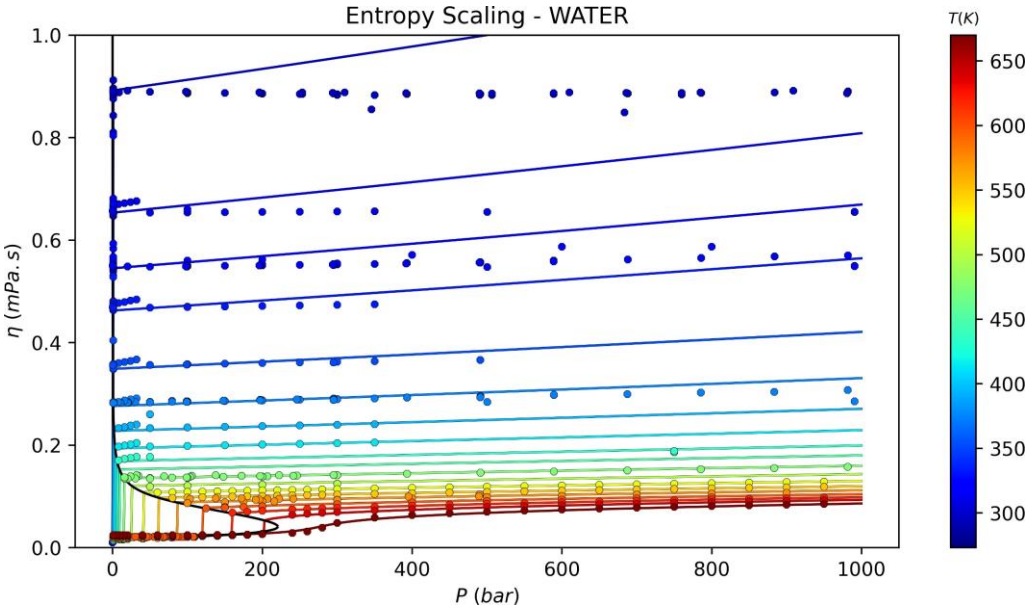

Figure III-14 - Pure-water isotherms in the (pressure, viscosity) plane. (●): experimental data; solid line: predictions using the *I*-PC-SAFT entropy-scaling based model developed in chapter 1.

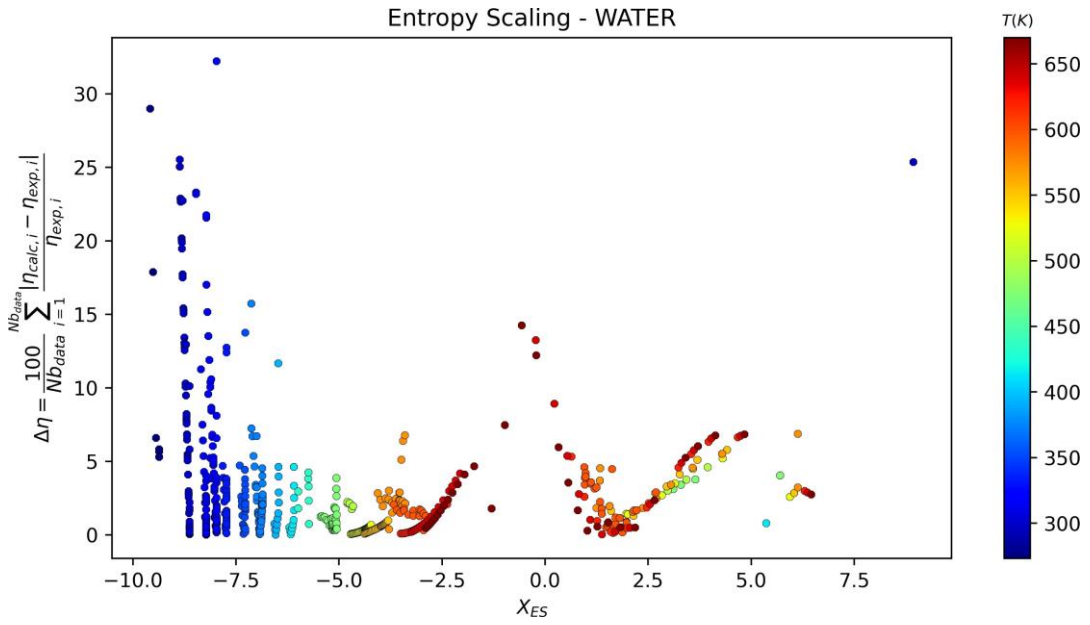

Figure III-15 - Deviations between experimental viscosity data and their prediction from I-PC-SAFT entropy- scaling based model. The experimental data considered are those reported in figures III-13 and III-14.

Although deviations increase in the high-density region (close to the triple point, i.e., for $X_{ES} \ll 0$), where equations of state also suffer from a lack of accuracy, figures III-12 and III-15 show that for most of fluid conditions, viscosity estimations from the I-PC-SAFT based model entropy-scaling based model are (very) satisfactory, lower than 5 %.

Model performance could be however improved for a given fluid and/or specific experimental conditions by:

- by selecting a more specific equation of state, including an association term for associating compounds like water or involving more parameters. The price to pay would be an increase of the model complexity through the increase of model parameters
- by selecting the experimental data in order to obtain equally-distributed experimental data. This would require to meticulously select experimental data and to be able to estimate their uncertainty and to use it in the fitting process

Note that this was not the aim of this study dedicated to propose a simple and broadly applicable approach.

III-C) *I*-PC-SAFT based model:

III-C-1) Equation of state parameters and viscosity experimental data informations:

PC-SAFT is a well-known equation of state, extensively described in the literature. For more information, the reader is referred to the original publication by Gross and Sadowski[82]. The difference between the PC-SAFT and the *I*-PC-SAFT model lies in (1) the way used to estimate the 3 molecular input parameters for a given non-associating compound (m, σ, ε), (2) the application of a Peneloux volume translation to the EoS.

More precisely, the 3 molecular parameters are constrained to exactly reproduce the experimental critical temperature and pressure and the vapor-pressure datum at a reduced temperature equal to 0.7. To do so, the following correlations were used:

$$\begin{cases} m_i \approx 0.5959\ \omega_{i,exp}^2 + 7.5437\omega_{i,exp} + 0.9729 \\ {\varepsilon_i}/{k_b} \approx {T_{c,i,exp}}/{(4.7968 \cdot 10^{-6} m_i^5 - 3.0895 \cdot 10^{-4} m_i^4 + 7.8649 \cdot 10^{-3} m_i^3 - 0.10215 \mathrm{m}_i^2 + 0.75358 m_i + 0.63659)} \\ \sigma_i \approx \left[{\varepsilon_i}/{k_b} \cdot \frac{k_b}{P_{c,i,exp}} 10^{(1.6345 \cdot 10^{-7} \mathrm{m}_i^6 - 1.1346 \cdot 10^{-5} m_i^5 + 3.1389 \cdot 10^{-4} m_i^4 - 4.4618 \cdot 10^{-3} m_i^3 + 3.6282 \cdot 10^{-2} \mathrm{m}_i^2 - 022498 m_i + 0.77655)} \right]^{1/3} \end{cases} \quad \text{(III-14)}$$

The application of a volume translation requires the knowledge of a component-dependent *c* parameter. It was determined in order to exactly reproduce the experimental saturated liquid molar volume at a reduced temperature of 0.8:

$$c = v_{liq}^{\mathrm{sat,u-EoS}}(T_r = 0.8) - v_{liq,exp}^{sat}(T_r = 0.8) \quad \text{(III-15)}$$

Where $v_{liq}^{sat,u-EoS}(T_r = 0.8)$ is the molar volume calculated with the original (untranslated) EoS at $T_r = 0.8$.

More details are available in the original paper introducing the *I*-PC-SAFT model[48]. The *I*-PC-SAFT parameters used in this study are reported in Table III-1.

Table III-1 - *I*-PC-SAFT EoS parameters and experimental viscosity data informations

		EoS parameters				Experimental viscosity data informations					
Name	CAS	m -	σ Å	$/k_b$ K	$c * 10^3$ m^3/mol	T_{min} K	T_{max} K	P_{min} MPa	P_{max} MPa	$\eta_{min} * 10^3$ $Pa.s$	$\eta_{max} * 10^3$ $Pa.s$
n-alkanes											
METHANE	74-82-8	1.0577	3.6335	145.557	0.0001	88.0	1050.0	0.0105	99.2433	0.0044	0.2220
ETHANE	74-84-0	1.74901	3.47261	181.204	0.0032	93.15	750.0	0.0267	78.4532	0.0081	1.1302
PROPANE	74-98-6	2.14983	3.61119	198.141	0.0074	88.1	750.0	0.0100	99.0472	0.0067	10.7221
n-BUTANE	106-97-8	2.51623	3.72001	211.407	0.0125	130.0	850.0	0.0267	70.0000	0.0073	2.5654
n-PENTANE	109-66-0	2.9127	3.80047	218.694	0.0195	137.15	900.0	0.0067	99.9900	0.0067	4.9900
n-HEXANE	110-54-3	3.30037	3.86477	224.08	0.0270	174.65	1000.0	0.0093	98.0665	0.0061	2.3900
n-HEPTANE	142-82-5	3.67922	3.91767	228.209	0.0342	180.15	620.0	0.0027	98.0600	0.0062	4.3800
n-OCTANE	111-65-9	4.0762	3.95828	230.949	0.0422	211.15	687.8	0.0093	99.9000	0.0069	3.3093
n-NONANE	111-84-2	4.4271	4.00172	234.238	0.0493	222.15	470.0	0.0980	98.0000	0.1850	2.8051
n-DECANE	124-18-5	4.82084	4.02795	236.136	0.0568	241.15	709.2	0.0500	98.0000	0.0074	2.4513
n-UNDECANE	1120-21-4	5.12925	4.07999	239.194	0.0660	246.65	520.15	0.0980	98.0000	0.1630	3.1700
n-DODECANE	112-40-3	5.50599	4.09659	240.655	0.0729	263.65	693.2	0.0500	97.1500	0.0074	3.6520
n-TRIDECANE	629-50-5	5.84391	4.14076	242.269	0.0841	263.05	503.15	0.0980	98.0000	0.2059	5.7700
n-TETRADECANE	629-59-4	6.0562	4.20981	246.012	0.0971	277.65	623.0	0.0500	80.0000	0.0070	4.7300
n-PENTADECANE	629-62-9	6.41709	4.2206	247.01	0.1037	293.15	543.16	0.0980	98.0000	0.1985	5.6000
n-HEXADECANE	544-76-3	6.67775	4.25727	249.329	0.1107	273.15	723.8	0.0500	99.6500	0.0073	6.1940
n-HEPTADECANE	629-78-7	7.11917	4.22813	249.246	0.1128	293.15	573.75	0.0980	98.0000	0.1985	7.0100
n-OCTADECANE	593-45-3	7.47364	4.23565	249.618	0.1194	305.15	583.15	0.0980	92.2000	0.2063	7.0000
n-NONADECANE	629-92-5	7.82356	4.2398	250.213	0.1247	313.15	603.15	0.0980	49.1500	0.1958	3.9570
n-EICOSANE	112-95-8	8.29483	4.20835	249.693	0.1213	310.6	613.15	0.0980	83.0000	0.1984	4.6420
n-HENEICOSANE	629-94-7	8.5998	4.22042	250.647	0.1292	323.15	496.65	0.0980	49.0000	0.4330	4.6000
n-DOCOSANE	629-97-0	8.86315	4.24425	251.658	0.1371	323.2	510.65	0.0980	49.0000	0.4240	4.1490
n-DOTRIACONTANE	544-85-4	12.4964	4.16931	253.235	0.1350	346.7	466.3	0.1000	0.3000	1.1680	6.5290
branched alkanes											
ISOBUTANE	75-28-5	2.38849	3.78831	207.777	0.0115	115.0	850.0	0.0223	68.6500	0.0069	9.3029
ISOPENTANE	78-78-4	2.72976	3.85923	220.615	0.0165	117.99	750.0	0.0015	98.0700	0.0069	21.6200
NEOPENTANE	463-82-1	2.4816	3.98539	217.112	0.0131	258.15	444.26	0.0500	99.0472	0.0079	0.5330
2,2-DIMETHYLBUTANE	75-83-2	2.77755	4.02794	232.508	0.0171	269.29	351.15	0.0500	88.2599	0.0076	0.7360
2,3-DIMETHYLBUTANE	79-29-8	2.89521	3.97732	233.416	0.0198	273.14	343.15	0.0981	88.2599	0.2132	0.6560
2-METHYLPENTANE	107-83-5	3.12767	3.90878	224.726	0.0221	143.15	485.65	0.0981	88.2599	0.0089	6.8668
3-METHYLPENTANE	96-14-0	3.05811	3.92458	230.038	0.0231	265.62	343.16	0.0981	88.2599	0.1980	0.5384
2,4-DIMETHYLPENTANE	108-08-7	3.30809	4.0227	229.245	0.0286	288.15	335.8	0.0981	88.2599	0.2377	0.6100
3-ETHYLPENTANE	617-78-7	3.3614	3.98054	236.849	0.0271	293.15	313.15	0.0981	88.2599	0.3070	0.6250
2,2,4-TRIMETHYLPENTANE	540-84-1	3.31755	4.16748	239.547	0.0292	173.15	548.15	0.0093	99.9000	0.0073	7.7700
2,3,4-TRIMETHYLPENTANE	565-75-3	3.41042	4.09852	246.683	0.0303	273.15	453.15	0.1000	80.0000	0.2770	1.2420

Continued on next page

Table III-1 – continued from previous page

Name	CAS	m -	σ Å	$/k_b$ K	$c * 10^3$ m^3/mol	T_{min} K	T_{max} K	P_{min} MPa	P_{max} MPa	$\eta_{min} * 10^3$ $Pa.s$	$\eta_{max} * 10^3$ $Pa.s$
2,3-DIMETHYLHEXANE	584-94-1	3.64816	4.04059	238.85	0.0345	273.15	313.15	0.1000	0.1000	0.3980	0.6430
2,2,4,4,6,8,8-HEPTAMETHYLNONANE	4390-04-9	5.27494	4.45318	256.641	0.0814	293.15	453.15	0.1000	80.0000	0.4210	15.9200
SQUALANE	111-01-3	8.36784	4.80043	279.955	0.1518	273.15	473.06	0.1000	98.8000	0.8530	442.3000
cycloalkanes											
CYCLOPENTANE	287-92-3	2.47558	3.75741	256.389	0.0139	218.74	449.1	0.0093	90.4000	0.0099	1.4380
CYCLOHEXANE	110-82-7	2.57692	3.93344	272.395	0.0152	273.15	673.15	0.0027	98.0665	0.0072	1.7920
CYCLOHEPTANE	291-64-5	2.83005	4.00491	284.904	0.0185	291.9	392.15	0.1000	40.1000	0.4250	2.9250
CYCLOOCTANE	292-64-8	2.91927	4.14912	301.043	0.0233	283.15	478.1	0.0093	40.1000	0.0070	3.2660
alkenes											
ETHYLENE	74-85-1	1.6482	3.41383	172.685	0.0026	105.0	575.15	0.0500	91.1925	0.0065	0.6600
PROPYLENE	115-07-1	2.03793	3.56538	200.642	0.0063	88.7	520.0	0.0068	80.0000	0.0052	14.4600
1-BUTENE	106-98-9	2.39595	3.69567	213.423	0.0111	103.15	263.15	0.1000	0.1000	0.1962	7.3583
1-PENTENE	109-67-1	2.80199	3.77011	220.139	0.0167	123.15	298.15	0.1000	0.1000	0.2085	5.6853
1-HEXENE	592-41-6	3.17425	3.83408	226.151	0.0222	133.15	473.15	0.0093	98.0600	0.0068	10.2780
1-HEPTENE	592-76-7	3.62973	3.84822	228.247	0.0273	163.15	490.0	0.0980	98.0600	0.0830	4.2843
1-OCTENE	111-66-0	4.0173	3.88808	231.485	0.0328	183.15	490.0	0.0980	98.0600	0.1280	3.9222
1-NONENE	124-11-8	4.37319	3.93983	234.685	0.0402	193.15	473.0	0.1000	50.0000	0.1440	10.5700
1-DECENE	872-05-9	4.72488	3.98774	237.365	0.0484	213.15	475.02	0.0980	98.0600	0.2011	4.4888
1-UNDECENE	821-95-4	5.06535	4.03419	239.748	0.0576	243.15	463.15	0.1000	0.1000	0.2019	2.8194
1-DODECENE	112-41-4	5.3878	4.08086	242.017	0.0673	243.15	483.15	0.1000	0.1000	0.2005	4.0253
1-TRIDECENE	2437-56-1	5.76092	4.10936	243.281	0.0767	263.15	503.15	0.1000	0.1000	0.1973	3.1259
1-TETRADECENE	1120-36-1	6.11674	4.13887	244.562	0.0870	273.15	523.15	0.1000	0.1000	0.1923	3.1045
1-PENTADECENE	13360-61-7	6.37683	4.14935	247.471	0.0836	273.15	533.15	0.1000	0.1000	0.2046	4.1104
1-HEXADECENE	629-73-2	6.73512	4.16202	248.371	0.0902	273.15	553.15	0.1000	0.1000	0.1977	5.4080
1-HEPTADECENE	6765-39-5	6.95515	4.19884	250.88	0.0938	303.15	563.15	0.1000	0.1000	0.2021	2.9120
alkynes											
ACETYLENE	74-86-2	2.44726	2.8751	155.302	0.0062	273.1	609.8	0.0133	10.1325	0.0094	0.0250
METHYLACETYLENE	74-99-7	2.60373	3.16481	196.989	0.0091	223.15	248.15	0.1000	0.1000	0.2200	0.2850
1-HEXYNE	693-02-7	3.54707	3.56485	221.268	0.0173	293.15	333.15	0.1000	0.1000	0.2420	0.3730
aromatics											
BENZENE	71-43-2	2.59421	3.71133	275.605	0.0151	273.15	673.15	0.0027	99.3000	0.0073	1.2580
TOLUENE	108-88-3	3.00982	3.79765	271.622	0.0233	169.6	673.15	0.0069	39.4120	0.0078	32.6000
m-XYLENE	108-38-3	3.4982	3.83078	265.958	0.0326	273.15	673.15	0.0981	98.0665	0.0102	1.1160
p-XYLENE	106-42-3	3.4617	3.85493	266.746	0.0332	273.15	673.15	0.0160	98.0665	0.0084	0.8880
ETHYLBENZENE	100-41-4	3.31766	3.88181	271.854	0.0292	191.4	673.15	0.1000	97.5200	0.0102	7.6400
MESITYLENE	108-67-8	4.0682	3.81367	258.999	0.0394	278.15	393.15	0.1000	51.5700	0.2770	0.9804
p-CYMENE	99-87-6	3.87147	4.06267	270.02	0.0456	290.15	413.15	0.0981	98.0665	0.3700	1.6190
n-HEPTYLBENZENE	1078-71-3	5.10359	4.08749	267.715	0.0634	293.15	353.15	0.1000	80.0000	0.8340	4.5100

Continued on next page

Table III-1 – continued from previous page

Name	CAS	m -	σ Å	$/k_b$ K	$c * 10^3$ m^3/mol	T_{min} K	T_{max} K	P_{min} MPa	P_{max} MPa	$\eta_{min} * 10^3$ $Pa.s$	$\eta_{max} * 10^3$ $Pa.s$
n-NONYLBENZENE	1081-77-2	5.97361	4.06633	264.16	0.0696	253.15	423.15	0.1000	40.0000	0.5600	12.9000
n-DODECYLBENZENE	123-01-3	6.81164	4.17615	267.456	0.0871	298.15	363.15	0.1000	80.0000	1.4210	11.9000
esters											
VINYL ACETATE	108-05-4	3.69372	3.41496	218.966	0.0307	273.25	373.15	0.1000	80.0000	0.2922	0.6790
n-PROPYL ACETATE	109-60-4	3.99149	3.57019	225.022	0.0337	273.15	494.16	0.0980	49.0000	0.0820	0.8010
n-BUTYL ACETATE	123-86-4	4.39448	3.59226	227.28	0.0322	273.15	492.46	0.0980	49.0000	0.1370	1.1035
ISOPENTYL ACETATE	123-92-2	4.79042	3.62822	224.546	0.0356	282.12	500.0	0.1000	50.1000	0.0105	1.1440
n-PENTYL ACETATE	628-63-7	4.46172	3.75548	235.665	0.0408	288.15	502.9	0.1000	50.1000	0.0083	1.1980
n-HEPTYL ACETATE	112-06-1	5.65343	3.69206	231.019	0.0414	283.15	500.0	0.1000	50.1000	0.0091	2.1400
ethers											
DIMETHYL ETHER	115-10-6	2.51666	3.24729	198.949	0.0083	227.22	423.15	0.1000	30.0000	0.0091	0.2589
METHYL tert-BUTYL ETHER	1634-04-4	2.87421	3.92426	232.807	0.0245	273.15	323.15	0.1000	0.1013	0.2760	0.4465
DI-n-PROPYL ETHER	111-43-3	3.83168	3.70975	220.622	0.0239	273.5	513.0	0.1000	58.8600	0.0610	0.6640
DI-n-BUTYL ETHER	142-96-1	4.4607	3.87277	229.477	0.0384	243.15	373.15	0.1000	21.1200	0.2900	2.2209
DI-n-PENTYL ETHER	693-65-2	5.70995	3.78253	224.872	0.0451	273.15	373.15	0.0981	98.0665	0.4100	2.3210
ketones											
ACETONE	67-64-1	3.3416	3.32279	223.197	0.0263	180.65	579.55	0.0027	98.0665	0.0078	2.1500
3-PENTANONE	96-22-0	3.64275	3.5897	237.909	0.0293	273.15	473.15	0.1000	98.0000	0.1460	1.0190
2-HEXANONE	591-78-6	3.95752	3.68916	241.311	0.0359	293.15	473.15	0.0980	98.0000	0.1950	1.3000
METHYL ISOBUTYL KETONE	108-10-1	3.72819	3.75161	241.481	0.0330	273.15	473.15	0.1000	80.0000	0.3160	1.3380
4-HEPTANONE	123-19-3	4.17521	3.79044	242.291	0.0402	273.0	473.0	0.1000	90.0000	0.1860	2.0000
2-OCTANONE	111-13-7	4.51877	3.86525	247.423	0.0482	288.15	473.15	0.0981	98.0660	0.2100	1.9800
HFC-CFC											
DIFLUOROMETHANE	75-10-5	3.11199	2.81359	158.941	0.0149	200.28	423.15	0.1000	50.0000	0.0108	0.5353
1,1-DIFLUOROETHANE	75-37-6	3.09574	3.15939	175.251	0.0189	200.21	423.15	0.1000	17.7000	0.0092	0.5907
TRIFLUOROMETHANE	75-46-7	3.01086	2.86827	137.23	0.0124	117.88	473.08	0.0979	58.9600	0.0101	1.9600
1,1,1-TRIFLUOROETHANE	420-46-2	2.98968	3.27705	159.225	0.0189	223.65	423.15	0.1000	10.0700	0.0111	0.2986
CHLORODIFLUOROMETHANE	75-45-6	2.66318	3.18061	178.941	0.0107	120.0	473.15	0.0960	60.0000	0.0103	7.8360
CARBON TETRAFLUORIDE	75-73-0	2.35371	3.10487	116.72	0.0038	203.15	873.0	0.1000	41.4916	0.0124	0.0883
1-CHLORO-1,1-DIFLUOROETHANE	75-68-3	2.75137	3.48938	195.907	0.0151	208.15	423.15	0.1000	5.0920	0.0105	0.6980
1,1,1,2-TETRAFLUOROETHANE	811-97-2	3.50128	3.09804	161.233	0.0168	175.0	438.15	0.0920	90.0000	0.0108	1.8410
DICHLOROFLUOROMETHANE	75-43-4	2.55216	3.40426	223.099	0.0107	193.15	473.15	0.0982	58.9200	0.0107	1.2320
CHLOROTRIFLUOROMETHANE	75-72-9	2.29771	3.40327	156.714	0.0067	93.1	433.31	0.1000	60.0000	0.0107	11.0420
PENTAFLUOROETHANE	354-33-6	3.33167	3.17152	149.142	0.0132	176.0	423.15	0.0900	53.0700	0.0103	1.0990
DICHLORODIFLUOROMETHANE	75-71-8	2.35936	3.57957	197.271	0.0086	117.6	575.0	0.0400	60.0000	0.0105	6.5700
1,1,1,3,3-PENTAFLUOROPROPANE	460-73-1	3.88501	3.22888	176.684	0.0177	263.15	396.46	0.1000	40.0000	0.0112	1.0153
TRICHLOROFLUOROMETHANE	75-69-4	2.4333	3.7056	237.998	0.0101	163.5	503.15	0.0983	60.0000	0.0113	5.2730
BROMOTRIFLUOROMETHANE	75-63-8	2.28781	3.51621	176.876	0.0079	101.95	448.15	0.1000	60.0000	0.0124	10.0050

Continued on next page

Table III-1 – continued from previous page

Name	CAS	m -	σ Å	$/k_b$ K	$c * 10^3$ m^3/mol	T_{min} K	T_{max} K	P_{min} MPa	P_{max} MPa	$\eta_{min} * 10^3$ $Pa.s$	$\eta_{max} * 10^3$ $Pa.s$
1,1,1,3,3,3-HEXAFLUOROPROPANE	690-39-1	4.00387	3.24822	162.751	0.0170	253.15	373.39	0.1000	40.0000	0.0110	0.8347
CHLOROPENTAFLUOROETHANE	76-15-3	2.91198	3.53216	164.446	0.0106	176.92	473.08	0.0979	58.9600	0.0104	1.5850
1,1,1,2,3,3,3-HEPTAFLUOROPROPANE	431-89-0	3.72471	3.38323	157.584	0.0185	243.16	371.78	0.1000	11.4900	0.0119	0.6250
1,2-DICHLOROTETRAFLUOROETHANE	76-14-2	2.91691	3.69685	194.896	0.0144	182.96	473.15	0.0979	58.9600	0.0113	2.6720
noble gases											
NEON	7440-01-9	0.666762	3.43647	39.3203	0.0025	20.43	2000.0	0.0013	99.2782	0.0034	0.1710
ARGON	7440-37-1	0.952492	3.44081	120.823	-0.0003	76.5	2100.0	0.0067	99.9000	0.0065	0.4798
KRYPTON	7439-90-9	0.952492	3.69199	167.668	0.0003	116.09	2000.0	0.0049	95.0000	0.0109	0.4582
XENON	7440-63-3	0.952492	4.03334	232.052	0.0012	153.2	2000.0	0.0067	95.0000	0.0125	0.7300
aldehydes											
ACETALDEHYDE	75-07-0	2.99801	3.17297	214.263	0.0206	273.15	350.95	0.0027	96.5263	0.0090	0.4889
PROPANAL	123-38-6	3.14408	3.30974	226.884	0.0214	273.15	320.95	0.1000	96.5263	0.2540	0.6227
2-METHYLPROPANAL	78-84-2	3.77964	3.31985	211.932	0.0237	293.15	501.88	0.1000	96.5263	0.1870	0.8411
BUTANAL	123-72-8	3.15421	3.53111	241.692	0.0230	283.0	495.13	0.0980	98.0000	0.2160	1.0500
3-METHYLBUTYRALDEHYDE	590-86-3	3.93688	3.4223	223.52	0.0201	294.25	358.15	0.1000	96.5263	0.2798	1.1058
HEPTANAL	111-71-7	4.12557	3.74553	250.649	0.0326	288.15	303.15	0.1000	96.5263	0.7910	1.6159
DECANAL	112-31-2	5.04583	3.79828	253.684	0.0210	293.87	318.15	0.1000	96.5263	1.2810	2.4778
amines											
METHYLAMINE	74-89-5	3.14535	2.75453	193.715	0.0110	194.85	673.0	0.0021	24.5166	0.0094	0.9120
n-PROPYLAMINE	107-10-8	3.13305	3.36706	224.224	0.0172	283.15	318.15	0.1000	51.8000	0.2910	0.5227
n-BUTYLAMINE	109-73-9	3.51929	3.43663	228.722	0.0184	278.15	348.15	0.1000	71.7500	0.2764	0.7690
DIETHYLAMINE	109-89-7	3.32069	3.57629	218.67	0.0234	288.15	353.15	0.1000	80.0000	0.5520	2.0740
n-PENTYLAMINE	110-58-7	4.13555	3.45949	224.169	0.0245	278.15	353.15	0.1000	80.0000	0.3104	1.2030
n-HEXYLAMINE	111-26-2	4.54125	3.53019	227.974	0.0303	278.15	373.15	0.1000	80.0000	0.3260	1.5610
alcohols											
METHANOL	67-56-1	5.41942	2.3078	188.401	0.0143	174.85	550.0	0.0027	99.7000	0.0101	13.9000
ETHANOL	64-17-5	6.06069	2.41836	182.427	0.0171	143.15	540.0	0.0815	98.0665	0.0108	467.0000
1-PROPANOL	71-23-8	5.87288	2.63227	192.371	0.0171	223.15	550.0	0.0815	98.2000	0.0099	21.6000
1-BUTANOL	71-36-3	5.60376	2.87407	204.791	0.0194	193.15	473.15	0.0815	98.0665	0.0092	217.6000
1-PENTANOL	71-41-0	5.49323	3.06448	215.25	0.0224	243.0	403.15	0.0981	80.0000	0.3900	24.5000
1-HEXANOL	111-27-3	5.36018	3.26659	225.525	0.0288	243.15	428.15	0.1000	50.2700	0.3400	35.5000
1-HEPTANOL	111-70-6	5.38889	3.42028	232.867	0.0244	243.15	435.05	0.1000	80.0000	0.3700	54.0000
1-OCTANOL	111-87-5	5.45109	3.56005	239.341	0.0367	283.15	603.15	0.1000	60.0000	0.1070	13.5200
1-NONANOL	143-08-8	5.56917	3.67874	244.479	0.0491	283.15	603.15	0.1000	60.0000	0.1500	17.4390
1-DECANOL	112-30-1	5.7579	3.77158	248.081	0.0531	283.15	593.15	0.1000	60.0000	0.1560	22.0640
1-UNDECANOL	112-42-5	5.8954	3.87226	251.955	0.0603	293.15	593.15	0.1000	60.0000	0.2070	17.2840
1-DODECANOL	112-53-8	6.16047	3.93338	253.817	0.0702	293.15	595.65	0.1000	60.0000	0.4140	19.7457
1-TETRADECANOL	112-72-1	6.67277	4.0467	257.074	0.0850	312.0	373.15	0.1000	0.1013	2.2000	13.0000

Continued on next page

Table III-1 – continued from previous page

Name	CAS	m -	σ Å	$/k_b$ K	$c * 10^3$ m^3/mol	T_{min} K	T_{max} K	P_{min} MPa	P_{max} MPa	$\eta_{min} * 10^3$ Pa.s	$\eta_{max} * 10^3$ Pa.s
1-OCTADECANOL	112-92-5	7.65199	4.24227	262.084	0.1255	333.15	423.15	0.0981	98.0665	1.2400	11.6000
others											
HYDROGEN	1333-74-0	0.421592	5.64646	24.8714	0.0163	14.0	1200.0	0.0010	99.5012	0.0007	0.0378
AMMONIA	7664-41-7	2.92125	2.41696	188.631	0.0089	203.15	989.15	0.0013	81.0600	0.0080	0.4750
WATER	7732-18-5	3.64287	2.08351	274.442	0.0071	251.15	2073.15	0.0012	99.5400	0.0097	4.9100
CARBON MONOXIDE	630-08-0	1.3574	3.21074	89.7577	-0.0002	68.55	911.0	0.0255	91.2938	0.0053	0.2870
NITROGEN	7727-37-9	1.27492	3.25959	87.9687	-0.0004	63.15	2150.0	0.0013	99.8200	0.0054	0.3914
OXYGEN	7782-44-7	1.14932	3.1795	113.452	-0.0001	54.4	1300.0	0.0015	78.4532	0.0054	0.8730
HYDROGEN SULFIDE	7783-06-4	1.70885	3.05537	224.31	0.0020	190.1	413.15	0.1000	50.0000	0.0125	0.5470
CARBON DIOXIDE	124-38-9	2.69691	2.60169	146.566	0.0049	190.0	1794.0	0.0067	99.8200	0.0097	0.3223
CHLOROFORM	67-66-3	2.68365	3.4792	259.011	0.0094	209.65	618.5	0.0046	99.6000	0.0128	1.9615

III-C-2) Component-specific parameters

Component-specific parameters (a_1, a_2, b_1, b_2, c and d) to be used in the below equation for the viscosity estimation are reported in table III-2.

$$\begin{cases} \ln\left(\frac{\eta}{\eta_{\mathrm{ref}}}\right)_{\mathrm{calc}} = \left[\left(\frac{a_1 + a_2\tilde{s}_{\mathrm{Tv-res}}}{1 + e^{cX_{\mathrm{ES}}}}\right) + \left(\frac{b_1 + b_2\tilde{s}_{\mathrm{Tv-res}}}{1 + e^{-cX_{\mathrm{ES}}}}\right)\right] X_{ES} + \frac{d}{\tilde{s}^{c}_{\mathrm{Tv-res}}} \\ X_{\mathrm{ES}} = -\left(\frac{s_{\mathrm{Tv-res}}}{s^{c}_{\mathrm{Tv-res}}}\right) - \ln\left(\frac{s_{\mathrm{Tv-res}}}{s^{c}_{\mathrm{Tv-res}}}\right) \\ \eta_{\mathrm{ref}} = \rho_{\mathrm{N}}^{2/3}\sqrt{\mathrm{m_0 k_b} T} \\ \tilde{s}_{\mathrm{Tv-res}} = \frac{s_{Tv-res}}{R} \end{cases} \quad \text{(III– 16)}$$

The Tv-residual entropy ($s_{\mathrm{Tv-res}}$) and the molecular density (ρ_{N}) were estimated using the *I*-PC-SAFT EoS.

Table III-2 - Component-specific parameters suitable for the *I*-PC-SAFT based model with the corresponding number of experimental data points and MAPE

Name	a_1	a_2	b_1	b_2	c	d	Data number	MAPE
n-alkanes							28105	3.11
METHANE	-0.054052	0.057284	0.577169	0.370991	0.513952	0.411486	3693	2.57
ETHANE	-0.077385	0.038358	0.563557	0.465858	0.609433	0.499328	3492	2.42
PROPANE	-0.091159	0.035387	0.587049	0.453097	0.542424	0.559930	3209	2.73
n-BUTANE	-0.214898	0.019051	0.565843	0.145485	0.808949	0.656786	1653	2.36
n-PENTANE	-0.153319	0.023466	0.557434	0.310143	0.660749	0.590314	2321	3.51
n-HEXANE	-0.155260	0.021596	0.556342	0.245134	0.611479	0.561363	2205	2.85
n-HEPTANE	-0.176902	0.019705	0.525655	0.091137	0.758887	0.594146	2291	2.68
n-OCTANE	-0.172956	0.019552	0.562592	0.190209	0.604875	0.658158	1900	2.58
n-NONANE	-0.212709	0.016146	0.159905	0.090961	2.400777	0.769518	766	2.37
n-DECANE	-0.268659	0.012767	0.586567	0.089148	2.756547	1.099282	1608	2.45
n-UNDECANE	-0.294529	0.011207	0.917902	0.238181	2.812801	1.298742	668	3.27
n-DODECANE	-0.231109	0.014081	0.552507	0.025095	0.858382	0.885632	1129	3.64
n-TRIDECANE	-0.281034	0.010807	0.722362	0.409981	1.886814	1.169567	195	4.84
n-TETRADECANE	-0.241798	0.013487	0.569195	0.151989	1.012786	1.040545	843	5.92
n-PENTADECANE	-0.213518	0.013010	0.491825	0.331752	2.626228	0.692914	226	5.80
n-HEXADECANE	-0.233624	0.014151	0.582260	0.460848	2.840359	1.119793	601	7.62
n-HEPTADECANE	-0.272035	0.010850	0.709956	0.348576	1.035669	1.312986	361	5.88
n-OCTADECANE	-0.194241	0.012493	0.384352	0.199204	2.218807	0.528248	416	6.28
n-NONADECANE	-0.145187	0.014569	0.765571	0.401980	1.681107	0.253272	309	4.98
n-EICOSANE	-0.116534	0.015778	0.988258	0.004388	3.000000	0.000010	138	5.04
n-HENEICOSANE	-0.246881	0.010962	0.341524	0.157937	2.943342	1.292534	39	9.18
n-DOCOSANE	-0.122095	0.015097	0.815008	0.191410	2.071020	0.184983	30	6.65
n-DOTRIACONTANE	-0.194929	0.009702	0.184696	0.027353	2.233454	0.546968	12	2.53
branched alkanes							4778	4.39
ISOBUTANE	-0.182116	0.030142	0.551316	0.323695	0.797773	0.630939	1943	2.93
ISOPENTANE	-0.108787	0.032654	0.564354	0.300737	0.627684	0.493520	863	3.48
NEOPENTANE	-0.197221	0.039826	0.546790	0.015798	2.035983	0.615072	77	3.11
2,2-DIMETHYLBUTANE	-0.229181	0.026897	0.573079	0.000010	2.706854	0.706622	23	1.20
2,3-DIMETHYLBUTANE	-0.240975	0.020995	0.587731	0.189775	2.675197	0.799515	92	1.55
2-METHYLPENTANE	-0.071261	0.027215	0.521427	0.199856	0.458857	0.176841	127	1.88
3-METHYLPENTANE	-0.267489	0.013496	0.689824	0.122334	2.653371	0.912765	108	0.99
2,4-DIMETHYLPENTANE	-0.187330	0.013730	0.564520	0.198386	0.357967	0.511182	15	1.25
3-ETHYLPENTANE	-0.366786	0.004157	0.614059	0.108918	0.630637	1.332715	7	0.87
2,2,4-TRIMETHYLPENTANE	-0.070638	0.029977	0.530967	0.200000	0.420944	0.117418	899	1.62
2,3,4-TRIMETHYLPENTANE	-0.052310	0.029768	0.509082	0.181140	0.436574	0.042686	23	5.59
2,3-DIMETHYLHEXANE	-0.448291	0.000200	0.691761	0.131829	0.442916	1.699942	16	1.48
2,2,4,4,6,8,8-HEPTAMETHYLNONANE	-0.080736	0.027827	0.537603	0.185324	0.436507	0.188156	161	3.65

Continued on next page

Table III-2 – continued from previous page

Name	a_1	a_2	b_1	b_2	c	d	Data number	MAPE
SQUALANE	-0.109993	0.016779	0.554859	0.173071	2.833187	0.000010	424	21.91
cycloalkanes							2142	3.24
CYCLOPENTANE	-0.378037	0.012189	0.682527	0.199977	1.562375	1.220129	266	0.82
CYCLOHEXANE	0.030331	0.071878	0.600136	0.739110	0.582655	0.616680	1732	3.68
CYCLOHEPTANE	0.065422	0.067149	0.526185	0.142739	1.786579	0.011659	62	2.43
CYCLOOCTANE	-0.042055	0.055022	0.500053	0.091445	1.262836	0.274847	82	2.29
alkenes							3178	3.19
ETHYLENE	-0.106644	0.038208	0.564195	0.350180	0.607574	0.458509	974	2.88
PROPYLENE	0.066286	0.052196	0.568249	0.598500	0.459916	0.438551	662	3.94
1-BUTENE	-0.047807	0.030493	0.552223	0.187703	0.563217	0.051114	19	3.10
1-PENTENE	-0.036418	0.027822	0.500001	0.199997	0.484683	0.000016	19	3.57
1-HEXENE	-0.037576	0.029887	0.504897	0.096225	2.433730	0.105832	461	5.13
1-HEPTENE	-0.141569	0.019115	0.508534	0.199153	0.412155	0.638555	331	2.09
1-OCTENE	-0.063155	0.022039	0.500000	0.139361	0.385857	0.000103	322	2.49
1-NONENE	0.013533	0.029626	0.511472	0.197118	0.387863	0.131358	107	4.34
1-DECENE	0.030659	0.028071	0.513237	0.200000	0.347198	0.000010	70	2.55
1-UNDECENE	-0.022411	0.025710	0.514666	0.189767	0.403574	0.141308	23	0.15
1-DODECENE	-0.133311	0.019626	0.545616	0.091486	0.913889	0.384690	44	0.89
1-TRIDECENE	-0.129319	0.019041	0.582463	0.124685	0.730275	0.356135	25	0.18
1-TETRADECENE	-0.106587	0.019784	0.511984	0.142398	0.571321	0.304529	26	0.16
1-PENTADECENE	-0.046931	0.022792	0.500103	0.168363	0.454677	0.164083	27	0.19
1-HEXADECENE	0.010049	0.025105	0.559641	0.194466	0.433329	0.000010	41	0.79
1-HEPTADECENE	-0.100424	0.018579	0.516026	0.103226	0.641413	0.092645	27	0.14
alkynes							160	2.31
ACETYLENE	-0.371503	0.000045	0.585341	-0.322563	0.507476	0.466353	148	2.50
METHYLACETYLENE	-0.309253	0.000012	0.520145	0.083111	0.438132	0.646956	2	0.00
1-HEXYNE	-0.236380	0.015577	0.657473	0.064724	0.547380	0.723993	10	0.04
aromatics							5660	2.51
BENZENE	-0.122131	0.040626	0.590348	0.309023	0.720466	0.667885	2296	2.41
TOLUENE	-0.128930	0.030384	0.564118	0.553610	1.387180	0.718135	437	5.00
m-XYLENE	-0.201608	0.016095	0.567602	-0.071592	1.000018	0.807556	857	1.37
p-XYLENE	-0.185178	0.019149	0.594124	0.088723	0.862959	0.790985	838	1.36
ETHYLBENZENE	-0.198473	0.018214	0.558299	0.482131	1.176220	0.739201	959	3.46
MESITYLENE	-0.121944	0.019107	0.603045	0.035577	2.109824	0.450815	165	2.05
p-CYMENE	-0.164543	0.012017	0.524429	0.198000	2.402824	0.000038	21	4.32
n-HEPTYLBENZENE	-0.099660	0.019463	0.574214	0.188713	0.362207	0.486152	35	3.51
n-NONYLBENZENE	0.020593	0.025436	0.500019	0.199966	0.380033	0.000161	27	5.80
n-DODECYLBENZENE	-0.012206	0.020609	0.629606	0.199855	0.371937	0.000029	25	6.95
esters							1013	3.18

Continued on next page

Table III-2 – continued from previous page

Name	a_1	a_2	b_1	b_2	c	d	Data number	MAPE
VINYL ACETATE	-0.089657	0.026130	0.689898	0.173726	2.393476	0.288704	30	0.81
n-PROPYL ACETATE	-0.196364	0.013931	0.606123	0.180224	0.278342	0.799306	193	3.37
n-BUTYL ACETATE	-0.144083	0.012972	0.520200	0.117990	0.207340	0.068415	291	1.97
ISOPENTYL ACETATE	-0.090742	0.016320	0.655233	0.181695	0.298190	0.183003	131	4.89
n-PENTYL ACETATE	-0.135241	0.025572	0.542054	0.160131	1.082717	0.780619	217	4.33
n-HEPTYL ACETATE	-0.163101	0.019681	0.555080	0.152132	0.897916	0.795565	151	2.63
ethers							494	2.48
DIMETHYL ETHER	-0.087716	0.035716	0.565191	0.337907	0.745279	0.597934	119	0.77
METHYL tert-BUTYL ETHER	-0.249832	0.003041	0.500064	0.199955	0.406644	0.297419	66	5.59
DI-n-PROPYL ETHER	-0.406534	0.000030	0.500000	0.199996	0.535939	1.547131	185	3.14
DI-n-BUTYL ETHER	-0.052108	0.026980	0.563274	0.200000	1.222858	0.000012	100	1.36
DI-n-PENTYL ETHER	-0.073083	0.021913	0.597450	0.063369	2.077188	0.000010	24	1.96
ketones							1101	3.68
ACETONE	-0.058017	0.026407	0.540329	0.194494	0.475416	0.215487	577	3.09
3-PENTANONE	-0.003580	0.032777	0.655603	0.200000	0.598178	0.000010	154	2.82
2-HEXANONE	-0.243975	0.016929	0.659065	0.063920	2.383468	1.192919	59	1.81
METHYL ISOBUTYL KETONE	-0.140300	0.016025	0.500000	0.200000	1.354124	0.000010	168	5.20
4-HEPTANONE	-0.305868	0.006124	0.652310	0.046898	0.253450	0.125438	75	4.86
2-OCTANONE	-0.217611	0.016516	0.638466	0.009781	2.092369	1.106230	68	7.18
HFC-CFC							9771	2.16
DIFLUOROMETHANE	0.344043	0.091837	0.586960	0.949680	0.519967	0.654929	234	2.17
1,1-DIFLUOROETHANE	-0.192957	0.022557	0.571080	0.163947	0.894263	0.691859	284	1.54
TRIFLUOROMETHANE	-0.146927	0.027143	0.561575	0.413241	0.968626	0.676744	591	3.20
1,1,1-TRIFLUOROETHANE	0.268579	0.088159	0.578051	0.912013	0.524019	0.673303	294	0.77
CHLORODIFLUOROMETHANE	-0.176961	0.026318	0.566040	0.295614	0.861963	0.671828	1151	2.25
CARBON TETRAFLUORIDE	0.017698	0.010741	0.595035	0.644138	0.395427	0.612949	658	1.47
1-CHLORO-1,1-DIFLUOROETHANE	0.481308	0.090116	0.567016	1.244702	0.423022	0.690885	109	1.66
1,1,1,2-TETRAFLUOROETHANE	-0.199941	0.027546	0.545610	0.280993	0.998893	0.758378	779	2.56
DICHLOROFLUOROMETHANE	-0.222677	0.019996	0.573059	0.125203	1.032374	0.720655	215	2.44
CHLOROTRIFLUOROMETHANE	-0.159173	0.031435	0.556479	0.284664	0.707801	0.625550	834	2.34
PENTAFLUOROETHANE	-0.219492	0.027442	0.548494	0.254930	0.867512	0.743785	464	1.89
DICHLORODIFLUOROMETHANE	-0.154805	0.030819	0.560272	0.321944	0.656624	0.583837	1322	2.65
1,1,1,3,3-PENTAFLUOROPROPANE	-0.225324	0.028565	0.565558	0.199904	0.868980	0.853518	149	1.50
TRICHLOROFLUOROMETHANE	-0.169145	0.033362	0.558090	0.408519	0.859223	0.645119	410	1.45
BROMOTRIFLUOROMETHANE	-0.152001	0.033556	0.548757	0.380585	0.790886	0.617391	1223	2.10
1,1,1,3,3,3-HEXAFLUOROPROPANE	-0.217334	0.025177	0.555976	0.200000	0.749337	0.789667	172	1.18
CHLOROPENTAFLUOROETHANE	-0.184197	0.039183	0.543420	0.389064	0.917866	0.723794	421	2.46
1,1,1,2,3,3,3-HEPTAFLUOROPROPANE	-0.245044	0.020866	0.564611	0.200000	0.596278	0.663861	113	1.90
1,2-DICHLOROTETRAFLUOROETHANE	-0.222824	0.029923	0.550655	0.304480	0.942374	0.723336	348	1.77

Continued on next page

Table III-2 – continued from previous page

Name	a_1	a_2	b_1	b_2	c	d	Data number	MAPE
noble gases							11456	3.33
NEON	0.185472	0.095887	0.611962	0.879246	0.348803	0.402718	2693	5.45
ARGON	-0.100847	0.054312	0.595747	0.385346	0.434477	0.392637	4586	3.10
KRYPTON	-0.088435	0.054106	0.591284	0.428331	0.475229	0.394950	2194	2.14
XENON	-0.081842	0.059605	0.585480	0.428216	0.506166	0.397021	1983	2.27
aldehydes							348	6.38
ACETALDEHYDE	0.049907	0.044705	0.552693	0.055903	1.992984	0.054186	33	7.09
PROPANAL	-0.417763	0.000392	0.634556	0.058411	0.222545	0.538757	22	2.92
2-METHYLPROPANAL	-0.186764	0.010343	0.649966	0.156232	2.961929	0.000010	57	7.19
BUTANAL	-0.032062	0.032992	0.500000	0.200000	1.621162	0.000010	197	6.92
3-METHYLBUTYRALDEHYDE	-0.002695	0.037528	0.668135	0.116210	1.982179	0.015658	20	3.33
HEPTANAL	-0.322318	0.002640	0.658617	0.120336	0.379473	0.577915	9	1.44
DECANAL	-0.310242	0.000010	0.541450	0.183733	0.381291	0.248936	10	6.98
amines							496	4.58
METHYLAMINE	0.058642	0.047542	0.559750	0.199732	0.623150	0.102471	122	1.50
n-PROPYLAMINE	-0.131341	0.027962	0.532061	0.052555	1.866606	0.335127	46	2.53
n-BUTYLAMINE	-0.047867	0.032850	0.634545	0.090256	1.493294	0.000086	169	5.76
DIETHYLAMINE	-0.342344	0.018834	0.655456	0.195038	0.795366	0.439670	30	11.67
n-PENTYLAMINE	-0.304911	0.009930	0.546343	0.044258	0.261753	0.242723	72	5.66
n-HEXYLAMINE	0.103176	0.027356	0.500004	0.199974	0.216165	0.000010	57	4.24
alcohols							9023	3.57
METHANOL	-0.162690	0.021103	0.632606	0.068956	0.789617	0.800006	1764	2.19
ETHANOL	-0.352574	0.013649	0.702106	0.013639	0.411033	0.802923	1829	3.04
1-PROPANOL	0.165251	0.041124	0.580884	0.214705	0.200042	0.085842	1348	2.87
1-BUTANOL	0.137368	0.045153	0.709011	0.279433	0.235913	0.835522	1246	2.79
1-PENTANOL	-0.048824	0.048531	1.228275	0.294381	0.406974	1.228878	514	2.98
1-HEXANOL	-0.106681	0.048796	0.669866	2.000000	1.264790	1.470363	492	2.95
1-HEPTANOL	-0.138980	0.047130	1.102721	0.393171	2.963129	1.740218	324	5.17
1-OCTANOL	0.082988	0.059424	0.628113	1.502520	1.169740	0.708614	394	4.33
1-NONANOL	0.069604	0.056960	0.847940	1.778817	1.066410	0.823872	221	6.62
1-DECANOL	0.075591	0.056921	1.077676	1.710334	0.927764	1.154518	346	6.35
1-UNDECANOL	0.895783	0.106050	1.273153	1.345521	0.474908	0.554738	235	10.50
1-DODECANOL	0.449436	0.077008	0.728974	1.745782	0.597610	1.163176	253	8.01
1-TETRADECANOL	-0.063742	0.038851	1.455643	0.934472	2.999303	1.473666	26	2.76
1-OCTADECANOL	-0.230949	0.013833	1.121907	0.320479	1.761448	0.592101	31	27.82
others							21179	3.42
HYDROGEN	0.351477	0.049581	0.641586	0.985197	0.258753	0.191413	2084	4.78
AMMONIA	0.264646	0.072909	0.607897	0.680870	0.462426	0.560856	1450	4.68
WATER	0.283943	0.068705	0.607352	0.633395	0.639701	0.553525	7496	3.12

Continued on next page

Table III-2 – continued from previous page

Name	a_1	a_2	b_1	b_2	c	d	Data number	MAPE
CARBON MONOXIDE	-0.018335	0.069632	0.585799	0.391369	0.492300	0.458438	422	2.10
NITROGEN	-0.046957	0.059045	0.596564	0.412618	0.433231	0.441384	4437	2.70
OXYGEN	0.039677	0.073449	0.573068	0.597376	0.533374	0.428259	1052	4.78
HYDROGEN SULFIDE	0.157456	0.071257	0.500151	0.819649	0.514761	0.071398	62	7.71
CARBON DIOXIDE	0.106803	0.074406	0.578254	0.674369	0.570497	0.643414	3833	3.39
CHLOROFORM	-0.167558	0.023817	0.562129	0.179466	0.602968	0.536076	343	2.89

III-C-3) Chemical-family specific parameters

These parameters have to be used with Eq. (III-16).

III-C-3.1) Paraffins

Table III-3 - Chemical-family specific parameters for paraffinic compounds to be used in the *I*-PC-SAFT based model.

Parameter	Value
Component number	33
Data number	25641
MAPE	8.98
a_1	-0.24189266
a_2	0.01056109
b_1	0.54639175
b_2	0.01884580
c	0.72652370
d	0.58165895

Table III-4 - Prediction of viscosity data of paraffins using chemical-family specific parameters for the *I*-PC-SAFT based model: data number and corresponding MAPE (Mean Average Percent Error).

Name	Data number	MAPE
PROPANE	3209	9.70
n-BUTANE	1652	6.60
n-PENTANE	2321	5.38
n-HEXANE	2205	4.15
n-HEPTANE	2291	5.47
n-OCTANE	1896	5.51
n-NONANE	767	4.23
n-DECANE	1610	5.26
n-UNDECANE	668	6.48
n-DODECANE	1123	7.28
n-TRIDECANE	195	6.83
n-TETRADECANE	843	8.03
n-PENTADECANE	226	8.20
n-HEXADECANE	601	10.23
n-HEPTADECANE	361	13.24
n-OCTADECANE	416	16.80
n-NONADECANE	311	21.16
n-EICOSANE	138	18.17
n-DOCOSANE	30	32.13
ISOBUTANE	1943	14.78
ISOPENTANE	863	8.57
NEOPENTANE	77	32.49
2,2-DIMETHYLBUTANE	23	29.59
2,3-DIMETHYLBUTANE	92	19.95
2-METHYLPENTANE	127	5.09
3-METHYLPENTANE	108	3.50
2,4-DIMETHYLPENTANE	15	5.30
3-ETHYLPENTANE	7	3.07
2,2,4-TRIMETHYLPENTANE	899	20.19
2,3,4-TRIMETHYLPENTANE	23	15.99

2,3-DIMETHYLHEXANE	16	7.41
2,2,4,4,6,8,8-HEPTAMETHYLNONANE	161	52.99
SQUALANE	424	28.44

III-C-3.2) Cycloalkanes

Table III-5 - Chemical-family specific parameters for cycloalkanes to be used in the *I*-PC-SAFT based model.

Parameter	Value
Component number	4
Data number	2142
MAPE	11.28
a_1	-0.20464329
a_2	0.03919542
b_1	0.57567523
b_2	0.36726369
c	0.90199805
d	0.65325721

Table III-6 - Prediction of viscosity data of cycloalkanes using chemical-family specific parameters for the *I*-PC-SAFT based model: data number and corresponding MAPE (Mean Average Percent Error).

Name	Data number	MAPE
CYCLOPENTANE	266	52.33
CYCLOHEXANE	1732	4.81
CYCLOHEPTANE	62	15.92
CYCLOOCTANE	82	11.27

III-C-3.3) Alkenes

Table III-7 - Chemical-family specific parameters for alkenes to be used in the *I*-PC-SAFT based model.

Parameter	Value
Component number	16
Data number	3178
MAPE	7.66
a_1	-0.17303094
a_2	0.01590895
b_1	0.53974381
b_2	0.17576301
c	0.85159064
d	0.47747754

Table III-8 - Prediction of viscosity data of alkenes using chemical-family specific parameters for the *I*-PC-SAFT based model: data number and corresponding MAPE (Mean Average Percent Error).

Name	Data number	MAPE
ETHYLENE	974	6.35
PROPYLENE	662	11.83
1-BUTENE	19	23.24
1-PENTENE	19	13.47
1-HEXENE	461	7.97
1-HEPTENE	331	6.64
1-OCTENE	322	3.02
1-NONENE	107	9.69
1-DECENE	70	3.87
1-UNDECENE	23	4.07
1-DODECENE	44	4.86
1-TRIDECENE	25	4.65
1-TETRADECENE	26	7.30
1-PENTADECENE	27	6.15
1-HEXADECENE	41	8.87
1-HEPTADECENE	27	12.07

III-C-3.4) Alkynes

Table III-9 - Chemical-family specific parameters for alkynes compounds to be used in the *I*-PC-SAFT based model.

Parameter	Value
Component number	3
Data number	160
MAPE	2.42
a_1	-0.19727728
a_2	0.01826123
b_1	0.58788698
b_2	0.05687695
c	0.46593451
d	0.46850716

Table III-10 - Prediction of viscosity data of alkynes using chemical-family specific parameters for the *I*-PC-SAFT based model: data number and corresponding MAPE (Mean Average Percent Error).

Name	Data number	MAPE
ACETYLENE	148	2.57
METHYLACETYLENE	2	3.24
1-HEXYNE	10	0.09

III-C-3.5) Aromatics compounds

Table III-11 - Chemical-family specific parameters for aromatic compounds to be used in the *I*-PC-SAFT based model.

Parameter	Value
Component number	8
Data number	2927
MAPE	6.88
a_1	-0.23714593
a_2	0.01130363
b_1	0.59274283
b_2	-0.03214776
c	0.67800132
d	0.71891464

Table III-12 - Prediction of viscosity data of aromatics using chemical-family specific parameters for the *I*-PC-SAFT based model: data number and corresponding MAPE (Mean Average Percent Error).

Name	Data number	MAPE
m-XYLENE	857	3.60
p-XYLENE	838	2.30
ETHYLBENZENE	959	11.46
MESITYLENE	165	19.22
p-CYMENE	21	6.78
n-HEPTYLBENZENE	35	8.43
n-NONYLBENZENE	27	9.99
n-DODECYLBENZENE	25	10.13

III-C-3.6) Esters

Table III-13 - Chemical-family specific parameters for esters to be used in the *I*-PC-SAFT based model.

Parameter	Value
Component number	6
Data number	1013
MAPE	4.59
a_1	-0.31764592
a_2	0.00722787
b_1	0.65257972
b_2	-0.04672593
c	0.50377108
d	0.78313973

Table III-14 - Prediction of viscosity data of esters using chemical-family specific parameters for the *I*-PC-SAFT based model: data number and corresponding MAPE (Mean Average Percent Error).

Name	Data number	MAPE
VINYL ACETATE	30	6.65
n-PROPYL ACETATE	193	3.89
n-BUTYL ACETATE	291	2.87
ISOPENTYL ACETATE	131	7.12
n-PENTYL ACETATE	217	5.74
n-HEPTYL ACETATE	151	4.55

III-C-3.7) Ethers

Table III-15 - Chemical-family specific parameters for ethers to be used in the *I*-PC-SAFT based model.

Parameter	Value
Component number	5
Data number	494
MAPE	6.78
a_1	-0.27021667
a_2	0.00899462
b_1	0.58258708
b_2	-0.15339942
c	0.68029876
d	0.63106356

Table III-16 - Prediction of viscosity data of ethers using chemical-family specific parameters for the *I*-PC-SAFT based model: data number and corresponding MAPE (Mean Average Percent Error).

Name	Data number	MAPE
DIMETHYL ETHER	119	4.69
METHYL tert-BUTYL ETHER	66	21.50
DI-n-PROPYL ETHER	185	4.03
DI-n-BUTYL ETHER	100	4.57
DI-n-PENTYL ETHER	24	7.06

III-C-3.8) Ketones

Table III-17 - Chemical-family specific parameters for ketones to be used in the *I*-PC-SAFT based model.

Parameter	Value
Component number	6
Data number	1101
MAPE	5.76
a_1	-0.26929016
a_2	0.01301093
b_1	0.66974115
b_2	1.19996547
c	1.19413920
d	1.13277291

Table III-18 - Prediction of viscosity data of ketones using chemical-family specific parameters for the *I*-PC-SAFT based model: data number and corresponding MAPE (Mean Average Percent Error).

Name	Data number	MAPE
ACETONE	577	3.41
3-PENTANONE	154	2.93
2-HEXANONE	59	5.44
METHYL ISOBUTYL KETONE	168	12.78
4-HEPTANONE	75	5.68
2-OCTANONE	68	15.11

III-C-3.9) HFC-CFC

Table III-19 - Chemical-family specific parameters for HFC-CFC compounds to be used in the *I*-PC-SAFT based model.

Parameter	Value
Component number	19
Data number	9771
MAPE	6.21
a_1	-0.18203119
a_2	0.02792084
b_1	0.55231149
b_2	0.28879044
c	0.78975181
d	0.64066123

Table III-20 - Prediction of viscosity data of HFC-CFCs using chemical-family specific parameters for the *I*-PC-SAFT based model: data number and corresponding MAPE (Mean Average Percent Error).

Name	Data number	MAPE
DIFLUOROMETHANE	234	10.08
1,1-DIFLUOROETHANE	284	8.07
TRIFLUOROMETHANE	591	8.46
1,1,1-TRIFLUOROETHANE	294	4.68
CHLORODIFLUOROMETHANE	1151	8.60
CARBON TETRAFLUORIDE	658	4.32
1-CHLORO-1,1-DIFLUOROETHANE	109	3.19
1,1,1,2-TETRAFLUOROETHANE	779	4.90
DICHLOROFLUOROMETHANE	215	8.06
CHLOROTRIFLUOROMETHANE	834	2.96
PENTAFLUOROETHANE	464	6.42
DICHLORODIFLUOROMETHANE	1322	3.35
1,1,1,3,3-PENTAFLUOROPROPANE	149	6.46
TRICHLOROFLUOROMETHANE	410	8.33
BROMOTRIFLUOROMETHANE	1223	2.99
1,1,1,3,3,3-HEXAFLUOROPROPANE	172	6.49
CHLOROPENTAFLUOROETHANE	421	13.52
1,1,1,2,3,3,3-HEPTAFLUOROPROPANE	113	8.64
1,2-DICHLOROTETRAFLUOROETHANE	348	15.29

III-C-3.10) Aldehydes

Table III-21 - Chemical-family specific parameters for aldehydes to be used in the *I*-PC-SAFT based model.

Parameter	Value
Component number	7
Data number	348
MAPE	9.04
a_1	-0.36502352
a_2	0.00697388
b_1	0.73276231
b_2	2.00000000
c	0.90230505
d	1.58297797

Table III-22 - Prediction of viscosity data of aldehydes using chemical-family specific parameters for the *I*-PC-SAFT based model: data number and corresponding MAPE (Mean Average Percent Error).

Name	Data number	MAPE
ACETALDEHYDE	33	16.66
PROPANAL	22	8.81
2-METHYLPROPANAL	57	5.63
BUTANAL	197	7.75
3-METHYLBUTYRALDEHYDE	20	14.32
HEPTANAL	9	2.96
DECANAL	10	24.14

III-C-3.11) Amines

Table III-23 - Chemical-family specific parameters for amines to be used in the *I*-PC-SAFT based model.

Parameter	Value
Component number	6
Data number	496
MAPE	12.13
a_1	-0.29904311
a_2	0.00791211
b_1	0.61015105
b_2	-0.38402168
c	0.76478670
d	0.65144352

Table III-24 - Prediction of viscosity data of amines using chemical-family specific parameters for the *I*-PC-SAFT based model: data number and corresponding MAPE (Mean Average Percent Error).

Name	Data number	MAPE
METHYLAMINE	122	14.90
n-PROPYLAMINE	46	5.87
n-BUTYLAMINE	169	6.35
DIETHYLAMINE	30	63.54
n-PENTYLAMINE	72	6.65
n-HEXYLAMINE	57	8.28

III-C-4) Universal parameters

Table III-25 - Universal parameters to be used in the *I*-PC-SAFT based model

Parameter	Value
Component number	131
Data number	82379
MAPE	12.31
a_1	-0.28758348
a_2	0.00593637
b_1	0.58243502
b_2	-0.03017106
c	0.50190584
d	0.39946247

Table III-26 - Data number and MAPE resulting from prediction with the *I*-PC-SAFT based model coupled with universal parameters

Name	Data number	MAPE
n-alkanes	28099	7.63
METHANE	3693	4.17
ETHANE	3492	6.99
PROPANE	3209	10.02
n-BUTANE	1652	9.62
n-PENTANE	2321	10.11
n-HEXANE	2205	7.95
n-HEPTANE	2291	8.39
n-OCTANE	1896	6.89
n-NONANE	767	4.11
n-DECANE	1610	4.12
n-UNDECANE	668	5.34
n-DODECANE	1123	6.54
n-TRIDECANE	195	8.94
n-TETRADECANE	843	11.81
n-PENTADECANE	226	8.58
n-HEXADECANE	601	13.92
n-HEPTADECANE	361	7.96
n-OCTADECANE	416	7.50
n-NONADECANE	311	7.65
n-EICOSANE	138	8.76
n-HENEICOSANE	39	12.37
n-DOCOSANE	30	10.39
n-DOTRIACONTANE	12	12.10
branched alkanes	4778	19.83
ISOBUTANE	1943	19.56
ISOPENTANE	863	6.08
NEOPENTANE	77	29.92
2,2-DIMETHYLBUTANE	23	23.45
2,3-DIMETHYLBUTANE	92	12.74
2-METHYLPENTANE	127	5.21
3-METHYLPENTANE	108	4.99
2,4-DIMETHYLPENTANE	15	2.04
3-ETHYLPENTANE	7	12.32
2,2,4-TRIMETHYLPENTANE	899	16.98
2,3,4-TRIMETHYLPENTANE	23	8.39
2,3-DIMETHYLHEXANE	16	1.99
2,2,4,4,6,8,8-HEPTAMETHYLNONANE	161	54.72
SQUALANE	424	51.60
cycloalkanes	2142	42.17
CYCLOPENTANE	266	26.42
CYCLOHEXANE	1732	43.66
CYCLOHEPTANE	62	49.41
CYCLOOCTANE	82	56.35
alkenes	3178	9.99
ETHYLENE	974	4.67
PROPYLENE	662	6.74
1-BUTENE	19	17.86
1-PENTENE	19	18.33
1-HEXENE	461	19.61
1-HEPTENE	331	16.60
1-OCTENE	322	11.65
1-NONENE	107	16.49
1-DECENE	70	7.35
1-UNDECENE	23	6.49
1-DODECENE	44	7.50
1-TRIDECENE	25	6.19
1-TETRADECENE	26	6.07

Continued on next page

Table III-26 – continued from previous page

Name	Data number	MAPE
1-PENTADECENE	27	6.30
1-HEXADECENE	41	9.58
1-HEPTADECENE	27	4.72
alkynes	160	5.68
ACETYLENE	148	5.40
METHYLACETYLENE	2	20.31
1-HEXYNE	10	6.87
aromatics	5660	18.05
BENZENE	2296	14.54
TOLUENE	437	13.46
m-XYLENE	857	27.62
p-XYLENE	838	23.22
ETHYLBENZENE	959	11.98
MESITYLENE	165	42.45
p-CYMENE	21	17.07
n-HEPTYLBENZENE	35	6.76
n-NONYLBENZENE	27	13.01
n-DODECYLBENZENE	25	13.48
esters	1013	8.44
VINYL ACETATE	30	16.75
n-PROPYL ACETATE	193	11.75
n-BUTYL ACETATE	291	4.25
ISOPENTYL ACETATE	131	6.02
n-PENTYL ACETATE	217	11.28
n-HEPTYL ACETATE	151	8.63
ethers	494	9.04
DIMETHYL ETHER	119	14.44
METHYL tert-BUTYL ETHER	66	13.55
DI-n-PROPYL ETHER	185	6.12
DI-n-BUTYL ETHER	100	5.80
DI-n-PENTYL ETHER	24	5.94
ketones	1101	17.94
ACETONE	577	22.55
3-PENTANONE	154	16.52
2-HEXANONE	59	16.86
METHYL ISOBUTYL KETONE	168	7.95
4-HEPTANONE	75	9.08
2-OCTANONE	68	17.42
HFC-CFC	9771	14.90
DIFLUOROMETHANE	234	11.85
1,1-DIFLUOROETHANE	284	7.19
TRIFLUOROMETHANE	591	13.20
1,1,1-TRIFLUOROETHANE	294	10.93
CHLORODIFLUOROMETHANE	1151	7.34
CARBON TETRAFLUORIDE	658	19.28
1-CHLORO-1,1-DIFLUOROETHANE	109	15.50
1,1,1,2-TETRAFLUOROETHANE	779	16.01
DICHLOROFLUOROMETHANE	215	3.37
CHLOROTRIFLUOROMETHANE	834	15.40
PENTAFLUOROETHANE	464	22.10
DICHLORODIFLUOROMETHANE	1322	12.86
1,1,1,3,3-PENTAFLUOROPROPANE	149	24.85
TRICHLOROFLUOROMETHANE	410	16.29
BROMOTRIFLUOROMETHANE	1223	13.17
1,1,1,3,3,3-HEXAFLUOROPROPANE	172	21.11
CHLOROPENTAFLUOROETHANE	421	26.23
1,1,1,2,3,3,3-HEPTAFLUOROPROPANE	113	23.23
1,2-DICHLOROTETRAFLUOROETHANE	348	28.28
aldehydes	348	13.38
ACETALDEHYDE	33	26.32

Continued on next page

Table III-26 – continued from previous page

Name	Data number	MAPE
PROPANAL	22	10.87
2-METHYLPROPANAL	57	21.99
BUTANAL	197	10.08
3-METHYLBUTYRALDEHYDE	20	8.26
HEPTANAL	9	4.94
DECANAL	10	9.95
amines	496	14.54
METHYLAMINE	122	13.11
n-PROPYLAMINE	46	9.23
n-BUTYLAMINE	169	11.56
DIETHYLAMINE	30	65.26
n-PENTYLAMINE	72	11.26
n-HEXYLAMINE	57	8.20
noble gases	11456	10.10
NEON	2693	14.65
ARGON	4586	7.93
KRYPTON	2194	8.47
XENON	1983	10.72
others	13683	12.73
HYDROGEN	2084	32.72
AMMONIA	1450	15.41
CARBON MONOXIDE	422	6.41
NITROGEN	4437	5.27
OXYGEN	1052	8.22
HYDROGEN SULFIDE	62	29.46
CARBON DIOXIDE	3833	11.93
CHLOROFORM	343	3.86

III-D) *tc*-PR based model:

III-D-1) Equation of state parameters and viscosity experimental data informations

The *translated-consistent* version of the Peng-Robinson (PR) EoS, denoted *tc*-PR[75,83] relies on consistent L, M and N parameters of the Twu 91 α-function (*consistent* means that these parameters passed a consistency test[83] ensuring safe calculations in the supercritical region). In this model, the volume translation parameter c was selected in order to exactly reproduce the experimental saturated liquid molar volume at a reduced temperature of 0.8:

$$c = v_{\mathrm{liq}}^{\mathrm{sat,u-EoS}}(T_{\mathrm{r}} = 0.8) - v_{\mathrm{liq,exp}}^{\mathrm{sat}}(T_{\mathrm{r}} = 0.8) \qquad \text{(III– 17)}$$

Where $v_{\mathrm{liq}}^{\mathrm{sat,u-EoS}}(T_{\mathrm{r}} = 0.8)$ is the molar volume calculated with the original (untranslated) EoS at $T_{\mathrm{r}} = 0.8$.

The final *tc*-PR EoS expression is:

$$P(T,v) = \frac{RT}{v-b} - \frac{a_c \cdot \alpha(T_{\mathrm{r}})}{(v+c)(v+b+2c)+(b+c)(v-b)}$$

$$\begin{cases} \alpha(T_{\mathrm{r}}) = T_{\mathrm{r}}^{N(M-1)}\exp[L(1-T_{\mathrm{r}}^{MN})] \\ c = v_{\mathrm{liq}}^{\mathrm{sat,u-EoS}}(T_{\mathrm{r}} = 0.8) - v_{\mathrm{liq,exp}}^{\mathrm{sat}}(T_{\mathrm{r}} = 0.8) \\ \eta_c = \left[1 + \sqrt[3]{4-2\sqrt{2}} + \sqrt[3]{4+2\sqrt{2}}\right] \approx 0.25308 \\ a_c = \dfrac{40\eta_c + 8}{49 - 37\eta_c}\dfrac{R^2T_{\mathrm{c,exp}}^2}{P_{\mathrm{c,exp}}} \approx 0.45724\dfrac{R^2T_{\mathrm{c,exp}}^2}{P_{\mathrm{c,exp}}} \\ b = \dfrac{\eta_c}{\eta_c + 3}\dfrac{RT_{\mathrm{c,exp}}}{P_{\mathrm{c,exp}}} - c \approx 0.07780\dfrac{RT_{\mathrm{c,exp}}}{P_{\mathrm{c,exp}}} - c \end{cases} \qquad \text{(III– 18)}$$

Table III-27 - *tc*-PR EoS parameters and experimental viscosity data informations

		EoS parameters				Experimental viscosity data informations					
Name	CAS	L -	M -	N -	$c * 10^6$ m^3/mol	T_{min} K	T_{max} K	P_{min} MPa	P_{max} MPa	$\eta_{min} * 10^3$ $Pa.s$	$\eta_{max} * 10^3$ $Pa.s$
n-alkanes											
METHANE	74-82-8	0.14738	0.90748	1.82411	-3.56049	88.0	1050.0	0.0105	99.2433	0.0044	0.2220
ETHANE	74-84-0	0.30533	0.86927	1.32966	-3.67453	93.15	750.0	0.0267	78.4532	0.0081	1.1302
PROPANE	74-98-6	0.74550	0.91333	0.76097	-3.73494	88.1	750.0	0.0100	99.0472	0.0067	10.7221
n-BUTANE	106-97-8	0.41536	0.84901	1.32049	-3.43648	130.0	850.0	0.0267	70.0000	0.0073	2.5654
n-PENTANE	109-66-0	0.29330	0.83662	1.82462	-1.59871	137.15	900.0	0.0067	99.9900	0.0067	4.9900
n-HEXANE	110-54-3	0.28726	0.83405	2.01991	0.81628	174.65	1000.0	0.0093	98.0665	0.0061	2.3900
n-HEPTANE	142-82-5	0.36295	0.82017	1.83664	3.10863	180.15	620.0	0.0027	98.0600	0.0062	4.3800
n-OCTANE	111-65-9	0.35700	0.81717	1.99996	6.42842	211.15	687.8	0.0093	99.9000	0.0069	3.3093
n-NONANE	111-84-2	0.41649	0.80811	1.89355	9.34517	222.15	470.0	0.0980	98.0000	0.1850	2.8051
n-DECANE	124-18-5	0.37696	0.81080	2.17809	12.82743	241.15	709.2	0.0500	98.0000	0.0074	2.4513
n-UNDECANE	1120-21-4	0.48046	0.80007	1.90454	18.32929	246.65	520.15	0.0980	98.0000	0.1630	3.1700
n-DODECANE	112-40-3	0.45843	0.80098	2.08729	22.22725	266.15	693.2	0.0500	97.1500	0.0074	3.6520
n-TRIDECANE	629-50-5	0.47740	0.79897	2.11999	30.13814	263.05	503.15	0.0980	98.0000	0.2059	5.7700
n-TETRADECANE	629-59-4	0.57041	0.78895	1.88879	39.90980	277.65	623.0	0.0500	80.0000	0.0070	4.7300
n-PENTADECANE	629-62-9	0.57955	0.78769	1.94902	45.35005	293.15	533.15	0.0980	98.0000	0.2116	5.6000
n-HEXADECANE	544-76-3	0.60685	0.78674	1.94340	52.13839	273.15	723.8	0.0500	99.6500	0.0073	6.1940
n-HEPTADECANE	629-78-7	0.56074	0.79245	2.18728	52.58577	293.15	573.75	0.0980	98.0000	0.1985	7.0100
n-OCTADECANE	593-45-3	0.58016	0.79247	2.21665	59.16994	305.15	583.15	0.0980	92.2000	0.2063	7.0000
n-NONADECANE	629-92-5	0.59247	0.79325	2.27181	64.88646	308.15	593.15	0.0980	49.1500	0.2079	3.9570
n-EICOSANE	112-95-8	0.56936	0.80387	2.50049	64.11107	310.6	613.15	0.0980	83.0000	0.1984	4.6420
n-HENEICOSANE	629-94-7	0.46937	0.81153	3.01913	72.69091	323.15	496.65	0.0980	49.0000	0.4330	4.6000
branched alkanes											
ISOBUTANE	75-28-5	1.07723	0.99213	0.57426	-3.80262	115.0	850.0	0.0223	68.6500	0.0069	9.3029
ISOPENTANE	78-78-4	0.24029	0.83746	1.95199	-3.60373	117.99	750.0	0.0015	98.0700	0.0069	21.6200
NEOPENTANE	463-82-1	0.12679	0.84939	2.55906	-5.96334	258.15	444.26	0.0500	99.0472	0.0079	0.5330
2,2-DIMETHYLBUTANE	75-83-2	0.22181	0.83374	2.03473	-6.28035	269.29	351.15	0.0500	88.2599	0.0076	0.7360
2,3-DIMETHYLBUTANE	79-29-8	0.18994	0.84369	2.36194	-4.22445	273.14	343.15	0.0981	88.2599	0.2132	0.6560
2-METHYLPENTANE	107-83-5	0.34965	0.82087	1.65903	-3.09737	143.15	485.65	0.0981	88.2599	0.0089	6.8668
3-METHYLPENTANE	96-14-0	0.30612	0.82268	1.77981	-1.66760	265.62	343.16	0.0981	88.2599	0.1980	0.5384
2,4-DIMETHYLPENTANE	108-08-7	0.33004	0.81906	1.79014	-0.96763	288.15	335.8	0.0981	88.2599	0.2377	0.6100
3-ETHYLPENTANE	617-78-7	0.38602	0.82159	1.64786	-2.12401	293.15	313.15	0.0981	88.2599	0.3070	0.6250
2,2,4-TRIMETHYLPENTANE	540-84-1	0.28256	0.83661	2.07206	-4.01104	173.15	548.15	0.0093	99.9000	0.0073	7.7700
2,3,4-TRIMETHYLPENTANE	565-75-3	0.27375	0.83040	2.11222	-2.27854	273.15	453.15	0.1000	80.0000	0.2770	1.2420
2,3-DIMETHYLHEXANE	584-94-1	0.22871	0.82862	2.44479	0.65156	273.15	313.15	0.1000	0.1000	0.3980	0.6430
2,2,4,4,6,8,8-HEPTAMETHYLNONANE	4390-04-9	0.35858	0.82217	2.48892	17.70508	293.15	453.15	0.1000	80.0000	0.4210	15.9200

Continued on next page

Table III-27 – continued from previous page

Name	CAS	L -	M -	N -	$c * 10^6$ m^3/mol	T_{min} K	T_{max} K	P_{min} MPa	P_{max} MPa	$\eta_{min} * 10^3$ $Pa.s$	$\eta_{max} * 10^3$ $Pa.s$
cycloalkanes											
CYCLOPENTANE	287-92-3	0.39596	0.82692	1.29392	-1.98829	218.74	449.1	0.0093	90.4000	0.0099	1.4380
CYCLOHEXANE	110-82-7	0.37295	0.81214	1.35210	-4.22316	273.15	673.15	0.0027	98.0665	0.0072	1.7920
CYCLOHEPTANE	291-64-5	0.24058	0.84705	2.08571	-5.35293	291.9	392.15	0.1000	40.1000	0.4250	2.9250
CYCLOOCTANE	292-64-8	0.13238	0.83720	2.69425	-4.11952	283.15	478.1	0.0093	40.1000	0.0070	3.2660
alkenes											
ETHYLENE	74-85-1	0.25059	0.85349	1.38986	-3.29106	105.0	575.15	0.0500	91.1925	0.0065	0.6600
PROPYLENE	115-07-1	0.49144	0.84580	1.00415	-3.54614	88.7	520.0	0.0068	80.0000	0.0052	14.4600
1-BUTENE	106-98-9	0.16900	0.86165	2.37074	-3.51399	103.15	263.15	0.1000	0.1000	0.1962	7.3583
1-PENTENE	109-67-1	0.93092	1.00000	0.77055	-2.77104	123.15	298.15	0.1000	0.1000	0.2085	5.6853
1-HEXENE	592-41-6	1.07672	1.00000	0.72580	-2.19294	133.15	473.15	0.0093	98.0600	0.0068	10.2780
1-HEPTENE	592-76-7	0.56499	0.84233	1.35286	-1.50579	163.15	490.0	0.0980	98.0600	0.0830	4.2843
1-OCTENE	111-66-0	0.27542	0.84919	2.56229	-1.08424	183.15	490.0	0.0980	98.0600	0.1280	3.9222
1-NONENE	124-11-8	0.30523	0.83019	2.41586	2.25852	193.15	473.0	0.1000	50.0000	0.1440	10.5700
1-DECENE	872-05-9	0.33273	0.82463	2.40215	6.30277	213.15	475.02	0.0980	98.0600	0.2011	4.4888
1-UNDECENE	821-95-4	0.38070	0.81660	2.28409	11.62682	243.15	463.15	0.1000	0.1000	0.2019	2.8194
1-DODECENE	112-41-4	0.47130	0.80552	2.02825	17.84439	243.15	483.15	0.1000	0.1000	0.2005	4.0253
1-TRIDECENE	2437-56-1	0.43221	0.80688	2.28050	24.19833	263.15	503.15	0.1000	0.1000	0.1973	3.1259
1-TETRADECENE	1120-36-1	0.48019	0.80161	2.20438	31.87092	273.15	523.15	0.1000	0.1000	0.1923	3.1045
1-PENTADECENE	13360-61-7	0.41834	0.80837	2.54360	27.08880	273.15	533.15	0.1000	0.1000	0.2046	4.1104
1-HEXADECENE	629-73-2	0.41849	0.80946	2.66470	32.32805	273.15	553.15	0.1000	0.1000	0.1977	5.4080
1-HEPTADECENE	6765-39-5	0.40655	0.81154	2.80699	34.07775	303.15	563.15	0.1000	0.1000	0.2021	2.9120
alkynes											
ACETYLENE	74-86-2	0.15046	0.85680	2.44390	-0.82881	273.1	609.8	0.0133	10.1325	0.0094	0.0250
METHYLACETYLENE	74-99-7	0.43408	0.80878	1.22458	-1.16083	223.15	248.15	0.1000	0.1000	0.2200	0.2850
1-HEXYNE	693-02-7	0.23577	0.85100	2.53335	-5.23855	293.15	333.15	0.1000	0.1000	0.2420	0.3730
aromatics											
BENZENE	71-43-2	0.13487	0.84816	2.57900	-1.43896	273.15	673.15	0.0027	99.3000	0.0073	1.2580
TOLUENE	108-88-3	0.31709	0.83024	1.75262	1.23818	169.6	673.15	0.0069	39.4120	0.0078	32.6000
m-XYLENE	108-38-3	0.41847	0.82958	1.62883	4.13384	273.15	673.15	0.0981	98.0665	0.0102	1.1160
p-XYLENE	106-42-3	0.22490	0.84934	2.55991	4.28703	273.15	673.15	0.0160	98.0665	0.0084	0.8880
ETHYLBENZENE	100-41-4	0.49914	0.82220	1.35401	2.70311	191.4	673.15	0.1000	97.5200	0.0102	7.6400
MESITYLENE	108-67-8	0.42214	0.83883	1.86363	7.29428	278.15	393.15	0.1000	51.5700	0.2770	0.9804
p-CYMENE	99-87-6	0.54407	0.83373	1.46158	8.97721	290.15	413.15	0.0981	98.0665	0.3700	1.6190
n-HEPTYLBENZENE	1078-71-3	0.31043	0.83670	2.77667	14.87721	293.15	353.15	0.1000	80.0000	0.8340	4.5100
n-DODECYLBENZENE	123-01-3	0.58896	0.80768	2.08226	29.00323	298.15	363.15	0.1000	80.0000	1.4210	11.9000
esters											
VINYL ACETATE	108-05-4	0.50644	0.76962	1.35637	10.25022	273.25	373.15	0.1000	80.0000	0.2922	0.6790

Continued on next page

Table III-27 – continued from previous page

Name	CAS	L -	M -	N -	$c * 10^6$ m^3/mol	T_{min} K	T_{max} K	P_{min} MPa	P_{max} MPa	$\eta_{min} * 10^3$ $Pa.s$	$\eta_{max} * 10^3$ $Pa.s$
n-PROPYL ACETATE	109-60-4	0.60227	0.80723	1.33319	8.21311	273.15	494.16	0.0980	49.0000	0.0820	0.8010
n-BUTYL ACETATE	123-86-4	0.22830	0.83168	2.87088	3.29714	273.15	492.46	0.0980	49.0000	0.1370	1.1035
ISOPENTYL ACETATE	123-92-2	0.27716	0.83598	2.78979	3.52813	282.12	500.0	0.1000	50.1000	0.0105	1.1440
n-PENTYL ACETATE	628-63-7	0.22449	0.82964	2.91053	7.29250	288.15	502.9	0.1000	50.1000	0.0083	1.1980
n-HEPTYL ACETATE	112-06-1	0.34941	0.82031	2.66490	3.47608	283.15	500.0	0.1000	50.1000	0.0091	2.1400
ethers											
DIMETHYL ETHER	115-10-6	0.61030	0.84979	0.96628	-2.19464	227.22	423.15	0.1000	30.0000	0.0091	0.2589
METHYL tert-BUTYL ETHER	1634-04-4	1.33854	0.99996	0.52864	1.74798	273.15	323.15	0.1000	0.1013	0.2760	0.4465
DI-n-PROPYL ETHER	111-43-3	0.27948	0.84272	2.37935	-3.93257	273.5	513.0	0.1000	58.8600	0.0610	0.6640
DI-n-BUTYL ETHER	142-96-1	0.45325	0.81484	1.82231	1.89035	243.15	373.15	0.1000	21.1200	0.2900	2.2209
DI-n-PENTYL ETHER	693-65-2	0.32305	0.83002	2.90319	3.99768	273.15	373.15	0.0981	98.0665	0.4100	2.3210
ketones											
ACETONE	67-64-1	0.36810	0.85384	1.83142	12.00988	180.65	579.55	0.0027	98.0665	0.0078	2.1500
3-PENTANONE	96-22-0	0.34554	0.81565	1.85642	5.70091	273.15	473.15	0.1000	98.0000	0.1460	1.0190
2-HEXANONE	591-78-6	0.22658	0.83834	2.74688	8.06710	293.15	473.15	0.0980	98.0000	0.1950	1.3000
METHYL ISOBUTYL KETONE	108-10-1	0.27658	0.82224	2.19503	5.32975	273.15	473.15	0.1000	80.0000	0.3160	1.3380
4-HEPTANONE	123-19-3	0.28391	0.82709	2.40709	7.94946	273.0	473.0	0.1000	90.0000	0.1860	2.0000
2-OCTANONE	111-13-7	0.23127	0.82931	2.91715	5.70781	288.15	473.15	0.0981	98.0660	0.2100	1.9800
HFC-CFC											
DIFLUOROMETHANE	75-10-5	0.28640	0.85516	2.05370	7.24952	200.28	423.15	0.1000	50.0000	0.0108	0.5353
1,1-DIFLUOROETHANE	75-37-6	0.29530	0.84627	1.95800	5.68966	200.21	423.15	0.1000	17.7000	0.0093	0.5907
TRIFLUOROMETHANE	75-46-7	0.38687	0.84268	1.57513	2.94268	117.88	473.08	0.0979	58.9600	0.0101	1.9600
1,1,1-TRIFLUOROETHANE	420-46-2	0.28849	0.84321	1.91206	4.85288	223.65	423.15	0.1000	10.0700	0.0111	0.2986
CHLORODIFLUOROMETHANE	75-45-6	0.52400	0.82812	1.11421	-0.09471	120.0	473.15	0.0960	60.0000	0.0103	7.8360
CARBON TETRAFLUORIDE	75-73-0	0.49866	0.84276	1.07530	-4.42118	203.15	873.0	0.1000	41.4916	0.0124	0.0883
1-CHLORO-1,1-DIFLUOROETHANE	75-68-3	0.36281	0.82781	1.49017	0.11017	208.15	423.15	0.1000	5.0920	0.0105	0.6980
1,1,1,2-TETRAFLUOROETHANE	811-97-2	0.28510	0.83200	2.11744	2.26973	175.0	438.15	0.0920	90.0000	0.0108	1.8410
DICHLOROFLUOROMETHANE	75-43-4	0.15072	0.84821	2.44409	-1.78708	193.15	473.15	0.0982	58.9200	0.0107	1.2320
CHLOROTRIFLUOROMETHANE	75-72-9	0.14133	0.85841	2.41981	-3.89034	93.1	433.31	0.1000	60.0000	0.0107	11.0420
PENTAFLUOROETHANE	354-33-6	0.25689	0.84291	2.24835	-1.53555	176.0	423.15	0.0900	53.0700	0.0112	1.0990
DICHLORODIFLUOROMETHANE	75-71-8	0.14934	0.85868	2.41594	-4.21947	117.6	575.0	0.0400	60.0000	0.0105	6.5700
1,1,1,3,3-PENTAFLUOROPROPANE	460-73-1	1.47972	0.95224	0.59279	-0.58486	263.15	396.46	0.1000	40.0000	0.0112	1.0153
TRICHLOROFLUOROMETHANE	75-69-4	0.35915	0.82967	1.36748	-4.73846	163.5	503.15	0.0983	60.0000	0.0113	5.2730
BROMOTRIFLUOROMETHANE	75-63-8	1.32456	0.89300	0.44573	-3.27621	101.95	448.15	0.1000	60.0000	0.0124	10.0050
1,1,1,3,3,3-HEXAFLUOROPROPANE	690-39-1	0.87288	0.85453	1.01805	-2.31167	253.15	373.39	0.1000	40.0000	0.0110	0.8347
CHLOROPENTAFLUOROETHANE	76-15-3	0.71852	0.87018	0.95712	-6.22075	176.92	473.08	0.0979	58.9600	0.0104	1.5850
1,1,1,2,3,3,3-HEPTAFLUOROPROPANE	431-89-0	1.18998	0.99998	0.72595	-1.70550	243.16	371.78	0.1000	11.4900	0.0119	0.6250
1,2-DICHLOROTETRAFLUOROETHANE	76-14-2	0.15228	0.84461	2.63850	-5.05369	182.96	473.15	0.0979	58.9600	0.0113	2.6720

Continued on next page

Table III-27 – continued from previous page

Name	CAS	L -	M -	N -	$c * 10^6$ m^3/mol	T_{min} K	T_{max} K	P_{min} MPa	P_{max} MPa	$\eta_{min} * 10^3$ $Pa.s$	$\eta_{max} * 10^3$ $Pa.s$
noble gases											
ARGON	7440-37-1	0.12268	0.90452	1.85408	-3.29332	76.5	1200.0	0.0067	99.9000	0.0065	0.4798
KRYPTON	7439-90-9	0.10130	0.89545	1.95004	-3.33250	116.09	1600.0	0.0049	95.0000	0.0109	0.4582
XENON	7440-63-3	0.17837	0.91982	1.70497	-3.77404	153.2	2000.0	0.0067	95.0000	0.0125	0.7300
aldehydes											
ACETALDEHYDE	75-07-0	1.00471	1.00000	0.74345	13.77891	273.15	350.95	0.0027	96.5263	0.0090	0.4889
PROPANAL	123-38-6	0.96884	1.00000	0.80394	5.97525	273.15	320.95	0.1000	96.5263	0.2540	0.6227
2-METHYLPROPANAL	78-84-2	0.15543	0.84033	2.71150	5.34491	293.15	501.88	0.1000	96.5263	0.1870	0.8411
BUTANAL	123-72-8	0.98654	0.99999	0.79134	4.15781	283.0	495.13	0.0980	98.0000	0.2160	1.0500
3-METHYLBUTYRALDEHYDE	590-86-3	1.09811	0.99269	0.83049	-2.16276	294.25	358.15	0.1000	96.5263	0.2798	1.1058
HEPTANAL	111-71-7	0.39590	0.85967	2.08077	1.54762	288.15	303.15	0.1000	96.5263	0.7910	1.6159
DECANAL	112-31-2	1.39518	1.00000	0.76727	-16.78859	293.87	318.15	0.1000	96.5263	1.2810	2.4778
amines											
METHYLAMINE	74-89-5	1.30335	1.00000	0.57812	2.17260	194.85	673.0	0.0021	24.5166	0.0094	0.9120
n-PROPYLAMINE	107-10-8	1.67447	0.95846	0.44429	1.19742	283.15	318.15	0.1000	51.8000	0.2910	0.5227
n-BUTYLAMINE	109-73-9	0.17659	0.81642	2.56447	-1.45129	278.15	348.15	0.1000	71.7500	0.2764	0.7690
DIETHYLAMINE	109-89-7	1.18755	0.94265	0.65976	2.69022	288.15	353.15	0.1000	80.0000	0.5520	2.0740
n-PENTYLAMINE	110-58-7	0.17435	0.82501	3.00408	0.35495	278.15	353.15	0.1000	80.0000	0.3104	1.2030
n-HEXYLAMINE	111-26-2	0.19688	0.82294	3.04755	2.25658	278.15	373.15	0.1000	80.0000	0.3260	1.5610
alcohols											
METHANOL	67-56-1	0.76822	0.93479	1.57159	9.17712	174.85	550.0	0.0027	99.7000	0.0101	13.9000
ETHANOL	64-17-5	1.11945	0.97724	1.14643	6.08287	143.15	540.0	0.0815	98.0665	0.0108	467.0000
1-PROPANOL	71-23-8	1.10666	0.93817	1.13228	3.07305	223.15	550.0	0.0815	98.2000	0.0099	21.6000
1-BUTANOL	71-36-3	1.38509	1.00000	0.85377	1.58248	193.15	473.15	0.0815	98.0665	0.0092	217.6000
1-PENTANOL	71-41-0	1.45953	1.00000	0.78797	1.17104	243.0	403.15	0.0981	80.0000	0.3900	24.5000
1-HEXANOL	111-27-3	1.58034	1.00000	0.70297	3.69615	243.15	428.15	0.1000	50.2700	0.3400	35.5000
1-HEPTANOL	111-70-6	1.78291	1.00000	0.61750	-4.37783	243.15	435.05	0.1000	80.0000	0.3700	54.0000
1-OCTANOL	111-87-5	2.25536	0.99996	0.48078	4.23212	283.15	603.15	0.1000	60.0000	0.1070	13.5200
1-NONANOL	143-08-8	2.30846	0.75926	0.53701	13.25322	283.15	603.15	0.1000	60.0000	0.1500	17.4390
1-DECANOL	112-30-1	2.43051	0.99998	0.45843	13.67306	283.15	593.15	0.1000	60.0000	0.1560	22.0640
1-UNDECANOL	112-42-5	1.87042	0.75624	0.68029	17.23437	293.15	593.15	0.1000	60.0000	0.2070	17.2840
1-DODECANOL	112-53-8	0.18171	0.79723	3.68542	23.01208	293.15	595.65	0.1000	60.0000	0.4140	19.7457
1-OCTADECANOL	112-92-5	0.25776	0.79520	3.74512	66.66800	333.15	423.15	0.0981	98.0665	1.2400	11.6000
others											
AMMONIA	7664-41-7	0.22737	0.86452	2.33201	4.03062	203.15	989.15	0.0013	81.0600	0.0080	0.4750
WATER	7732-18-5	0.38720	0.87198	1.96692	5.27106	251.15	2073.15	0.0012	99.5400	0.0097	4.9100
CARBON MONOXIDE	630-08-0	0.09967	0.87823	2.15086	-3.67664	68.55	911.0	0.0255	91.2938	0.0053	0.2870
NITROGEN	7727-37-9	0.12427	0.88981	2.01285	-3.64285	63.9	1000.0	0.0013	99.8200	0.0054	0.3914

Continued on next page

Table III-27 – continued from previous page

Name	CAS	L -	M -	N -	$c * 10^6$ m^3/mol	T_{min} K	T_{max} K	P_{min} MPa	P_{max} MPa	$\eta_{min} * 10^3$ $Pa.s$	$\eta_{max} * 10^3$ $Pa.s$
OXYGEN	7782-44-7	0.23391	0.88957	1.30528	-2.76205	54.4	1211.0	0.0015	78.4532	0.0054	0.8730
HYDROGEN SULFIDE	7783-06-4	0.11219	0.86878	2.27341	-2.50757	190.1	413.15	0.1000	50.0000	0.0125	0.5470
CARBON DIOXIDE	124-38-9	0.17800	0.85903	2.41074	-1.13352	190.0	1794.0	0.0067	99.8200	0.0097	0.3223
CHLOROFORM	67-66-3	0.22533	0.83791	1.98744	-4.91516	209.65	618.5	0.0046	99.6000	0.0128	1.9615

III-D-2) Component-specific parameters

Component-specific parameters (a_1, a_2, b_1, b_2, c and d) to be used in the below equation for the viscosity estimation are reported in Table III-28.

$$\begin{cases} \ln\left(\frac{\eta}{\eta_{\mathrm{ref}}}\right)_{\mathrm{calc}} = \left[\left(\frac{a_1 + a_2\tilde{s}_{\mathrm{Tv-res}}}{1 + e^{cX_{\mathrm{ES}}}}\right) + \left(\frac{b_1 + b_2\tilde{s}_{\mathrm{Tv-res}}}{1 + e^{-cX_{\mathrm{ES}}}}\right)\right] X_{ES} + \frac{d}{\tilde{s}^{c}_{\mathrm{Tv-res}}} \\ X_{\mathrm{ES}} = -\left(\frac{s_{\mathrm{Tv-res}}}{s^{c}_{\mathrm{Tv-res}}}\right) - \ln\left(\frac{s_{\mathrm{Tv-res}}}{s^{c}_{\mathrm{Tv-res}}} \times f_{\mathrm{corr}}(T)\right) \\ f_{\mathrm{corr}}(T) = 1 + \left(\frac{T - T_{\mathrm{c}}}{T_{\mathrm{c}}}\right)^{3} \\ \eta_{\mathrm{ref}} = \rho_{\mathrm{N}}^{2/3}\sqrt{\mathrm{m_0 k_b} T} \\ \tilde{s}_{\mathrm{Tv-res}} = \frac{s_{\mathrm{Tv-res}}}{R} \end{cases} \quad \text{(III– 19)}$$

The Tv-residual entropy ($s_{\mathrm{Tv-res}}$) and the molecular density (ρ_{N}) were estimated using the *tc*-PR EoS.

Table III-28 - Component-specific parameters suitable for the *tc*-PR based model with the corresponding number of experimental data points and MAPE

Name	a_1	a_2	b_1	b_2	c	d	α	Data number	MAPE
n-alkanes								27981	4.45
METHANE	0.166301	0.036814	0.603401	0.249291	0.387417	1.135243	0.002961	3686	2.58
ETHANE	-0.123276	0.027327	0.570573	0.252339	0.574119	0.740239	0.000000	3492	2.31
PROPANE	-0.055614	0.045098	0.573474	0.484177	0.544990	0.578176	0.000000	3197	2.21
n-BUTANE	-0.130962	0.044716	0.574252	0.364025	0.575470	0.503497	0.000000	1652	2.33
n-PENTANE	-0.109097	0.048770	0.545919	0.466066	0.604016	0.386243	0.000000	2309	3.88
n-HEXANE	-0.087161	0.057172	0.533845	0.456573	0.553793	0.307552	0.000000	2197	3.75
n-HEPTANE	-0.016656	0.075827	0.523520	0.629464	0.518750	0.281273	0.000000	2258	3.63
n-OCTANE	-0.031651	0.078139	0.533271	0.690599	0.537658	0.282773	0.000000	1896	4.09
n-NONANE	-0.027700	0.074369	0.534006	0.170371	1.422928	0.078540	0.000000	767	4.29
n-DECANE	-0.127983	0.062553	0.500002	0.119121	2.849758	0.276442	0.000000	1609	4.93
n-UNDECANE	-0.084258	0.070572	0.588243	0.173583	2.084758	0.203159	0.000000	668	6.44
n-DODECANE	-0.244249	0.049777	0.660712	1.774219	0.838413	0.542320	0.000000	1123	6.87
n-TRIDECANE	-0.053946	0.072977	0.634227	0.123414	2.751049	0.043591	0.000000	195	9.18
n-TETRADECANE	-0.137863	0.064153	0.500000	0.187847	2.518995	0.248667	0.000000	843	10.14
n-PENTADECANE	-0.048513	0.071093	0.657142	0.164734	2.550343	0.000010	0.000000	224	12.05
n-HEXADECANE	-0.106717	0.072412	0.500000	0.199697	1.055140	0.191156	0.000000	601	15.38
n-HEPTADECANE	-0.022105	0.081123	0.501979	0.198535	2.856684	0.000010	0.000000	361	12.95
n-OCTADECANE	-0.039413	0.075195	0.522944	0.191176	2.674767	0.000010	0.000000	416	14.39
n-NONADECANE	-0.027242	0.078857	0.696800	0.140126	2.402062	0.000026	0.000000	310	13.12
n-EICOSANE	-0.037487	0.082761	0.624733	0.088438	2.380113	0.000010	0.000000	138	13.42
n-HENEICOSANE	-0.043839	0.084313	0.690594	0.037592	1.257186	0.091417	0.000000	39	20.14
branched alkanes								4335	3.60
ISOBUTANE	-0.074449	0.058852	0.561002	0.621708	0.625365	0.503092	0.000000	1943	2.72
ISOPENTANE	-0.110407	0.049337	0.548775	0.308040	0.499947	0.305619	0.000000	844	3.92
NEOPENTANE	-0.224952	0.059351	0.582176	1.400910	1.235812	0.612666	0.000000	77	4.26
2,2-DIMETHYLBUTANE	-0.387992	0.013621	0.661626	0.032414	0.443613	0.453458	0.000000	23	1.33
2,3-DIMETHYLBUTANE	-0.041150	0.072409	0.616791	0.068972	1.931246	0.132175	0.000000	92	1.80
2-METHYLPENTANE	-0.125699	0.048000	0.500000	0.151022	1.385306	0.290492	0.000000	127	2.16
3-METHYLPENTANE	-0.059568	0.059316	0.699229	0.029094	2.348665	0.158075	0.000000	108	1.20
2,4-DIMETHYLPENTANE	-0.340836	0.017112	0.519864	0.129870	0.842204	0.685567	0.000000	15	1.45
3-ETHYLPENTANE	-0.500000	0.000075	0.637520	0.092669	2.969575	1.185999	0.000000	7	1.34
2,2,4-TRIMETHYLPENTANE	-0.105419	0.070802	0.515072	1.643289	2.335661	0.242504	0.000000	899	4.40
2,3,4-TRIMETHYLPENTANE	-0.005429	0.086176	0.634487	0.122318	2.788305	0.116965	0.000000	23	5.15
2,3-DIMETHYLHEXANE	-0.500000	0.000156	0.500424	0.199076	0.505209	1.052706	0.000000	16	1.54
2,2,4,4,6,8,8-HEPTAMETHYLNONANE	-0.056278	0.097802	0.594623	0.136739	2.328043	0.043026	0.000000	161	12.06
cycloalkanes								2142	3.54
CYCLOPENTANE	-0.299219	0.033458	0.644639	0.078475	2.968894	0.754458	0.000000	266	1.42

Continued on next page

Table III-28 – continued from previous page

Name	a_1	a_2	b_1	b_2	c	d	α	Data number	MAPE
CYCLOHEXANE	-0.055003	0.100000	0.539907	1.045791	0.770940	0.372327	0.000000	1732	3.89
CYCLOHEPTANE	-0.141666	0.100000	0.523836	0.176381	0.200000	0.201986	0.000000	62	3.79
CYCLOOCTANE	-0.101032	0.095881	0.525209	0.088341	1.302456	0.319907	0.000000	82	2.84
alkenes								3168	3.61
ETHYLENE	-0.233067	0.012937	0.568461	0.089713	0.595105	0.763856	0.000000	974	2.67
PROPYLENE	-0.018352	0.040590	0.561774	0.445324	0.479890	0.488780	0.000000	652	3.58
1-BUTENE	-0.207631	0.020157	0.512445	0.155074	0.403802	0.341960	0.000000	19	0.41
1-PENTENE	0.084351	0.081146	0.500000	0.200000	2.963879	0.012854	0.000000	19	7.64
1-HEXENE	0.075398	0.080415	0.500000	0.200000	2.698483	0.000010	0.000000	461	6.57
1-HEPTENE	-0.039045	0.064963	0.500000	0.200000	0.596462	0.180692	0.000000	331	2.52
1-OCTENE	-0.106190	0.061707	0.620889	0.083390	2.234771	0.285295	0.000000	322	3.43
1-NONENE	0.064522	0.092649	0.689096	0.154891	2.594631	0.000048	0.000000	107	6.30
1-DECENE	-0.008216	0.079758	0.517577	0.018550	1.524122	0.022765	0.000000	70	4.23
1-UNDECENE	0.008580	0.086021	0.513936	0.032148	1.893788	0.000010	0.000000	23	0.74
1-DODECENE	0.019019	0.091090	0.579018	0.104281	2.820843	0.000010	0.000000	44	1.98
1-TRIDECENE	0.004853	0.088737	0.514282	0.198967	2.465879	0.000010	0.000000	25	1.49
1-TETRADECENE	0.002063	0.088640	0.518525	0.115766	2.412606	0.000021	0.000000	26	1.84
1-PENTADECENE	0.003197	0.092570	0.521811	0.189084	1.950309	0.000010	0.000000	27	2.13
1-HEXADECENE	0.011642	0.097282	0.572003	0.030740	1.971685	0.000010	0.000000	41	3.09
1-HEPTADECENE	-0.005799	0.092044	0.577946	0.189653	1.768897	0.000010	0.000000	27	1.79
alkynes								160	1.77
ACETYLENE	-0.120254	0.000026	0.598822	0.072826	0.420560	0.832625	0.000000	148	1.92
METHYLACETYLENE	-0.232781	0.012770	0.620745	0.158386	0.899874	0.791003	0.000000	2	0.02
1-HEXYNE	-0.336084	0.032791	0.513162	0.126076	1.577389	1.030168	0.000000	10	0.04
aromatics								5621	3.00
BENZENE	0.048665	0.088833	0.589620	0.742714	0.475062	0.435443	0.000000	2286	2.47
TOLUENE	-0.046416	0.076683	0.545201	1.157512	1.082507	0.391215	0.000000	435	4.89
m-XYLENE	-0.115004	0.057270	0.540765	0.200000	1.000885	0.387029	0.000000	857	2.38
p-XYLENE	-0.135002	0.055010	0.575113	0.183009	0.599996	0.365573	0.000000	838	2.23
ETHYLBENZENE	-0.139512	0.051199	0.502187	0.200000	1.187191	0.358712	0.000000	959	4.20
MESITYLENE	0.004606	0.078482	0.598732	0.137363	1.439807	0.132138	0.000000	165	2.33
p-CYMENE	-0.147627	0.041226	0.587587	0.115390	1.698666	0.115056	0.000000	21	5.11
n-HEPTYLBENZENE	-0.111162	0.069369	0.547112	0.132206	2.187319	0.197786	0.000000	35	6.82
n-DODECYLBENZENE	-0.046188	0.090536	0.536486	0.101675	2.409777	0.221948	0.000000	25	15.76
esters								1013	3.83
VINYL ACETATE	-0.033015	0.045098	0.582352	0.131778	1.442920	0.035150	0.000000	30	1.22
n-PROPYL ACETATE	-0.189131	0.038129	0.650879	0.200000	0.359719	0.380494	0.000000	193	3.43
n-BUTYL ACETATE	-0.116685	0.050521	0.679068	0.048999	0.539757	0.129695	0.000000	291	2.15
ISOPENTYL ACETATE	-0.323564	0.029670	0.695828	0.170212	1.440411	0.740553	0.000000	131	6.31

Continued on next page

Table III-28 – continued from previous page

Name	a_1	a_2	b_1	b_2	c	d	α	Data number	MAPE
n-PENTYL ACETATE	-0.085979	0.070900	0.500000	0.180287	1.801030	0.353558	0.000000	217	5.02
n-HEPTYL ACETATE	-0.099025	0.074500	0.510764	0.158273	2.368234	0.367790	0.000000	151	4.23
ethers								494	2.78
DIMETHYL ETHER	0.129615	0.062798	0.577685	0.603167	0.532290	0.660933	0.000000	119	0.92
METHYL tert-BUTYL ETHER	-0.331115	0.000014	0.595802	0.123080	2.240539	0.441140	0.000000	66	5.59
DI-n-PROPYL ETHER	-0.471484	0.005996	0.549077	0.196063	0.712194	1.110047	0.000000	185	3.22
DI-n-BUTYL ETHER	0.035905	0.087508	0.513040	0.165319	1.915235	0.014107	0.000000	100	2.23
DI-n-PENTYL ETHER	-0.057552	0.076086	0.554379	0.095821	1.222474	0.155949	0.000000	24	3.20
ketones								1101	4.01
ACETONE	-0.016911	0.059158	0.500206	0.200000	0.646256	0.196482	0.000000	577	3.16
3-PENTANONE	-0.042550	0.058909	0.661661	0.145445	2.558350	0.158594	0.000000	154	3.37
2-HEXANONE	-0.070715	0.069337	0.549345	0.113396	2.143655	0.360522	0.000000	59	2.70
METHYL ISOBUTYL KETONE	-0.075806	0.049320	0.535879	0.037257	1.728826	0.000010	0.000000	168	5.31
4-HEPTANONE	-0.143534	0.060687	0.667216	0.137327	2.177875	0.454484	0.000000	75	6.49
2-OCTANONE	0.029032	0.082093	0.697147	0.118258	2.343689	0.054980	0.000000	68	7.90
HFC-CFC								9743	2.28
DIFLUOROMETHANE	0.139290	0.053914	0.583095	0.425485	0.563487	0.953508	0.000000	234	2.26
1,1-DIFLUOROETHANE	0.033183	0.056289	0.591278	0.469684	0.489406	0.689885	0.000000	281	1.51
TRIFLUOROMETHANE	-0.092000	0.029866	0.560812	0.251433	0.785427	1.070556	0.000000	591	3.27
1,1,1-TRIFLUOROETHANE	0.205652	0.088669	0.559103	0.756920	0.572203	0.715007	0.000000	294	1.05
CHLORODIFLUOROMETHANE	-0.136383	0.030911	0.563704	0.313689	0.698974	0.738046	0.000000	1128	2.29
CARBON TETRAFLUORIDE	-0.247988	0.019332	0.550043	0.101061	0.637075	1.246251	0.000000	658	3.57
1-CHLORO-1,1-DIFLUOROETHANE	0.188752	0.071921	0.585313	0.993656	0.431557	0.582102	0.000000	109	0.93
1,1,1,2-TETRAFLUOROETHANE	0.145484	0.076531	0.566463	0.671158	0.535005	0.743204	0.000000	779	2.52
DICHLOROFLUOROMETHANE	-0.215925	0.020782	0.569827	0.181027	0.503290	0.453404	0.000000	215	2.06
CHLOROTRIFLUOROMETHANE	-0.309798	0.011657	0.569516	-0.001506	0.644405	0.813364	0.000000	834	2.75
PENTAFLUOROETHANE	0.034593	0.065304	0.565746	0.517226	0.549138	0.781884	0.000000	463	1.63
DICHLORODIFLUOROMETHANE	-0.263250	0.018496	0.594316	0.166486	0.461760	0.520424	0.000000	1322	2.47
1,1,1,3,3-PENTAFLUOROPROPANE	-0.247869	0.029088	0.555195	0.200000	0.800904	0.632564	0.000000	149	1.47
TRICHLOROFLUOROMETHANE	-0.126382	0.055873	0.539715	0.609615	0.810710	0.497463	0.000000	410	1.57
BROMOTRIFLUOROMETHANE	-0.222160	0.017045	0.547158	0.251851	0.760615	0.657320	0.000000	1223	1.90
1,1,1,3,3,3-HEXAFLUOROPROPANE	-0.264459	0.021927	0.577399	0.199996	0.553641	0.573611	0.000000	172	1.85
CHLOROPENTAFLUOROETHANE	-0.106792	0.062466	0.543976	0.514969	0.747531	0.633606	0.000000	421	2.05
1,1,1,2,3,3,3-HEPTAFLUOROPROPANE	-0.292026	0.018413	0.583084	0.195920	0.498066	0.506488	0.000000	112	1.93
1,2-DICHLOROTETRAFLUOROETHANE	-0.268462	0.034540	0.562860	0.141568	0.636147	0.529092	0.000000	348	1.98
noble gases								8565	2.72
ARGON	-0.460829	0.000010	0.580159	-0.104931	0.671210	1.682354	0.012774	4406	2.81
KRYPTON	-0.407071	0.000010	0.582788	-0.096522	0.656828	1.073248	0.009032	2187	2.29
XENON	-0.144010	0.047359	0.579838	0.086168	0.587360	0.697640	0.012168	1972	2.99

Continued on next page

Table III-28 – continued from previous page

Name	a_1	a_2	b_1	b_2	c	d	α	Data number	MAPE
aldehydes								348	6.99
ACETALDEHYDE	-0.220391	0.028518	0.664326	0.123566	2.939826	1.016180	0.000000	33	7.61
PROPANAL	0.144767	0.094323	0.527546	0.139936	1.339003	0.089709	0.000000	22	2.82
2-METHYLPROPANAL	-0.142971	0.028785	0.500000	0.200000	2.586692	0.000010	0.000000	57	6.64
BUTANAL	0.038579	0.073439	0.615871	0.121457	2.001779	0.000010	0.000000	197	8.05
3-METHYLBUTYRALDEHYDE	0.125124	0.100000	0.636890	0.028705	2.339660	0.013758	0.000000	20	3.81
HEPTANAL	-0.493381	0.002394	0.588568	0.148539	1.608195	0.856743	0.000000	9	1.53
DECANAL	-0.337756	0.001733	0.528353	0.059416	2.702960	0.093158	0.000000	10	6.65
amines								496	4.23
METHYLAMINE	0.040191	0.038164	0.561405	0.108290	1.473835	0.220625	0.000000	122	1.82
n-PROPYLAMINE	-0.003833	0.053119	0.683926	0.172185	1.550378	0.052951	0.000000	46	3.00
n-BUTYLAMINE	-0.033999	0.053849	0.610750	0.064248	2.758578	0.029153	0.000000	169	5.47
DIETHYLAMINE	-0.189804	0.055333	0.550751	0.015246	1.707389	0.080927	0.000000	30	10.11
n-PENTYLAMINE	0.016634	0.070176	0.579146	0.082713	2.735342	0.002358	0.000000	72	4.61
n-HEXYLAMINE	-0.004852	0.068852	0.500252	0.200000	2.990311	0.023516	0.000000	57	3.11
alcohols								8995	3.26
METHANOL	0.839597	0.155416	0.604767	1.240319	0.696234	0.970610	0.000000	1762	2.44
ETHANOL	0.511222	0.124630	0.557043	0.796910	0.566280	0.607537	0.000000	1829	2.61
1-PROPANOL	0.066788	0.102021	0.642146	1.594645	1.030270	0.982002	0.000000	1348	2.24
1-BUTANOL	0.768240	0.189651	0.735990	1.530678	0.400242	1.126372	0.000000	1246	2.35
1-PENTANOL	0.350734	0.158669	0.866120	1.225570	0.439920	0.900720	0.000000	514	2.78
1-HEXANOL	0.164996	0.139498	0.713986	1.767158	0.689570	0.445080	0.000000	492	2.72
1-HEPTANOL	0.174734	0.132490	1.250770	0.374960	1.037639	0.025442	0.000000	324	4.63
1-OCTANOL	0.085263	0.115290	0.875519	1.497508	0.741884	0.217179	0.000000	394	3.56
1-NONANOL	0.050700	0.096444	1.364158	1.824045	0.964930	0.034994	0.000000	221	4.16
1-DECANOL	0.376911	0.177308	0.623347	1.809256	0.408769	0.311143	0.000000	346	6.07
1-UNDECANOL	0.279428	0.151072	0.500006	1.999978	0.493085	0.006442	0.000000	235	8.42
1-DODECANOL	0.286043	0.160270	0.500048	1.999479	0.455570	0.000010	0.000000	253	10.65
1-OCTADECANOL	-0.033738	0.077923	0.823644	1.042787	0.404877	0.000109	0.000000	31	31.40
others								18838	3.96
AMMONIA	0.158227	0.036096	0.616510	0.218933	0.386808	1.106626	0.000000	1433	5.86
WATER	0.500000	0.082898	0.596291	0.639114	0.940985	0.932397	0.000000	7445	4.56
CARBON MONOXIDE	0.109960	0.022053	0.602154	0.155689	0.453356	2.006286	0.022343	422	1.88
NITROGEN	0.169677	0.020197	0.612566	0.179286	0.382340	2.059329	0.028901	4288	2.99
OXYGEN	-0.089990	0.013273	0.585376	0.100463	0.489195	1.803688	0.022505	1033	4.02
HYDROGEN SULFIDE	0.028021	0.029756	0.500000	0.370698	0.495036	0.134451	0.000000	61	7.97
CARBON DIOXIDE	0.106976	0.033995	0.601472	0.267889	0.426357	1.416130	0.087427	3813	3.38
CHLOROFORM	-0.343246	0.018864	0.649473	0.107131	1.618529	0.975325	0.000000	343	3.02

III-D-3) Chemical-family specific parameters

These parameters have to be used with Eq. (III-19).

III-D-3.1) Paraffins

Table III-29 - Chemical-family specific parameters for paraffinic compounds to be used in the *tc*-PR based model.

Parameter	Value
Component number	33
Data number	25099
MAPE	10.88
a_1	-0.38044223
a_2	0.00496815
b_1	0.64386422
b_2	0.01221408
c	0.33690576
d	0.31802325

Table III-30 - Prediction of viscosity data of paraffins using chemical-family specific parameters for the tc-PR based model: data number and corresponding MAPE (Mean Average Percent Error).

Name	Data number	MAPE
PROPANE	3197	11.69
n-BUTANE	1652	8.43
n-PENTANE	2309	7.77
n-HEXANE	2197	6.71
n-HEPTANE	2258	7.99
n-OCTANE	1896	7.13
n-NONANE	767	5.48
n-DECANE	1609	7.01
n-UNDECANE	668	8.47
n-DODECANE	1123	10.84
n-TRIDECANE	195	13.05
n-TETRADECANE	843	13.91
n-PENTADECANE	224	14.56
n-HEXADECANE	601	18.90
n-HEPTADECANE	361	16.58
n-OCTADECANE	416	17.09
n-NONADECANE	310	18.21
n-EICOSANE	138	21.22
ISOBUTANE	1943	15.51
ISOPENTANE	844	8.37
NEOPENTANE	77	31.61
2,2-DIMETHYLBUTANE	23	25.95
2,3-DIMETHYLBUTANE	92	15.96
2-METHYLPENTANE	127	5.49
3-METHYLPENTANE	108	5.26
2,4-DIMETHYLPENTANE	15	2.50
3-ETHYLPENTANE	7	12.24
2,2,4-TRIMETHYLPENTANE	899	23.01
2,3,4-TRIMETHYLPENTANE	23	11.41
2,3-DIMETHYLHEXANE	16	1.68
2,2,4,4,6,8,8-HEPTAMETHYLNONANE	161	59.40

III-D-3.2) Cycloalkanes

Table III-31 - Chemical-family specific parameters for cycloalkanes to be used in the *tc*-PR based model.

Parameter	Value
Component number	4
Data number	2142
MAPE	11.97
a_1	-0.53130923
a_2	0.00001000
b_1	0.63786725
b_2	-0.33665528
c	0.43719479
d	0.45000000

Table III-32 - Prediction of viscosity data of cycloalkanes using chemical-family specific parameters for the *tc*-PR based model: data number and corresponding MAPE (Mean Average Percent Error).

Name	Data number	MAPE
CYCLOPENTANE	266	41.28
CYCLOHEXANE	1732	7.58
CYCLOHEPTANE	62	12.55
CYCLOOCTANE	82	9.21

III-D-3.3) Alkenes

Table III-33 - Chemical-family specific parameters for alkenes to be used in the *tc*-PR based model.

Parameter	Value
Component number	16
Data number	3168
MAPE	11.42
a_1	-0.44507179
a_2	0.00000000
b_1	0.67810597
b_2	-0.01635567
c	0.31163434
d	0.41586438

Table III-34 - Prediction of viscosity data of alkenes using chemical-family specific parameters for the *tc*-PR based model: data number and corresponding MAPE (Mean Average Percent Error).

Name	Data number	MAPE
ETHYLENE	974	10.68
PROPYLENE	652	10.48
1-BUTENE	19	15.35
1-PENTENE	19	15.25
1-HEXENE	461	15.67
1-HEPTENE	331	8.78
1-OCTENE	322	11.22
1-NONENE	107	12.36
1-DECENE	70	9.39
1-UNDECENE	23	11.23
1-DODECENE	44	8.86
1-TRIDECENE	25	9.67
1-TETRADECENE	26	9.32
1-PENTADECENE	27	14.54
1-HEXADECENE	41	18.10
1-HEPTADECENE	27	14.48

III-D-3.4) Alkynes

Table III-35 - Chemical-family specific parameters for alkynes to be used in the *tc*-PR based model.

Parameter	Value
Component number	3
Data number	160
MAPE	2.85
a_1	-0.47893811
a_2	0.00000000
b_1	0.58052188
b_2	-0.29484829
c	0.54598975
d	0.81836633

Table III-36 - Prediction of viscosity data of alkynes using chemical-family specific parameters for the *tc*-PR based model: data number and corresponding MAPE (Mean Average Percent Error).

Name	Data number	MAPE
ACETYLENE	148	2.05
METHYLACETYLENE	2	73.04
1-HEXYNE	10	0.55

III-D-3.5) Aromatics compounds

Table III-37 - Chemical-family specific parameters for aromatic compounds to be used in the *tc*-PR based model.

Parameter	Value
Component number	9
Data number	5621
MAPE	5.14
a_1	-0.11239348
a_2	0.06022209
b_1	0.56892276
b_2	0.35505868
c	0.62160203
d	0.39582666

Table III-38 - Prediction of viscosity data of aromatics using chemical-family specific parameters for the *tc*-PR based model: data number and corresponding MAPE (Mean Average Percent Error).

Name	Data number	MAPE
BENZENE	2286	2.94
TOLUENE	435	7.73
m-XYLENE	857	6.21
p-XYLENE	838	3.90
ETHYLBENZENE	959	6.00
MESITYLENE	165	3.50
p-CYMENE	21	23.68
n-HEPTYLBENZENE	35	52.14
n-DODECYLBENZENE	25	63.05

III-D-3.6) Esters

Table III-39 - Chemical-family specific parameters for esters to be used in the *tc*-PR based model.

Parameter	Value
Component number	6
Data number	1013
MAPE	9.61
a_1	-0.02450351
a_2	0.05804304
b_1	0.16253136
b_2	-1.54999151
c	0.59918351
d	-0.43088357

Table III-40 - Prediction of viscosity data of esters using chemical-family specific parameters for the *tc*-PR based model: data number and corresponding MAPE (Mean Average Percent Error).

Name	Data number	MAPE
VINYL ACETATE	30	41.00
n-PROPYL ACETATE	193	10.70
n-BUTYL ACETATE	291	6.78
ISOPENTYL ACETATE	131	13.72
n-PENTYL ACETATE	217	7.21
n-HEPTYL ACETATE	151	7.32

III-D-3.7) Ethers

Table III-41 - Chemical-family specific parameters for ethers to be used in the *tc*-PR based model.

Parameter	Value
Component number	5
Data number	494
MAPE	7.64
a_1	-0.41993711
a_2	0.00000000
b_1	0.59897303
b_2	-0.24371851
c	0.45616690
d	0.43066178

Table III-42 - Prediction of viscosity data of ethers using chemical-family specific parameters for the *tc*-PR based model: data number and corresponding MAPE (Mean Average Percent Error).

Name	Data number	MAPE
DIMETHYL ETHER	119	7.99
METHYL tert-BUTYL ETHER	66	9.82
DI-n-PROPYL ETHER	185	5.24
DI-n-BUTYL ETHER	100	9.38
DI-n-PENTYL ETHER	24	11.19

III-D-3.8) Ketones

Table III-43 - Chemical-family specific parameters for ketones to be used in the *tc*-PR based model.

Parameter	Value
Component number	6
Data number	1101
MAPE	6.86
a_1	-0.45273818
a_2	0.02343088
b_1	-0.48409999
b_2	-0.27305913
c	0.26309638
d	0.77336072

Table III-44 - Prediction of viscosity data of ketones using chemical-family specific parameters for the *tc*-PR based model: data number and corresponding MAPE (Mean Average Percent Error).

Name	Data number	MAPE
ACETONE	577	5.68
3-PENTANONE	154	8.63
2-HEXANONE	59	3.08
METHYL ISOBUTYL KETONE	168	8.81
4-HEPTANONE	75	8.07
2-OCTANONE	68	10.05

III-D-3.9) HFC-CFC

Table III-45 - Chemical-family specific parameters for HFC-CFC compounds to be used in the *tc*-PR based model.

Parameter	Value
Component number	19
Data number	9743
MAPE	11.66
a_1	-0.41501535
a_2	0.00000000
b_1	0.57328803
b_2	-0.13501287
c	0.53795228
d	0.58379137

Table III-46 - Prediction of viscosity data of HFC-CFCs using chemical-family specific parameters for the *tc*-PR based model: data number and corresponding MAPE (Mean Average Percent Error).

Name	Data number	MAPE
DIFLUOROMETHANE	234	13.12
1,1-DIFLUOROETHANE	281	6.06
TRIFLUOROMETHANE	591	15.84
1,1,1-TRIFLUOROETHANE	294	3.78
CHLORODIFLUOROMETHANE	1128	12.78
CARBON TETRAFLUORIDE	658	34.25
1-CHLORO-1,1-DIFLUOROETHANE	109	8.83
1,1,1,2-TETRAFLUOROETHANE	779	8.70
DICHLOROFLUOROMETHANE	215	12.41
CHLOROTRIFLUOROMETHANE	834	9.48
PENTAFLUOROETHANE	463	14.41
DICHLORODIFLUOROMETHANE	1322	5.89
1,1,1,3,3-PENTAFLUOROPROPANE	149	8.26
TRICHLOROFLUOROMETHANE	410	7.75
BROMOTRIFLUOROMETHANE	1223	6.84
1,1,1,3,3,3-HEXAFLUOROPROPANE	172	8.26
CHLOROPENTAFLUOROETHANE	421	12.78
1,1,1,2,3,3,3-HEPTAFLUOROPROPANE	112	12.57
1,2-DICHLOROTETRAFLUOROETHANE	348	21.91

III-D-3.10) Aldehydes

Table III-47 - Chemical-family specific parameters for aldehydes to be used in the *tc*-PR based model.

Parameter	Value
Component number	7
Data number	348
MAPE	9.36
a_1	0.77959684
a_2	0.14685457
b_1	0.17479301
b_2	-1.36284174
c	0.59649990
d	-2.77076302

Table III-48 - Prediction of viscosity data of aldehydes using chemical-family specific parameters for the *tc*-PR based model: data number and corresponding MAPE (Mean Average Percent Error).

Name	Data number	MAPE
ACETALDEHYDE	33	10.74
PROPANAL	22	13.85
2-METHYLPROPANAL	57	11.00
BUTANAL	197	6.81
3-METHYLBUTYRALDEHYDE	20	11.73
HEPTANAL	9	17.56
DECANAL	10	23.81

III-D-3.11) Amines

Table III-49 - Chemical-family specific parameters for amines to be used in the *tc*-PR based model.

Parameter	Value
Component number	6
Data number	496
MAPE	9.81
a_1	-0.18785796
a_2	0.02423144
b_1	0.54749540
b_2	-0.10386684
c	0.28794771
d	-0.60735281

Table III-50 - Prediction of viscosity data of amines using chemical-family specific parameters for the *tc*-PR based model: data number and corresponding MAPE (Mean Average Percent Error).

Name	Data number	MAPE
METHYLAMINE	122	3.07
n-PROPYLAMINE	46	14.13
n-BUTYLAMINE	169	5.85
DIETHYLAMINE	30	58.74
n-PENTYLAMINE	72	7.31
n-HEXYLAMINE	57	9.90

III-D-4) Universal parameters

Table III-51 - Universal parameters to be used with the *tc*-PR based model

Parameter	Value
Component number	126
Data number	75866
MAPE	16.49
a_1	-0.40758780
a_2	0.00253490
b_1	0.59340800
b_2	-0.03077821
c	0.38279452
d	0.45826483

Table III-52 - Data number and MAPE resulting from prediction with the *tc*-PR based model coupled with universal parameters

Name	Data number	MAPE
n-alkanes	27973	12.83
METHANE	3678	20.33
ETHANE	3492	12.09
PROPANE	3197	11.17
n-BUTANE	1652	9.86
n-PENTANE	2309	12.44
n-HEXANE	2197	12.43
n-HEPTANE	2258	10.92
n-OCTANE	1896	10.05
n-NONANE	767	5.43
n-DECANE	1609	7.77
n-UNDECANE	668	8.29
n-DODECANE	1123	12.62
n-TRIDECANE	195	14.72
n-TETRADECANE	843	15.46
n-PENTADECANE	224	15.03
n-HEXADECANE	601	20.61
n-HEPTADECANE	361	16.38
n-OCTADECANE	416	16.54
n-NONADECANE	310	16.31
n-EICOSANE	138	24.76
n-HENEICOSANE	39	22.82
branched alkanes	4335	18.50
ISOBUTANE	1943	15.21
ISOPENTANE	844	14.67
NEOPENTANE	77	33.66
2,2-DIMETHYLBUTANE	23	28.93
2,3-DIMETHYLBUTANE	92	14.66
2-METHYLPENTANE	127	6.95
3-METHYLPENTANE	108	6.85
2,4-DIMETHYLPENTANE	15	3.46
3-ETHYLPENTANE	7	13.79
2,2,4-TRIMETHYLPENTANE	899	24.18
2,3,4-TRIMETHYLPENTANE	23	10.81
2,3-DIMETHYLHEXANE	16	1.66
2,2,4,4,6,8,8-HEPTAMETHYLNONANE	161	61.22
cycloalkanes	2142	39.64
CYCLOPENTANE	266	18.61
CYCLOHEXANE	1732	41.87
CYCLOHEPTANE	62	52.07
CYCLOOCTANE	82	51.45
alkenes	3168	13.80
ETHYLENE	974	11.99
PROPYLENE	652	12.87
1-BUTENE	19	21.90
1-PENTENE	19	18.91
1-HEXENE	461	22.91
1-HEPTENE	331	14.50
1-OCTENE	322	6.03
1-NONENE	107	15.04
1-DECENE	70	8.74
1-UNDECENE	23	11.71
1-DODECENE	44	12.07
1-TRIDECENE	25	12.11
1-TETRADECENE	26	10.68
1-PENTADECENE	27	18.08
1-HEXADECENE	41	24.06
1-HEPTADECENE	27	18.41

Continued on next page

Table III-52 – continued from previous page

Name	Data number	MAPE
alkynes	160	8.30
ACETYLENE	148	7.80
METHYLACETYLENE	2	50.08
1-HEXYNE	10	7.37
aromatics	5621	14.76
BENZENE	2286	10.90
TOLUENE	435	18.54
m-XYLENE	857	22.37
p-XYLENE	838	11.47
ETHYLBENZENE	959	16.31
MESITYLENE	165	21.27
p-CYMENE	21	11.78
n-HEPTYLBENZENE	35	26.77
n-DODECYLBENZENE	25	34.77
esters	1013	11.24
VINYL ACETATE	30	47.81
n-PROPYL ACETATE	193	17.15
n-BUTYL ACETATE	291	4.18
ISOPENTYL ACETATE	131	13.00
n-PENTYL ACETATE	217	8.28
n-HEPTYL ACETATE	151	12.77
ethers	494	11.33
DIMETHYL ETHER	119	21.52
METHYL tert-BUTYL ETHER	66	7.18
DI-n-PROPYL ETHER	185	7.31
DI-n-BUTYL ETHER	100	7.50
DI-n-PENTYL ETHER	24	19.08
ketones	1101	12.47
ACETONE	577	12.27
3-PENTANONE	154	18.55
2-HEXANONE	59	10.35
METHYL ISOBUTYL KETONE	168	8.61
4-HEPTANONE	75	10.35
2-OCTANONE	68	14.13
HFC-CFC	9743	14.26
DIFLUOROMETHANE	234	15.61
1,1-DIFLUOROETHANE	281	10.48
TRIFLUOROMETHANE	591	17.47
1,1,1-TRIFLUOROETHANE	294	9.33
CHLORODIFLUOROMETHANE	1128	10.71
CARBON TETRAFLUORIDE	658	26.81
1-CHLORO-1,1-DIFLUOROETHANE	109	12.43
1,1,1,2-TETRAFLUOROETHANE	779	15.71
DICHLOROFLUOROMETHANE	215	12.27
CHLOROTRIFLUOROMETHANE	834	12.27
PENTAFLUOROETHANE	463	18.69
DICHLORODIFLUOROMETHANE	1322	8.70
1,1,1,3,3-PENTAFLUOROPROPANE	149	15.96
TRICHLOROFLUOROMETHANE	410	13.59
BROMOTRIFLUOROMETHANE	1223	10.39
1,1,1,3,3,3-HEXAFLUOROPROPANE	172	15.80
CHLOROPENTAFLUOROETHANE	421	20.04
1,1,1,2,3,3,3-HEPTAFLUOROPROPANE	112	16.82
1,2-DICHLOROTETRAFLUOROETHANE	348	26.64
aldehydes	348	15.26
ACETALDEHYDE	33	37.51
PROPANAL	22	9.17
2-METHYLPROPANAL	57	21.24
BUTANAL	197	10.03
3-METHYLBUTYRALDEHYDE	20	10.44

Continued on next page

Table III-52 – continued from previous page

Name	Data number	MAPE
HEPTANAL	9	34.27
DECANAL	10	16.56
amines	496	21.31
METHYLAMINE	122	44.78
n-PROPYLAMINE	46	29.95
n-BUTYLAMINE	169	7.32
DIETHYLAMINE	30	60.01
n-PENTYLAMINE	72	5.57
n-HEXYLAMINE	57	5.08
noble gases	8337	20.47
NEON	858	41.21
ARGON	3848	21.46
KRYPTON	1789	16.37
XENON	1842	12.74
others	10935	22.23
AMMONIA	1433	18.08
CARBON MONOXIDE	418	21.76
NITROGEN	3914	27.32
OXYGEN	1009	16.45
HYDROGEN SULFIDE	61	23.08
CARBON DIOXIDE	3757	21.54
CHLOROFORM	343	6.30

III-E) Validation cases:

A validation case is proposed to help potential users to verify the implementation of the models introduced in this article. Calculations are performed with pure n-hexane.

III-E-1) *I*-PC-SAFT based model

Table II-53 - Validation cases for the *I*-PC-SAFT based model. Model parameters related to pure n-hexane can be found in Tables III-1 and III-2.

Variable	Case 1	Case 2	Cas 3
T **(*K*)**	198.15	440.0	900.0
p **(*bar*)**	1.000	1.000	60.00
$\eta_{\text{experimental}}$ **(*Pa.s*)**	0.001265	0.0000095	0.0000217
ρ **(mol.m^{-3})**	9364.371331	27.93899672	854.2957831
$\frac{s_{\text{Tv-res}}}{R}$	-9.096773398	-0.019221457	-0.318273562
$\frac{s^{c}_{\text{Tv-res}}}{R}$	-1.172261033	-1.172261033	-1.172261033
X_{ES}	-9.809009089	4.09426556	1.032274398
η_{ref} **(*Pa.s*)**	0.00006269	0.00000194	0.00002707
$\eta_{\text{prediction}}$ **(*Pa.s*)**	0.001263151	0.00000922	0.00002184
$\Delta\eta$ **(%)**	0.146175672	2.956112896	0.660320278

III-E-2) *tc*-PR based model

Table II-54 - Validation cases for the *tc*-PR based model. Model parameters related to pure n-hexane can be found in Tables III-27 and III-28.

Variable	Case 1	Case 2	Cas 3
T **(*K*)**	198.15	440	900
p **(*bar*)**	1.000	1.000	60.00
$\eta_{\text{experimental}}$ **(*Pa.s*)**	0.001265	0.0000095	0.0000217
ρ **(mol.m^{-3})**	8499.433742	27.88530923	829.6265173
$\frac{s_{\text{Tv-res}}}{R}$	-4.904025668	-0.009074876	-0.178457713
$\frac{s^{c}_{\text{Tv-res}}}{R}$	-0.661375936	-0.661375936	-0.661375936
X_{ES}	-9.41837302	4.275091526	1.040142793
η_{ref} **(*Pa.s*)**	0.00005876	0.00000193	0.00002655
$\eta_{\text{prediction}}$ **(*Pa.s*)**	0.00125907	0.00000932	0.00002173
$\Delta\eta$ **(%)**	0.468411087	1.845421065	0.147306134

IV- Chapitre 2 : Le coefficient d'auto-diffusion des corps purs

Ce chapitre a donné lieu à la publication suivante :

A new entropy-scaling based model for estimating the self-diffusion coefficients of pure fluids.

Aghilas Dehlouz[1,2], Jean-Noël Jaubert[1(*)], Guillaume Galliero[3], Marc Bonnissel[2], Romain Privat[1(*)]

[1] *Université de Lorraine, École Nationale Supérieure des Industries Chimiques, Laboratoire Réactions et Génie des Procédés (UMR CNRS 7274), 1 rue Grandville, 54000 Nancy, France*

[2] *Gaztransport & Technigaz (GTT), 1 route de Versailles, 78470 Saint-Rémy-lès-Chevreuse, France*

[3] *Université de Pau et des Pays de l'Adour, E2S UPPA, CNRS TotalEnergies, LFCR UMR 5150, Pau, France*

Abstract :

A new model for providing self-diffusion coefficients is proposed here. It is based on the entropy-scaling concept and makes it possible to quantitatively estimate self-diffusion coefficients in any fluid state (subcritical gas and liquid as well as supercritical states). A general relation between a dimensionless form of self-diffusion coefficient and a function of the Tv-residual entropy is proposed. This relation involves thermodynamic properties only that were estimated using the *I*-PC-SAFT and *tc*-PR equations of state (EoS).

Firstly, the proposed model was parameterized using component-specific parameters. To do so, 72 pure components and around 2400 experimental data were considered.

Secondly, a chemical-family parametrization was used. Four chemical families were defined and parameter sets valid for all the compounds of each given family were estimated. Eventually, regardless of the considered EoS, the component-specific parametrization enables to describe data with an average accuracy of 7.5% while using a chemical-family parametrization, the deviation reaches 9.5%.

IV-A) Introduction:

Transport phenomena characterize the situation where the flux density of a property α (amount of substance, momentum, heat) is generated by a driving force that is defined as the gradient of an intensive property f such as concentration or temperature. This force can thus be seen as a stimulus and the flux as the response to this stimulus.

Macroscopically speaking, transport phenomena are characterized all by similar constitutive laws expressing a linear relationship between the flux density $\boldsymbol{J}$ (per unit of time and area) of the property α and the gradient, $\boldsymbol{\nabla} f$, of the associated intensive quantity f: $\boldsymbol{J_\alpha} = -k\boldsymbol{\nabla} f$. The proportionality constant k is called transport coefficient and is a positive scalar.

For $\boldsymbol{J_\alpha}$ being a diffusion flux density of which the dimension is amount of substance (e.g., kg or mol) per unit area and per unit time (e.g., if the amount is a mass, the flux density is expressed in $kg.s^{-1}.m^{-2}$), f is the corresponding concentration of this amount (e.g., $kg.m^{-3}$), $k = D$ is the mass diffusion coefficient ($m^2.s^{-1}$) and the corresponding constitutive law is known as Fick's law.

In the present article, the estimation of *self-diffusion coefficients* (denoted D_{self} thereafter) - a specific class of diffusion coefficients - is addressed.

In practice, self-diffusion coefficients are used to describe quantitatively various phenomena that are driven by molecular dynamics at the microscopic scale; for instance, this property is involved in the characterization of nanoporous material for gas production, storage and separation[84–86], in the analysis of protein hydration layer[87]. It is used to correlate ionic transport behaviour[88] or the glass transition of nanoconfined polymers[89] as well as for expressing the binary mass diffusion coefficients D_{ij}[70,90–92]. It is also widely used to quantify the migration of tracers in various context [93,94] as the mass diffusion of a tracer is fully defined by its self-diffusion coefficient. Experimentally, various experimental techniques[95] such as the Tracer Method, the Nuclear Magnetic Resonance or the Neutron Scattering Method can be implemented to measure self-diffusion coefficients.

To estimate this property, different methodologies and corresponding models were proposed in the literature. Unfortunately, and this is also the case for shear viscosity and thermal conductivity, most of methods are specific to either liquid or gas states, to particular classes of substances. There is no current theory capable of unifying the description of transport properties of the subcritical liquid, gas and supercritical states, for any type of substance, independently of its chemical nature, that obtains a scientific consensus.

As a noticeable exception, the concept of entropy scaling[1] is a semi-theoretical approach that has taken a considerable step in this direction, while keeping a valuable potential for industrial applications. As suggested by its name, this theory postulates that any given reduced transport property ($\tilde{\psi} = \psi/\psi_{\mathrm{ref}}$) can be univocally expressed as a function of a residual-entropy variable (the reduced Tv-residual entropy sometimes called "excess entropy"), denoted $\tilde{s}_{\mathrm{Tv-res}} = -s_{\mathrm{Tv-res}}/R$ and defined in detail elsewhere[96]. For the sake of clarity, the notations used in the

rest of this article are commented briefly. Reduced transport properties are topped by a tilde symbol, $\tilde{\psi}$, and are defined as the ratio of the experimental (real) value ψ over a corresponding reference property ψ_{ref}, obtained from a dimensional analysis and involving macroscopic variables (temperature, density, molecular mass) and potentially microscopic parameters like, e.g., the collision diameter.

While most of literature models express usually a transport property as a function of the temperature and pressure variables, $\psi(T,P)$, the entropy scaling concept offers a simplified framework by reducing the number of variables governing the problem. It is claimed indeed that any appropriately reduced transport property only depends on one variable $\tilde{\psi}(\tilde{s}_{\mathrm{Tv-res}})$. This idea was originally developed by Rosenfeld[1] through his work on simple theoretical fluids at dense states. He showed that when plotting the logarithm of shear viscosity and self-diffusion coefficient data, reduced in an appropriate way, against reduced residual entropy $\tilde{s}_{\mathrm{Tv-res}}$, nearly-universal linear laws were obtained (by *universal*, it is meant here that the law is the same for any type of substance). Later[2], he showed that the entropy-scaling concept could be extended to another property, the thermal conductivity, and to wider density domains, in particular, the low-density region. These studies and subsequent literature works[30,31,38,41,72,80,96] highlighted that the dependence between the logarithm of reduced transport properties and the reduced residual entropy:

- Can be considered as linear on specific domains but is non-linear overall,
- Is not universal, i.e., curves are component-specific.

As a noticeable success of the proposed approach, the monovariable relationship $\tilde{\psi}(\tilde{s}_{\mathrm{Tv-res}})$ remains valid over the three fluid-state regions (liquid, sub- and super-critical gas).

The formalism and the corresponding model for self-diffusion coefficients proposed by Rosenfeld[2] are recalled in Table IV-1.

Table IV-55 - Rosenfeld's Entropy Scaling variables[1,2] for expressing the self-diffusion coefficient at dense states; ρ_N is the number density (number of molecules in a volume unit), m_0 is the molecular mass, k_b is the Boltzmann constant.

Entropy-scaling variables:	**X-axis**	**Y-axis**	$\boldsymbol{D_{\mathrm{self}}^{\mathrm{reference}}}$	**Proposed model: for $\tilde{s}_{\mathrm{Tv-res}} \gtrsim 0.5$**
Expressions:	$\tilde{s}_{\mathrm{Tv-res}} = -\frac{s_{\mathrm{Tv-res}}}{R}$	$\ln(\tilde{D}_{self}) = \ln\left(\frac{D_{\mathrm{self}}^{\mathrm{experimental}}}{D_{\mathrm{self}}^{\mathrm{reference}}}\right)$	$\rho_{\mathrm{N}}^{-1/3}\sqrt{\frac{k_{\mathrm{b}}T}{m_0}}$	$Y = -0.8X + \ln(0.6)$

For illustration, Figure IV-1 shows the curve obtained when applying Rosenfeld's entropy scaling concept to the self-diffusion coefficient of pure methane. Note that a diverging behaviour arises at low density (when $\frac{s_{\mathrm{Tv-res}}}{R} \to 0$).

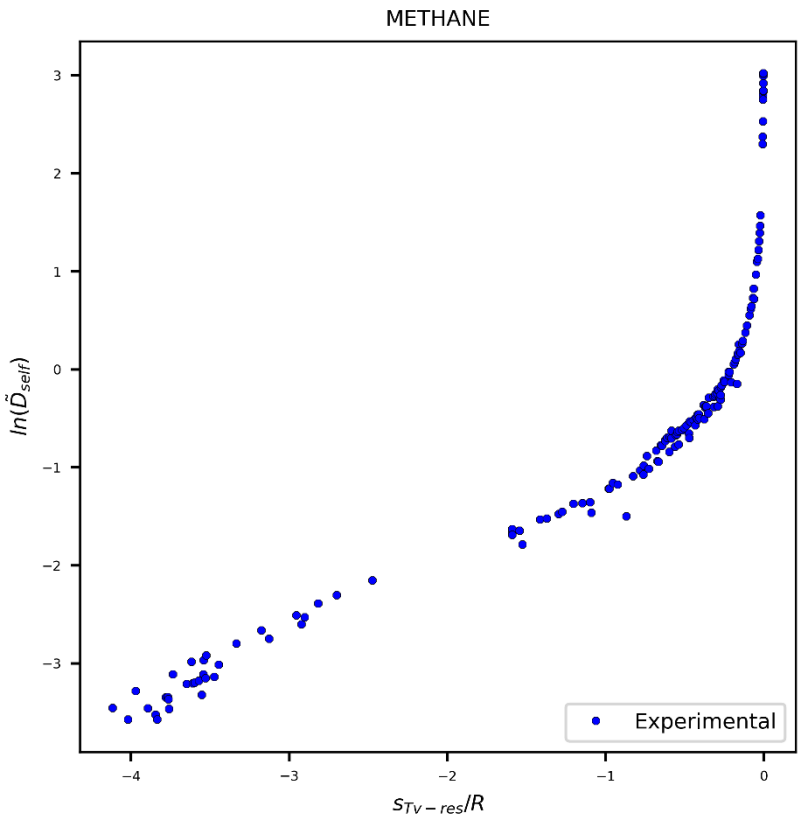

Figure IV-16 - Rosenfeld's entropy scaling concept applied to self-diffusion coefficient for pure methane.

Inspired by Rosenfeld's initial concept[1,2], several authors have proposed entropy-scaling approaches for self-diffusion coefficient that mainly differ through the way used to reduce the transport property.

Addressing the case of atomic diffusion in condensed matter, Dzugutov[3] developed an expression for the $D_{\text{self}}^{\text{reference}}$ property derived from the Chapman-Enskog theory[10] by considering Enskog collision rate. Therefore, in addition to the molecular density and temperature, the proposed $D_{\text{self}}^{\text{reference}}$ was expressed with respect to molecular descriptors such as the hard-sphere diameter and the value of the radial distribution function at the contact distance. Subsequently, Bretonnet[97] considered the same reference term. On the contrary, Krekelberg et al.[98] derived a reference term by multiplying $[\rho D]_0$, the temperature-dependent product of the number density and diffusion coefficient of the considered species in dilute conditions, and the factor $\left(B + T\frac{dB}{dT}\right)$, where B is the second virial coefficient, resulting in an expression valid in low-density conditions. To derive this expression, Krekelberg et al.[98] used as approximate expression for self-diffusion coefficient $[\rho D]_0/\rho$ and replaced the number density by its expression with respect to $s_{\text{Tv-res}}$ according to the truncated virial equation of state. Doing so, they proved that the ratio $D/\left[[\rho D]_0\left(B + T\frac{dB}{dT}\right)\right]$ is proportional to $1/s_{\text{Tv-res}}$.

In the same spirit, Novak[34] also used a reference term valid in dilute gas conditions, derived from the Chapman-Enskog theory, that involves molecular density and Lennard-Jones

parameters such as a characteristic collision diameter, a characteristic energy of attraction between identical molecules and collision integrals. Novak made this choice to preserve the universality of the concept and to improve the description of the low-density region (i.e., to avoid the diverging behaviour at low density illustrated in Figure IV-1). Although Novak's proposal has been widely used recently to develop models for the prediction of transport properties of pure fluids[30,31,35,38] and mixtures[80], there is currently no consensus on this approach. Indeed, it appeared that considering a $D_{\text{self}}^{\text{reference}}$ property valid in dilute-gas conditions is not appropriate to describe both liquids and dense gases. Nevertheless, it is worth noting that Novak's proposal made it possible to improve dramatically the low-density behaviour[99].

Differently from the aforementioned studies, some others are in accordance with Rosenfeld's initial idea: let us cite the isomorph theory[69] as well as Bell's approach[40,41] wherein self-diffusion coefficients are reduced in a similar manner.

In a recent study dealing with the modelling of pure-component shear viscosity from a revisited entropy-scaling formulation, we proposed a new general expression for the residual entropy variable and selected Rosenfeld's method for reducing the shear viscosity. Representing experimental data in this reduced space, V-shape curves were systematically obtained, regardless of the considered compound, and a strictly-universal behaviour was observed in the gas region. Using a rather-simple functional form to correlate experimental data in the reduced space, a high accuracy was achieved over the entire fluid region[96].

In this study, the same methodology is applied to self-diffusion coefficients in order to achieve the best formulation of the concept and thus to propose reliable models enabling to estimate self-diffusion coefficients of a pure fluid in the liquid, gas or supercritical regions. To estimate residual entropies and densities, the *I*-PC-SAFT[100] and *translated*[101,102]*-consistent*[51,52] Peng-Robinson (*tc*-PR[5]) equations of state (EoS) were used. The choice to consider two different EoS, one belonging to the Van der Waals EoS family and the other belonging to the SAFT EoS family is justified by: (i) the industrial success of cubic EoS and their excellent capacity to model thermodynamic properties of any type of fluid[103], (ii) the promising capacity of SAFT EoS to model pure species[100] and in particular, associating fluids.

IV-B) Theoretical background:

IV-B-1) Use of the entropy scaling concept to describe self-diffusion:

The Tv-residual entropy, denoted $s_{\mathrm{Tv-res}}$, is a departure function expressing the difference between the entropy of a real fluid and the one of a perfect gas at the same temperature and molar volume as the real fluid; it can be estimated using an equation of state in a straightforward manner.

From a reasoning based on the kinetic theory, Rosenfeld[1,2] postulated that reduced self-diffusion coefficients could be univocally expressed as a function of the reduced Tv-residual entropy. He introduced a so-called *macroscopic reduction* where D_{self} are divided by a temperature (T) and a molecular density (ρ_{N}) dependent term (here called "reference property" and denoted $D_{\mathrm{self}}^{\mathrm{reference}}$), having the same dimension as the transport coefficient. As shown in Table 1, T and ρ_{N}-independent quantities like the molecular mass or the Boltzmann constant can be used to define the reference property in order to get the dimensionless transport property $\widetilde{D}_{\mathrm{self}}$. Rosenfeld showed that reference property depending on T and ρ_{N} are predisposed to scale with the Tv-residual entropy. Indeed, such a reference property has the potential to qualitatively mimic the dynamic behaviour of molecules / particles animated with rectilinear translations over a maximum distance $l = \rho_{\mathrm{N}}^{-1/3}$, at the mean thermal velocity $v = \sqrt{k_{\mathrm{b}}T/\mathrm{m}_0}$, before a collision occurs.

Such a technique has the advantage to introduce variables revealing the change of fluid structure in the definition of the reference property. Therefore, the resulting reduced transport property can be interpreted as a ratio unveiling how much the real system deviates from a representation of simple (fictitious) liquid systems deduced from the kinetic theory due to the local structure. Deviations from these simple representations are observed whenever:

- Additional pathways of transfer, accessible to the system molecules, exist (e.g., vibrational degrees of freedom for polyatomic fluids at low density),
- Shape effects, intermolecular forces, association through hydrogen bonding etc. are taking place in the fluid.

When important deviations from simple liquid-system behaviours are observed, entropy-scaling laws depart from universality, thus restricting the scope of its application. This issue can be partially counteracted with the introduction of empirical parameters fitted to experimental data and / or by modifying the expression of the reference property used for the reduction.

It is worth noting that the choice to use an exponential function in Rosenfeld's formulation (see Table 1) of entropy scaling in dense-fluid conditions can be justified by the close relation existing between system microstates (evaluated through the exponential of entropy, according to Boltzmann's formula) and transport properties. For addressing dilute-gas states, Rosenfeld

derived a power-law dependence based on Enskog's theory[10] but did not propose a relation unifying dense and dilute fluid state. In a recent work focusing on the modelling of shear viscosity through the entropy-scaling approach[96], we proposed to keep the same reduced viscosity as Rosenfeld but to modify the definition of the entropy variable. While Rosenfeld used $s = -s_{\mathrm{Tv-res}}/R$, we used a different definition with the ambition to:

- Avoid the low-density divergence observed using Rosenfeld's approach (see Figure IV-2),
- Obtain a quasi-universal behaviour at low density,
- Make the entropy-scaling law less dependent on (i) the considered component and (ii) the EoS model selected to estimate density and residual entropy.

The new entropy scaling (ES) X-coordinate is defined as:

$$X_{\mathrm{ES}} = -\left(\frac{s_{\mathrm{Tv-res}}}{s^{\mathrm{c}}_{\mathrm{Tv-res}}}\right) - \ln\left(\frac{s_{\mathrm{Tv-res}}}{s^{\mathrm{c}}_{\mathrm{Tv-res}}}\right) = -\left(\frac{\tilde{s}_{\mathrm{Tv-res}}}{\tilde{s}^{\mathrm{c}}_{\mathrm{Tv-res}}}\right) - \ln\left(\frac{\tilde{s}_{\mathrm{Tv-res}}}{\tilde{s}^{\mathrm{c}}_{\mathrm{Tv-res}}}\right) \qquad \text{(IV–1)}$$

In Eq. (IV-1) where $s^{\mathrm{c}}_{\mathrm{Tv-res}}$ is the critical value of the reduced molar entropy, the 1st term is dominant in dense-fluid condition while the 2nd term dominates at low density. By noticing that (i) the ratio $\frac{s_{\mathrm{Tv-res}}}{s^{\mathrm{c}}_{\mathrm{Tv-res}}}$, calculated from a given EoS, is similar for components belonging to the same homologous family and (ii) that for a given component, all EoS provide comparable estimations of this ratio (while EoS estimations of residual entropies can be strongly different from one EoS to another), it was decided to introduce this ratio instead of $s_{\mathrm{Tv-res}}/R$ in the entropy variable definition (see Eq. (IV-1)).

Furthermore, as an important feature, the X_{ES} definition yields a quasi-universal behaviour in the $\ln(\widetilde{D}_{\mathrm{self}})$ versus X_{ES} plane: at low density (i.e., for $X_{\mathrm{ES}} \to +\infty$), an oblique asymptote appears, consequence of a well-defined limit behaviour of $\ln(\widetilde{D}_{\mathrm{self}})$ in such conditions. Analogically to what was demonstrated for the viscosity (see section 1.2 in the supporting information of reference [96]), the reduced self-diffusion coefficient can be re-written as follows at the zero-density limit.

$$\begin{cases} \ln(\widetilde{D}_{\mathrm{self}}) \underset{\rho_{\mathrm{N}}\to 0}{\sim} \ln\left[\frac{(\rho_{\mathrm{N}} D_{\mathrm{self}})_{\rho_{\mathrm{N}}\to 0}}{\sqrt{\mathrm{k_b}T/\mathrm{m_0}}}\left[B_{\mathrm{N}}(T) + \frac{dB_{\mathrm{N}}(T)}{dT}\right]^{2/3}\right] + \frac{2}{3}X_{\mathrm{ES}} \\ with \quad \widetilde{D}_{\mathrm{self}} = \frac{D_{\mathrm{self}}}{\rho_{\mathrm{N}}^{-1/3}\sqrt{\mathrm{k_b}T/\mathrm{m_0}}} \end{cases} \qquad \text{(IV–2)}$$

Where B_{N} denotes the molecular second viral coefficient (in m^3 per molecule). Eq. (IV-2) was obtained by assuming that the relation between the self-diffusion coefficient and the density is well represented by a virial-expansion law in dilute-gas conditions. It is recalled that the quantity ρD_{self} only depends on the temperature at the zero-density limit. Therefore, in such conditions, $\ln(\widetilde{D}_{\mathrm{self}}) \sim K(T) + \frac{2}{3}X_{\mathrm{ES}}$, where $K(T)$ is a temperature function. In a previous

study[96], we shown that $K(T)$ can be considered as a linear function of X_{ES}. It appears thus that $\widetilde{D}_{\mathrm{self}}$ is a linear function of X_{ES} when $X_{\mathrm{ES}} \to +\infty$. This particular feature is illustrated in Figure IV-2.

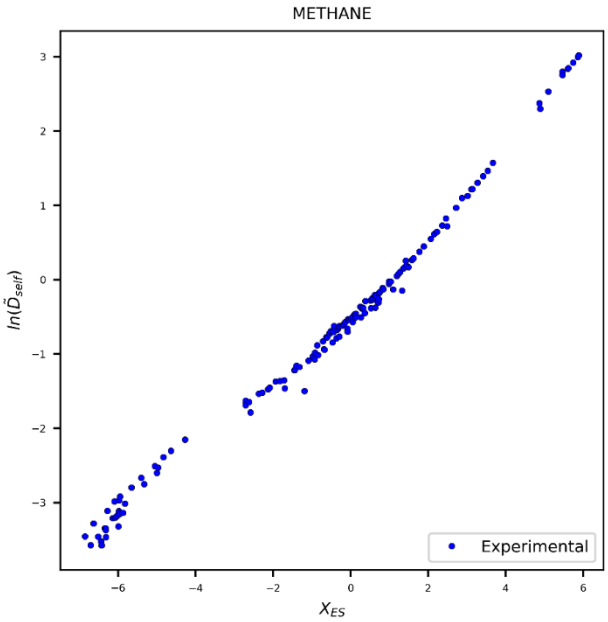

Figure IV-2 – Illustration of the entropy-scaling formulation proposed here applied to the modelling of methane self-diffusion coefficient. Tv-residual entropies and density values were calculated using the *I*-PC-SAFT[100] EoS.

As shown in Figure IV-2, the liquid and gas-like states align along a single curve in the $(Y_{\mathrm{ES}}, X_{\mathrm{ES}})$ plane. According to Eq. (IV-1), the critical point is located at $X_{\mathrm{ES}} = -1$. For a better visualisation of the distribution of the various pressure and temperature conditions, Figure IV-3 shows characteristic vapour−liquid saturation curves as well as series of liquid, gas and supercritical branches of various isotherms for the case of methane modelled with the *I*-PC-SAFT EoS[100]. These curves are represented in the $(P_{\mathrm{r}}, Y_{\mathrm{ES}}, X_{\mathrm{ES}})$ space (see Figure IV-3.A), where $P_{\mathrm{r}} = P/P_{\mathrm{c}}$ denotes the reduced pressure and $Y_{\mathrm{ES}} = \ln(\widetilde{D}_{\mathrm{self}})$ is the natural logarithm of the reduced self-diffusion coefficient (following Rosenfeld's definition), in the $(P_{\mathrm{r}}, X_{\mathrm{ES}})$ plane (see Figure IV-3.B), and in the $(Y_{\mathrm{ES}}, X_{\mathrm{ES}})$ plane (see Figure IV-3.C).

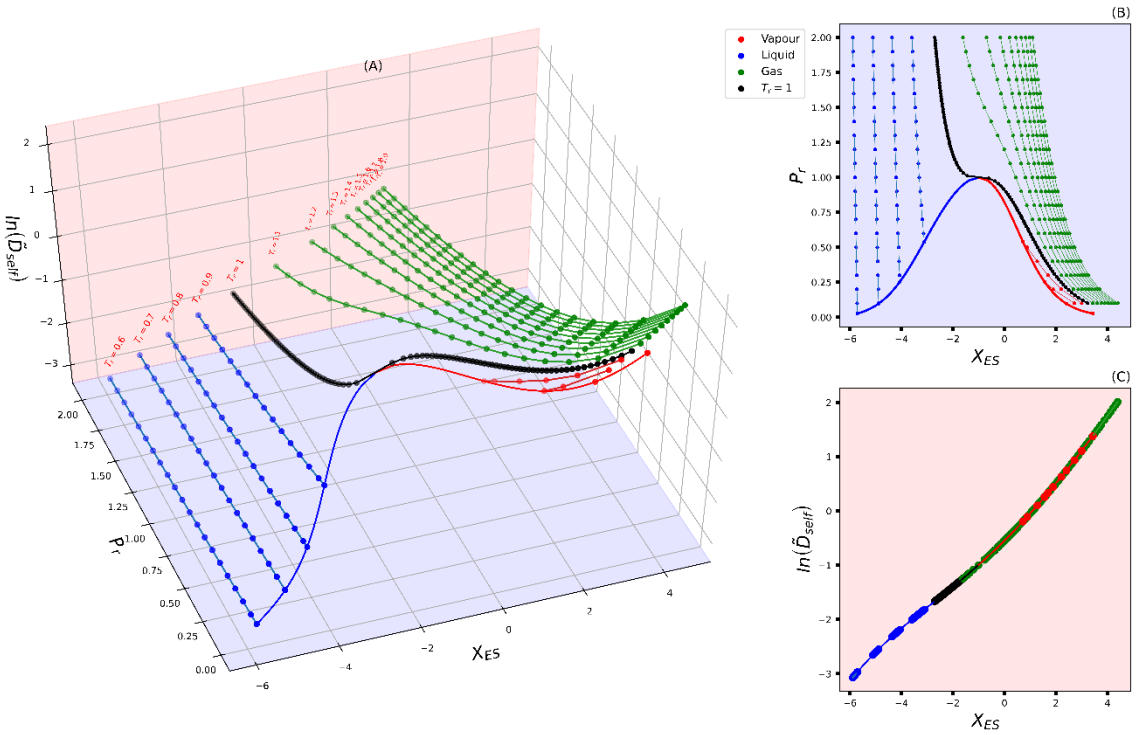

Figure IV-3 – Graphical illustration of the entropy scaling formulation proposed here through the representation of isotherms and saturation curves of pure methane in 3 different diagrams. Reduced temperatures of isotherms range from $T_r = 0.6$ to 1.9 while reduced pressures span from $P_r = 0.1$ to 2. Panel (A): representation in the (P_r, Y_{ES}, X_{ES}) space, Panel (B): representation in the (P_r, X_{ES}) plane. Panel (C): representation in the (Y_{ES}, X_{ES}) plane.

IV-B-2) Search for a functional form for describing the relation between self-diffusion coefficient and residual-entropy variable

Unlike the change of the reduced viscosity as a function of X_{ES} for which a global minimum is systematically observed around $X_{ES} = 0$, for all substances, and which can be interpreted as a demarcation between liquid- and gas-like behaviours (or equivalently, between an interaction- and a kinetic- driven regime)[96], the reduced self-diffusion coefficient does not present this specificity and increases from dense to dilute fluids (i.e., when density decreases). In pure fluids, this is mainly due to the fact that mass diffusion is a simpler phenomenon than heat conduction or transfer of momentum. Mass diffusion is essentially governed by translations of molecules (more specifically, the intercellular translations in the case of self-diffusion) while the viscosity and the thermal conductivity are consequently impacted by other phenomena such as the intracellular motions or the microscopic collisions[4].

Nevertheless, depending on the chemical nature of a considered substance, intermolecular forces (dispersive and repulsive) gain a considerable influence on molecular kinetics (translations) as long as intermolecular distance between molecules decreases (i.e., when

density increases such as, e.g., in liquid states). As a consequence, the dependence of self-diffusion coefficients with density, i.e., from low ($X_{\mathrm{ES}} > 0$) to high density ($X_{\mathrm{ES}} < 0$) changes severely with fluid conditions (temperature and pressure). In diagrams reporting $Y_{\mathrm{ES}} = \ln\left(\widetilde{D}_{\mathrm{self}}\right)$ versus X_{ES}, this dependence-changeover induces:

- component-dependent curves slopes,
- from moderately dense ($X_{\mathrm{ES}} \approx 0$) to dense fluids ($X_{\mathrm{ES}} \ll 0$), the curve departs from a linear behaviour.

In order to capture satisfactorily those mass-transport regimes and to maintain a high flexibility of the functional form for the prediction of the self-diffusion coefficients, it is proposed here to keep the same expression as the one previously used for shear viscosity (see Eq. (IV-3)).

$$\ln\left(\widetilde{D}_{\mathrm{self}}\right)_{\mathrm{calc}} = f_{\mathrm{dense}}(\tilde{s}_{\mathrm{Tv-res}}) \times g_{\mathrm{dense}} + f_{\mathrm{gas}}(\tilde{s}_{\mathrm{Tv-res}}) \times g_{\mathrm{gas}} + d \qquad \text{(IV–3)}$$

where f_{dense} and f_{gas} are functions describing the dense-state behaviour (i.e., for $X_{\mathrm{ES}} < 0$; note that the term "dense" concerns both subcritical liquid and supercritical fluids) and the dilute-gas behaviours (i.e., for $X_{\mathrm{ES}} > 0$; note that the term "gas" means both subcritical and supercritical fluids); g_{dense} and g_{gas} are damping factors making f_{dense} dominating in the dense region, and conversely, f_{gas} dominating in the gas region; d is a component-specific constant. The following expressions are introduced to express these various quantities:

$$\begin{cases} f_{\mathrm{dense}}(\tilde{s}_{\mathrm{Tv-res}}) = (a_1 + a_2\tilde{s}_{\mathrm{Tv-res}} + a_3\tilde{s}_{\mathrm{Tv-res}}^2)X_{\mathrm{ES}} \\ g_{\mathrm{dense}} = \frac{1}{1+e^{cX_{\mathrm{ES}}}} \\ f_{\mathrm{gas}}(\tilde{s}_{Tv-res}) = bX_{\mathrm{ES}} \\ g_{\mathrm{gas}} = \frac{1}{1+e^{-cX_{\mathrm{ES}}}} \end{cases} \qquad \text{(IV–4)}$$

In Eq. (IV-4), $(a_1, a_2, a_3), b, c$ and d are six adjustable parameters. Therefore, the final model proposed here is:

$$\begin{cases} \ln\left(\frac{D_{\mathrm{self}}}{D_{\mathrm{self}}^{\mathrm{reference}}}\right)_{\mathrm{calc}} = \left[\left(\frac{a_1+a_2\tilde{s}_{\mathrm{Tv-res}}+a_3\tilde{s}_{\mathrm{Tv-res}}^2}{1+e^{cX_{\mathrm{ES}}}}\right) + \left(\frac{b}{1+e^{-cX_{\mathrm{ES}}}}\right)\right]X_{\mathrm{ES}} + d \\ D_{\mathrm{self}}^{\mathrm{reference}} = \rho_{\mathrm{N}}^{-1/3}\sqrt{\frac{k_{\mathrm{b}}T}{m_0}} \end{cases} \qquad \text{(IV–5)}$$

Recalling that the Tv-residual entropy is a non-measurable thermodynamic property and that EoS are most often benchmarked to correlate the behaviour of other thermodynamic quantities, quantitative and qualitative differences may exist on the estimation of $\tilde{s}_{\mathrm{Tv-res}}$. This makes the adjusted parameters specific to the considered EoS.

IV-C) Methods, results & discussions:

IV-C-1) Methodology for model derivation:

For developing our entropy-scaling based models for the estimation of self-diffusion coefficients, around 2400 subcritical gas, subcritical liquid and supercritical data associated with 72 different pure substances were considered. All these data, stemming from the database of self-diffusion coefficient measurements proposed by Suárez-Iglesias et al.[95], are graphically represented in Figure IV-4 and were used to determine the sets of parameters a_1, a_2, a_3, b, c and d by minimizing the following objective function:

$$F_{\text{obj}}^{D_{\text{self}}} = \frac{100}{Nb_{\text{data}}} \sum_{\text{i}=1}^{Nb_{\text{data}}} 0.5 \times \left(\left| \frac{D_{\text{self,i}}^{\text{calc}} - D_{\text{self,i}}^{\text{exp}}}{D_{\text{self,i}}^{\text{exp}}} \right| + \left| \frac{Y_{\text{ES,i}}^{\text{calc}} - Y_{\text{ES,i}}^{\text{exp}}}{Y_{\text{ES,i}}^{\text{exp}}} \right| \right) \qquad \text{(IV–6)}$$

Where Nb_{data} is the total number of data taken into account, $Y_{\text{ES,i}}^{\text{exp}}$ and $Y_{\text{ES,i}}^{\text{calc}}$ are respectively, the logarithm of the experimental and the calculated (i.e. according to Eq. (IV-5)) values of the reduced self-diffusion coefficient at the given temperature and pressure of the data point i, $D_{\text{self,i}}^{\text{exp}}$ and $D_{\text{self,i}}^{\text{calc}}$ are respectively the equivalent experimental and calculated values of the self-diffusion coefficient. Eq. (IV-6) averages relative deviations on self-diffusion coefficient (D_{self}) but also on $Y_{\text{ES}} = \ln(\widetilde{D}_{\text{self}})$. Mean Absolute Percentage Error (MAPE) on D_{self} is included in Eq. (IV-6) since our primary objective is to model accurately self-diffusion coefficients. It was decided to add MAPE on Y_{ES} to help the convergence of the minimization procedure. Note that some experimental data points were removed from the database after application of the following filters:

- Data associated with pressures out of the range [10^{-3} MPa; 10^{2} MPa] were considered as (i) potentially inaccurate and, (ii) out of pressure range for most of applications. Therefore, they were disregarded.
- To eliminate out-of-chart data, the absolute deviation $\Delta Y_{\text{i}} = |Y_{\text{ES,i}}^{\text{calc}} - Y_{\text{ES,i}}^{\text{exp}}|$ was calculated for each data and compared to the average deviation ΔY estimated for the species under consideration. It was decided to disregard data such that $\Delta Y_{\text{i}} > \Delta\bar{Y} + 3\sigma$ (where σ denotes the standard deviation, and $\Delta\bar{Y}$, the MAPE on Y_{ES}). As a double check, it was verified graphically that each datum eliminated by the test was deviating strongly from the general trend and could be considered as an outlier.
- For the case of the *tc*-PR based model, data at temperatures above $4 \cdot T_{\text{c}}$ (with T_{c}, the critical temperature of the pure fluid considered) were voluntary discarded because it was observed previously that cubic EoS may fail to predict Tv-residual entropy in this specific temperature region. Note however that the quasi-totality of practical applications use temperature lower than $4 \cdot T_{\text{c}}$. For more details, the reader is referred to our previous work dealing with the modelling of shear viscosity[96].

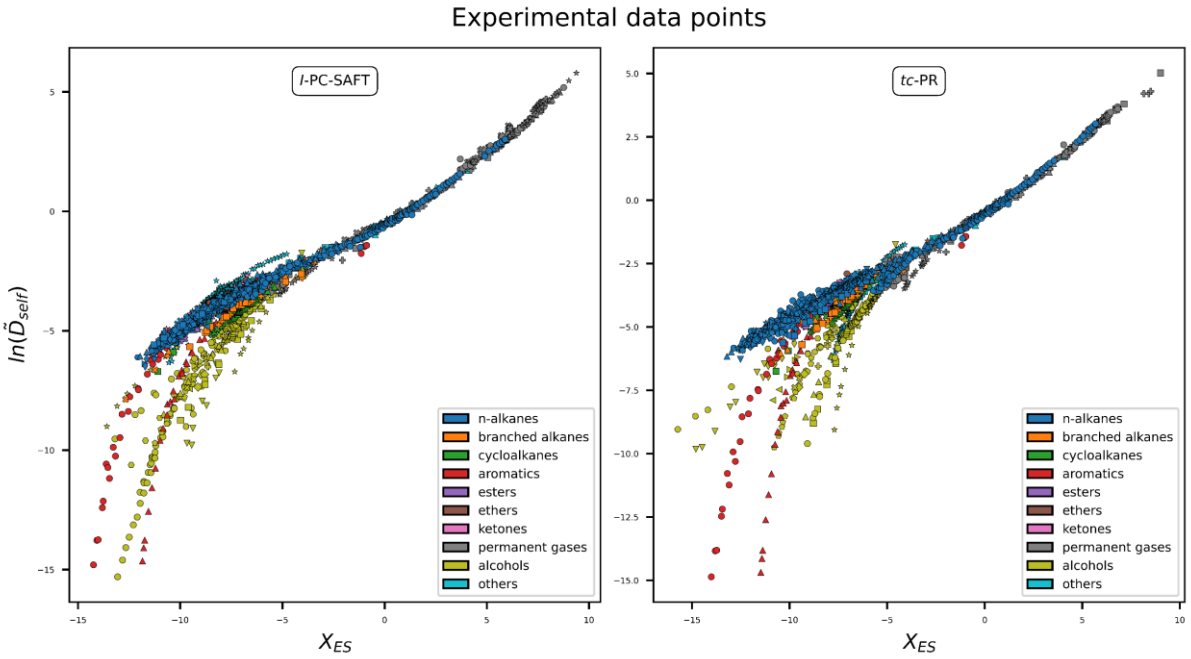

Figure IV-4 – Overview of all experimental data in the $ln(\tilde{D}_{self})$ vs X_{ES} plane. Thermodynamic properties involved in the definition of $\tilde{D}_{self}$ and X_{ES} were estimated using the *I*-PC-SAFT EoS (left panel) and the *tc*-PR EoS (right panel). Each colour corresponds to a specific chemical family and each symbol to a specific compound.

The minimization procedure was based on the Broyden-Fletcher-Goldfarb-Shanno (BFGS) algorithm, a quasi-Newton optimization method. To ensure the consistency of the optimized parameter sets, it was necessary to verify that the algorithm converged to global (i.e., nonlocal) minima. To do so, multiple initialization sets were systematically generated using a random process for each compound. Among all the parameter sets returned by the routine, the optimal one was identified as follows:

- At least half of the initial guesses led to the same optimal parameter set,
- This parameter set was associated with the lowest objective function value and a nearly zero gradient norm.

IV-C-2) A universal behaviour for dilute gas:

As observed in Figure IV-4, dilute gases characterized by low-density conditions (or, equivalently, by positive X_{ES} values) exhibit a quasi-universal behaviour. In such conditions, the model proposed in this paper (see Eq. (IV-5)) can be approximated by:

$$\ln\left(\frac{D_{\mathrm{self}}}{D_{\mathrm{self}}^{\mathrm{reference}}}\right)_{\mathrm{calc}} \underset{\rho_{\mathrm{N}}\to 0}{\sim} \left(\frac{b}{1+e^{-cX_{\mathrm{ES}}}}\right) X_{\mathrm{ES}} + d \qquad \text{(IV–7)}$$

From a graphical point of view:

- b is the slope of the asymptote arising at $X_{\mathrm{ES}} \gg 0$;
- c characterizes the sharpness of the transition between the dense and the dilute parts of the $(Y_{\mathrm{ES}}, X_{\mathrm{ES}})$ curve,
- d is the Y_{ES} value at the origin ($X_{\mathrm{ES}} = 0$).

From Eq. (IV-5), it is noticeable that parameters c and d also affect the representation of dense-fluid data (i.e., they have an influence on the modelling of data at $X_{\mathrm{ES}} < 0$). It is thus impossible to estimate universal values of parameters b, c and d (simply denoted b_{univ}, c_{univ}, d_{univ} thereafter) by considering dilute-gas data only. For this reason, it was decided to include data at dense state in the fitting procedure aimed at determining b_{univ}, c_{univ} and d_{univ}. n-alkanes experimental data at dense state were considered (and the data for all the other molecules were excluded) because Figure IV-4 shows that n-alkanes have a nearly universal behaviour in the dense region. In other words, it is a satisfactorily approximation to use in Eq. (IV-5) the same a_{i} coefficients (i = 1,2,3) for all the n-alkanes. In summary, parameters b_{univ}, c_{univ} and d_{univ}, as well as a_{i} coefficients for n-alkanes were fitted against (i) dilute-gas data (such that $X_{\mathrm{ES}} > 0$) of all the compounds for which such data were available and (ii) the dense-liquid n-alkane data. The obtained results are reported in Table IV-2.

Table IV-2 - Universal parameters for the self-diffusion model in the dilute-gas region ($X_{ES} \geq 0$) associated with 2 different EoS (used for estimating density and residual entropy) namely, the *I*-PC-SAFT and *tc*-PR models.

Parameter	***I*-PC-SAFT EoS**	***tc*-PR EoS**
$\boldsymbol{b_{\mathrm{univ}}}$	0.668634	0.618974
$\boldsymbol{c_{\mathrm{univ}}}$	0.286121	0.499326
$\boldsymbol{d_{\mathrm{univ}}}$	-0.545059	-0.515105

IV-C-3) Parametrization strategy 1: use of component-specific parameters:

In this model version, parameters a_{i} (i = 1,2,3), b, c and d of Eq. (IV-5) were determined for all pure substances for which this determination was possible.

Note that when experimental data were lacking in the dilute-gas regions, parameters b, c and d were set to b_{univ}, c_{univ} and d_{univ}, respectively (see Table IV-2). More generally, the estimation of component-specific parameters (i.e., a_1, a_2, a_3) [and (b, c, d), when possible] was performed as follows:

1- If at least 5 experimental data points are available at dense state ($X_{\mathrm{ES}} < 0$) and simultaneously at least 3 experimental data points are available in the dilute-gas region ($X_{\mathrm{ES}} \geq 0$) then, specific parameters a_1, a_2, a_3 and b, c, d are fitted to these data.
2- If at least 5 experimental data points are available at dense state ($X_{\mathrm{ES}} < 0$) and simultaneously less than 3 experimental data points are available in the dilute-gas region

($X_{ES} \geq 0$) then, specific parameters a_1, a_2, a_3 are fitted to these data whereas and b, c, d are fixed to the universal values.

3- If less than 5 experimental data points are available at dense state ($X_{ES} < 0$), no parameter are fitted (the component is disregarded and no deviations with experimental data are calculated) but universal b, c, d parameters can be used to predict self-diffusion coefficients in the dilute gas region.

Two sets of component-specific parameters were determined for 72 chemical species: one to be used with the *I*-PC-SAFT EoS, and the second, with the *tc*-PR EoS (EoS were used for estimating thermodynamic properties: density and residual entropy). Numerical values of these parameters are available in the *supporting information* file.

Figure IV-5, below, provides a graphical overview of the achieved results. Similar accuracies in the correlation of self-diffusion coefficients are obtained using either the *I*-PC-SAFT EoS (MAPE on $D_{self} = 7.5\%$) or the *tc*-PR EoS (MAPE = 7.9%), with a slight advantage for the *I*-PC-SAFT model.

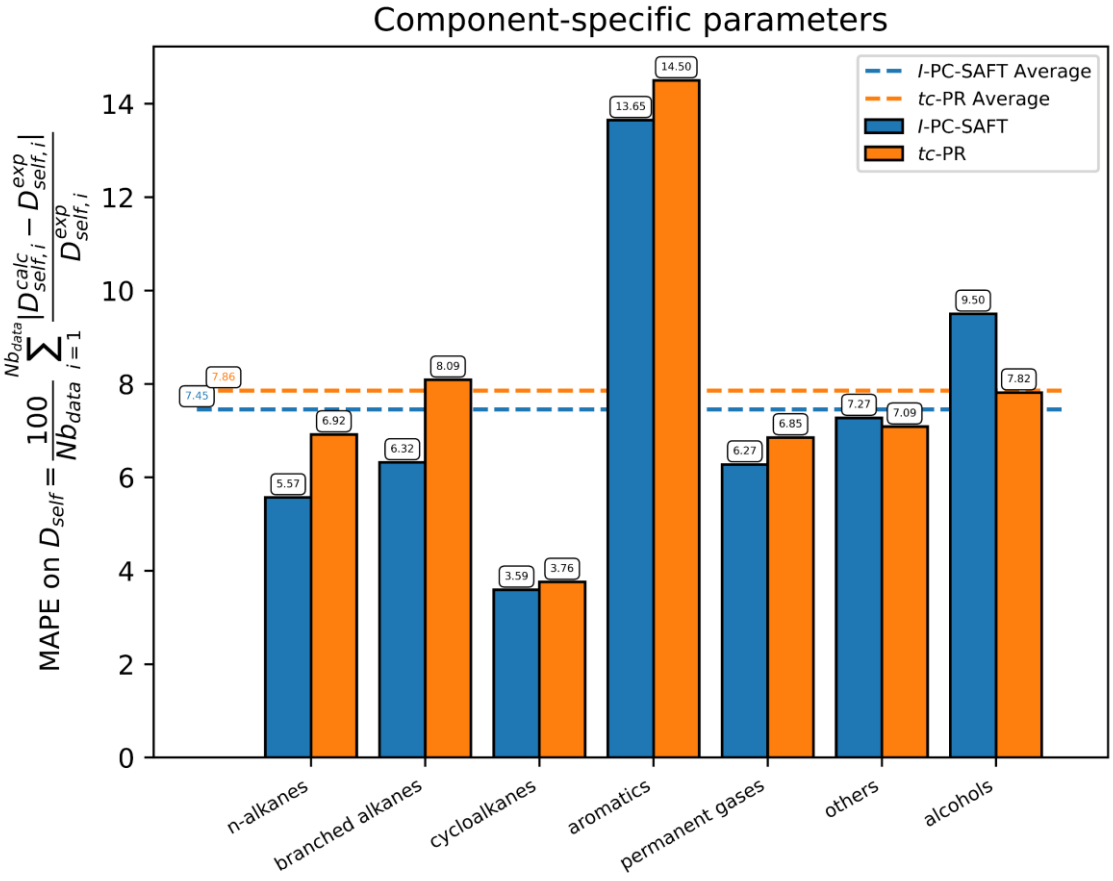

Figure IV-5 – Prediction of self-diffusion coefficients using the model given by Eq. (IV-5) and parametrization strategy 1 (component-specific parameters). Summary of the MAPEs obtained using either the *I*-PC-SAFT or the *tc*-PR EoS for estimating density and residual entropy.

Examples of results obtained with the model described by equation (IV-5) and parametrization strategy 1 (involving component-specific parameters) are provided in Figures IV-6 to IV-13 in the $(X_{\mathrm{ES}}, Y_{\mathrm{ES}})$ and in the (ln (D_{self}), ln P) planes for both the *I*-PC-SAFT and the *tc*-PR based models.

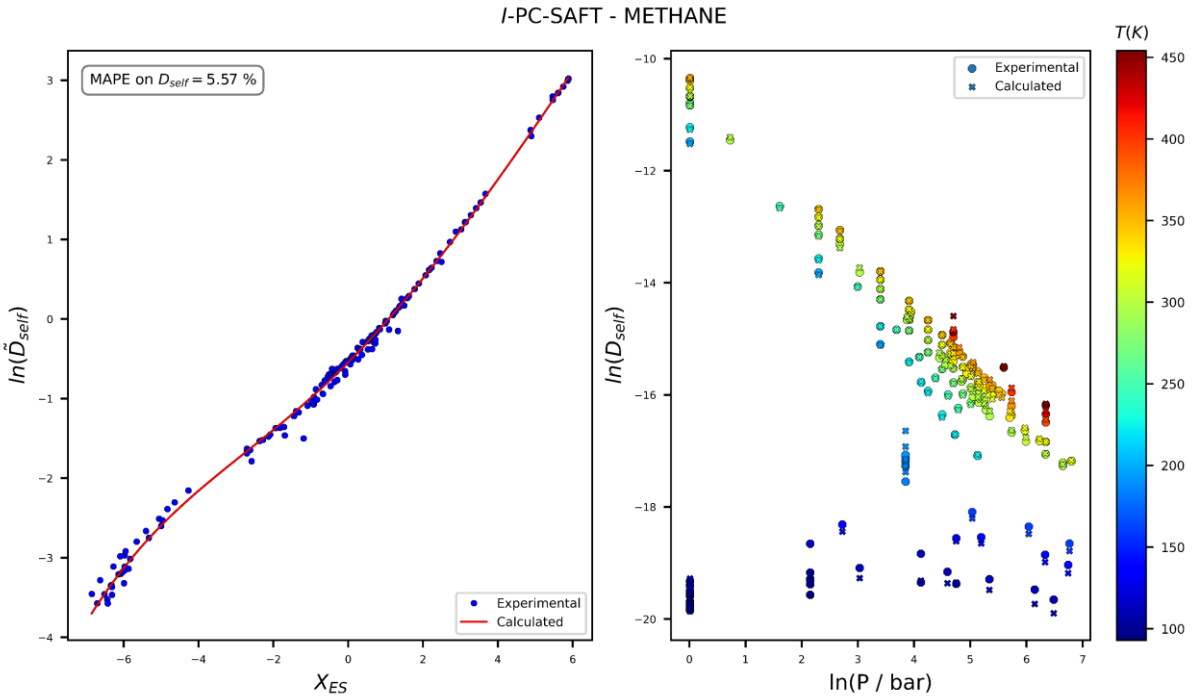

Figure IV-6 – Application of the entropy-scaling (ES)-based model combining Eq. (IV-5) and parametrization strategy 1 to methane, using the *I*-PC-SAFT EoS to estimate density and residual entropy. Left panel: (X_{ES}, Y_{ES}) plane. Right panel: self-diffusion coefficient versus pressure (log-log scale).

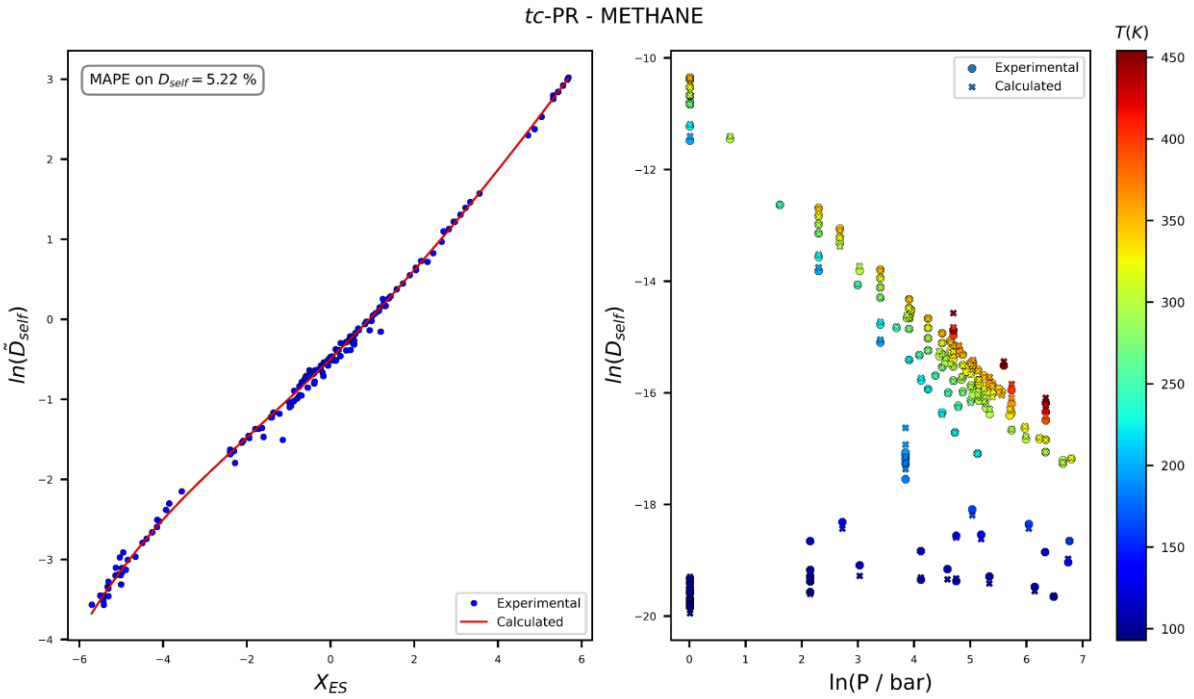

Figure IV-7 - Application of the ES-based model combining Eq. (IV-5) and parametrization strategy 1 to methane, using the *tc*-PR EoS (for more details, see caption of Fig. IV-7).

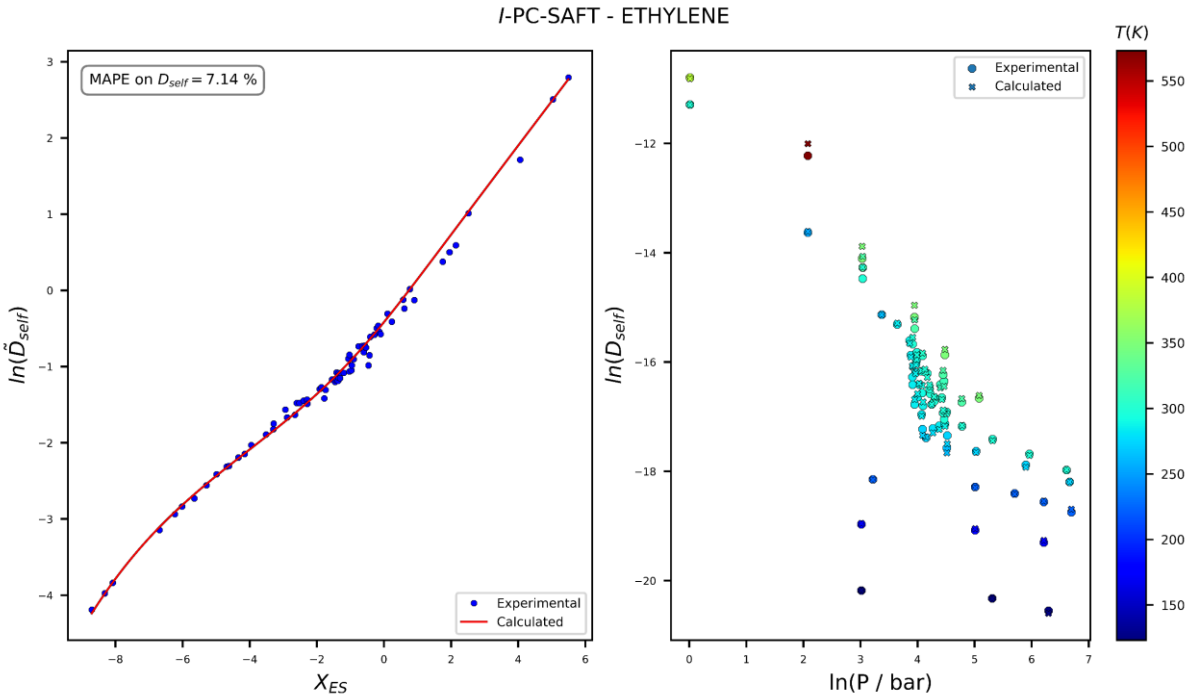

Figure IV-8 - Application of the ES-based model combining Eq. (IV-5) and parametrization strategy 1 to ethylene, using the *I*-PC-SAFT EoS (for more details, see caption of Fig. IV-7).

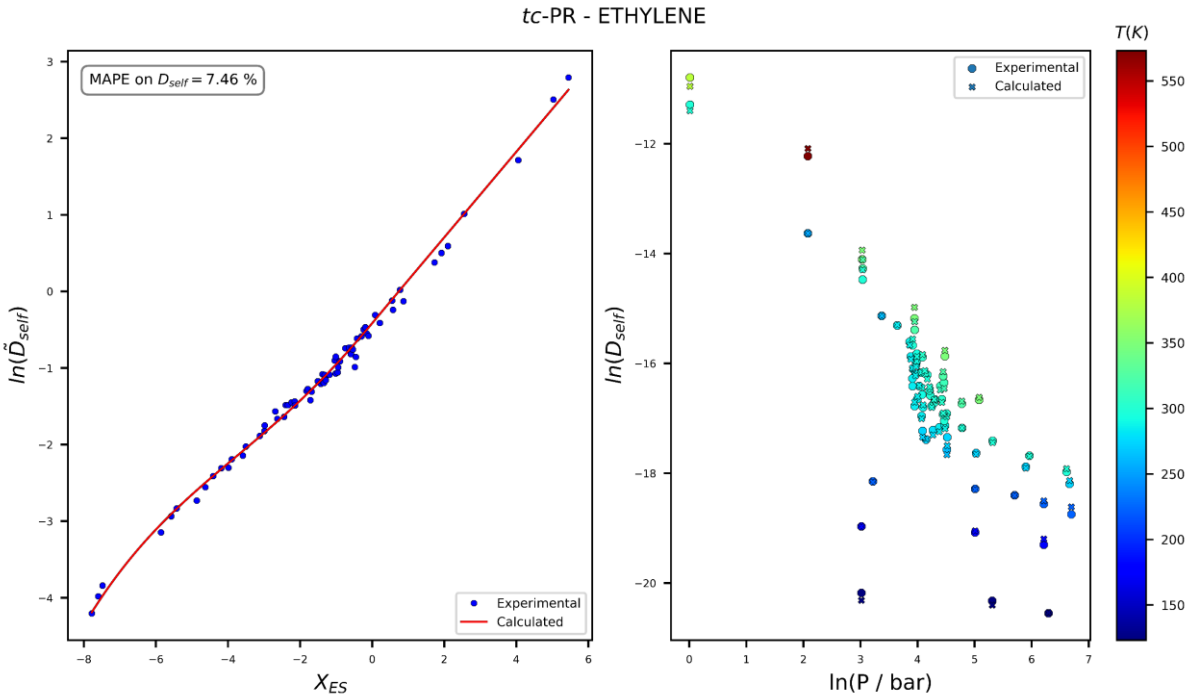

Figure IV-9 - Application of the ES-based model combining Eq. (IV-5) and parametrization strategy 1 to ethylene, using the *tc*-PR EoS (for more details, see caption of Fig. IV-7).

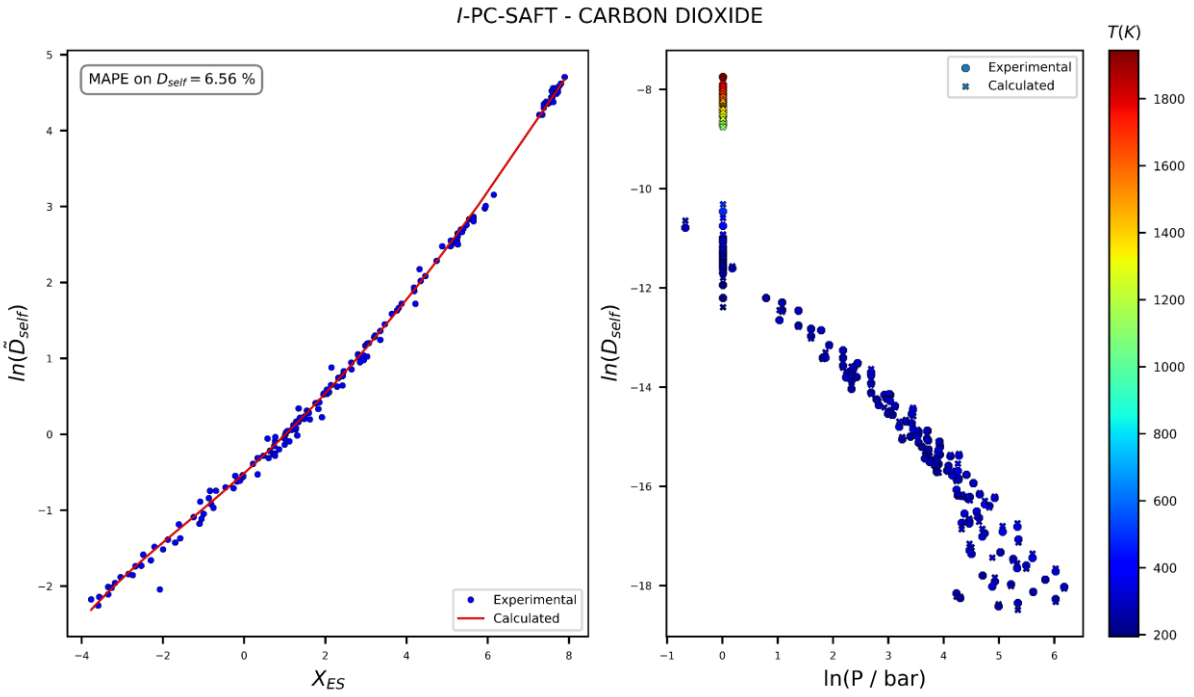

Figure IV-10 - Application of the ES-based model combining Eq. (IV-5) and parametrization strategy 1 to CO_2, using the *I*-PC-SAFT EoS (for more details, see caption of Fig. IV-7).

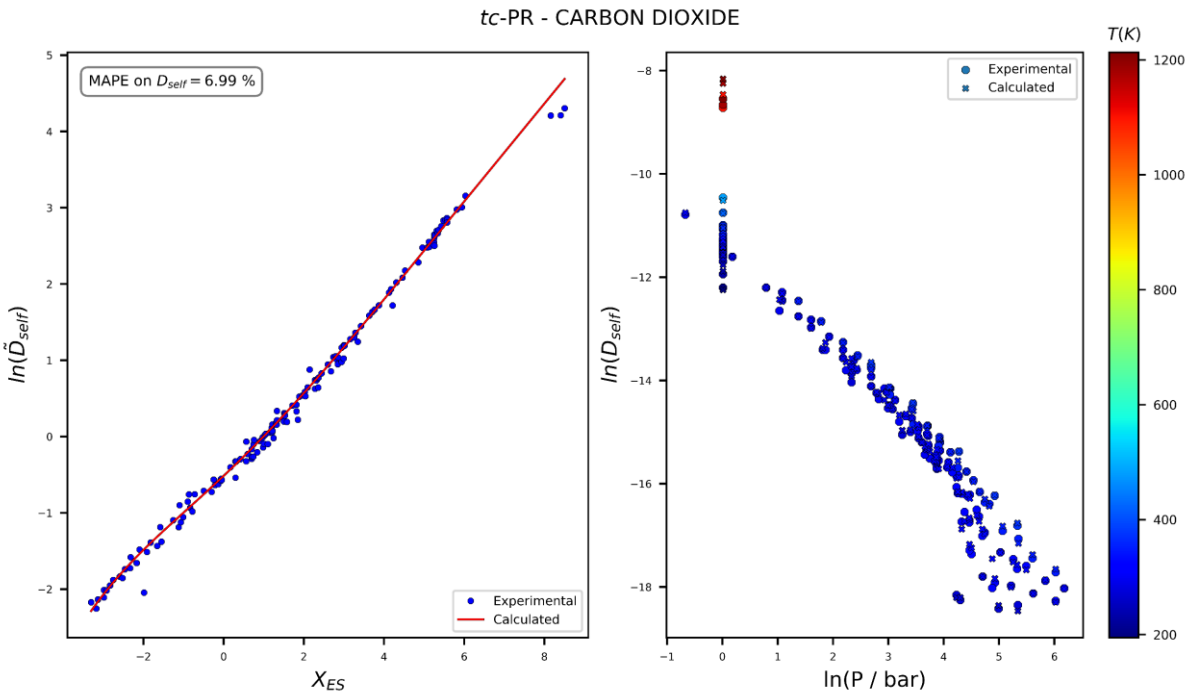

Figure IV-11 - Application of the ES-based model combining Eq. (IV-5) and parametrization strategy 1 to CO_2, using the *tc*-PR EoS (for more details, see caption of Fig. IV-7).

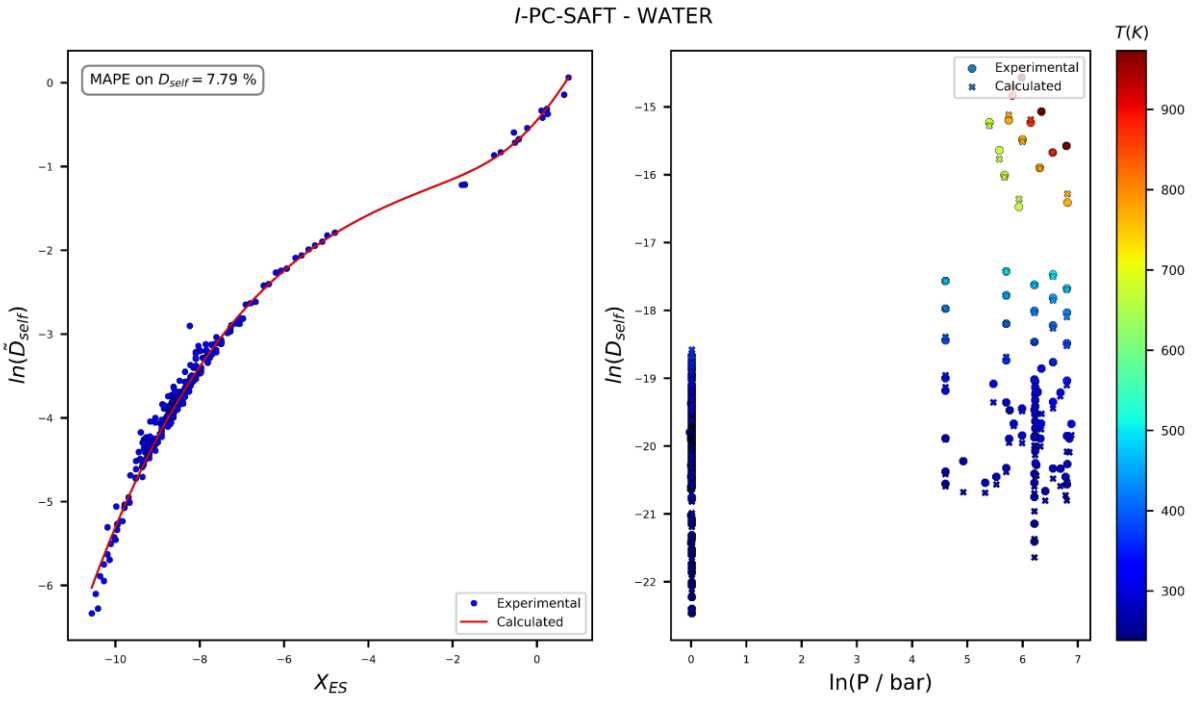

Figure IV-12 - Application of the ES-based model combining Eq. (IV-5) and parametrization strategy 1 to water, using the *I*-PC-SAFT EoS (for more details, see caption of Fig. IV-7).

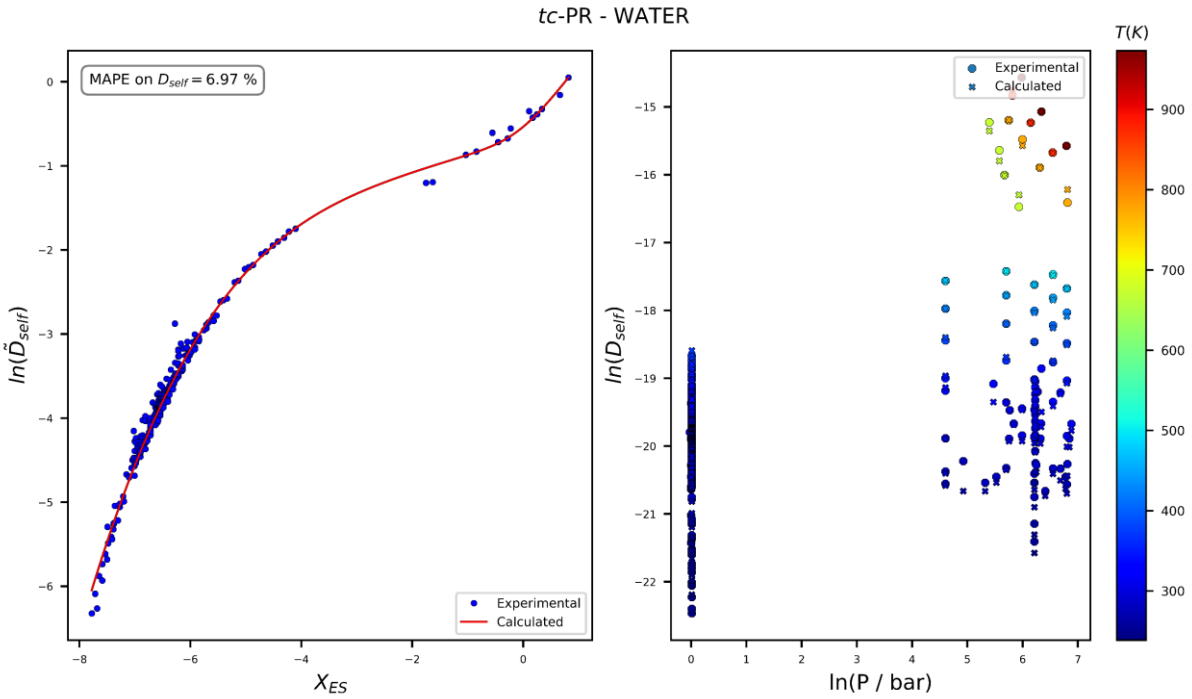

Figure IV-13 - Application of the ES-based model combining Eq. (IV-5) and parametrization strategy 1 to water, using the *tc*-PR EoS (for more details, see caption of Fig. IV-7).

As it can be observed from Figures IV-6 to IV-13, parametrization strategy 1 (PS1) proposed here enables to achieve a quite-reasonable description of self-diffusion coefficients. A similar accuracy is obtained with both the *I*-PC-SAFT and *tc*-PR based models, from dense-liquid to dilute-gas conditions, by including supercritical states. For water, which is yet a fluid acknowledged as complex and difficult to be modelled, accurate results are obtained, as attested by Figure IV-12 and IV-13 (MAPE on D_{self} is around 7%). To provide the readers a fair overview of PS1 capacities, Figures IV-14 to IV-17 show results obtained for the nonpolar and non-associating molecules, that is for n-alkanes, permanent gases, branches alkanes and cycloalkanes. Figures IV-18 and IV-19 show results obtained for n-alcohols and aromatic compounds that contains polar and / or associating compounds (through hydrogen bonding or pi-stacking).

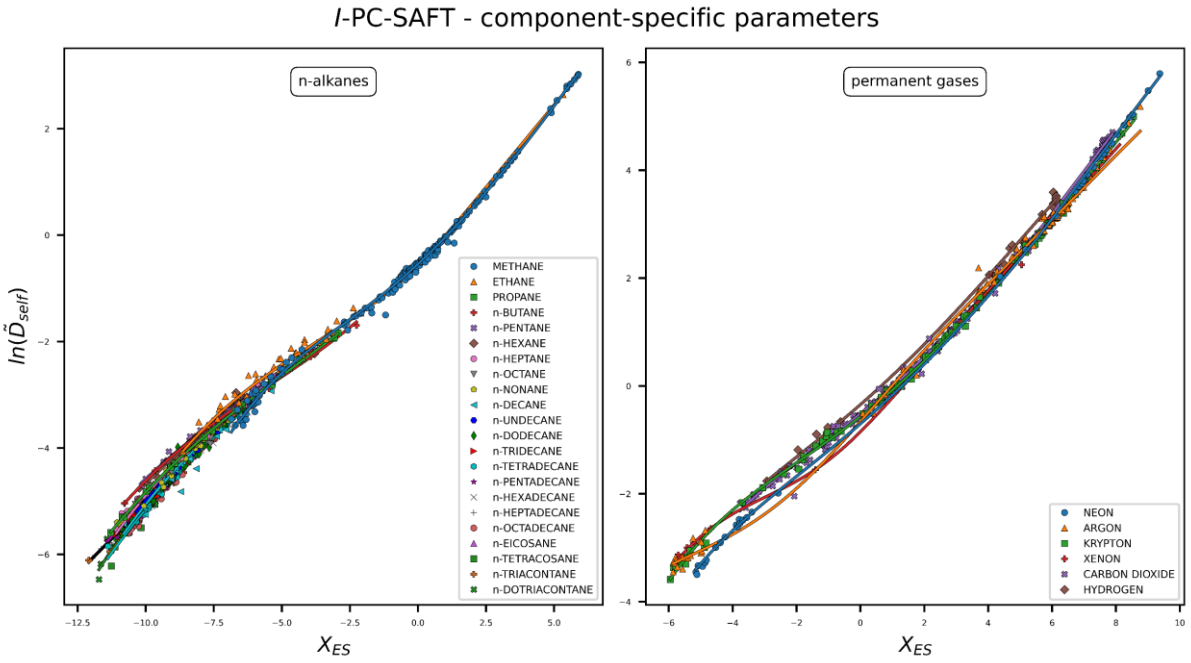

Figure IV-14 - Application of the ES-based model combining Eq. (IV-5) and parametrization strategy 1 to n-alkanes and permanent gases, using the *I*-PC-SAFT EoS. Points: experimental data. Solid line: model.

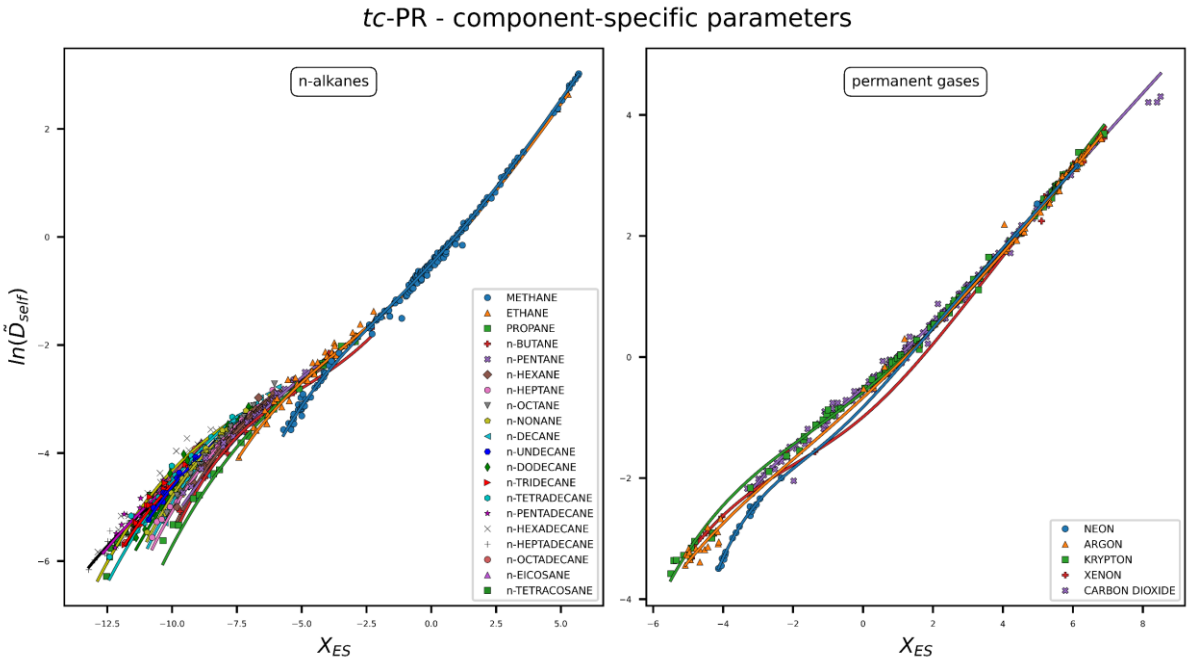

Figure IV-15 - Application of the ES-based model combining Eq. (IV-5) and parametrization strategy 1 to n-alkanes and permanent gases, using the *tc*-PR EoS. Points: experimental data. Solid line: model.

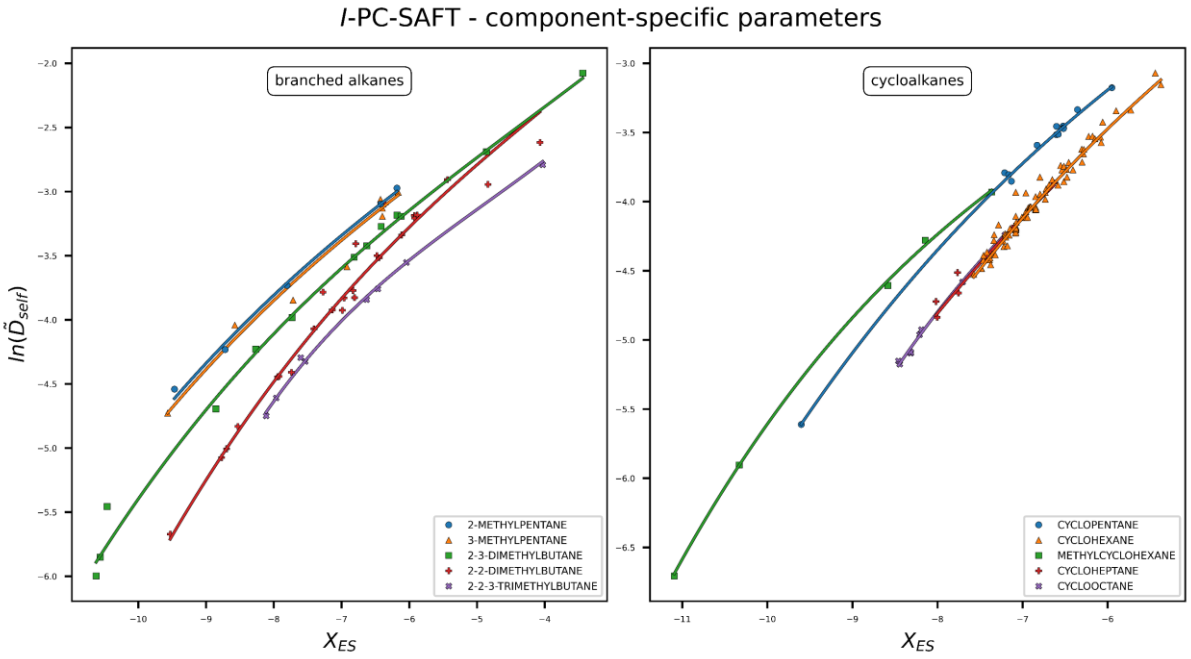

Figure IV-16 - Application of the ES-based model combining Eq. (IV-5) and parametrization strategy 1 to branched alkanes and aromatic cycloalkanes, using the *I*-PC-SAFT EoS. Points: experimental data. Solid line: model.

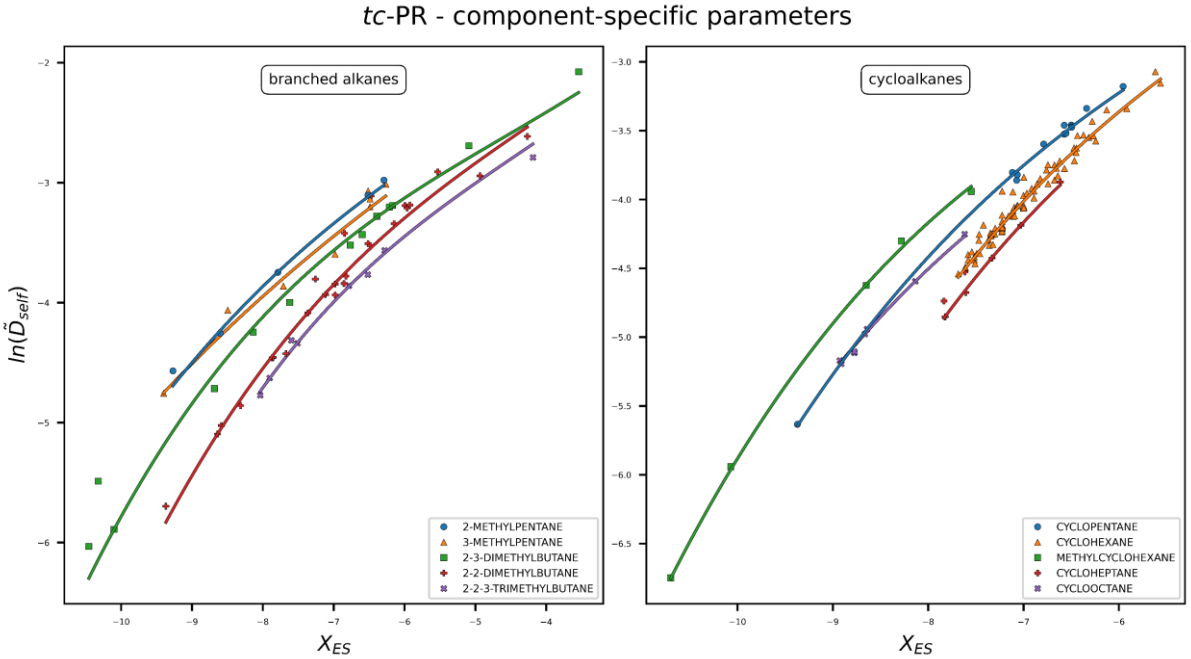

Figure IV-17 - Application of the ES-based model combining Eq. (IV-5) and parametrization strategy 1 to branched alkanes and cycloalkanes, using the *tc*-PR EoS. Points: experimental data. Solid line: model.

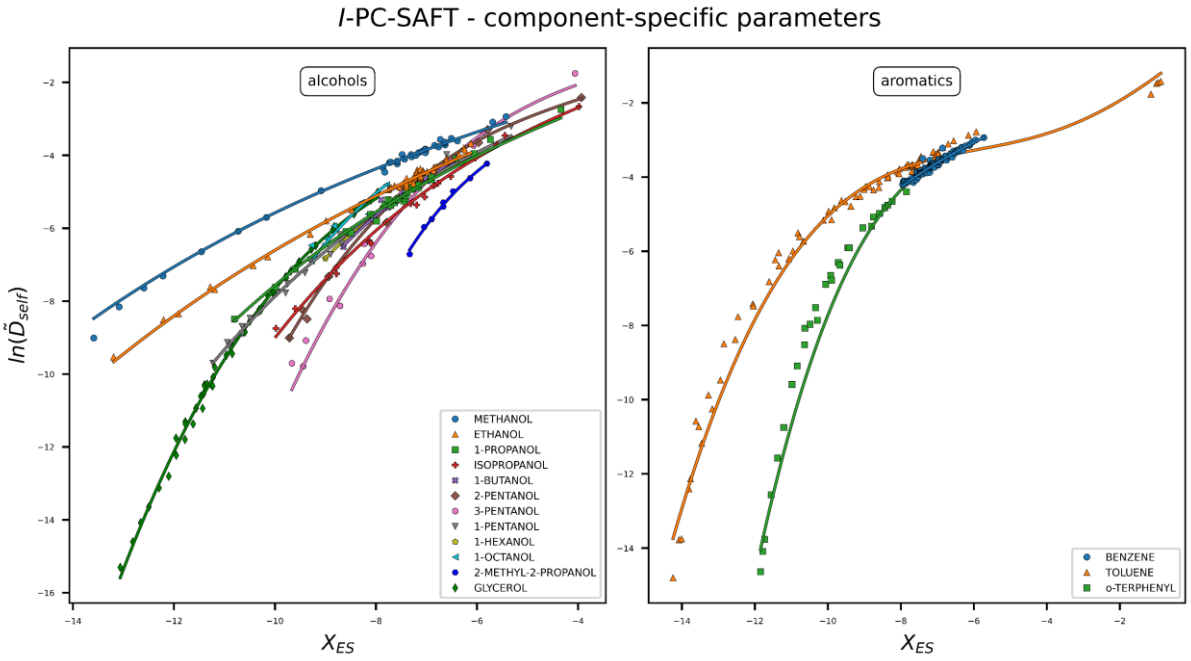

Figure IV-18 - Application of the ES-based model combining Eq. (IV-5) and parametrization strategy 1 to n-alcohols and aromatic compounds, using the *I*-PC-SAFT EoS. Points: experimental data. Solid line: model.

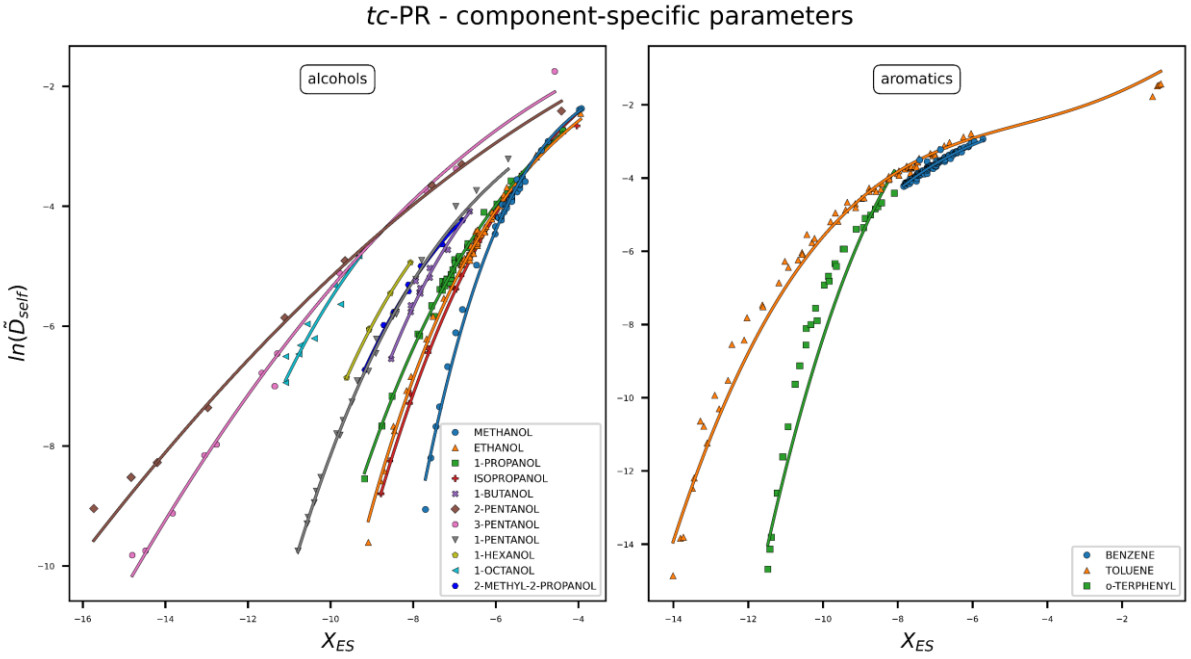

Figure IV-19 - Application of the ES-based model combining Eq. (IV-5) and parametrization strategy 1 to n-alcohols and aromatic compounds, using the *tc*-PR EoS. Points: experimental data. Solid line: model.

Considering measurement uncertainties[95] which are relatively more important for self-diffusion coefficients than for shear viscosities, it can be concluded that the flexibility of the functional form proposed here allows an accurate description of self-diffusion coefficient regardless of the chemical species of interest. Note that the use of universal parameters in the low-density region makes it possible to overcome the absence of experimental data for dilute gas.

In the dense-fluid region, self-associating and polar substances are departing strongly from a universal behavior, as attested by the comparison between Figures IV-14 to IV-17 (quasi-universal behavior), on one side, and Figures IV-18 and IV-19 (non-universal behavior), on the other side.

A loss of accuracy is observed nonetheless in very-dense fluid conditions (near the solid-state region), where the self-diffusion phenomenon tends to cancel out. This is, e.g., visible with toluene (see Figure IV-19) for which the available D_{self} experimental data moves from a magnitude of 10^{-6} to 10^{-15} m²/s. The addition of a 4th parameter (a_4) in Eq. (IV-5) (and more specifically, in the dense-fluid part of this equation) would be necessary to model this extreme behavior. However, in the absence of a more comprehensive database and because 3 a_{i} parameters were enough to represent most of the studied substances in the dense state, the a_4 parameter was not introduced.

IV-C-4) Parametrization strategy 2: use of chemical-family specific parameters:

In order to overcome the potential lack of experimental data for a given compound, a second parametrization strategy for the proposed model [Eq. (IV-5)], involving chemical-family specific parameters instead of component-specific parameters, is proposed. These parameters can be estimated provided a sufficient number of representative compounds and data are available. For this reason, only 4 different chemical families were defined eventually: n-alkanes, branched alkanes, cycloalkanes, and permanent gases. Parameters related to a given chemical family were fitted against all the experimental data available for all the components of the chemical family. Therefore, sets of parameters a_1, a_2, a_3, b, c and d in Eq. (IV-5) were determined for each of the 4 chemical families defined above and are provided in the supporting information file. As for parametrization strategy 1, parameters b, c and d were set to b_{univ}, c_{univ} and d_{univ} when less than 3 experimental data points were available in the dilute-gas region ($X_{\mathrm{ES}} \geq 0$).

As expected, chemical-family specific parameters entail a less accurate estimation of self-diffusion coefficients than component-specific ones, especially at high absolute values of the Tv-residual entropy (i.e. at high densities) and for the branched alkanes family. For a dense fluid described by a lattice model, vacant positions enabling intercellular translations becomes

scarcer and thus, the probability for self-diffusion to occur vanishes, thus entailing a dramatic decrease of the coefficient with the density increase.

To counterbalance the decrease of accuracy when switching from parametrization strategy 1 to 2, it can be emphasized that the second strategy makes it possible to predict self-diffusion coefficients for new molecules provided these molecules belong to one of the aforementioned chemical families.

Eventually, chemical-family-specific parameters provide a reasonable alternative to parametrization strategy 1 when this latter cannot be used.

Overall statistical results for parametrization strategy 2 (PS2) are shown in Figure IV-20. It can be seen that similar deviations are obtained with the *I*-PC-SAFT based and *tc*-PR based model (MAPE = 9.5% in both cases).

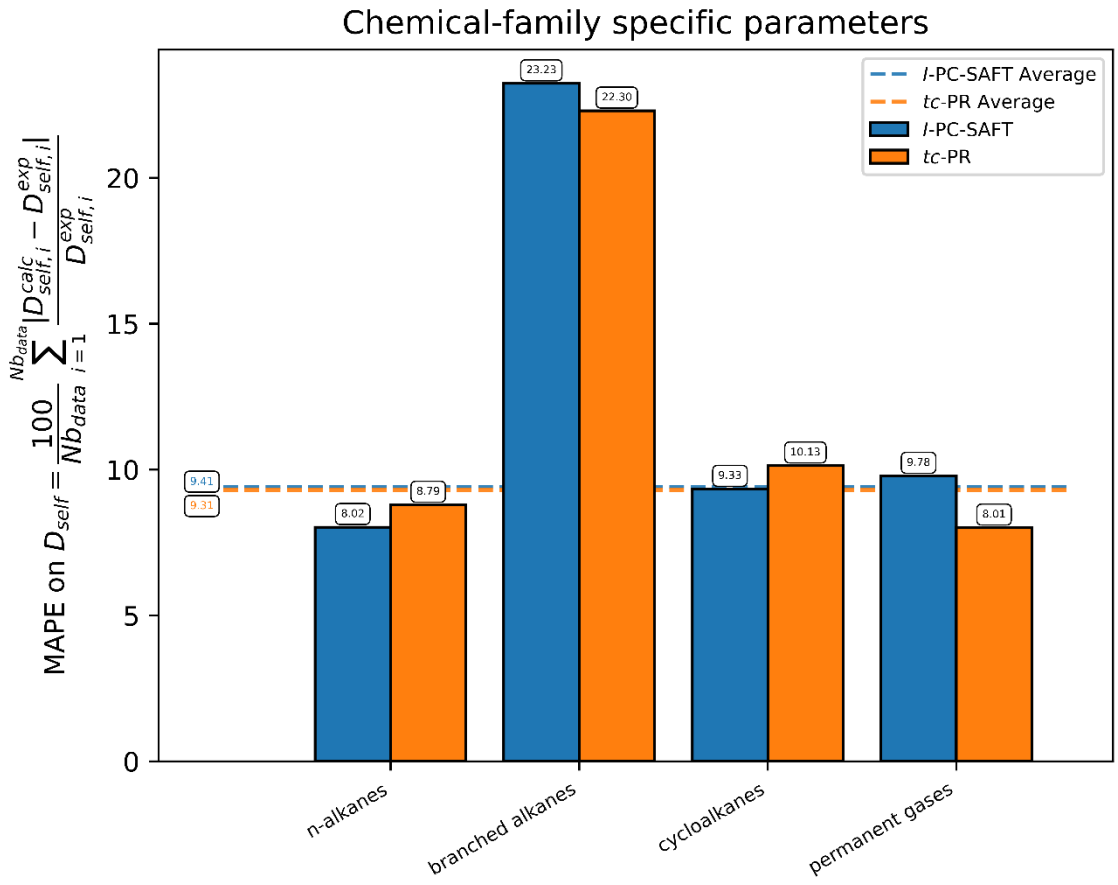

Figure IV-20 - Prediction of self-diffusion coefficients using model given by Eq. (IV-5) and parametrization strategy 2 (with chemical-family-specific parameters). Summary of the MAPEs obtained using either the *I*-PC-SAFT or the *tc*-PR EoS for estimating density and residual entropy.

The performance of the model combining Eq. (IV-5) and PS 2 is illustrated in Figures IV-21 to IV-24.

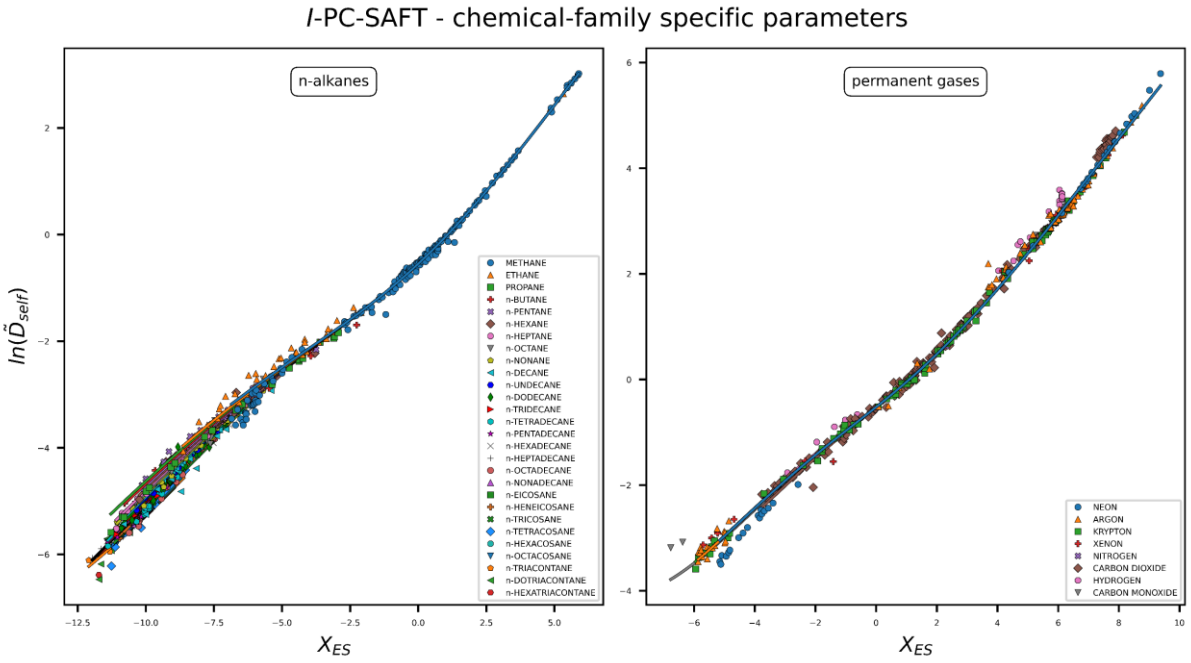

Figure IV-21 - Application of the ES-based model combining Eq. (IV-5) and parametrization strategy 2 to n-alkanes and permanent gases, using the *I*-PC-SAFT EoS. Points: experimental data. Solid line: model.

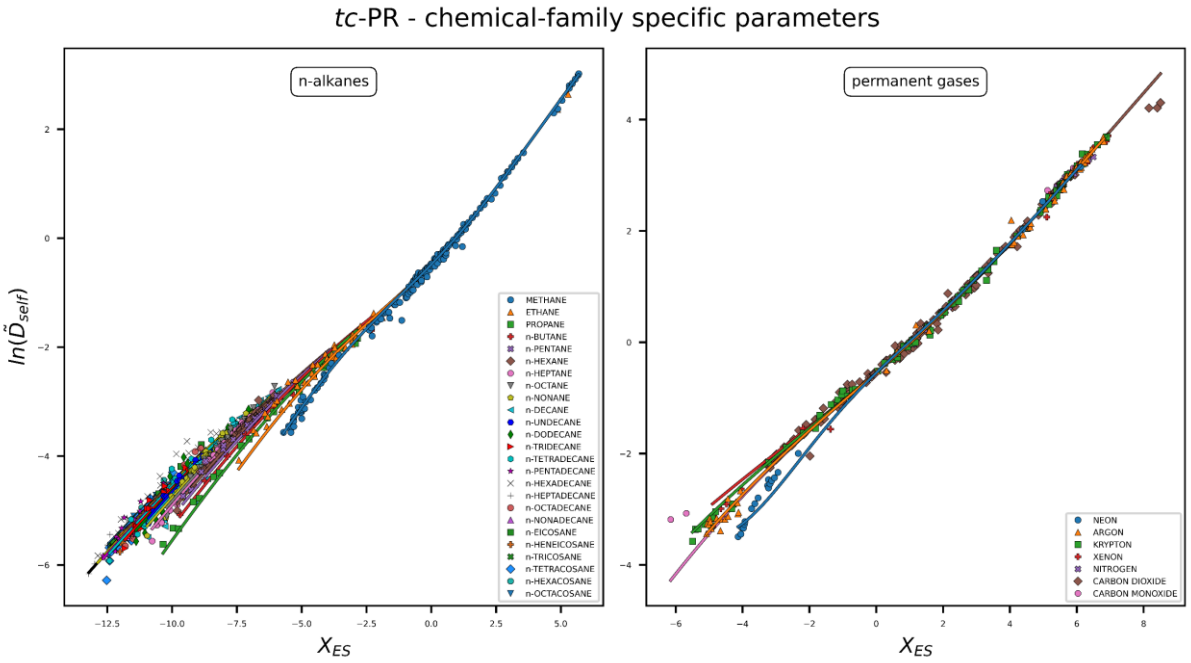

Figure IV-22 - Application of the ES-based model combining Eq. (IV-5) and parametrization strategy 2 to n-alkanes and permanent gases, using the *tc*-PR EoS. Points: experimental data. Solid line: model.

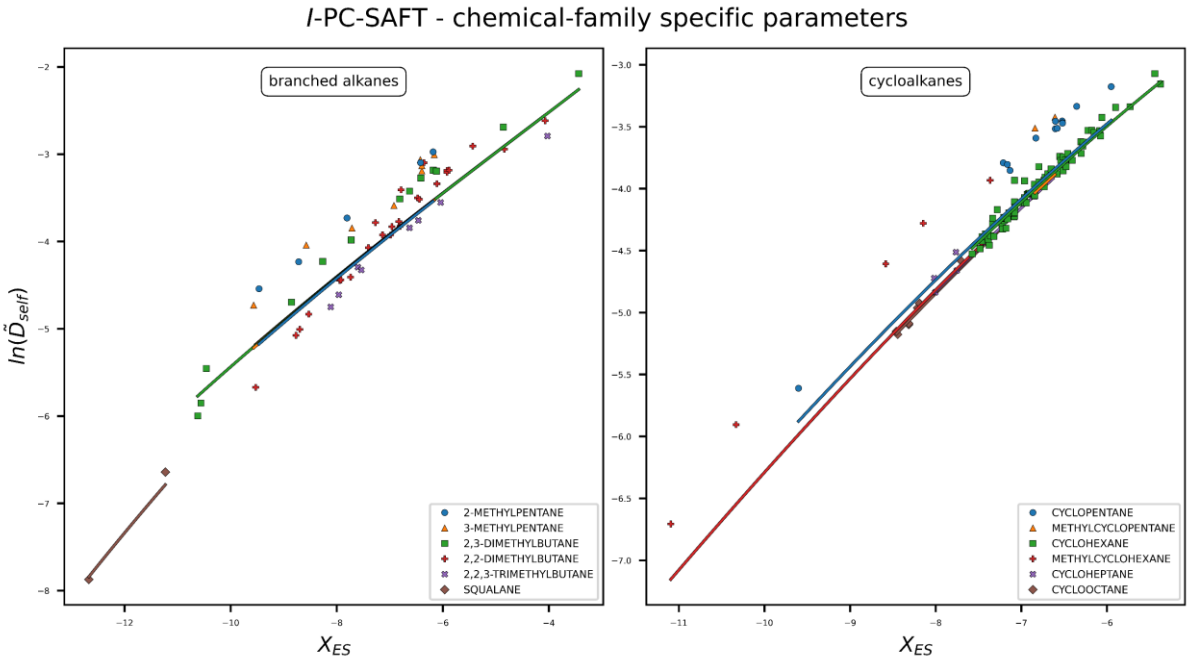

Figure IV-23 - Application of the ES-based model combining Eq. (IV-5) and parametrization strategy 2 to aromatic compounds and ketones, using the *I*-PC-SAFT EoS. Points: experimental data. Solid line: model.

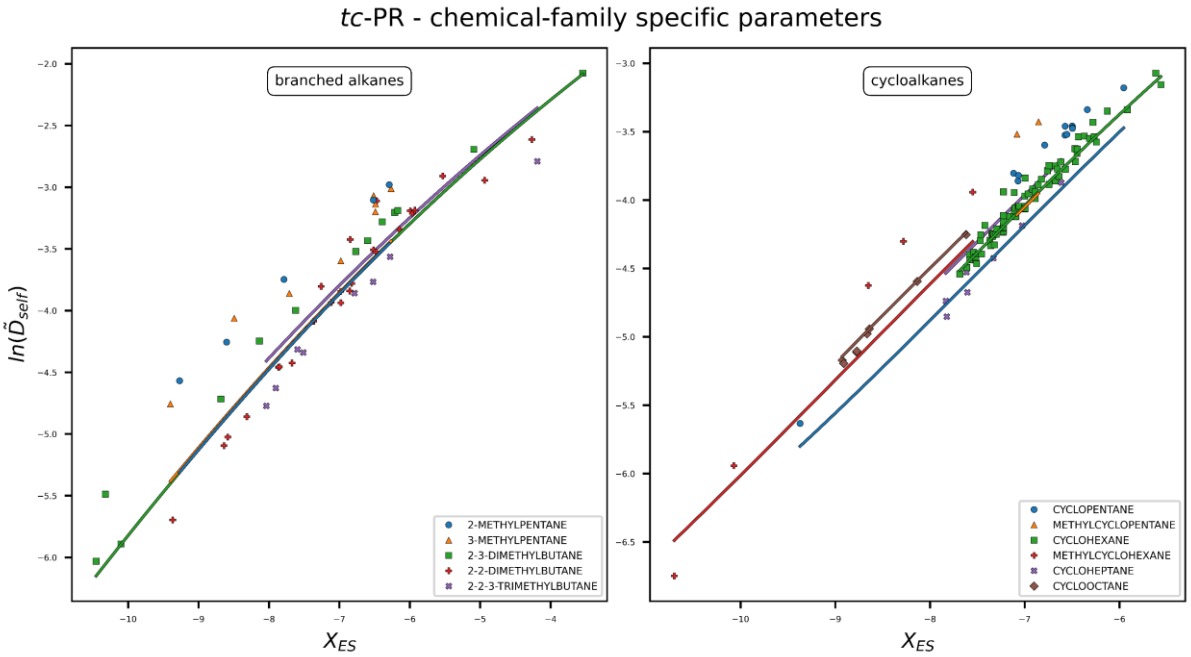

Figure IV-24 - Application of the ES-based model combining Eq. (IV-5) and parametrization strategy 2 to aromatic compounds and ketones, using the *tc*-PR EoS. Points: experimental data. Solid line: model.

To conclude this section, it can be highlighted that although showing higher deviations than PS 1, PS 2 extends the prediction capacity of the ES-based. PS 2 affords a reasonable estimation and a consistent description of temperature and pressure dependence of the self-diffusion coefficient (see Figures IV-21 to IV-24).

Recalling that both EoS used in this study do not include term accounting specifically for association, we observed that it was not possible to model properly the high component dependence of the curve slopes at dense states for some chemical families including associating compounds (e.g., alcohols) using PS 2. For this reason, these chemical families were disregarded.

Similarly to the case where the parameters are component specific (PS 1) and for which we observed that the cubic and SAFT models were equivalent, the same conclusion can be drawn when PS 2 is used: the *I*-PC-SAFT EoS and *tc*-PR EoS show equivalent performances.

IV-D) Conclusion:

The present study was devoted to the development of a new model for the correlation of self-diffusion coefficients based on the entropy-scaling concept. The main advantage of this approach lies in the applicability of the concept to the prediction of transport property in any fluid state, from dense liquid to supercritical gas.

In this article, following a methodology developed for the correlation of shear viscosity in a previous article[96], a model relating a dimensionless form of self-diffusion coefficient involving temperature and density [$Y_{\mathrm{ES}} = \ln\left(\widetilde{D}_{\mathrm{self}}\right)$], and a function X_{ES} of the Tv-residual entropy has been proposed.

As shown in Figure 3.C, such a model allows, for a given pure component, to define a unique mathematical relationship between Y_{ES} and X_{ES} whatever the state of the fluid (liquid, gas or supercritical). In addition, a universal behaviour at low density (i.e., for $X_{\mathrm{ES}} > 0$) has been highlighted.

To estimate the thermodynamic properties involved in the definition of X_{ES} and Y_{ES} (density and residual entropy), two EoS were selected: a SAFT-like EoS (*I*-PC-SAFT) and a cubic EoS (*tc*-PR).

Using a database containing around 2400 data for 72 pure species, two parametrization sets were determined for each EoS:

- a component-specific set (i.e., for each component, model parameters were fit to data associated with this pure component),
- a chemical-family set (i.e., 4 chemical families were considered; for each of them, model parameters were determined on data associated to all components belonging to the chemical family of interest).

Using a component-specific parametrization, both EoS lead to similar mean absolute deviations around 7.5% while using a chemical-family parametrization, the deviation (which is, once again, nearly the same for both EoS) is about 9.5%.

V- Complément d'information du chapitre 2

Supporting information:

A new entropy-scaling based model for estimating the self-diffusion coefficients of pure fluids.

Aghilas Dehlouz[1,2], Jean-Noël Jaubert[1(*)], Guillaume Galliero[3], Marc Bonnissel[2], Romain Privat[1(*)]

[1] *Université de Lorraine, École Nationale Supérieure des Industries Chimiques, Laboratoire Réactions et Génie des Procédés (UMR CNRS 7274), 1 rue Grandville, 54000 Nancy, France*

[2] *Gaztransport & Technigaz (GTT), 1 route de Versailles, 78470 Saint-Rémy-lès-Chevreuse, France*

[3] *Université de Pau et des Pays de l'Adour, E2S UPPA, CNRS TotalEnergies, LFCR UMR 5150, Pau, France*

V-A) Database user for the ES-based model development

The database containing experimental values of self-diffusion coefficients is the one proposed by Suàrez-Iglesias et al.[95]

Table S1 reports general informations of the considered data from the database. For each pure specie, it indicates:

- The lowest and the highest temperatures of the related data
- The lowest and the highest pressures of the related data
- The lowest and the highest values of the related self-diffusion data

Table V-1 - Experimental self-diffusion data information

Name	CAS	T_{min} K	T_{max} K	P_{min} MPa	P_{max} MPa	$D_{self}^{min} \cdot 10^3$ cm^2/s	$D_{self}^{max} \cdot 10^3$ cm^2/s
n-alkanes							
METHANE	74-82-8	93.00	454.00	0.1013	89.8300	0.0241000	319.0000
ETHANE	74-84-0	136.00	454.00	0.1013	97.8473	0.0142000	170.0000
PROPANE	74-98-6	112.00	453.00	1.4700	50.0000	0.0024900	0.2340
n-BUTANE	106-97-8	150.00	451.00	5.0000	50.0000	0.0046800	0.3000
n-PENTANE	109-66-0	174.00	450.00	0.1013	98.1000	0.0068200	0.1620
n-HEXANE	110-54-3	188.54	443.00	0.1000	99.8000	0.0052430	0.1460
n-HEPTANE	142-82-5	186.12	360.60	0.1000	98.1000	0.0028893	0.0641
n-OCTANE	111-65-9	248.14	383.66	0.1000	99.8000	0.0050900	0.0737
n-NONANE	111-84-2	235.52	403.20	0.1000	99.0000	0.0035406	0.0595
n-DECANE	124-18-5	247.86	448.00	0.1013	75.0000	0.0034500	0.0726
n-UNDECANE	1120-21-4	293.00	353.00	0.1000	98.1000	0.0046500	0.0242
n-DODECANE	112-40-3	268.75	434.76	0.1000	51.0000	0.0031549	0.0483
n-TRIDECANE	629-50-5	288.16	353.00	0.1000	98.1000	0.0028500	0.0140
n-TETRADECANE	629-59-4	279.36	443.00	0.1000	75.0000	0.0022377	0.0381
n-PENTADECANE	629-62-9	288.16	353.00	0.1000	98.1000	0.0025000	0.0102
n-HEXADECANE	544-76-3	292.68	472.50	0.1000	99.6000	0.0025200	0.0390
n-HEPTADECANE	629-78-7	303.00	353.00	0.1000	98.1000	0.0017700	0.0077
n-OCTADECANE	593-45-3	301.86	425.78	0.1013	0.1013	0.0028974	0.0212
n-NONADECANE	629-92-5	313.16	333.16	0.1013	0.1013	0.0034448	0.0052
n-EICOSANE	112-95-8	323.16	443.66	0.1013	0.1013	0.0036600	0.0229
n-HENEICOSANE	629-94-7	310.16	323.16	0.1013	0.1013	0.0025800	0.0037
n-TRICOSANE	638-67-5	316.16	328.16	0.1013	0.1013	0.0028400	0.0034
n-TETRACOSANE	646-31-1	318.16	423.66	0.1013	0.1013	0.0015200	0.0129
n-HEXACOSANE	630-01-3	343.66	423.66	0.1013	0.1013	0.0028947	0.0111
n-OCTACOSANE	630-02-4	343.66	423.66	0.1013	0.1013	0.0024100	0.0083
n-TRIACONTANE	638-68-6	343.66	469.00	0.1000	50.0000	0.0017000	0.0106
n-DOTRIACONTANE	544-85-4	339.16	443.66	0.1013	0.1013	0.0011700	0.0098
n-HEXATRIACONTANE	630-06-8	353.16	423.66	0.1013	0.1013	0.0012846	0.0059
branched alkanes							
2-METHYLPENTANE	107-83-5	200.00	308.16	0.1013	0.1013	0.0084000	0.0530
3-METHYLPENTANE	96-14-0	200.00	313.16	0.1013	0.1013	0.0069000	0.0514
2-3-DIMETHYLBUTANE	79-29-8	174.00	453.00	0.1013	50.0000	0.0017900	0.1740
2-2-DIMETHYLBUTANE	75-83-2	193.00	450.00	0.1000	60.0000	0.0026600	0.0968
2-2-3-TRIMETHYLBUTANE	464-06-2	263.00	450.00	5.0000	50.0000	0.0077700	0.0795
SQUALANE	111-01-3	293.00	333.00	0.1013	0.1013	0.0002700	0.0010
cycloalkanes							
CYCLOPENTANE	287-92-3	194.66	328.00	0.1000	75.0000	0.0028000	0.0442
METHYLCYCLOPENTANE	96-37-7	298.16	308.16	0.1013	0.1013	0.0290000	0.0324
CYCLOHEXANE	110-82-7	281.70	393.20	0.1000	90.0000	0.0102100	0.0524
METHYLCYCLOHEXANE	108-87-2	203.00	298.16	0.1000	50.0000	0.0008910	0.0184
CYCLOHEPTANE	291-64-5	288.16	348.82	0.1013	0.1013	0.0071672	0.0214
CYCLOOCTANE	292-64-8	292.57	345.90	0.1012	0.1013	0.0049800	0.0141
aromatics							
BENZENE	71-43-2	279.96	373.15	0.0981	98.0665	0.0134818	0.0573
TOLUENE	108-88-3	136.67	729.16	0.1000	99.7000	0.0000002	0.5072
o-TERPHENYL	84-15-1	281.55	438.16	0.1013	0.1013	0.0000003	0.0114
ethers							
DIMETHYL ETHER	115-10-6	184.50	458.00	50.0000	50.0000	0.0153000	0.2971
ketones							
ACETONE	67-64-1	182.86	323.16	0.1013	0.1013	0.0053000	0.0686
permanent gases							
NEON	7440-01-9	25.00	3273.15	0.1013	10.1325	0.0091758	29046.2000
ARGON	7440-37-1	77.50	3273.00	0.0115	24.6200	0.0153000	11248.3000
KRYPTON	7439-90-9	117.20	3273.00	0.0943	19.0350	0.0115000	6470.5000
XENON	7440-63-3	169.78	2773.00	0.0175	11.0400	0.0157000	3093.5000
NITROGEN	7727-37-9	233.17	421.80	0.1013	9.0000	2.1700000	381.6990
CARBON DIOXIDE	124-38-9	194.66	1944.00	0.0513	48.2630	0.1000000	4300.0000

Continued on next page

Table V-1 – continued from previous page

Name	CAS	T_{min} K	T_{max} K	P_{min} MPa	P_{max} MPa	$D^{min}_{self} \cdot 10^3$ cm^2/s	$D^{max}_{self} \cdot 10^3$ cm^2/s
HYDROGEN	1333-74-0	55.50	297.16	0.1013	75.0000	0.3600000	1285.0000
CARBON MONOXIDE	630-08-0	68.97	421.80	0.0930	0.1013	0.0225000	388.8180
alcohols							
METHANOL	67-56-1	154.00	453.00	0.0980	98.1000	0.0000892	0.1370
ETHANOL	64-17-5	158.66	437.00	0.1000	93.1000	0.0000500	0.1200
1-PROPANOL	71-23-8	212.00	441.00	0.1000	75.0000	0.0001610	0.0851
ISOPROPANOL	67-63-0	221.00	435.50	0.1000	50.0000	0.0001290	0.0938
1-BUTANOL	71-36-3	268.16	353.16	0.1013	0.1013	0.0013200	0.0182
1-3-PROPYLENE GLYCOL	504-63-2	304.00	315.00	0.1013	0.1013	0.0005500	0.0008
1-2-PROPYLENE GLYCOL	57-55-6	304.00	315.00	0.1013	0.1013	0.0005600	0.0010
2-PENTANOL	6032-29-7	237.10	483.10	5.0000	50.0000	0.0000975	0.1190
3-PENTANOL	584-02-1	242.20	474.50	5.0000	50.0000	0.0000451	0.2260
1-PENTANOL	71-41-0	213.00	428.60	0.1013	50.0000	0.0000457	0.0477
1-4-BUTANEDIOL	110-63-4	304.00	315.00	0.1013	0.1013	0.0003300	0.0005
1-3-BUTANEDIOL	107-88-0	227.16	276.46	0.1013	0.1013	0.0000180	0.0004
1-HEXANOL	111-27-3	278.16	338.16	0.1013	0.1013	0.0009250	0.0071
1-OCTANOL	111-87-5	288.16	343.16	0.1013	0.1013	0.0008440	0.0077
ETHYLENE GLYCOL	107-21-1	298.00	318.00	0.1013	0.1013	0.0008300	0.0019
2-METHYL-2-PROPANOL	75-65-0	283.40	344.25	0.1013	0.1013	0.0011400	0.0157
GLYCEROL	56-81-5	255.71	435.05	0.1013	0.1013	0.0000002	0.0065
others							
WATER	7732-18-5	238.60	973.16	0.0981	97.6000	0.0017500	4.7100
TETRAHYDROFURAN	109-99-9	180.56	308.16	0.1013	0.1013	0.0040000	0.0340
PROPYLENE CARBONATE	108-32-7	288.00	303.16	0.1013	0.1013	0.0044000	0.0058
ETHYLENE	74-85-1	123.15	573.00	0.1013	81.0600	0.0118600	205.0000
CYCLOPENTENE	142-29-0	182.16	253.16	0.1013	0.1013	0.0053887	0.0227
AMMONIA	7664-41-7	199.16	473.00	0.1013	75.0000	0.0233000	0.4340
CARBON DISULFIDE	75-15-0	268.20	313.20	0.1000	81.1000	0.0218000	0.0495
CHLOROFORM	67-66-3	200.00	397.00	0.1000	99.7000	0.0050000	0.0630
FLUOROBENZENE	462-06-6	235.33	349.37	0.1013	0.1013	0.0078007	0.0504

V-B) *I*-PC-SAFT based model

V-B-1) Equation of state parameters

PC-SAFT is a well-known equation of state, extensively described in the literature. For more information, the reader is referred to the original publication by Gross and Sadowski[82]. The difference between the PC-SAFT and the *I*-PC-SAFT model lies in (1) the way used to estimate the 3 molecular input parameters for a given non-associating compound (m, σ, ε), (2) the application of a Peneloux volume translation to the EoS.

More precisely, the 3 molecular parameters are constrained to exactly reproduce the experimental critical temperature and pressure and the vapor-pressure datum at a reduced temperature equal to 0.7. To do so, the following correlations were used:

$$\begin{cases} \mathrm{m}_i \approx 0.5959\,\omega_{i,\mathrm{exp}}^2 + 7.5437\omega_{i,\mathrm{exp}} + 0.9729 \\ {\varepsilon_i}/{\mathrm{k_b}} \approx {T_{c,i,\mathrm{exp}}}/{(4.7968\cdot 10^{-6}\mathrm{m}_i^5 - 3.0895\cdot 10^{-4}\mathrm{m}_i^4 + 7.8649\cdot 10^{-3}\mathrm{m}_i^3 - 0.10215\mathrm{m}_i^2 + 0.75358\mathrm{m}_i + 0.63659)} \\ \sigma_i \approx \left[{\varepsilon_i}/{\mathrm{k_b}}\cdot\frac{\mathrm{k_b}}{P_{c,i,\mathrm{exp}}}10^{(1.6345\cdot 10^{-7}\mathrm{m}_i^6 - 1.1346\cdot 10^{-5}\mathrm{m}_i^5 + 3.1389\cdot 10^{-4}\mathrm{m}_i^4 - 4.4618\cdot 10^{-3}\mathrm{m}_i^3 + 3.6282\cdot 10^{-2}\mathrm{m}_i^2 - 022498\mathrm{m}_i + 0.77655)}\right]^{1/3} \end{cases} \quad (\mathrm{V}-1)$$

The application of a volume translation requires the knowledge of a component-dependent *c* parameter. It was determined in order to exactly reproduce the experimental saturated liquid molar volume at a reduced temperature of 0.8:

$$c = v_{\mathrm{liq}}^{\mathrm{sat,u-EoS}}(T_{\mathrm{r}} = 0.8) - v_{\mathrm{liq,exp}}^{\mathrm{sat}}(T_{\mathrm{r}} = 0.8) \quad (\mathrm{V}-2)$$

Where $v_{\mathrm{liq}}^{\mathrm{sat,u-EoS}}(T_{\mathrm{r}} = 0.8)$ is the molar volume calculated with the original (untranslated) EoS at $T_{\mathrm{r}} = 0.8$.

More details are available in the original paper introducing the *I*-PC-SAFT model[48]. The *I*-PC-SAFT parameters used in this study are reported in Table V-2.

Table V-2 - *I*-PC-SAFT EoS parameters

Name	CAS	m -	σ Å	$/k_b$ K	$c \cdot 10^3$ m^3/mol
n-alkanes					
METHANE	74-82-8	1.0577	3.6335	145.557	0.0001
ETHANE	74-84-0	1.74901	3.47261	181.204	0.0032
PROPANE	74-98-6	2.14983	3.61119	198.141	0.0074
n-BUTANE	106-97-8	2.51623	3.72001	211.407	0.0125
n-PENTANE	109-66-0	2.9127	3.80047	218.694	0.0195
n-HEXANE	110-54-3	3.30037	3.86477	224.08	0.0270
n-HEPTANE	142-82-5	3.67922	3.91767	228.209	0.0342
n-OCTANE	111-65-9	4.0762	3.95828	230.949	0.0422
n-NONANE	111-84-2	4.4271	4.00172	234.238	0.0493
n-DECANE	124-18-5	4.82084	4.02795	236.136	0.0568
n-UNDECANE	1120-21-4	5.12925	4.07999	239.194	0.0660
n-DODECANE	112-40-3	5.50599	4.09659	240.655	0.0729
n-TRIDECANE	629-50-5	5.84391	4.14076	242.269	0.0841
n-TETRADECANE	629-59-4	6.0562	4.20981	246.012	0.0971
n-PENTADECANE	629-62-9	6.41709	4.2206	247.01	0.1037
n-HEXADECANE	544-76-3	6.67775	4.25727	249.329	0.1107
n-HEPTADECANE	629-78-7	7.11917	4.22813	249.246	0.1128
n-OCTADECANE	593-45-3	7.47364	4.23565	249.618	0.1194
n-NONADECANE	629-92-5	7.82356	4.2398	250.213	0.1247
n-EICOSANE	112-95-8	8.29483	4.20835	249.693	0.1213
n-HENEICOSANE	629-94-7	8.5998	4.22042	250.647	0.1292
n-TRICOSANE	638-67-5	9.33691	4.21456	251.347	0.1356
n-TETRACOSANE	646-31-1	9.73329	4.20453	251.398	0.1366
n-HEXACOSANE	630-01-3	10.477	4.19074	251.824	0.1382
n-OCTACOSANE	630-02-4	11.2258	4.17187	251.984	0.1353
n-TRIACONTANE	638-68-6	11.8597	4.16678	252.669	0.1353
n-DOTRIACONTANE	544-85-4	12.4964	4.16931	253.235	0.1350
n-HEXATRIACONTANE	630-06-8	13.885	4.1208	253.573	0.1074
branched alkanes					
2-METHYLPENTANE	107-83-5	3.12767	3.90878	224.726	0.0221
3-METHYLPENTANE	96-14-0	3.05811	3.92458	230.038	0.0231
2-3-DIMETHYLBUTANE	79-29-8	2.89521	3.97732	233.416	0.0198
2-2-DIMETHYLBUTANE	75-83-2	2.77755	4.02794	232.508	0.0171
2-2-3-TRIMETHYLBUTANE	464-06-2	2.90142	4.14466	247.7	0.0219
SQUALANE	111-01-3	8.36784	4.80043	279.955	0.1518
cycloalkanes					
CYCLOPENTANE	287-92-3	2.47558	3.75741	256.389	0.0139
METHYLCYCLOPENTANE	96-37-7	2.73659	3.89635	254.973	0.0172
CYCLOHEXANE	110-82-7	2.57692	3.93344	272.395	0.0152
METHYLCYCLOHEXANE	108-87-2	2.793	4.07577	271.347	0.0202
CYCLOHEPTANE	291-64-5	2.83005	4.00491	284.904	0.0185
CYCLOOCTANE	292-64-8	2.91927	4.14912	301.043	0.0233
aromatics					
BENZENE	71-43-2	2.59421	3.71133	275.605	0.0151
TOLUENE	108-88-3	3.00982	3.79765	271.622	0.0233
o-TERPHENYL	84-15-1	5.30019	3.85061	317.335	-0.0049
ethers					
DIMETHYL ETHER	115-10-6	2.51666	3.24729	198.949	0.0083
ketones					
ACETONE	67-64-1	3.3416	3.32279	223.197	0.0263
permanent gases					
NEON	7440-01-9	0.666762	3.43647	39.3203	0.0025
ARGON	7440-37-1	0.952492	3.44081	120.823	-0.0003
KRYPTON	7439-90-9	0.952492	3.69199	167.668	0.0003
XENON	7440-63-3	0.952492	4.03334	232.052	0.0012
NITROGEN	7727-37-9	1.27492	3.25959	87.9687	-0.0004
CARBON DIOXIDE	124-38-9	2.69691	2.60169	146.566	0.0049

Continued on next page

Table 2.1 – continued from previous page

Name	CAS	m -	σ $\AA$	$/k_b$ K	$c \cdot 10^3$ m^3/mol
HYDROGEN	1333-74-0	0.421592	5.64646	24.8714	0.0163
CARBON MONOXIDE	630-08-0	1.3574	3.21074	89.7577	-0.0002
alcohols					
METHANOL	67-56-1	5.41942	2.3078	188.401	0.0143
ETHANOL	64-17-5	6.06069	2.41836	182.427	0.0171
1-PROPANOL	71-23-8	5.87288	2.63227	192.371	0.0171
ISOPROPANOL	67-63-0	6.22242	2.59274	178.972	0.0178
1-BUTANOL	71-36-3	5.60376	2.87407	204.791	0.0194
1-3-PROPYLENE GLYCOL	504-63-2	6.85531	2.2247	247.803	-0.0148
1-2-PROPYLENE GLYCOL	57-55-6	10.0487	2.07202	194.304	0.0019
2-PENTANOL	6032-29-7	5.33057	3.10702	207.343	0.0244
3-PENTANOL	584-02-1	4.99872	3.18175	211.293	0.0260
1-PENTANOL	71-41-0	5.49323	3.06448	215.25	0.0224
1-4-BUTANEDIOL	110-63-4	10.6792	2.21594	204.219	0.0120
1-3-BUTANEDIOL	107-88-0	6.56733	2.94968	234.251	0.0362
1-HEXANOL	111-27-3	5.36018	3.26659	225.525	0.0288
1-OCTANOL	111-87-5	5.45109	3.56005	239.341	0.0367
ETHYLENE GLYCOL	107-21-1	4.9379	2.67065	272.99	0.0202
2-METHYL-2-PROPANOL	75-65-0	5.82577	2.82756	181.86	0.0176
GLYCEROL	56-81-5	4.9859	2.89659	321.223	0.0225
others					
WATER	7732-18-5	3.64287	2.08351	274.442	0.0071
TETRAHYDROFURAN	109-99-9	2.71029	3.53701	259.662	0.0146
PROPYLENE CARBONATE	108-32-7	4.47771	3.27181	305.238	0.0298
ETHYLENE	74-85-1	1.6482	3.41383	172.685	0.0026
CYCLOPENTENE	142-29-0	2.48508	3.66398	253.582	0.0100
AMMONIA	7664-41-7	2.92125	2.41696	188.631	0.0089
CARBON DISULFIDE	75-15-0	1.83386	3.54318	319.894	0.0009
CHLOROFORM	67-66-3	2.68365	3.4792	259.011	0.0094
FLUOROBENZENE	462-06-6	2.87918	3.66127	262.108	0.0188

V-B-2) Parameters for parametrization strategy 1 (i.e., involving component-specific parameters in combination with the *I*-PC-SAFT EoS)

Component-specific parameters (a_1, a_2, a_3, b, c and d) to be used in the below equation for the viscosity estimation are reported in Table V-3.

$$\begin{cases} \ln\left(\frac{D_{\text{self}}}{D_{\text{self}}^{\text{ref}}}\right)_{\text{calc}} = \left[\left(\frac{a_1 + a_2\tilde{s}_{\text{Tv-res}} + a_3\tilde{s}_{\text{Tv-res}}^2}{1 + e^{cX_{\text{ES}}}}\right) + \left(\frac{b}{1 + e^{-cX_{\text{ES}}}}\right)\right] X_{\text{ES}} + d \\ X_{\text{ES}} = -\left(\frac{s_{\text{Tv-res}}}{s_{\text{Tv-res}}^c}\right) - \ln\left(\frac{s_{\text{Tv-res}}}{s_{\text{Tv-res}}^c}\right) \\ D_{\text{self}}^{\text{ref}} = \rho_{\text{N}}^{-1/3}\sqrt{\text{k}_\text{b}T/\text{m}_0} \\ \tilde{s}_{\text{Tv-res}} = \frac{s_{\text{Tv-res}}}{R} \end{cases} \quad \text{(V-3)}$$

The Tv-residual entropy ($s_{\text{Tv-res}}$) and the molecular density (ρ_{N}) were estimated using the *I*-PC-SAFT EoS.

Table V-3 - Component-specific parameters suitable for the *I*-PC-SAFT based model with the corresponding number of experimental data points and MAPE (MAPE = Mean Absolute Percentage Error)

Name	a_1	a_2	a_3	b	c	d	Data number	MAPE
n-alkanes							708	5.57
METHANE	0.274849	0.010650	0.011561	0.674936	0.271708	-0.545220	156	5.57
ETHANE	0.437620	0.039076	0.005576	0.604804	0.739505	-0.560599	56	7.24
PROPANE	0.346534	0.000783	0.001253	0.668634	0.286121	-0.545060	21	2.45
n-BUTANE	0.416839	0.022535	0.002375	0.668634	0.286121	-0.545060	9	3.97
n-PENTANE	0.343884	0.001760	0.000781	0.668634	0.286121	-0.545060	29	3.51
n-HEXANE	0.332367	0.000000	0.000771	0.668634	0.286121	-0.545060	72	3.15
n-HEPTANE	0.335598	0.002541	0.001157	0.668634	0.286121	-0.545060	47	3.57
n-OCTANE	0.344278	0.000539	0.000745	0.668634	0.286121	-0.545060	36	5.38
n-NONANE	0.392393	0.008702	0.001035	0.668634	0.286121	-0.545060	38	4.86
n-DECANE	0.333314	0.000084	0.000838	0.668634	0.286121	-0.545060	40	8.79
n-UNDECANE	0.345060	0.000005	0.000639	0.668634	0.286121	-0.545060	17	3.28
n-DODECANE	0.364615	0.002471	0.000724	0.668634	0.286121	-0.545060	33	7.61
n-TRIDECANE	0.673652	0.047848	0.002265	0.668634	0.286121	-0.545060	18	5.10
n-TETRADECANE	0.359433	0.000005	0.000545	0.668634	0.286121	-0.545060	23	6.09
n-PENTADECANE	0.432376	0.002465	0.000228	0.668634	0.286121	-0.545060	16	7.42
n-HEXADECANE	0.354210	0.000039	0.000498	0.668634	0.286121	-0.545060	31	8.14
n-HEPTADECANE	0.436839	0.001975	0.000176	0.668634	0.286121	-0.545060	14	6.15
n-OCTADECANE	0.360179	0.000001	0.000460	0.668634	0.286121	-0.545060	11	4.80
n-EICOSANE	0.346559	0.000926	0.000486	0.668634	0.286121	-0.545060	6	2.20
n-TETRACOSANE	0.366479	0.000000	0.000272	0.668634	0.286121	-0.545060	11	9.74
n-TRIACONTANE	0.415716	0.000063	0.000076	0.668634	0.286121	-0.545060	14	6.20
n-DOTRIACONTANE	0.557369	0.020089	0.000714	0.668634	0.286121	-0.545060	10	9.93
branched alkanes							59	6.32
2-METHYLPENTANE	0.311062	0.000082	0.001407	0.668634	0.286121	-0.545060	5	3.30
3-METHYLPENTANE	0.329723	0.003473	0.001669	0.668634	0.286121	-0.545060	8	8.65
2-3-DIMETHYLBUTANE	0.396136	0.013791	0.002583	0.668634	0.286121	-0.545060	13	5.19
2-2-DIMETHYLBUTANE	0.360892	0.002792	0.002904	0.668634	0.286121	-0.545060	25	8.12
2-2-3-TRIMETHYLBUTANE	0.791221	0.122439	0.011557	0.668634	0.286121	-0.545060	8	2.08
cycloalkanes							117	3.59
CYCLOPENTANE	0.356060	0.006751	0.003551	0.668634	0.286121	-0.545060	13	2.41
CYCLOHEXANE	0.383853	0.004450	0.004161	0.668634	0.286121	-0.545060	84	3.99
METHYLCYCLOHEXANE	0.616249	0.069494	0.006443	0.668634	0.286121	-0.545060	5	2.06
CYCLOHEPTANE	0.416398	0.005363	0.003013	0.668634	0.286121	-0.545060	7	4.19
CYCLOOCTANE	0.693606	0.092078	0.009673	0.668634	0.286121	-0.545060	8	1.81
aromatics							250	13.65
BENZENE	0.303287	0.001846	0.003674	0.668634	0.286121	-0.545060	146	3.19

Continued on next page

Table V-3 – continued from previous page

Name	a_1	a_2	a_3	b	c	d	Data number	MAPE
TOLUENE	0.988787	0.181355	0.013454	0.668634	0.286121	-0.545060	76	23.63
o-TERPHENYL	1.109265	0.192299	0.012805	0.668634	0.286121	-0.545060	28	41.09
ethers							10	4.30
DIMETHYL ETHER	0.263931	0.000050	0.002296	0.668634	0.286121	-0.545060	10	4.30
ketones							20	9.07
ACETONE	0.628627	0.091878	0.007360	0.668634	0.286121	-0.545060	20	9.07
permanent gases							429	6.27
NEON	0.155965	0.000000	0.020000	0.867058	0.115214	-0.703275	39	2.95
ARGON	0.806516	0.174388	0.019646	0.611704	0.467839	-0.663230	84	8.79
KRYPTON	0.230100	0.000038	0.018815	0.697956	0.231662	-0.569721	89	4.65
XENON	0.602168	0.194124	0.041463	0.655887	0.972667	-0.852486	29	6.69
CARBON DIOXIDE	0.001780	0.000076	0.017085	0.954210	0.100394	-0.514797	167	6.56
HYDROGEN	0.379281	0.000033	0.019966	0.651987	0.336301	-0.347987	21	6.46
alcohols							267	9.50
METHANOL	0.404933	0.000000	0.000623	0.668634	0.286121	-0.545060	42	6.64
ETHANOL	0.498607	0.000005	0.000631	0.668634	0.286121	-0.545060	52	6.90
1-PROPANOL	0.496082	0.000095	0.001291	0.668634	0.286121	-0.545060	32	7.82
ISOPROPANOL	0.438955	0.000033	0.002415	0.668634	0.286121	-0.545060	16	10.09
1-BUTANOL	0.599023	0.048717	0.005411	0.668634	0.286121	-0.545060	11	7.38
2-PENTANOL	0.554664	0.065161	0.007981	0.668634	0.286121	-0.545060	9	13.82
3-PENTANOL	0.156559	0.000380	0.007148	0.668634	0.286121	-0.545060	12	24.46
1-PENTANOL	0.452128	0.000008	0.001875	0.668634	0.286121	-0.545060	22	12.11
1-HEXANOL	0.383984	0.001959	0.002908	0.668634	0.286121	-0.545060	5	1.20
1-OCTANOL	0.704436	0.096410	0.008418	0.668634	0.286121	-0.545060	9	16.33
2-METHYL-2-PROPANOL	1.076373	0.195113	0.018754	0.668634	0.286121	-0.545060	8	4.93
GLYCEROL	0.938997	0.116876	0.008466	0.668634	0.286121	-0.545060	49	10.81
others							454	7.27
WATER	0.318994	0.032247	0.005221	0.864698	0.971024	-0.450270	289	7.79
TETRAHYDROFURAN	0.748592	0.110692	0.008104	0.668634	0.286121	-0.545060	7	4.87
ETHYLENE	0.537000	0.071040	0.009127	0.580149	0.988389	-0.418434	70	7.14
AMMONIA	0.216226	0.002572	0.004146	0.668634	0.286121	-0.545060	18	4.63
CARBON DISULFIDE	0.334432	0.033144	0.006051	0.668634	0.286121	-0.545060	10	3.36
CHLOROFORM	0.322396	0.000373	0.001561	0.668634	0.286121	-0.545060	51	7.34
FLUOROBENZENE	0.301864	0.000268	0.002123	0.668634	0.286121	-0.545060	9	2.75

V-B-3) Parameters for parametrization strategy 2 (i.e., involving chemical-family specific parameters in com- bination with the *I*-PC-SAFT EoS)

These parameters have to be used with Eq. (V-3).

V-B-3.1) n-alkane family:

Table V-4 - Chemical-family specific parameters for n-alkanes compounds to be used in the *I*-PC-SAFT based model.

Variable	Value
Number of compounds	28
Data number	726
MAPE	8.02
a_1	0.307528
a_2	-0.014906
a_3	-0.000343
b	0.640654
c	0.365670
d	-0.550066

Table V-5 - Prediction of self-diffusion data of n-alkanes using chemical-family specific parameters for the *I*-PC-SAFT based model: data number and corresponding MAPE (Mean Absolute Percentage Error).

Name	Data number	MAPE
METHANE	156	9.64
ETHANE	56	7.90
PROPANE	21	14.80
n-BUTANE	9	8.14
n-PENTANE	29	5.25
n-HEXANE	72	5.12
n-HEPTANE	47	3.46
n-OCTANE	36	5.97
n-NONANE	38	5.37
n-DECANE	40	10.22
n-UNDECANE	17	2.68
n-DODECANE	33	8.78
n-TRIDECANE	18	4.95
n-TETRADECANE	23	9.49
n-PENTADECANE	16	7.81
n-HEXADECANE	31	8.63
n-HEPTADECANE	14	6.53
n-OCTADECANE	11	9.22
n-NONADECANE	2	3.93
n-EICOSANE	6	6.39
n-HENEICOSANE	4	7.05
n-TRICOSANE	3	14.56
n-TETRACOSANE	11	11.63
n-HEXACOSANE	3	10.51
n-OCTACOSANE	3	7.19
n-TRIACONTANE	14	14.50
n-DOTRIACONTANE	10	18.22
n-HEXATRIACONTANE	3	23.75

V-B-3.1) Branched alkane family:

Table V-6 - Chemical-family specific parameters for branched alkanes compounds to be used in the *I*-PC-SAFT based model.

Variable	Value
Number of compounds	6
Data number	61
MAPE	23.23
a_1	0.415587
a_2	-0.006792
a_3	0.000045
b	0.668634
c	0.286121
d	-0.545059

Table V-7 - Prediction of self-diffusion data of branched alkanes using chemical-family specific parameters for the *I*-PC-SAFT based model: data number and corresponding MAPE (Mean Absolute Percentage Error).

Name	Data number	MAPE
2-METHYLPENTANE	5	44.08
3-METHYLPENTANE	8	38.73
2,3-DIMETHYLBUTANE	13	23.29
2,2-DIMETHYLBUTANE	25	17.16
2,2,3-TRIMETHYLBUTANE	8	17.32
SQUALANE	2	8.33

V-B-3.1) Cycloalkane family:

Table V-8 - Chemical-family specific parameters for cycloalkanes compounds to be used in the *I*-PC-SAFT based model.

Variable	Value
Number of compounds	6
Data number	119
MAPE	9.33
a_1	0.280659
a_2	-0.043467
a_3	-0.001168
b	0.668634
c	0.286121
d	-0.545059

Table V-9 - Prediction of self-diffusion data of cycloalkanes using chemical-family specific parameters for the *I*-PC-SAFT based model: data number and corresponding MAPE (Mean Absolute Percentage Error).

Name	Data number	MAPE
CYCLOPENTANE	13	28.51
METHYLCYCLOPENTANE	2	38.92
CYCLOHEXANE	84	4.53
METHYLCYCLOHEXANE	5	42.77
CYCLOHEPTANE	7	5.53
CYCLOOCTANE	8	3.59

V-B-3.1) Permanent gas family:

Table V-10 - Chemical-family specific parameters for permanent gases to be used in the *I*-PC-SAFT based model.

Variable	Value
Number of compounds	8
Data number	458
MAPE	9.78
a_1	0.169366
a_2	-0.151883
a_3	-0.020000
b	0.682951
c	0.282622
d	-0.524472

Table V-11 - Prediction of self-diffusion data of permanent gases using chemical-family specific parameters for the *I*-PC-SAFT based model: data number and corresponding MAPE (Mean Absolute Percentage Error).

Name	Data number	MAPE
NEON	39	17.84
ARGON	84	11.54
KRYPTON	89	4.76
XENON	29	9.58
NITROGEN	13	4.32
CARBON DIOXIDE	167	8.83
HYDROGEN	21	22.05
CARBON MONOXIDE	16	7.41

V-C) *tc*-PR based model

V-C-1) Equation of state parameters

The *translated-consistent* version of the Peng-Robinson (PR) EoS, denoted *tc*-PR[75,83] relies on consistent L, M and N parameters of the Twu 91 α-function (*consistent* means that these parameters passed a consistency test[83] ensuring safe calculations in the supercritical region). In this model, the volume translation parameter c was selected in order to exactly reproduce the experimental saturated liquid molar volume at a reduced temperature of 0.8:

$$c = v_{\mathrm{liq}}^{\mathrm{sat,u-EoS}}(T_{\mathrm{r}} = 0.8) - v_{\mathrm{liq,exp}}^{\mathrm{sat}}(T_{\mathrm{r}} = 0.8) \qquad \text{(V-4)}$$

Where $v_{\mathrm{liq}}^{\mathrm{sat,u-EoS}}(T_{\mathrm{r}} = 0.8)$ is the molar volume calculated with the original (untranslated) EoS at $T_r = 0.8$.

The final *tc*-PR EoS expression is:

$$P(T,v) = \frac{RT}{v-b} - \frac{a_c \cdot \alpha(T_{\mathrm{r}})}{(v+c)(v+b+2c)+(b+c)(v-b)}$$

$$\begin{cases} \alpha(T_r) = T_r^{N(M-1)}\exp[L(1-T_r^{MN})] \\ c = v_{\mathrm{liq}}^{\mathrm{sat,u-EoS}}(T_{\mathrm{r}} = 0.8) - v_{\mathrm{liq,exp}}^{\mathrm{sat}}(T_{\mathrm{r}} = 0.8) \\ \eta_c = \left[1 + \sqrt[3]{4-2\sqrt{2}} + \sqrt[3]{4+2\sqrt{2}}\right] \approx 0.25308 \\ a_c = \dfrac{40\eta_c + 8}{49 - 37\eta_c}\dfrac{R^2T_{\mathrm{c,exp}}^2}{P_{\mathrm{c,exp}}} \approx 0.45724\dfrac{R^2T_{\mathrm{c,exp}}^2}{P_{\mathrm{c,exp}}} \\ b = \dfrac{\eta_c}{\eta_c+3}\dfrac{RT_{\mathrm{c,exp}}}{P_{\mathrm{c,exp}}} - c \approx 0.07780\dfrac{RT_{\mathrm{c,exp}}}{P_{\mathrm{c,exp}}} - c \end{cases} \qquad \text{(V-5)}$$

The *tc*-PR parameters used in this study are reported in Table V-12.

Table V-12 - *tc*-PR EoS parameters

Name	CAS	*L* -	*M* -	*N* -	$c \cdot 10^6$ m^3/mol
n-alkanes					
METHANE	74-82-8	0.14738	0.90748	1.82411	-3.56049
ETHANE	74-84-0	0.30533	0.86927	1.32966	-3.67453
PROPANE	74-98-6	0.74550	0.91333	0.76097	-3.73494
n-BUTANE	106-97-8	0.41536	0.84901	1.32049	-3.43648
n-PENTANE	109-66-0	0.29330	0.83662	1.82462	-1.59871
n-HEXANE	110-54-3	0.28726	0.83405	2.01991	0.81628
n-HEPTANE	142-82-5	0.36295	0.82017	1.83664	3.10863
n-OCTANE	111-65-9	0.35700	0.81717	1.99996	6.42842
n-NONANE	111-84-2	0.41649	0.80811	1.89355	9.34517
n-DECANE	124-18-5	0.37696	0.81080	2.17809	12.827436
n-UNDECANE	1120-21-4	0.48046	0.80007	1.90454	18.32929
n-DODECANE	112-40-3	0.45843	0.80098	2.08729	22.22725
n-TRIDECANE	629-50-5	0.47740	0.79897	2.11999	30.13814
n-TETRADECANE	629-59-4	0.57041	0.78895	1.88879	39.90980
n-PENTADECANE	629-62-9	0.57955	0.78769	1.94902	45.35005
n-HEXADECANE	544-76-3	0.60685	0.78674	1.94340	52.13839
n-HEPTADECANE	629-78-7	0.56074	0.79245	2.18728	52.58577
n-OCTADECANE	593-45-3	0.58016	0.79247	2.21665	59.16994
n-NONADECANE	629-92-5	0.59247	0.79325	2.27181	64.88646
n-EICOSANE	112-95-8	0.56936	0.80387	2.50049	64.11107
n-HENEICOSANE	629-94-7	0.46937	0.81153	3.01913	72.69091
n-TRICOSANE	638-67-5	0.47273	0.81012	3.20180	84.63427
n-TETRACOSANE	646-31-1	0.46905	0.81025	3.33744	89.64608
n-HEXACOSANE	630-01-3	0.51088	0.81036	3.33463	100.20264
n-OCTACOSANE	630-02-4	0.56000	0.81096	3.31984	107.89305
branched alkanes					
2-METHYLPENTANE	107-83-5	0.34965	0.82087	1.65903	-3.09737
3-METHYLPENTANE	96-14-0	0.30612	0.82268	1.77981	-1.66760
2-3-DIMETHYLBUTANE	79-29-8	0.18994	0.84369	2.36194	-4.22445
2-2-DIMETHYLBUTANE	75-83-2	0.22181	0.83374	2.03473	-6.28035
2-2-3-TRIMETHYLBUTANE	464-06-2	0.17671	0.84973	2.51494	-5.39360
cycloalkanes					
CYCLOPENTANE	287-92-3	0.39596	0.82692	1.29392	-1.98829
METHYLCYCLOPENTANE	96-37-7	0.88602	0.88162	0.75449	-3.34392
CYCLOHEXANE	110-82-7	0.37295	0.81214	1.35210	-4.22316
METHYLCYCLOHEXANE	108-87-2	0.44822	0.82056	1.28350	-4.19185
CYCLOHEPTANE	291-64-5	0.24058	0.84705	2.08571	-5.35293
CYCLOOCTANE	292-64-8	0.13238	0.83720	2.69425	-4.11952
aromatics					
BENZENE	71-43-2	0.13487	0.84816	2.57900	-1.43896
TOLUENE	108-88-3	0.31709	0.83024	1.75262	1.23818
o-TERPHENYL	84-15-1	0.26545	0.82496	3.00517	-46.15007
ethers					
DIMETHYL ETHER	115-10-6	0.61030	0.84979	0.96628	-2.19464
ketones					
ACETONE	67-64-1	0.36810	0.85384	1.83142	12.00988
permanent gases					
NEON	7440-01-9	0.18850	0.94691	1.47057	-2.35725
ARGON	7440-37-1	0.12268	0.90452	1.85408	-3.29332
KRYPTON	7439-90-9	0.10130	0.89545	1.95004	-3.33250
XENON	7440-63-3	0.17837	0.91982	1.70497	-3.77404
NITROGEN	7727-37-9	0.12427	0.88981	2.01285	-3.64285
CARBON DIOXIDE	124-38-9	0.17800	0.85903	2.41074	-1.13352
CARBON MONOXIDE	630-08-0	0.09967	0.87823	2.15086	-3.67664
alcohols					
METHANOL	67-56-1	0.76822	0.93479	1.57159	9.17712
ETHANOL	64-17-5	1.11945	0.97724	1.14643	6.08287

Continued on next page

Table V-12 – continued from previous page

Name	CAS	*L* -	*M* -	*N* -	$c \cdot 10^6$ m^3/mol
1-PROPANOL	71-23-8	1.10666	0.93817	1.13228	3.07305
ISOPROPANOL	67-63-0	1.31643	1.00000	0.98017	4.10196
1-BUTANOL	71-36-3	1.38509	1.00000	0.85377	1.58248
1-3-PROPYLENE GLYCOL	504-63-2	1.47031	0.99999	0.82047	6.67077
1-2-PROPYLENE GLYCOL	57-55-6	0.91796	0.82040	1.26503	8.04443
2-PENTANOL	6032-29-7	0.27429	0.00000	0.96806	3.87821
3-PENTANOL	584-02-1	0.32989	0.00000	0.93122	4.80420
1-PENTANOL	71-41-0	1.45953	1.00000	0.78797	1.17104
1-4-BUTANEDIOL	110-63-4	1.78655	1.00000	0.68346	4.23278
1-HEXANOL	111-27-3	1.58034	1.00000	0.70297	3.69615
1-OCTANOL	111-87-5	2.25536	0.99996	0.48078	4.23212
ETHYLENE GLYCOL	107-21-1	1.52720	0.99998	0.69328	8.24660
2-METHYL-2-PROPANOL	75-65-0	2.74566	0.76371	0.46554	1.14775
others					
WATER	7732-18-5	0.38720	0.87198	1.96692	5.27106
TETRAHYDROFURAN	109-99-9	0.52904	0.82981	1.12360	-0.60455
ETHYLENE	74-85-1	0.25059	0.85349	1.38986	-3.29106
CYCLOPENTENE	142-29-0	0.58167	0.85909	1.00774	-4.80044
AMMONIA	7664-41-7	0.22737	0.86452	2.33201	4.03062
CARBON DISULFIDE	75-15-0	0.63354	0.89765	0.72757	-0.58303
CHLOROFORM	67-66-3	0.22533	0.83791	1.98744	-4.91516
FLUOROBENZENE	462-06-6	0.61813	0.86561	1.08642	0.28950

V-C-2) Parameters for parametrization strategy 1 (i.e., involving component-specific parameters in combination with the *tc*-PR EoS)

Component-specific parameters (a_1, a_2, a_3, b, c and d) to be used in the below equation for the viscosity estimation are reported in Table V-13.

$$\begin{cases} \ln\left(\frac{D_{\text{self}}}{D_{\text{self}}^{\text{ref}}}\right)_{\text{calc}} = \left[\left(\frac{a_1 + a_2\tilde{s}_{\text{Tv-res}} + a_3\tilde{s}_{\text{Tv-res}}^2}{1 + e^{cX_{\text{ES}}}}\right) + \left(\frac{b}{1 + e^{-cX_{\text{ES}}}}\right)\right] X_{\text{ES}} + d \\ X_{\text{ES}} = -\left(\frac{s_{\text{Tv-res}}}{s_{\text{Tv-res}}^c}\right) - \ln\left(\frac{s_{\text{Tv-res}}}{s_{\text{Tv-res}}^c}\right) \\ D_{\text{self}}^{\text{ref}} = \rho_{\text{N}}^{-1/3}\sqrt{\text{k}_\text{b}T/\text{m}_0} \\ \tilde{s}_{\text{Tv-res}} = \frac{s_{\text{Tv-res}}}{R} \end{cases} \quad \text{(V-6)}$$

The Tv-residual entropy ($s_{\text{Tv-res}}$) and the molecular density (ρ_{N}) were estimated using the *tc*-PR EoS.

Table V-13- Component-specific parameters suitable for the *tc*-PR based model with the corresponding number of experimental data points and MAPE (MAPE = Mean Absolute Percentage Error)

Name	a_1	a_2	a_3	b	c	d	Data number	MAPE
n-alkanes							684	6.92
METHANE	0.318063	0.000100	0.001921	0.712319	0.200000	-0.495170	156	5.23
ETHANE	0.361185	0.023983	0.004326	0.676628	0.229575	-0.548079	56	7.38
PROPANE	0.472876	0.032253	0.004772	0.618974	0.499327	-0.515105	21	7.54
n-BUTANE	0.744906	0.149810	0.017101	0.618974	0.499327	-0.515105	9	10.53
n-PENTANE	0.429863	0.026132	0.005771	0.618974	0.499327	-0.515105	29	6.58
n-HEXANE	0.663685	0.162093	0.024718	0.618974	0.499327	-0.515105	72	3.81
n-HEPTANE	0.560900	0.113567	0.019146	0.618974	0.499327	-0.515105	47	4.25
n-OCTANE	0.622901	0.159137	0.027149	0.618974	0.499327	-0.515105	36	6.56
n-NONANE	0.663041	0.181352	0.029897	0.618974	0.499327	-0.515105	38	6.93
n-DECANE	0.578307	0.147937	0.028322	0.618974	0.499327	-0.515105	40	10.40
n-UNDECANE	0.563773	0.127374	0.023004	0.618974	0.499327	-0.515105	17	5.10
n-DODECANE	0.468069	0.088183	0.020592	0.618974	0.499327	-0.515105	33	8.90
n-TRIDECANE	0.705899	0.195918	0.031496	0.618974	0.499327	-0.515105	18	9.30
n-TETRADECANE	0.474733	0.100437	0.023699	0.618974	0.499327	-0.515105	23	7.89
n-PENTADECANE	0.557900	0.101749	0.016579	0.618974	0.499327	-0.515105	16	12.31
n-HEXADECANE	0.590569	0.174671	0.034448	0.618974	0.499327	-0.515105	31	13.80
n-HEPTADECANE	0.707734	0.169491	0.024209	0.618974	0.499327	-0.515105	14	10.64
n-OCTADECANE	0.508460	0.135621	0.031986	0.618974	0.499327	-0.515105	11	4.97
n-EICOSANE	0.512781	0.150749	0.036220	0.618974	0.499327	-0.515105	6	1.09
n-TETRACOSANE	0.600367	0.193902	0.041060	0.618974	0.499327	-0.515105	11	9.64
branched alkanes							59	8.09
2-METHYLPENTANE	0.447777	0.053911	0.011179	0.618974	0.499327	-0.515105	5	3.95
3-METHYLPENTANE	0.401055	0.013456	0.004807	0.618974	0.499327	-0.515105	8	8.82
2-3-DIMETHYLBUTANE	0.632942	0.132787	0.021320	0.618974	0.499327	-0.515105	13	10.81
2-2-DIMETHYLBUTANE	0.589709	0.107664	0.021022	0.618974	0.499327	-0.515105	25	8.57
2-2-3-TRIMETHYLBUTANE	0.721813	0.179589	0.033670	0.618974	0.499327	-0.515105	8	4.02
cycloalkanes							117	3.76
CYCLOPENTANE	0.583684	0.098777	0.017090	0.618974	0.499327	-0.515105	13	2.59
CYCLOHEXANE	0.568714	0.109342	0.025694	0.618974	0.499327	-0.515105	84	4.15
METHYLCYCLOHEXANE	0.725995	0.194985	0.033003	0.618974	0.499327	-0.515105	5	2.39
CYCLOHEPTANE	0.670073	0.160385	0.035162	0.618974	0.499327	-0.515105	7	4.14
CYCLOOCTANE	0.737448	0.187921	0.034623	0.618974	0.499327	-0.515105	8	2.03
aromatics							250	14.50
BENZENE	0.678271	0.172882	0.028942	0.618974	0.499327	-0.515105	146	2.90
TOLUENE	0.684911	0.193867	0.031641	0.618974	0.499327	-0.515105	76	22.69
o-TERPHENYL	0.056423	0.152592	0.075707	0.618974	0.499327	-0.515105	28	52.78

Continued on next page

Table V-13 – continued from previous page

Name	α_1	α_2	α_3	b	c	d	Data number	MAPE
ethers							10	3.30
DIMETHYL ETHER	0.345100	0.000010	0.001664	0.618974	0.499327	-0.515105	10	3.30
ketones							20	7.36
ACETONE	0.664631	0.130902	0.016823	0.618974	0.499327	-0.515105	20	7.36
permanent gases							357	6.85
NEON	0.718250	0.019555	0.000334	0.638166	0.273426	-0.830012	20	2.77
ARGON	0.356956	0.000100	0.000749	0.707142	0.200000	-0.672319	77	7.62
KRYPTON	0.166693	0.000100	0.004251	0.759171	0.200427	-0.582339	84	6.98
XENON	0.278184	0.000107	0.005872	0.697071	0.612631	-0.992518	26	6.58
CARBON DIOXIDE	0.367923	0.000100	0.004082	0.617613	0.420221	-0.516313	150	6.98
alcohols							223	7.82
METHANOL	0.805845	0.162467	0.018597	0.618974	0.499327	-0.515105	44	7.80
ETHANOL	0.599584	0.065246	0.010102	0.618974	0.499327	-0.515105	55	7.05
1-PROPANOL	0.512509	0.038617	0.009913	0.618974	0.499327	-0.515105	32	5.59
ISOPROPANOL	0.384578	0.013339	0.009992	0.618974	0.499327	-0.515105	16	6.53
1-BUTANOL	0.718439	0.152775	0.024551	0.618974	0.499327	-0.515105	11	7.50
2-PENTANOL	0.299966	-0.029067	0.000000	0.618974	0.499327	-0.515105	9	12.56
3-PENTANOL	0.198532	-0.049182	0.000352	0.618974	0.499327	-0.515105	12	14.32
1-PENTANOL	0.645422	0.117704	0.021843	0.618974	0.499327	-0.515105	22	7.90
1-HEXANOL	0.775523	0.199752	0.034440	0.618974	0.499327	-0.515105	5	1.35
1-OCTANOL	0.570161	0.149098	0.030209	0.618974	0.499327	-0.515105	9	16.37
2-METHYL-2-PROPANOL	0.880434	0.169613	0.020636	0.618974	0.499327	-0.515105	8	4.18
others							454	7.09
WATER	0.362246	0.049333	0.006175	0.771729	2.379275	-0.535812	289	6.96
TETRAHYDROFURAN	0.820939	0.168436	0.017192	0.618974	0.499327	-0.515105	7	5.40
ETHYLENE	0.600107	0.050789	0.004178	0.559184	1.862570	-0.416643	70	7.47
AMMONIA	0.258116	-0.017620	0.000445	0.618974	0.499327	-0.515105	18	4.60
CARBON DISULFIDE	0.635667	0.165409	0.024180	0.618974	0.499327	-0.515105	10	3.59
CHLOROFORM	0.692335	0.141938	0.018350	0.618974	0.499327	-0.515105	51	9.62
FLUOROBENZENE	0.566950	0.132489	0.024358	0.618974	0.499327	-0.515105	9	3.75

V-C-3) Parameters for parametrization strategy 2 (i.e., involving chemical-family specific parameters in com- bination with the *tc*-PR EoS)

V-C-3.1) n-alkane family:

Table V-14 - Chemical-family specific parameters for n-alkanes compounds to be used in the *tc*-PR based model.

Variable	Value
Number of compounds	25
Data number	699
MAPE	8.79
a_1	0.317614
a_2	-0.029067
a_3	-0.000684
b	0.627360
c	0.528488
d	-0.482980

Table V-15 - Prediction of self-diffusion data of n-alkanes using chemical-family specific parameters for the *tc*-PR based model: data number and corresponding MAPE (Mean Absolute Percentage Error).

Name	Data number	MAPE
METHANE	156	5.89
ETHANE	56	11.57
PROPANE	21	10.76
n-BUTANE	9	10.84
n-PENTANE	29	5.40
n-HEXANE	72	4.37
n-HEPTANE	47	5.07
n-OCTANE	36	7.27
n-NONANE	38	7.95
n-DECANE	40	13.40
n-UNDECANE	17	6.42
n-DODECANE	33	11.91
n-TRIDECANE	18	9.34
n-TETRADECANE	23	10.87
n-PENTADECANE	16	12.60
n-HEXADECANE	31	14.66
n-HEPTADECANE	14	11.02
n-OCTADECANE	11	13.65
n-NONADECANE	2	10.97
n-EICOSANE	6	15.67
n-HENEICOSANE	4	21.79
n-TRICOSANE	3	7.27
n-TETRACOSANE	11	24.48
n-HEXACOSANE	3	12.61
n-OCTACOSANE	3	9.77

V-C-3.1) Branched alkane family:

Table V-16 - Chemical-family specific parameters for branched alkanes compounds to be used in the *tc*-PR based model.

Variable	Value
Number of compounds	6
Data number	59
MAPE	22.30
a_1	0.352550
a_2	-0.035768
a_3	-0.000404
b	0.618974
c	0.499326
d	-0.515105

Table V-17 - Prediction of self-diffusion data of branched alkanes using chemical-family specific parameters for the *tc*-PR based model: data number and corresponding MAPE (Mean Absolute Percentage Error).

Name	Data number	MAPE
2-METHYLPENTANE	5	43.83
3-METHYLPENTANE	8	36.62
2-3-DIMETHYLBUTANE	13	17.69
2-2-DIMETHYLBUTANE	25	13.16
2-2-3-TRIMETHYLBUTANE	8	30.53

V-C-3.1) Cycloalkane family:

Table V-18 - Chemical-family specific parameters for cycloalkanes compounds to be used in the *tc*-PR based model.

Variable	Value
Number of compounds	6
Data number	119
MAPE	10.13
a_1	0.204066
a_2	-0.120355
a_3	-0.009952
b	0.618974
c	0.499326
d	-0.515105

Table V-19 - Prediction of self-diffusion data of cycloalkanes using chemical-family specific parameters for the *tc*-PR based model: data number and corresponding MAPE (Mean Absolute Percentage Error).

Name	Data number	MAPE
CYCLOPENTANE	13	30.73
METHYLCYCLOPENTANE	2	42.69
CYCLOHEXANE	84	4.37
METHYLCYCLOHEXANE	5	29.48
CYCLOHEPTANE	7	25.51
CYCLOOCTANE	8	3.52

V-C-3.1) Permanent gas family:

Table V-20 - Chemical-family specific parameters for permanent gases to be used in the *tc*-PR based model.

Variable	Value
Number of compounds	7
Data number	386
MAPE	8.01
a_1	0.342558
a_2	-0.018519
a_3	-0.000228
b	0.660996
c	0.269945
d	-0.551324

Table V-21 - Prediction of self-diffusion data of permanent gases using chemical-family specific parameters for the *tc*-PR based model: data number and corresponding MAPE (Mean Absolute Percentage Error).

Name	Data number	MAPE
NEON	20	14.46
ARGON	77	8.14
KRYPTON	84	5.37
XENON	26	13.21
NITROGEN	13	5.39
CARBON DIOXIDE	150	7.28
CARBON MONOXIDE	16	13.59

VI- Chapitre 3 : La conductivité thermique des corps purs

Ce chapitre a donné lieu à la publication suivante :

Thermal conductivities of pure fluids by combining the entropy-scaling concept with cubic- and SAFT-type equations of state

Aghilas Dehlouz[1,2], Jean-Noël Jaubert[1(*)], Guillaume Galliero[3], Marc Bonnissel[2], Romain Privat[1(*)]

[1] *Université de Lorraine, École Nationale Supérieure des Industries Chimiques, Laboratoire Réactions et Génie des Procédés (UMR CNRS 7274), 1 rue Grandville, 54000 Nancy, France*

[2] *Gaztransport & Technigaz (GTT), 1 route de Versailles, 78470 Saint-Rémy-lès-Chevreuse, France*

[3] *Université de Pau et des Pays de l'Adour, E2S UPPA, CNRS TotalEnergies, LFCR UMR 5150, Pau, France*

Abstract :

The transport properties of a fluid evolve in a complex way with temperature and pressure due to the combination of different phenomena occurring at the microscopic scale. The entropy scaling concept aims at simplifying this complex behaviour into a monovariable relationship between a reduced form of the transport properties and the Tv-residual entropy, a thermodynamic quantity that can be straightforwardly estimated with an equation of state (EoS). In this work, a reformulated version of Rosenfeld's original entropy scaling approach is proposed in order to calculate the thermal conductivities of pure fluids. A specifically developed reduced thermal conductivity expression was correlated to a function of the Tv-residual entropy that was recently proposed by our group to correlate viscosities and self-diffusion coefficients. The involved thermodynamic properties (residual entropies, densities, heat capacities) were estimated with either the *I*-PC-SAFT or the *tc-PR* EoS thus leading to the definition of two different models. Each of them was validated against a large database of around 90,000 experimental thermal conductivities encompassing liquid, gas and supercritical states for 119 chemical species belonging to 11 chemical families such as n-alkanes, alkenes, alcohols, HFC-CFC... For each model, component-specific, chemical-family specific and universal parameters were proposed. Working with the *I*-PC-SAFT and *tc*-PR EoSs, the obtained MAPEs (Mean Absolute Percent Errors) are respectively 3.3% and 3.4% when the model's parameters are taken component-specific, 9.7% and 5.6% when they are selected as chemical-family specific meanwhile they are 11.2% and 9.2% when they are taken universal.

VI-A) Introduction:

Convection and conduction are two mechanisms that allow a fluid to transfer thermal energy within itself when it is under a temperature gradient. In the absence of macroscopic flows, characterizing the convection process, the energy is transferred by conduction due to molecules dynamics at the microscopic scale. According to Fourier's law, the thermal conductivity which characterizes the ability of a material to transfer thermal energy by conduction, is of great interest whenever it's a question of designing industrial processes or products [104]. However, accurate measurement of thermal conductivity is a challenging task because heat transfer most often combines conduction and convection simultaneously. Thus, apart from the transient and the stationary methods to experimentally measure the thermal conductivity, there are several empirical or semi-empirical methods that allow its estimation with an affordable time-efficiency/precision compromise. Among those methods, one can find:

- Empirical correlations [6] that link the thermal conductivity to temperature or density for a given range of fluid conditions
- Cubic equations of state used to take benefit of [105] the observed geometric similitude between the (P,v,T) and the (T, λ,P) plots of a pure fluid if λ designates the thermal conductivity.
- Approaches based on a dimensional analysis [106] that correlate the thermal conductivity of a fluid to its specific properties (e.g. temperature, critical constants, molecular weight …).
- Corresponding-state methods [107] that predict the thermal conductivity of a fluid from the mere knowledge of its critical constants, acentric factor, molecular weight and ideal gas heat capacity.
- The scheme by Assael and Dymond [12] in which the thermal conductivity is defined as a function of the close-packed volume V_0, the temperature and the number of carbon atoms.
- The Friction Theory [108] in which the thermal conductivity is correlated to the residual entropy stemming from an equation of state.
- The entropy scaling approach [2,31,32,42,46,109–114] which relates the reduced transport property (the dimensionless thermal conductivity) to the Tv-residual entropy.

In addition to the above-mentioned approaches, it is worth recalling that the kinetic theory of gases [10], which relates transport properties to the dynamics of binary collisions, remains one of the most physically-sound approaches used today. In particular, it can be used to ensure a correct zero density limit for approaches that estimate a residual transport property rather than the actual property itself like the friction theory [108] or models based on the entropy scaling concept [113]. However, it is only applicable to dilute gas states and suffers from not considering the multiple internal degrees of freedom possessed by polyatomic molecules that strongly impact the thermal conductivities. It is indeed well-acknowledged that a comprehensive understanding of the actual mechanics associated with the different modes of energy transfer in polyatomic molecules requires an understanding of the steps associated with the individual translational, rotational and vibrational contributions for the prediction of thermal conductivity.

Despite considerable efforts to develop and/or extend the scope of the above-mentioned methods, a rigorous theory applicable to all fluid states and all pure compounds regardless of their chemical structure is still missing. We are however convinced that the entropy scaling concept [2] is a remarkably robust concept to model the different transport properties: the dynamic viscosity, the mass diffusion coefficient and the thermal conductivity. The technic is based on the existence of a relationship between the transport properties and the Tv-residual entropy; the latter revealing information about the internal structure of fluids. This concept was originally developed by Rosenfeld through his work on simple fluids. He discovered that the reduced transport properties share a monovariable relationship with the Tv-residual entropy ($s_{\mathrm{Tv-res}}$) regardless of the fluid state (liquid, gas or supercritical). For the sake of clarity, let us recall that reduced transport property refers to a dimensionless number that is the ratio of an actual transport property (e.g., a thermal conductivity) and a reference property having the same units while the Tv-residual entropy refers to the entropy of a pure component in its actual state minus that of the corresponding perfect gas at the same temperature and volume. Since Rosenfeld's pioneering work, several studies investigated this concept to assess its range of applicability and/or to improve it. A literature review on the work conducted by Rosenfeld leads to the following observations:

- The relation between the transport properties, specifically the thermal conductivity, and the Tv-residual entropy is not universal; it depends instead on the considered component.
- A systematic divergence of the transport properties appears at low-density states (it approximately starts for $s_{\mathrm{Tv-res}} > -0.5$).
- After defining an appropriate reference property, it is however possible to maintain a monovariable relationship between the Tv-residual entropy and the transport properties over the entire fluid region.

After reviewing the main advances in the modelling of thermal conductivity through the entropy scaling concept, this study proposes a new approach in which either a SAFT-type or a cubic equation of state [namely the *I*-PC-SAFT[100] and the *translated*[101,102]*-consistent*[51,52] Peng-Robinson (*tc*-PR[5])], are used to correlate the thermal conductivity of a pure fluid whatever its physical state (liquid, gas or supercritical). The presented method was successfully applied to a comprehensive database of experimental thermal conductivities for 119 chemical components and regrouping around 90,000 data points. Component-specific, chemical-family specific and universal versions of the model's parameters are proposed in order to be used according to the availability of the experimental data.

VI-B) Theoretical background:

VI-B-1) Modelling the thermal conductivity of fluids:

While the transport phenomena are mainly governed by microscopic phenomena (molecules translations, collisions…), the transport properties, and the thermal conductivity in particular, relate at the macroscopic scale the concerned flux (e.g. the heat flux) and the corresponding driving force (e.g. the temperature gradient) through a linear relationship (e.g. of the form $\boldsymbol{q} = -\lambda \boldsymbol{\nabla} T$ which is the well-known Fourier's law for the thermal conduction). It is usual to express the thermal conductivity λ as the sum of three independent contributions [115] as:

$$\lambda(\rho, T) = \lambda_0(T) + \Delta\lambda_c(\rho, T) + \Delta\lambda(\rho, T) \qquad (VI-1)$$

Where:

- $\lambda(\rho, T)$ is the thermal conductivity of the real fluid which depends on the temperature T and the density ρ.
- $\lambda_0(T) = \lambda(0, T)$ is the zero-density (or the dilute-gas) contribution which only depends on the temperature. In addition, only the two-body collisions are considered.
- $\Delta\lambda_c(\rho, T)$ represents the critical enhancement contribution resulting from the long-range density fluctuations [116].
- $\Delta\lambda(\rho, T)$ is known as the residual property and represents the contribution of all other effects to the thermal conductivity of the fluid at elevated densities including many-body collisions, molecular-velocity correlations , and collisional transfer [115].

A similar decomposition can be used for the viscosity. Nevertheless, the following significant differences exist between the two transport properties:

- While the viscosity critical enhancement is asymptotic and is restrained to a close region in the vicinity of the critical point, the thermal conductivity enhancement is significant over a substantial range of fluid conditions. It is to be noted that despite the considerable effort provided to model the critical enhancement of the thermal conductivity [117–119], an efficient and broadly applicable theory or model is still lacking. For this reason, this phenomenon was not considered in the present study.
- While viscosity is mainly governed by the transfer of a translational energy, thermal conductivity of polyatomic gases is also considerably affected by vibrational and rotational degrees of freedom. Consequently, and contrary to the case of viscosity, the Chapman-Enskog relation [10], reported in Eq. 2 and derived to estimate $\lambda_0(T)$ of monoatomic gases, is not suited for the estimation of this contribution ($\lambda_0(T)$) when it's up to polyatomic gases.

$$\lambda^{CE} = \frac{75}{64}\sqrt{\frac{k_b T}{m_0 \pi}}\frac{1}{\sigma^2 \Omega^{(2,2)*}} \qquad (VI-2)$$

In Equation VI-2, k_b is the Boltzmann constant, m_0 is the molecular mass, σ and $\Omega^{(2,2)*}$ are the Lennard-Jones characteristic collision diameter and the Lennard-Jones collision integral respectively.

Empirically, Eucken [6,120] proposed to decompose the dilute-gas contribution of the thermal conductivity into two independent parts: a translational contribution (λ_{tr}) and an internal part (λ_{int}) which takes account of the internal energy transferred through rotational and vibrational degrees of freedom (see equations VI-3 and VI-4).

$$\lambda_0 = \lambda_{\mathrm{tr}} + \lambda_{\mathrm{int}} \tag{VI-3}$$

With:

$$\begin{cases} \lambda_{\mathrm{tr}} = \eta \times f_{\mathrm{tr}} \times c_{\mathrm{v,tr}} \\ \lambda_{\mathrm{int}} = \eta \times f_{\mathrm{int}} \times c_{\mathrm{v,int}} \end{cases} \tag{VI-4}$$

Where η is the dynamic viscosity, $c_{\mathrm{v,tr}} = 3R/2$ and $c_{\mathrm{v,int}}$ are the translational and the internal contribution to the specific heat capacity at constant volume c_{v} respectively. They are related as: $c_{\mathrm{v}} = c_{\mathrm{v,tr}} + c_{\mathrm{v,int}}$. The factors f_{int} and f_{tr} are usually fixed to 1 and 5/2 although those values are still open to question. Therefore, some authors such as Chapman and Cowling [10] proposed to modify Eucken's formula assuming that the transport of internal energy is governed by a diffusion mechanism. This assumption led to the introduction of the self-diffusion coefficient D_{self} in the definition of the factor f_{int} ($f_{int} = {}^{\rho D_{self}}/_{\eta}$) thus leading to:

$$\lambda_{\mathrm{int}} = \rho D_{\mathrm{self}} c_{\mathrm{v,int}} \tag{VI-5}$$

Equation (VI-3) can thus be rewritten as:

$$\lambda_0 = \lambda_{\mathrm{tr}} + \rho D_{\mathrm{self}} c_{\mathrm{v,int}} \tag{VI-6}$$

VI-B-2) Key advancements on application of the entropy scaling concept to thermal conductivity:

The entropy scaling concept is based on the relation between the transport properties (reflecting the dynamic behaviour of molecules at the microscopic scale) and the Tv-residual entropy (providing information on the structure of the fluid). Such a quantity can be estimated from an equation of state in a straightforward manner, according to the following expression:

$$\begin{cases} s_{\mathrm{Tv-res}} = s_{\mathrm{real}}(T,v) - s_{\mathrm{perfect\ gas}}(T,v) = -\left(\dfrac{\partial a_{\mathrm{Tv-res}}}{\partial T}\right)_v \\ \qquad with\ :\ a_{\mathrm{Tv-res}} = -\displaystyle\int_{+\infty}^{v} \left[P(T,v) - \frac{RT}{v}\right] dv \end{cases} \tag{VI-7}$$

where $s_{\mathrm{Tv-res}}$ is the Tv-residual entropy, s_{real} is the actual molar entropy of the real fluid (liquid, gas, supercritical), $s_{\mathrm{perfect\ gas}}$ is the perfect-gas entropy, R is the universal gas constant, $a_{\mathrm{Tv-res}}$ is the Tv-residual molar Helmholtz energy, and $P(T,v)$ is the equation of state. The existence of a relation between $s_{\mathrm{Tv-res}}$ and the transport properties was discovered by Rosenfeld during his study of simple theoretical fluids at dense states. He pointed out that the reduced viscosity, self-diffusion coefficient [1] and thermal conductivity [2] can be formulated as functions that only depend on the Tv-residual entropy. In his approach, a transport property is reduced, i.e., is made dimensionless by its division by a temperature and density dependent expression obtained from elementary kinetics analysis. For the case of thermal conductivity, the reduced property is defined as:

$$\tilde{\lambda} = \frac{\lambda_{\text{real}}}{\lambda_{\text{reference}}} = \frac{\lambda_{\text{real}}}{\rho_{\text{N}}^{\frac{2}{3}} k_{\text{b}} \sqrt{k_{\text{b}} T / m_0}} \qquad \text{(VI– 8)}$$

where ρ_N is the molecular density and m_0 is the molecular weight. The actual property (λ_{real}) is thus calculated as the product of a reference property by a Tv-residual entropy depending function:

$$\lambda_{\text{real}} = \lambda_{\text{reference}} \times f(s_{\text{Tv-residual}}) \qquad \text{(VI– 9)}$$

As pointed out by Rosenfeld [2], this approach that combines simplicity and broad applicability is more a semi-quantitative model than a real theory. On one hand, it offers many advantages:

- it involves easily accessible and straightforwardly calculable quantities (the density and the Tv-residual entropy are obtained from an EoS),
- it can be applied to the three transport properties (viscosity, self-diffusion and thermal conductivity).

On the other hand, the application of the concept to real substances suffers of several deficiencies:

- A systematic divergence at low densities
- The non-universality of the function f in equation (VI-9) (each component has a specific form and/or specific parameters characterizing the function f)

In the previously published studies on thermal conductivity, the efforts aimed at extending/improving the validity of the entropy scaling concept focused on the research of a new formulation for the reference property or a correction that counteracts the low-density divergence, improves the universality of the concept and incidentally considers the translational, rotational, vibrational internal degrees of freedom in polyatomic gases. Based on Novak's proposal [33,34] and the success of using the Chapman-Enskog relations [10] as a reference property for viscosity reduction [38,80], Hopp and Gross [32] proposed a new expression for the reference thermal conductivity where i) both the segment diameter sigma and the pair energy parameter were replaced by those of the PCP-SAFT EoS and; ii) the mass of the molecule m_0 is divided by the number of segment m. In order to take account of the rotational and vibrational degrees of freedom in polyatomic gases, Hopp and Gross – in their research for an optimal reference thermal conductivity – have investigated several corrections to the Chapman-Enskog relation. They proposed: $\lambda_{\text{ref}} = \lambda^{CE} + \lambda_{\text{int}}$ and introduced a temperature-dependent correlation for λ_{int}. The latter was restrained to the low-density states using an empirical activation function of the form $e^{-\left(s_{\text{Tv-res}} / s^{\text{c}}_{\text{Tv-res}}\right)}$. Their finding led them to make their model predictive by adding a group contribution method [109]. Although the model allowed accurate results in the prediction of the low-density region of polyatomic molecules, the proposed temperature-dependent correlation for λ_{int} was still not suitable for substances with a small number of internal degrees of freedom (e.g. Xenon, Nitrogen). As an alternative, Hopp et al. [31] proposed to introduce the complete temperature and density dependent self-diffusion coefficient and the constant volume heat capacity in the expression of λ_{int} (see Eq. VI-5). The description of the thermal conductivities of simple gases and diatomic fluids was thus considerably improved but the use of Eq. (VI-5) requires the knowledge of the self-diffusion coefficient.

Most of the studies dealing with the application of the entropy scaling to thermal conductivities concern refrigerants and their mixtures because of their immediate involvement in current heating and cooling systems. In this context, several authors have followed a similar path for the definition of the reference thermal conductivity. As an example, in their study on HFC and HFO, Liu et al.[112] used the Eucken's approach (see Eqs. (VI-3) and (VI-4)) to define the reference thermal conductivity but replaced the translational contribution by the Chapman-Enskog relation reported in Eq. (VI-2) and correlated f_{int} as a temperature-dependent polynomial for each fluid.

In order to predict the thermal conductivities of hydrocarbon mixtures and fuels, Rokni et al. [42,110] proposed to use a pseudo-component technic where the mixture is represented as a homogeneous substance of a single chain-type hydrocarbon. The model is focused on dense states and thus neglects λ_{int} in the mathematical of the reference thermal conductivity (i.e., the thermal conductivty contribution induced by the vibrational and rotational degrees of freedom). The reference property used for the reduction is based on the Chapman-Enskog relation ($\lambda_{\mathrm{ref}} = \lambda_{\mathrm{tr}} = \lambda^{CE}$) while σ and ε are taken as those of the defined pseudo component. In addition, the molecular mass m_0 is divided by the chain number.

Compared to the previously cited approaches, a different pathway was followed by Bell in his investigation of the zero-density limit [81]. As in the isomorph theory [69] where the macroscopic reduction (using $l = \rho_{\mathrm{N}}^{-1/3}$ as the mean intermolecular distance, $v = \sqrt{k_{\mathrm{b}}T/m_0}$ as the mean thermal velocity and $t = \rho_N^{-1/3}\sqrt{m_0/k_bT}$ as the time for a collision to occur) is found to be the adequate reduction for transport properties, he kept Rosenfeld's proposal for $\lambda_{\mathrm{reference}}$ (see Eq. (VI-8)) while subtracting the zero-density value to the actual thermal conductivity. Therefore, in his approach, Bell correlated a residual conductivity to the Tv-residual entropy. In addition, he introduced an empirical correction in the form of $(-\tilde{s}_{Tv-res})^{2/3}$ that multiplies the reduced residual conductivity in order to overcome the low-density divergence. The approach enhanced a better global behaviour and well characterized low-density limit but a significant scatter of experimental data remains for several substances at low densities. Recently, this approach was applied to refrigerant and their mixtures with the consideration of the critical enhancement contribution in the definition of the residual conductivity. The latter contribution was estimated using the Olchowy and Sengers model [117] and the dilute-gas contribution was calculated with REFPROP 10.0. Following Liu et al. proposal's [112], a component specific parameter was used to normalize the T-v-residual entropies values and to collapse the considered experimental data to a single curve.

VI-B-3) A new approach:

Despite all the efforts devoted to improve the entropy scaling concept in the last few years, its optimal formulation is still open to question. As shown in Figure VI-1-A, Rosenfeld's proposal was found to be valid at dense state but shows a diverging behaviour at low density. As pointed by Dzugutov [3], the monovariable relationship observed at dense state ($\tilde{s}_{\mathrm{Tv-res}} < -0.5$) can be ascribed to the strong correlation between the dynamical behaviour of molecules, which is reflected in the transport properties, and the structural relaxations, which are proportional to the

number of accessible configurations per atom evaluated through the exponential of entropy (according to Boltzmann's formula). By increasing with density and thus with the Tv-residual entropy in absolute values, this strong correlation overrides the effect of the reduction and makes it barely needed – at dense states – to correlate the thermal conductivity and the Tv-residual entropy. As the density decreases and as the molecule kinetics plays a more prominent role, more parameters are necessary to correlate the behaviour of the transport properties, a task which should be fulfilled by their reduction (e.g. by introducing the mean velocity of molecules or the intermolecular distance). It is worth recalling that, if the use of the Chapman-Enskog relations to reduce the transport properties (the thermal conductivity in the present case) partially counteracts the low-density divergence by allowing a well-defined limit at the low-density states, this solution is not optimal because:

- The entropy scaling concept has the ambition to be applicable to the entire fluid region while the CE relation was derived to estimate the dilute gas contribution of the thermal conductivity. A direct consequence is the appearance of scattered experimental data for several fluid conditions when the reduced thermal conductivity is plotted against the reduced residual entropy. This phenomenon (scatter of the experimental data at low and moderate densities) is particularly visible with argon in Figure VI-1B. This component was selected as an illustrative example because the CE relation is acknowledged to be a good approximation to describe the thermal conductivity of monoatomic gases.
- This approach requires the knowledge of additional component-specific parameters: the collision diameter and the molecular attraction parameter.
- In the case of the thermal conductivity, the CE relation does not account for the rotational and vibrational degrees of freedom possessed by polyatomic molecules so that a strong scattering of experimental data is observed in Figure VI-1B for methane, ethane and n-hexane at $\tilde{s}_{\mathrm{Tv-res}} > -2$.

Such weaknesses also apply when a residual approach (i.e., when the zero-density contribution is subtracted to the actual transport property) is combined with the entropy scaling concept.

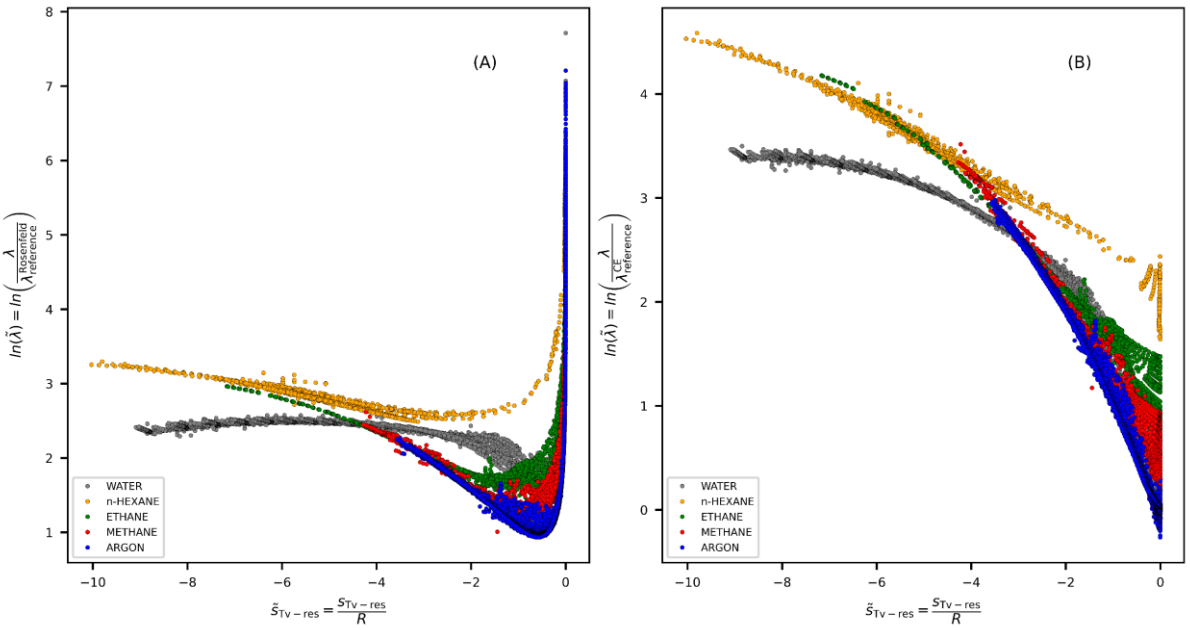

Figure VI-1 – Plot of the experimental reduced thermal conductivity as a function of the reduced Tv-residual entropy. Panel (A): using Rosenfeld's original reduction. Panel (B): using the Chapman-Enskog relation as the reference thermal conductivity (data source: Dortmund Data Bank; the data selection procedure is described in section VI-C).

Based on the results obtained for viscosities of simple fluids at dense states, Rosenfeld [1,2] proposed an exponential form to describe the relation between the reduced transport property and the Tv-residual entropy. This empirical proposal was convenient since the experimental data enhance straight lines in the semi log scale for a large range of dense-fluid conditions. For dilute states, he derived a power law dependence based on Enskog results [2]. Inspired by this finding, a new variable, noted X_{ES}, depending on the Tv-residual entropy was recently introduced by our group [96] in order to gather between a semi-log scale at high-densities and a log-log scale at low densities.

$$X_{\mathrm{ES}} = -\left(\frac{s_{\mathrm{Tv-res}}}{s^{\mathrm{c}}_{\mathrm{Tv-res}}}\right) - \ln\left(\frac{s_{\mathrm{Tv-res}}}{s^{\mathrm{c}}_{\mathrm{Tv-res}}}\right) = -\left(\frac{\tilde{s}_{\mathrm{Tv-res}}}{\tilde{s}^{\mathrm{c}}_{\mathrm{Tv-res}}}\right) - \ln\left(\frac{\tilde{s}_{\mathrm{Tv-res}}}{\tilde{s}^{\mathrm{c}}_{\mathrm{Tv-res}}}\right) \qquad \text{(VI– 10)}$$

In Eq. (VI-10), $s^{\mathrm{c}}_{\mathrm{Tv-res}}$ is the critical value of the reduced molar entropy $\tilde{s}_{\mathrm{Tv-res}}$, the 1st term is dominant in dense-fluid condition while the 2nd term dominates at low density. Remarkably, the X_{ES} variable makes it possible:

- To avoid the low-density divergence and to reach a well-characterized zero-density limit when it is combined with Rosenfeld's macroscopic reduction
- To achieve a quasi-universal behaviour at low densities for both the viscosity and the self-diffusion coefficient

- To obtain more closely packed curves since the $\frac{\tilde{s}_{\mathrm{Tv-res}}}{\tilde{s}^{\mathrm{c}}_{\mathrm{Tv-res}}}$ ratio was found to take similar values for different chemical species and was found to slightly depend on the selected EoS.

Our paper devoted to viscosity [96] underlined that numerical values of $s_{\mathrm{Tv-res}}$ could differ significantly from one EoS to another. Although dividing the Tv-residual entropy by its value at the critical point strongly attenuates this difference, we found necessary to add a temperature-dependent term in the mathematical expression of the X_{ES} variable (see Eq. (VI-11)) when the *tc*-PR EoS is used. This patch, specific to the *tc*-PR EoS and only needed at very high temperatures ($4T_C < T < 8T_C$) was introduced to keep the same mathematical expression of the X_{ES} variable (see Eq. (VI-10)) whatever the EoS: it is indeed enough to select $f_{\mathrm{corr}}(T) = 1$ in Eq. (VI-11) when one works with the *I*-PC-SAFT EoS.

To sum up, for heavy molecules for which the temperature domain $T > 4T_C$ is not of practical interest, a null α value is selected in Eq. (VI-11). In return, for light molecules (having a low T_C) such as Ar, N_2 or Krypton for which experimental thermal conductivities are available at high reduced temperatures ($4T_C < T < 8T_C$) a non-zero coefficient was selected. The influence of this correction is illustrated with Argon in Figure VI-16 of Appendix A.

$$\begin{cases} X^{\mathrm{corrected}}_{\mathrm{ES}-tc-\mathrm{PR}} = -\left(\frac{\tilde{s}_{Tv-res}}{\tilde{s}^{c}_{Tv-res}}\right) - \ln\left(\frac{\tilde{s}_{\mathrm{Tv-res}}}{\tilde{s}^{\mathrm{c}}_{\mathrm{Tv-res}}} \times f_{\mathrm{corr}}(T)\right) \\ f_{\mathrm{corr}}(T) = 1 + \alpha\left(\frac{T - T_{\mathrm{c}}}{T_{\mathrm{c}}}\right)^3 \end{cases} \qquad \text{(VI– 11)}$$

In order to investigate the effect of using the X_{ES} variable to correlate the thermal conductivity, the entropy scaling curves obtained by combining both the X_{ES} variable and successively Ronsenfeld's macroscopic reduction (reported in Eq. (VI-8)) and the Chapman-Enskog relation (reported in Eq. (VI-2)) as the reference thermal conductivity are shown in Figure VI-2 for water, argon, methane, ethane and n-hexane.

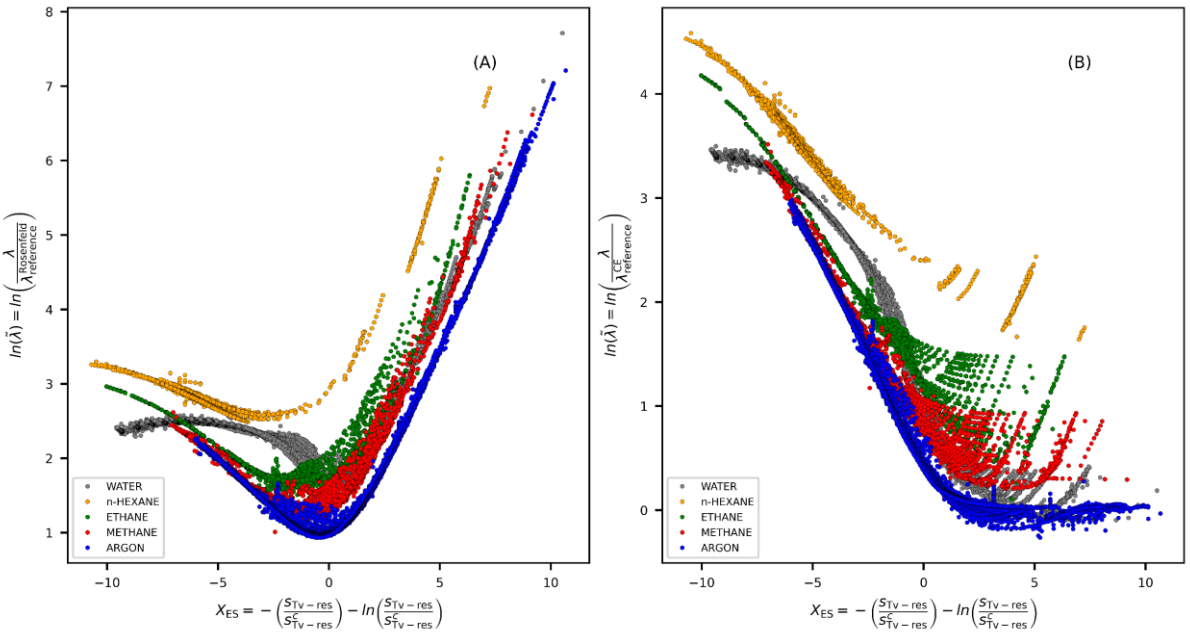

Figure VI-2 - Plot of the experimental reduced thermal conductivity as a function of the proposed X_{ES} variable. Panel (A): using the original Rosenfeld reduction. Panel (B): using the Chapman-Enskog relation as the reference thermal conductivity

Figure VI-2 demonstrates that both reductions return an acceptable scaling at high densities (i.e. $X_{\mathrm{ES}} < 0$). The Chapman-Enskog relation (not corrected to account for the many degrees of freedom possessed by polyatomic molecules) results in a scatter of the experimental data at the low-density conditions (see the case of n-hexane, ethane at $X_{\mathrm{ES}} \geq 0$ in the panel B). For the case of Argon for which the contribution of the vibrational and rotational degrees of freedom to the thermal conductivity is negligible, a horizontal asymptote appears due to the ability of the CE relation to satisfactorily reproduce the thermal conductivity of simple gases at low density and thus making $ln(\tilde{\lambda})$ tend to 0. However, since the CE relation is not suitable for moderately dense gases and/or supercritical states, the dispersion of several experimental data points is visible at $X_{\mathrm{ES}} \geq 0$.

The use of the macroscopic reduction $\lambda_{\mathrm{reference}}^{Rosenfeld}$, as defined in equation 8, also leads to dispersed data for molecules that possess vibrational and rotational degrees of freedom whereas the data collapse on a master curve when the latter degrees of freedom are negligible (see the case of argon at $X_{\mathrm{ES}} \geq 0$ in Figure VI-2-A).

To account for these specific phenomena encountered in polyatomic molecules (e.g. the transfer of vibrational energy during molecules collision) and thus to extend the scope of the entropy scaling concept to such molecules, it was decided in the following to test Eucken's approach along with the Chapman and Cowling assumption (see Eq. (VI-6)) to prospect (i) a corrected macroscopic reduction based on Rosenfeld proposal and (ii) a microscopic corrected reduction based on the Chapman-Enskog relation. Both of the investigated reductions are reported in Table VI-1.

Table VI-1 - Expressions of the reference thermal conductivity, corrected to account for the internal degrees of freedom encountered in polyatomic molecules

Macroscopic corrected reduction	*Microscopic corrected reduction*
$\lambda_{\text{reference}}^{\text{Rosenfeld,intDoF}} = \lambda_{\text{reference}}^{\text{Rosenfeld}} + g(\rho)\rho D_{\text{self,referencce}}^{\text{Rosenfeld}} c_v^{real}$ (VI−12)	$\lambda_{\text{reference}}^{\text{CE,intDoF}} = \lambda_{\text{refernce}}^{\text{CE}} + g(\rho)\rho D_{\text{self,reference}}^{\text{CE}} c_v^{real}$ (VI−13)
Where: $\begin{cases} \lambda_{\text{reference}}^{\text{Rosenfeld}} = \rho_{\text{N}}^{\frac{2}{3}} k_{\text{b}} \sqrt{k_{\text{b}}T/\text{m}_0} \\ D_{\text{self,reference}}^{\text{Rosenfeld}} = \rho_{\text{N}}^{-\frac{1}{3}} \sqrt{k_{\text{b}}T/\text{m}_0} \\ g(\rho) = e^{-\left(\rho/\rho_c\right)} \end{cases}$	Where: $\begin{cases} \lambda_{\text{reference}}^{\text{CE}} = \frac{75}{64}\sqrt{\frac{k_{\text{b}}T}{\text{m}_0\pi}}\frac{1}{\sigma^2\Omega^{(2,2)*}} \\ D_{\text{self,reference}}^{\text{CE}} = \frac{3}{8\rho_{\text{N}}}\sqrt{\frac{k_{\text{b}}T}{\text{m}_0\pi}}\frac{1}{\sigma^2\Omega^{(1,1)*}} \\ g(\rho) = e^{-\left(\rho/\rho_c\right)} \end{cases}$

In Table VI-1, $c_{\text{v}}^{\text{real}}$ is the specific heat capacity at constant volume in (J.mol^{-1}.K^{-1}) defined as $c_{\text{v}}^{\text{real}} = c_{\text{v}}^{\text{residual}} + c_{\text{v}}^{0}$. The residual specific heat capacity at constant volume $c_{\text{v}}^{\text{residual}}$ was obtained from the considered EoS (the *I*-PC-SAFT or the *tc*-PR EoS) while the ideal gas contribution c_{v}^{0} was estimated with the DIPPR correlations. ρ is the molar density in mol.m^{-3} and ρ_{N} is the molecular density in m^{-3}. σ and $\Omega^{(*,*)*}$ are the Lennard-Jones characteristic collision diameter and the Lennard-Jones collision integral respectively. In this paper, the collision integrals $\Omega^{(1,1)*}$ and $\Omega^{(2,2)*}$ were estimated using Neufeld's empirical equation [73] while both the Lennard-Jones characteristic collision diameter (σ) and the molecular attraction parameter (ε) required to estimate $\Omega^{(1,1)*}$ and $\Omega^{(2,2)*}$ were taken from reference [74]. In both of the reductions, the $c_{\text{v}}^{\text{real}}$ is considered rather than c_{v}^{0} in order to ensure a better applicability of the reductions beyond the ideal gas state condition. In addition, it was chosen to neglect the subtraction of the $c_{\text{v,tr}}$ term from the $c_{\text{v}}^{\text{real}}$ since i) the usual fixed value of 3R/2 for $c_{\text{v,tr}}$ is a valid assumption for simple gases at the ideal gas limit only, while these reductions are meant to be used in the entire fluid region; ii) neglecting this constant value has a quantitative impact only, while our goal is a qualitative reproduction of the evolution of the thermal conductivity.

Finally, this choice was confirmed to be more suitable since it allows a more universal behaviour as it is shown in Appendix VI-B. Similarly to what has been proposed by Hopp and Gross[32], the function $g(\rho)$ was introduced in order the correction added to the original Rosenfeld (see Eq. (VI-12)) or Chapman-Enskog (see Eq. (VI-13)) expressions are particularly effective in the low density region. It can be observed in Figure VI-3 that both of the prospected reductions result on a significant improvement compared to the case where the internal degrees of freedom are not accounted (see Figure VI-2). Indeed, while the curves remain closely packed at dense states ($X_{\text{ES}} < 0$), except for the case of water, the experimental data at dilute states ($X_{\text{ES}} \geq 0$) collapse into an oblique asymptote for the case of the macroscopic corrected reduction (panel A) whereas a rough horizontal asymptote appears when the microscopic corrected reduction is used (panel B).

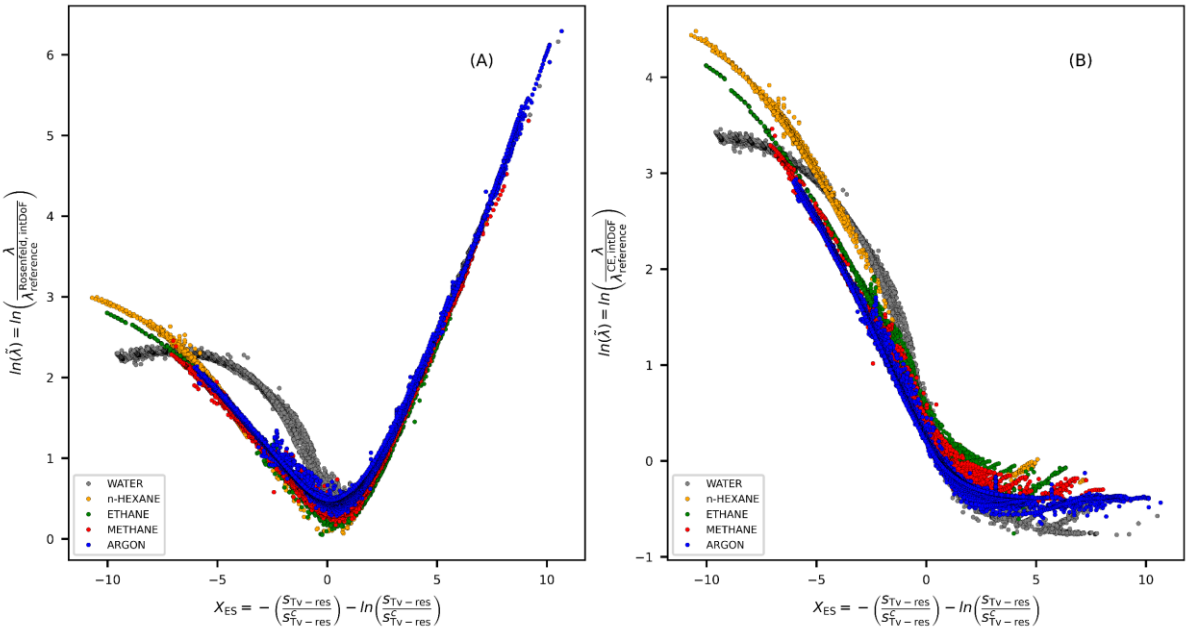

Figure VI-3 - Plot of the experimental reduced thermal conductivity as a function of the X_{ES} variable. Panel (A): using the macroscopic corrected reduction (Eq. (VI-12) in Table VI-1). Panel (B): using the microscopic corrected reduction (Eq. (VI-13) in Table VI-1)

Figure VI-3A clearly shows that by correcting Rosenfeld's reference thermal conductivity by Eq. (VI-12) makes it possible to achieve a satisfying qualitative description of the thermal conductivity along liquid, gas and supercritical states. Indeed, a monovariable relationship between the reduced thermal conductivity and the X_{ES} variable is maintained in the entire fluid region with the enhancement of a quasi-universal oblique asymptote at low-density states, including water. At dense states, although the curves remain closely packed, they exhibit component-specific slopes which can be ascribed to the specificities of the chemical species (e.g. association, shape, chain length …). In conclusion, the macroscopic corrected reduction $\lambda_{\mathrm{reference}}^{\mathrm{Rosenfeld,intDoF}}$, which only involves thermodynamic quantities that can be estimated by an EoS appears as well suited to be combined with the X_{ES} variable.

VI-B-4) Functional form for the calculation of the thermal conductivity of real pure fluids:

Analogously, to what has been observed for the dynamic viscosity, a quasi-common global minimum is obtained in the $\left(X_{\mathrm{ES}}, ln\left(\lambda/\lambda_{\mathrm{reference}}^{\mathrm{Rosenfeld,intDoF}}\right)\right)$ plane at $X_{\mathrm{ES}} \approx 0$ (see Figure VI-3A). As pointed by Rosenfeld and as prospected by bell et al. [63,121] later, this minimum reflects a regime changeover between a liquid-like behaviour (predominated by intermolecular interactions/forces effects) and a gas-like behaviour (predominated by kinetic effects). Following the procedure developed to correlate the viscosities and aimed at capturing the

entropy scaling curve behaviour with a relatively simple fitting function, we adopted a decomposition of the reduced thermal conductivity in a logarithm scale into a dense and a gas parts (see Eq. (VI-14)).

$$\ln\left(\tilde{\lambda}\right)_{\text{calc}} = f_{\text{dense}}(\tilde{s}_{\text{Tv-res}}) \times g_{\text{dense}} + f_{\text{gas}}(\tilde{s}_{\text{Tv-res}}) \times g_{\text{gas}} + d \qquad \text{(VI-14)}$$

In Eq. (VI-14), f_{dense} and f_{gas} are polynomial functions describing the dense-state behaviour (i.e., for $X_{\text{ES}} < 0$; note that the term "dense" concerns both subcritical liquid and supercritical fluids) and the dilute-gas behaviours (i.e., for $X_{\text{ES}} > 0$; note that the term "gas" means both subcritical and supercritical fluids); g_{dense} and g_{gas} are damping factors making f_{dense} dominating in the dense region, and conversely, f_{gas} dominating in the gas region; d is a component-specific constant. For the thermal conductivity, we propose to define the latter quantities as follow:

$$\begin{cases} f_{\text{dense}}(\tilde{s}_{\text{Tv-res}}) = \left(a_1 + a_2 X_{\text{ES}}^{1/3}\right) X_{\text{ES}} \\ g_{\text{dense}} = \dfrac{1}{1 + e^{cX_{\text{ES}}}} \\ f_{\text{gas}}(\tilde{s}_{\text{Tv-res}}) = \left(b_1 + b_2 X_{\text{ES}}^{1/3}\right) X_{\text{ES}} \\ g_{\text{gas}} = \dfrac{1}{1 + e^{-cX_{\text{ES}}}} \end{cases} \qquad \text{(VI-15)}$$

where a_1, a_2, b_1, b_2, c and d are six adjustable parameters. Ultimately, the functional form proposed to calculate the thermal conductivities of a pure fluid is defined as follow:

$$\begin{cases} \ln\left(\dfrac{\lambda}{\lambda_{\text{reference}}^{\text{Rosenfeld,intDoF}}}\right)_{\text{calc}} = \left[\left(\dfrac{a_1 + a_2 X_{\text{ES}}^{1/3}}{1 + e^{cX_{\text{ES}}}}\right) + \left(\dfrac{b_1 + b_2 X_{\text{ES}}^{1/3}}{1 + e^{-cX_{\text{ES}}}}\right)\right] X_{\text{ES}} + d \\ \lambda_{\text{reference}}^{\text{Rosenfeld,intDoF}} = \rho_{\text{N}}^{\frac{2}{3}} k_{\text{b}} \sqrt{k_{\text{b}} T / \text{m}_0} \left[1 + \left(\dfrac{c_{\text{v}}^{\text{real}}}{R}\right) e^{-\left(\rho/\rho_{\text{c}}\right)}\right] \\ X_{\text{ES}} = -\left(\dfrac{\tilde{s}_{\text{Tv-res}}}{\tilde{s}_{\text{Tv-res}}^{\text{c}}}\right) - \ln\left(\dfrac{\tilde{s}_{\text{Tv-res}}}{\tilde{s}_{\text{Tv-res}}^{\text{c}}}\right) \text{ for the } \textit{I}\text{-PC-SAFT EoS} \\ X_{\text{ES}} = -\left(\dfrac{\tilde{s}_{\text{Tv-res}}}{\tilde{s}_{\text{Tv-res}}^{\text{c}}}\right) - \ln\left\{\left(\dfrac{\tilde{s}_{\text{Tv-res}}}{\tilde{s}_{\text{Tv-res}}^{\text{c}}}\right)\left[1 + \alpha\left(\dfrac{T - T_c}{T_c}\right)^3\right]\right\} \text{ for the } \textit{tc}\text{-PR EoS} \end{cases} \qquad \text{(VI-16)}$$

As previously stated, in Eq. (VI-16), the α coefficient is an optional component-specific parameter to be used with the *tc*-PR EoS only and with light components. It enables one to improve thermal conductivity predictions for $4 < T_{\text{r}} < 8$.

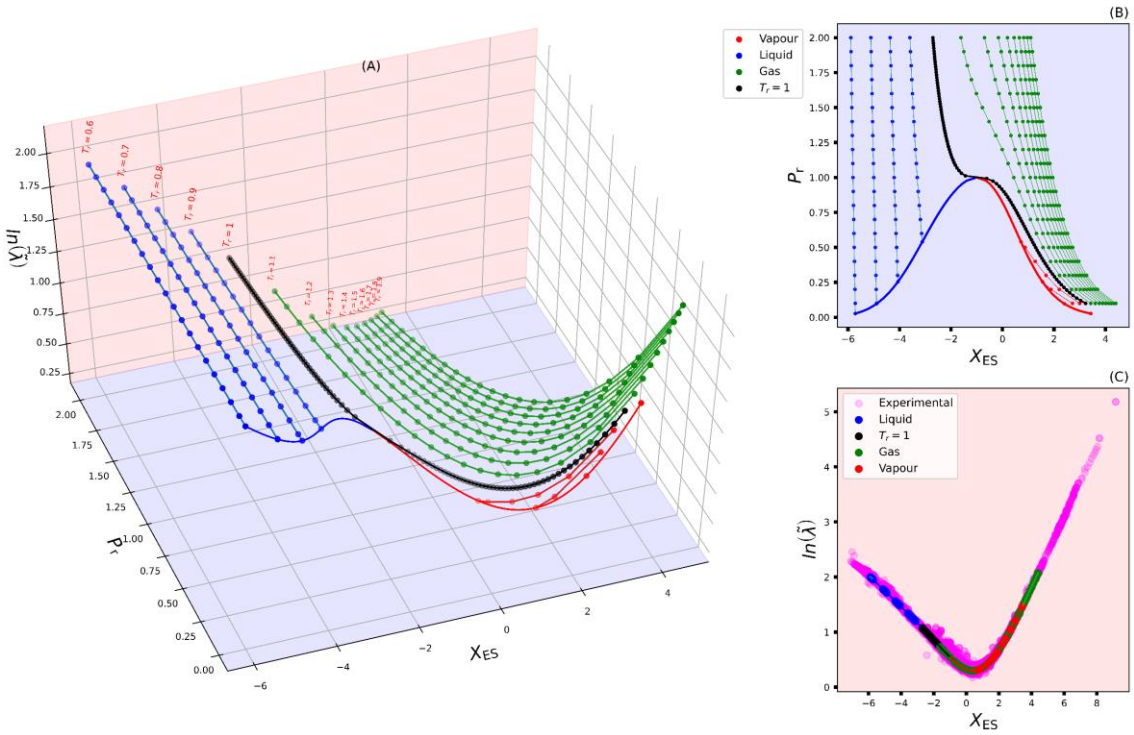

Figure VI-4 - Graphical illustration of the entropy scaling formulation proposed in this paper through the representation of isotherms and saturation curves of pure methane in 3 different diagrams. Reduced temperatures of isotherms range from T_r = 0.6 to 1.9 while reduced pressures span from P_r = 0.1 to 2. Panel (A): representation in the (P_r, $ln(\tilde{\lambda})$, X_{ES}) space as calculated with the *I*-PC-SAFT EoS, Panel (B): representation in the (P_r, X_{ES}) plane as calculated with the *I*-PC-SAFT EoS. Panel (C): representation in the ($ln(\tilde{\lambda})$, X_{ES}) plane of the same isotherms and saturation curves and comparison with the experimental data.

Figure VI-4 shows characteristic vapour−liquid saturation curves as well as series of liquid, gas and supercritical branches of various isotherms for the case of methane modelled with the *I*-PC-SAFT EoS [100]. These curves are represented in the (P_r, Y_{ES}, X_{ES}) space (see Figure VI-4-A), where $P_r = P/P_c$ denotes the reduced pressure and $Y_{ES} = ln(\tilde{\lambda})$ is the natural logarithm of the reduced thermal conductivity, in the (P_r, X_{ES}) plane (see Figure VI-4-B), and in the (Y_{ES}, X_{ES}) plane (see Figure VI-4-C). As shown in Figure VI-4-C, equation (VI-16) achieves an excellent correlation of the reduced thermal conductivity all along the fluid conditions, when the parameters a_1, a_2, b_1, b_2, c and d are adjusted against the experimental data of a given chemical component. Moreover, the combination of the X_{ES} variable and the $\lambda_{reference}^{Rosenfeld,intDoF}$ reference thermal conductivity ensures that the liquid and gas-like states align along a single curve in the ($ln(\tilde{\lambda}), X_{ES}$) plane. According to Eq. (VI-10), the critical point is located at $X_{ES} = -1$.

VI-C) Results & Discussion:

A large database of experimental thermal conductivities was extracted from the commercial Dortmund Data Bank (DDB: http://www.ddbst.com) in order to determine 3 sets of parameters: component-specific, chemical-family specific and universal for each of the two proposed models, i.e., combination of Eq. 16 with the *tc*-PR or the *I*-PC-SAFT EoS. The database encompasses liquid, gas and supercritical data for 119 chemical components belonging to 11 different chemical families. Around 90,000 experimental data points were included for temperatures ranging from 25 to 3600 K, pressures ranging from 10^{-4} to 10^{3} MPa and thermal conductivities spanning from 0.004 to 0.78 $W.m^{-1}.K^{-1}$.
Some experimental data points were removed from the database after application of the following filters:

- Data associated with pressures out of the range $[10^{-3}$ MPa ; 10^{2} MPa] were considered as potentially inaccurate and disregarded,
- The present model does not account for the *critical enhancement of the thermal conductivity*, so that data in the close critical region ($0.95 < T_r < 1.05$ and $0.95 < P_r < 1.05$) were also removed. In addition, data such that $T_r > 8$ were removed when the *tc*-PR EoS was used because they are outside the domain of validity of Eq. (VI-11).

To eliminate out-of-chart data, the absolute deviation $\Delta Y^i = |Y^i_{\text{calc}} - Y^i_{\text{exp}}|$, where $Y = \ln \tilde{\lambda}$, was calculated for each data point of a given component and compared to the corresponding average deviation $\overline{\Delta Y}$ estimated over all the data points for the species under consideration. It was decided to disregard data such that: $\Delta Y^i > \overline{\Delta Y} + 3\sigma$ (where σ denotes the standard deviation). For clarity, it is recalled that ΔY^i is calculated as: $\Delta Y^i = \left|\ln\left(\frac{\lambda_{\text{calc,i}}}{\lambda_{ref}}\right) - \ln\left(\frac{\lambda_{\text{exp},i}}{\lambda_{\text{ref}}}\right)\right|$ where $\lambda_{\text{ref}} = \rho_{\text{N}}^{\frac{2}{3}} k_{\text{b}} \sqrt{k_{\text{b}}T/m_0}\left[1 + \left(\frac{c_{\text{v}}^{\text{real}}}{R}\right) e^{-\left(\rho/\rho_{\text{c}}\right)}\right]$ is calculated by the EoS.
To determine the values of the 6 parameters defined in Equation (VI-16) (a_1, a_2, b_1, b_2, c and d) as well as the α coefficient when necessary (i.e., for light molecules modelled with the *tc*-PR EoS), the following objective function F^{λ}_{obj} was minimized with respect to the 6 (or 7, with α) coefficients:

$$F^{\lambda}_{\text{obj}} = \frac{100}{Nb_{\text{data}}} \sum_{i=1}^{Nb_{\text{data}}} 0.5 \frac{|\lambda_{\text{calc},i} - \lambda_{\text{exp},i}|}{\lambda_{\text{exp},i}} + 0.5 \frac{|Y_{\text{calc},i} - Y_{\text{exp},i}|}{Y_{\text{exp},i}} \qquad \text{(VI– 17)}$$

where Nb_{data} denotes the total number of the considered experimental data and Y is the logarithm of the reduced thermal conductivity.

The minimization of Equation (VI-17) was performed using the Broyden-Fletcher-Goldfarb-Shanno (BFGS) algorithm, a quasi-Newton optimization method. To ensure the robustness of

the optimized parameter sets by avoiding dependence on initial estimates and convergence to local minima, multiple initialization sets were systematically generated using a random process for each compound.

Among all the parameter sets returned by the routine, the optimal one was identified as follows:

- At least half of the initial guesses led to the same optimal parameter set,
- This parameter set was associated with the lowest objective function value and a nearly-zero gradient norm.

Figure VI-5, regroups all the obtained entropy scaling curves with both the EoS for all the chemical components in the $(\ln\tilde{\lambda}, X_{\mathrm{ES}})$ plane. A detailed description of experimental data is provided in Tables VII-1 and VII-25. As pointed above, V-shapes curves are obtained for the thermal conductivity with a quasi-common minimum in the vicinity of $X_{\mathrm{ES}} \approx 0$ and a quasi-universal linear behaviour at low densities. In addition, it is also noticeable that the entropy scaling curves enhance a concave profile at high density.

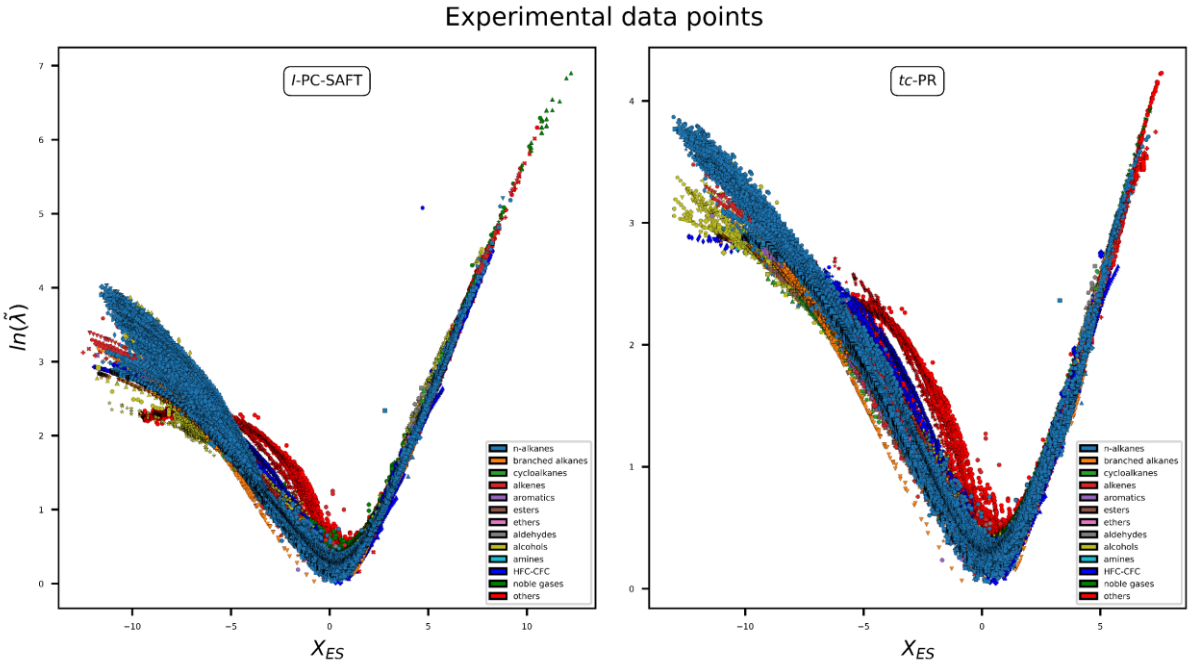

Figure VI-5 – Overview of all the experimental data in the $(ln\,\tilde{\lambda}, X_{ES})$ plane. The thermodynamic properties involved in the calculation were estimated with the *I*-PC-SAFT EoS in the left panel and with *tc*-PR EoS in the right panel. Each colour corresponds to a chemical family and each symbol corresponds to a given chemical specie.

VI-C-1) Component-specific parameters:

The component-specific parameters were obtained by minimizing Eq. (VI-17) against the experimental data of each chemical component. Some important details regarding the strategy used to fit parameters of the model, depending on the availability of experimental data, is detailed in Table VI-2 of appendix VI-C. Figures VI-6 to VI-9 report the obtained results by

combining the *I*-PC-SAFT and the *tc*-PR EoS with their respective component specific values of (a_1, a_2, b_1, b_2, c and d). The latter values are provided for all the considered chemical species in Tables VII-2 and VII-26 of the supporting information file. As observable in such Figures, the functional form proposed in equation 16 is flexible enough to ensure a very accurate description of the thermal conductivity all over the fluid conditions. Regardless the considered EoS, the thermal conductivities are correlated with high accuracy for all the studied chemical species, from non-associating and non-polar species like n-alkanes to more complex molecules like alcohols or water. The detailed MAPEs for several chemical families (calculated by averaging the MAPEs of all the compounds present in a given chemical family) are shown in Figure VI-10; nearly all the deviations are below 3%, regardless of the chemical family considered, which is really excellent.

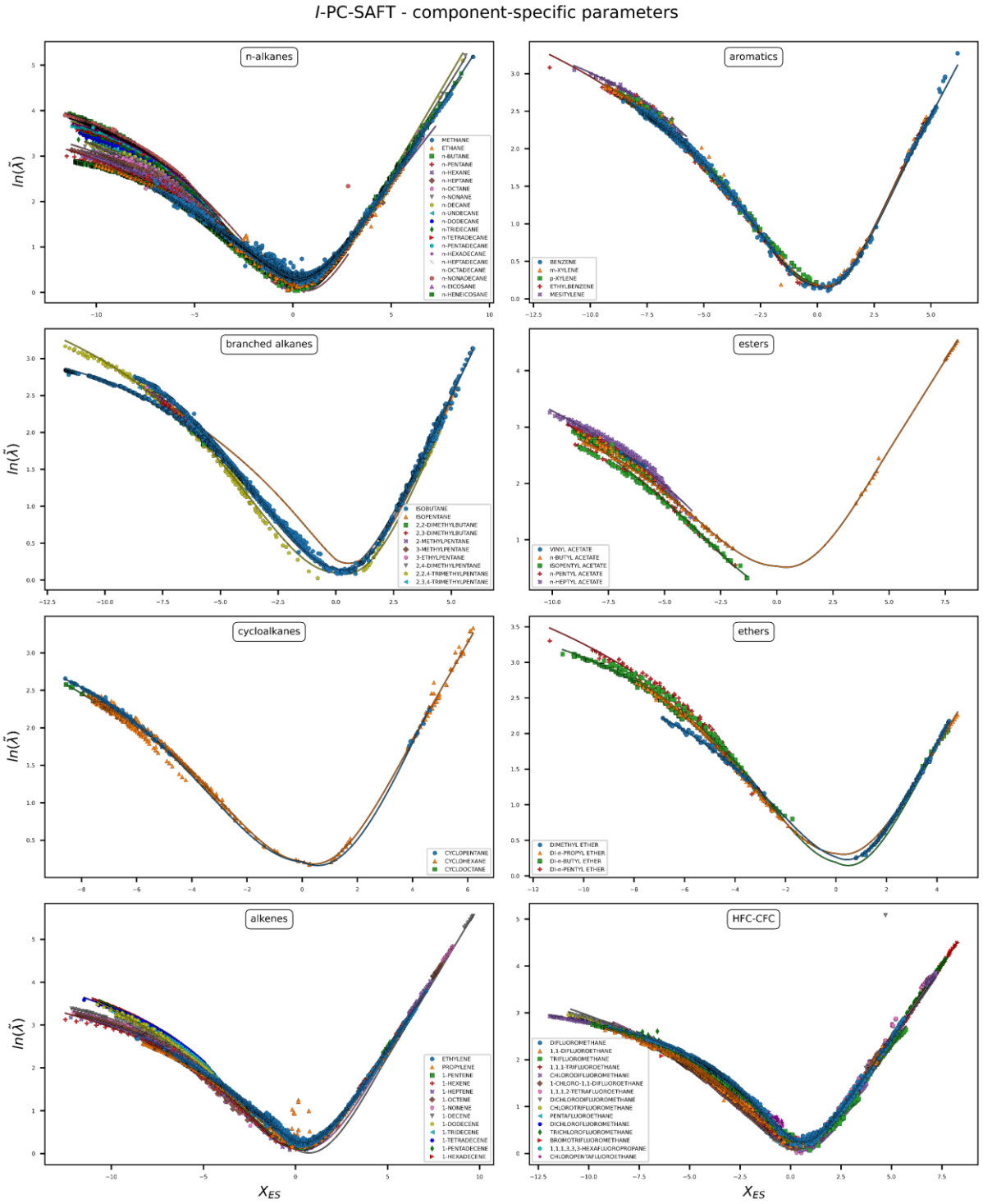

Figure VI-6 - Results of the combination of the component-specific parameters with the *I*-PC-SAFT EoS for modelling the thermal conductivity of n-alkanes, branched alkanes, cycloalkanes, alkenes, aromatics, esters, ethers and HFC-CFCs. Symbols represent the experimental data points; Solid lines represent the calculated values.

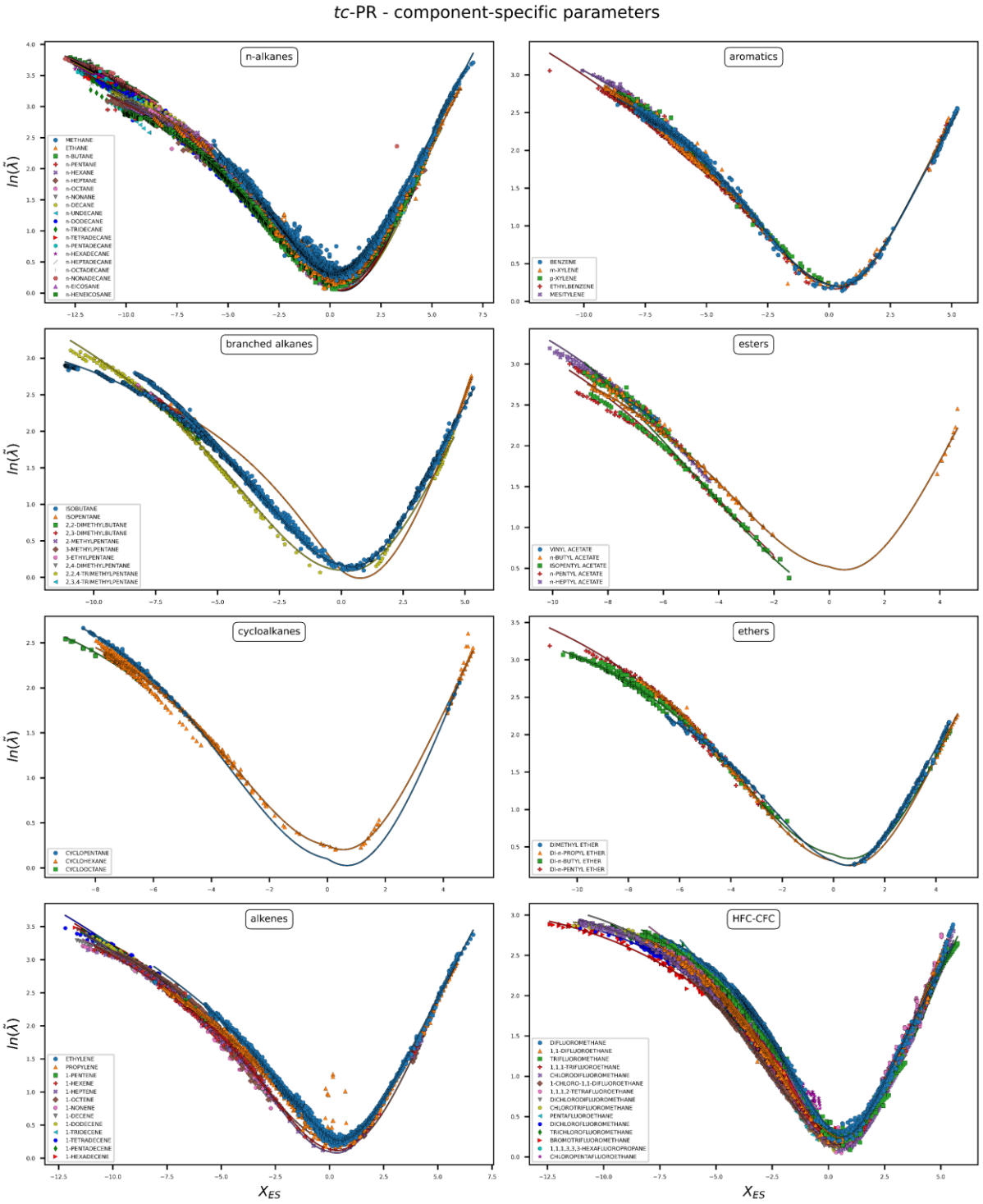

Figure VI-7 - Results of the combination of the component-specific parameters with the *tc*-PR EoS for modelling the thermal conductivity of n-alkanes, branched alkanes, cycloalkanes, alkenes, aromatics, esters, ethers and HFC-CFCs. Symbols represent the experimental data points; Solid lines represent the calculated values.

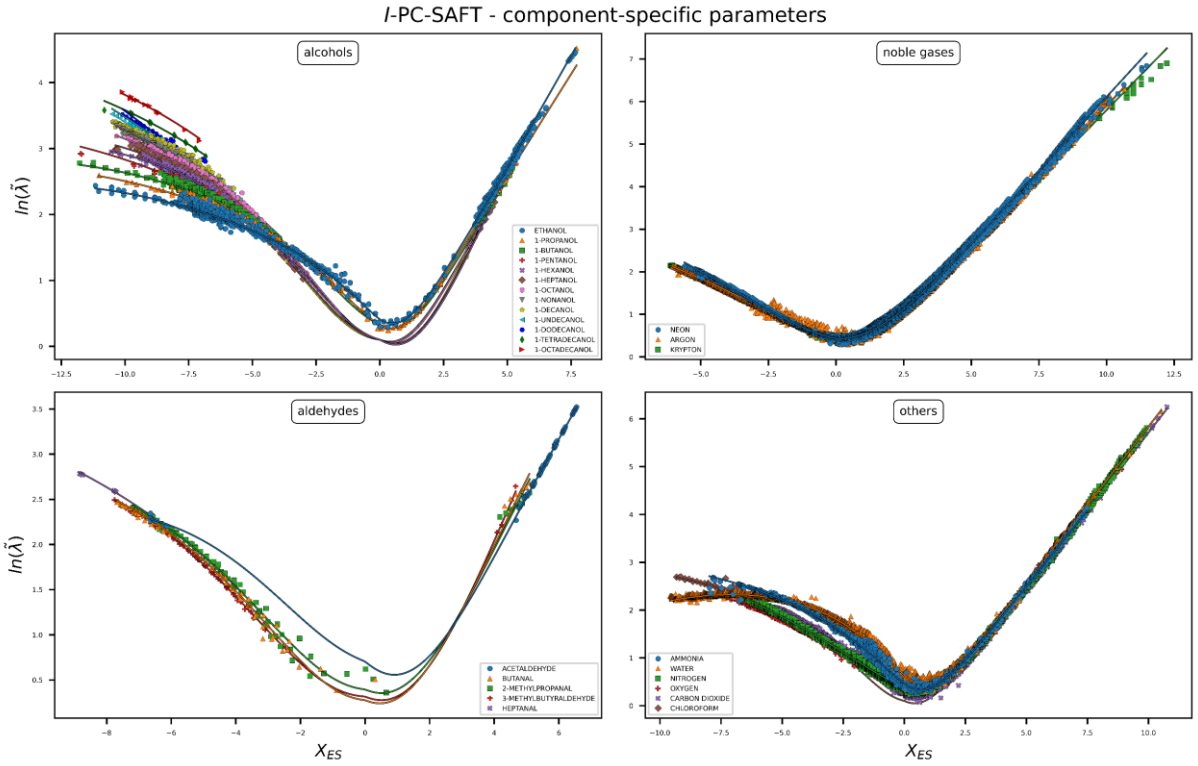

Figure VI-8 - Results of the combination of the component-specific parameters with the *I*-PC-SAFT EoS for modelling the thermal conductivity of alcohols, noble gases, aldehydes and other chemical species. Symbols represent the experimental data points; Solid lines represent the calculated values.

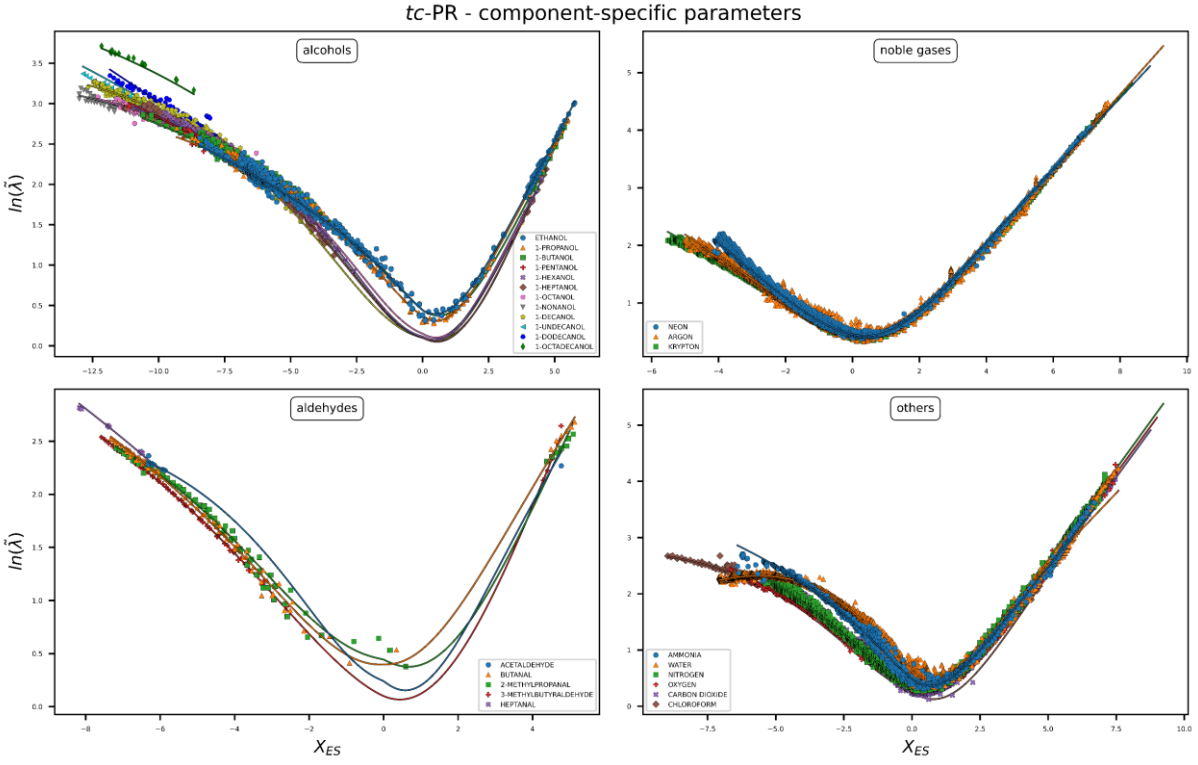

Figure VI-9 - Results of the combination of the component-specific parameters with the *tc*-PR EoS for modelling the thermal conductivity of alcohols, noble gases,

aldehydes and other chemical species. Symbols represent the experimental data points; Solid lines represent the calculated values.

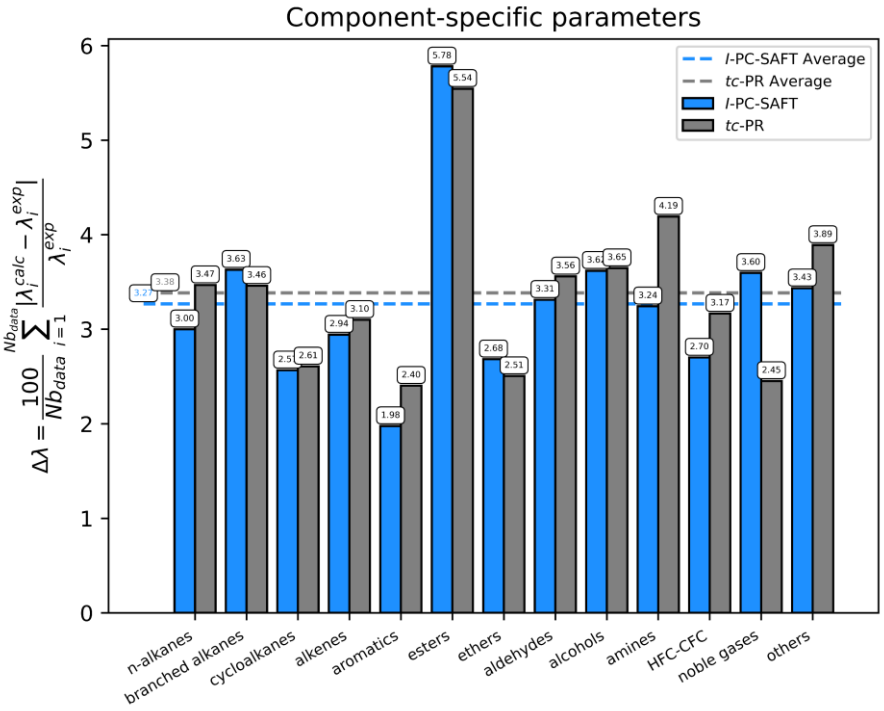

Figure VI-10 – Summary of MAPEs obtained with the *I*-PC-SAFT and the *tc*-PR EoS in combination with the component-specific parameters

VI-C-2) Chemical-family specific parameters:

In order to estimate the thermal conductivity of a particular species for which a limited number or no experimental data at all is available but that is a member of a chemical family (e.g., paraffins, alcohols …) for which many data are available, it was decided to determine chemical-family specific parameters. 10 families including alcohols and amines were selected.

Figures VI-11 and VI-12 show the obtained results for the paraffins (n-alkanes and branched alkanes) and the HFC-CFCs families with both the *I*-PC-SAFT and the *tc*-PR based models. As stated above, in this section, each chemical family was considered as a whole to optimise the (a_1, a_2, b_1, b_2, c and d) parameters. A detailed analysis of such figures makes it possible to draw the following conclusion: regarding the dense states, it has to be noted that although the same reduction of the thermal conductivity is applied to both EoS, a different behaviour of the entropy scaling curves (more or less pronounced curves slopes, different ordering …) is observed. This effect is the consequence of different values of the Tv-residual entropy returned by each EoS and can also be revealed by comparing the curves of chemical components belonging to a same homologous series and calculated with the two considered EoS with component-specific parameters. For illustrative purpose, let us consider the particular cases of the n-alkanes and alcohols molecules. For these 2 chemical families, packed curves were obtained with the *tc*-PR model (see Figure VI-7 and VI-9) whereas component-specific curves stand out at high absolute values of $\tilde{s}_{\mathrm{Tv-res}}$ with the *I*-PC-SAFT model (see Figures VI-6 and

VI-9) what has an immediate impact on the ability of a common set of parameters to describe the thermal conductivity of a whole family. This impact is depicted in Figure VI-13 where the thermal conductivities of paraffins (which encompass n-alkanes and branched-alkanes) and alcohols respectively report a MAPE of 15.6 and 17 % for the *I*-PC-SAFT model while these values are respectively 5.9 and 5.5 % with the *tc*-PR model. For all the other chemical families such as HFC-CFCs, the predicted thermal conductivities agree with the experimental data (see Figures VI-11 and VI-12) and the MAPEs (see Figure VI-13) remain low with the two EoS.

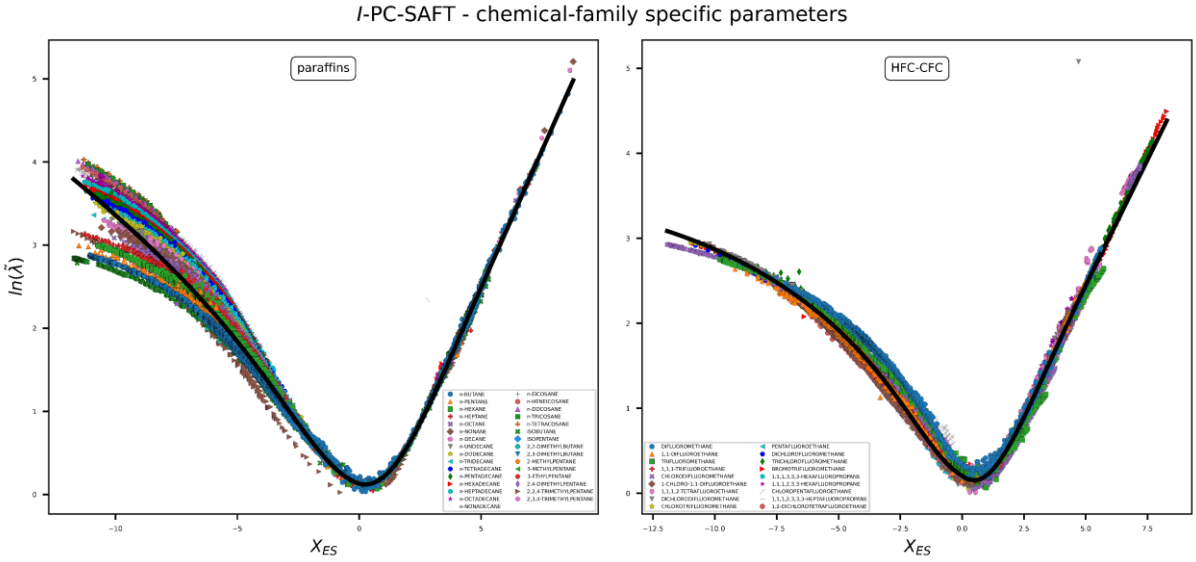

Figure VI-11 - Results of the combination of the chemical-family specific parameters with the *I*-PC-SAFT EoS for modelling the thermal conductivity of paraffins and HFC-CFCs. Symbols represent the experimental data points; Solid lines represent the calculated values.

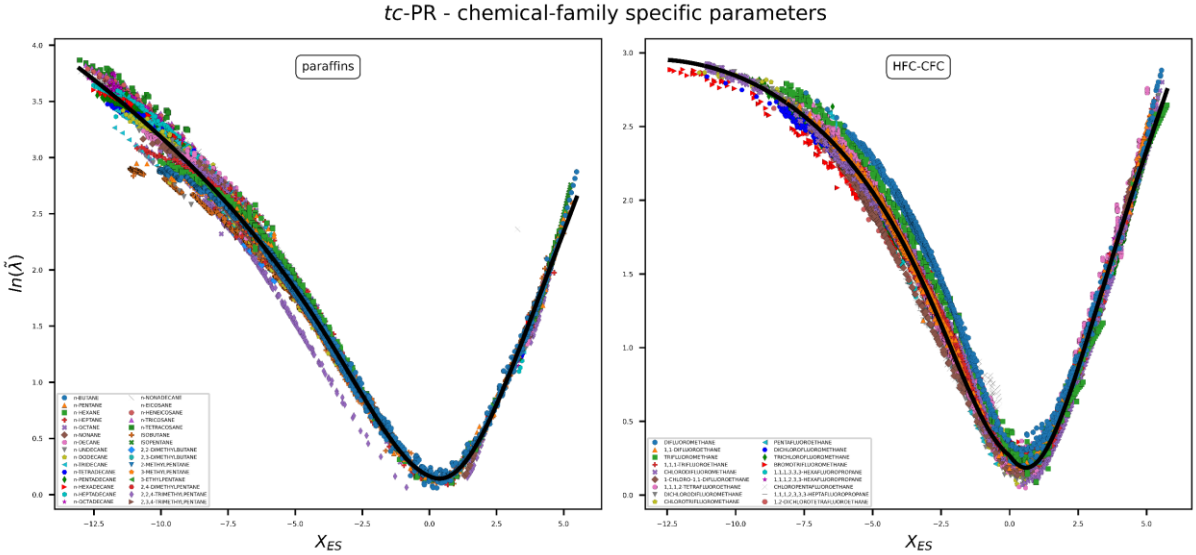

Figure VI-12 - Results of the combination of the chemical-family specific parameters with the *tc*-PR EoS for modelling the thermal conductivity of paraffins and HFC-CFCs. Symbols represent the experimental data points; Solid lines represent the calculated values.

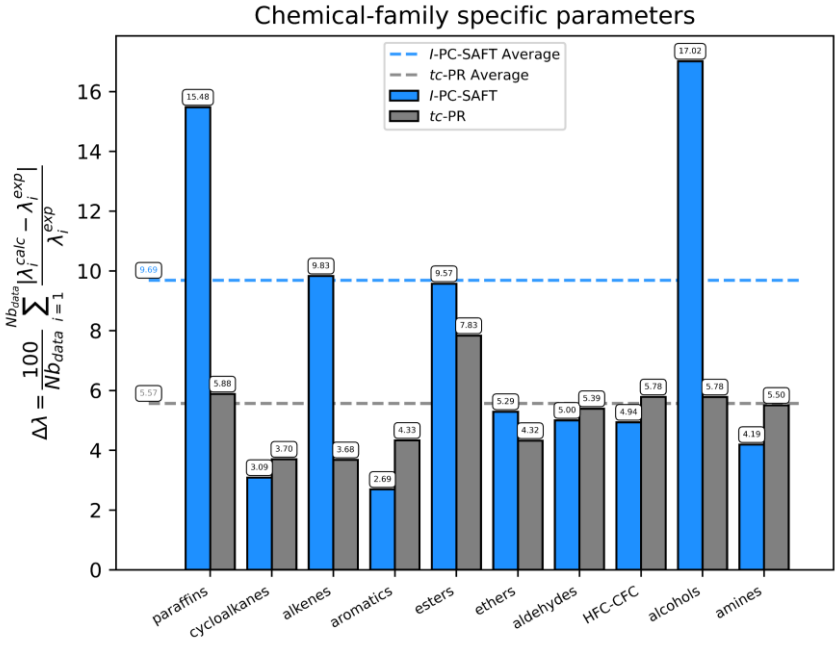

Figure VI-13 - Summary of MAPEs obtained with the *I*-PC-SAFT and the *tc*-PR EoS in combination with the chemical-family specific parameters

VI-C-3) Universal parameters:

As a last resort for chemical species that do not belong to one of the ten chemical families previously defined and for which a limited number of experimental data is available, it was decided to optimise universal parameters considering all the available experimental data as a whole. Some components with a specific behaviour such like water or noble gases which possess a small number of internal degrees of freedom were disregarded in order not to bias the optimisation of these parameters. Such universal parameters (one set per equation) aim to enable a reasonable estimation of the thermal conductivity of a pure fluid knowing its critical temperature Tc, critical pressure Pc, acentric factor and the volume translation c for the *I*-PC-SAFT model or Tc, Pc, c and the three component-specific alpha-function parameters (L,M,N) for the *tc*-PR model. These parameters make it possible:

- to qualitatively reproduce the temperature and pressure dependence of the pure fluid thermal conductivities.
- to predict with a satisfactorily accuracy the thermal conductivities of any chemical species as reported in figure VI-15 where the overall MAPEs are respectively 11.2% and 9.2% for the *I*-PC-SAFT and the *tc*-PR models (more detailed information is provided in Tables VII-23, VII-23, VII-47 and VII-48)
- to get a continuous representation over the three fluid states (liquid, gas and supercritical) for any given component as represented in Figure VI-14

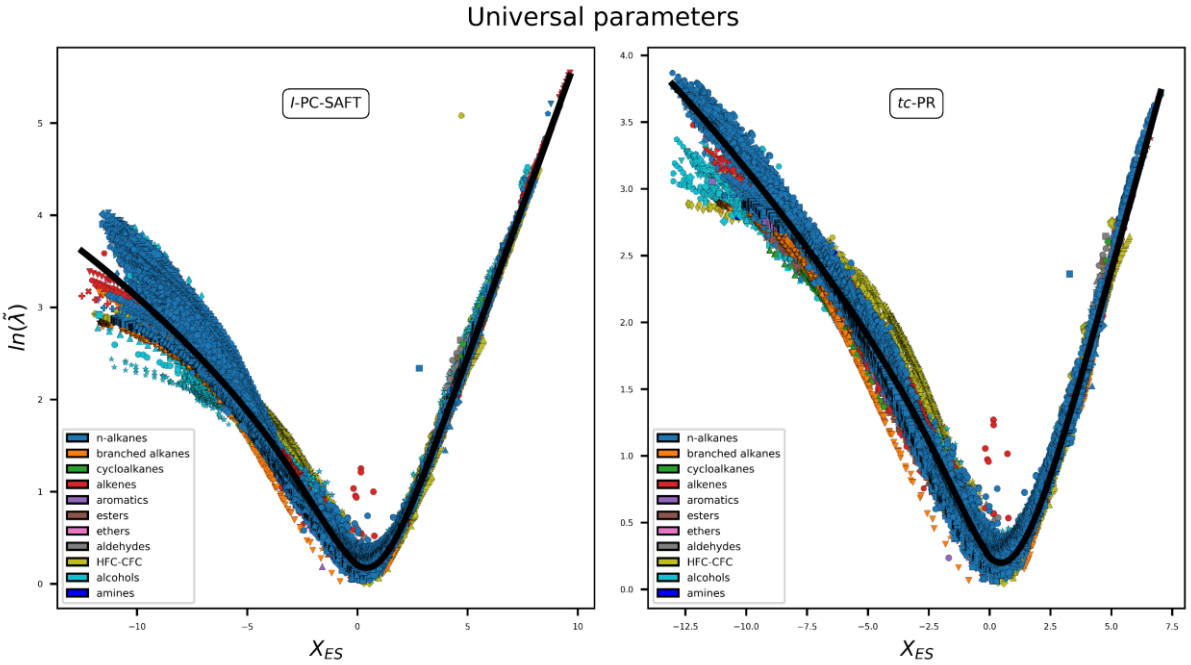

Figure VI-14 - Results of the combination of the universal parameters with the *I*-PC-SAFT and the *tc*-PR EoS for modelling the thermal conductivity. Each colour corresponds to a chemical family and each symbol correspond to a given chemical specie; Solid lines represent the calculated values.

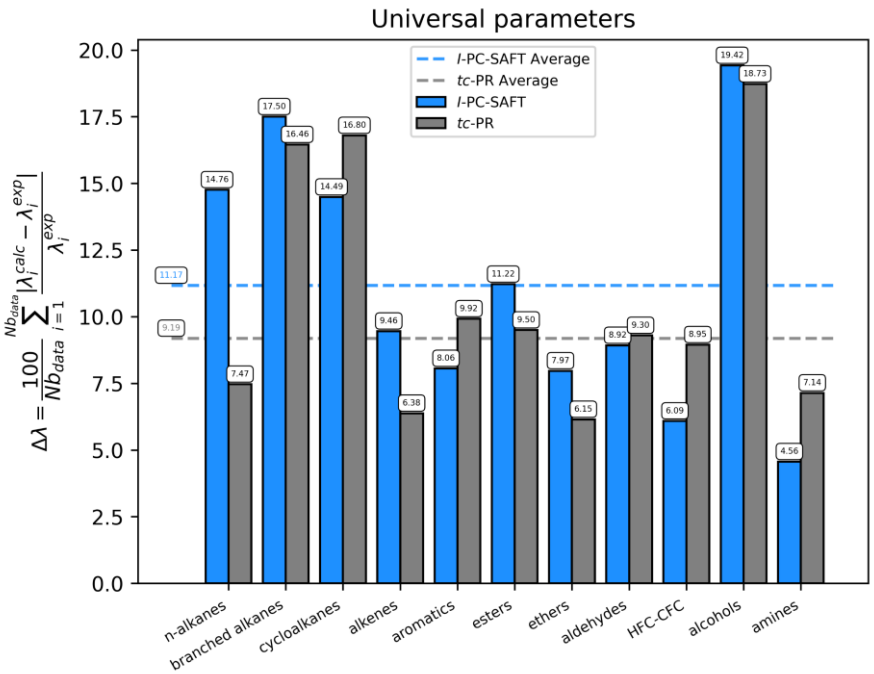

Figure VI-15 - Summary of MAPEs obtained with the *I*-PC-SAFT and the *tc*-PR EoS in combination with the universal parameters.

VI-D) Conclusion:

In this study, a successful combination between a Tv-residual entropy dependent function, which was previously derived for the dynamic viscosity, and a corrected thermal conductivity reference are proposed for the calculation of the thermal conductivities of pure fluids through the entropy scaling concept. Two equations of states (*I*-PC-SAFT and *tc*-PR) were used to predict the residual entropies and other needed properties (densities, heat capacities) thus yielding to the definition of two models. The approach was validated against a large experimental database and made it possible to conclude that:

- using component-dependent parameters, the thermal conductivities of pure fluids could be accurately correlated with an average deviation of only 3% which is really excellent.
- The thermal conductivities can be estimated whatever the fluid state: liquid, gas and supercritical. The critical region has however to be excluded since the critical enhancement of thermal conductivities was not considered in this study.
- The developed equation writes: $\lambda_{\mathrm{real}} = \lambda_{\mathrm{reference}} \times f(s_{\mathrm{Tv-residual}})$. The quantities: $\lambda_{\mathrm{reference}}$ and $f(s_{\mathrm{Tv-residual}})$ are defined in Eq. (VI-16) and can be straightforwardly estimated with an EoS. In this paper, both the *I*-PC-SAFT and *tc*-PR EoS were used.
- To overcome the lack or the unavailability of experimental data of some chemical species, chemical-family specific and universal versions of the model's parameters were optimized in addition to the component-specific ones. The obtained overall MAPEs obtained with the *I*-PC-SAFT and the *tc*-PR EoS are respectively 9.7% and 5.6 % when the parameters are taken chemical-family specific and 11.2% and 9.2% when they are taken universal which is accurate enough for industrial applications.

As this approached involves only macroscopic thermodynamic quantities, accessible via an equation of state, it is believed that it can be straightforwardly extended to mixtures.

VI-E) Appendix:

VI-E-1) Graphical illustration of the effect of the *tc*-PR specific patch to correlate the thermal conductivity at high temperatures

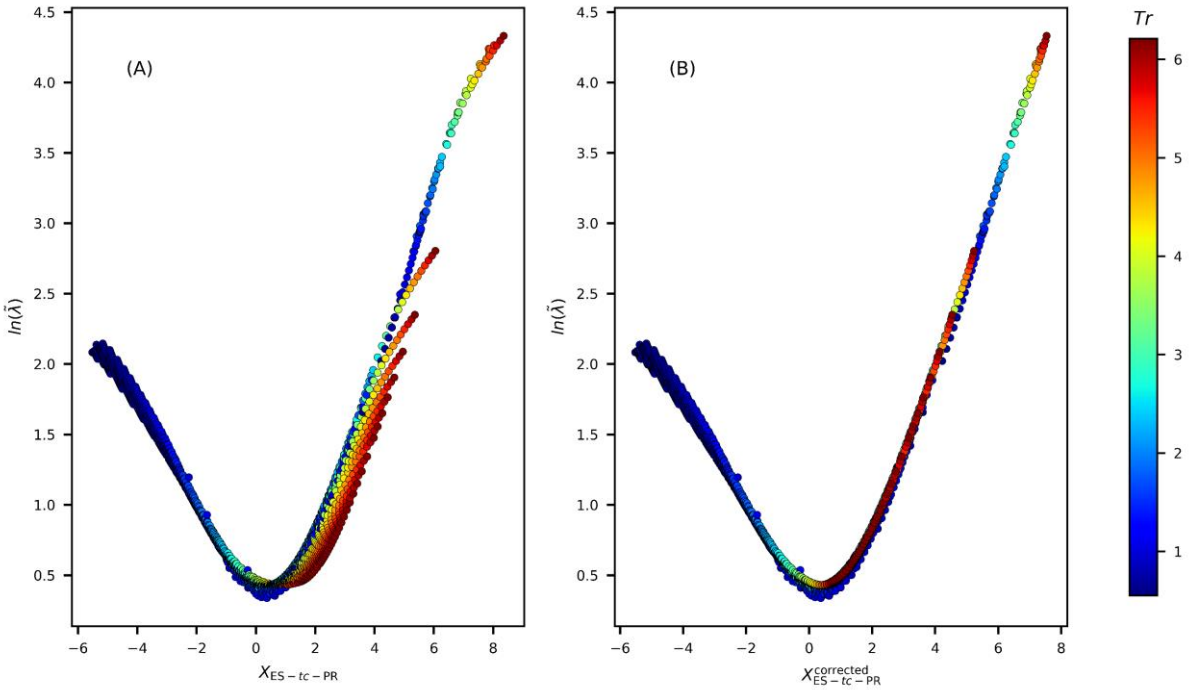

Figure VI-16 - Comparison between the non-corrected version of the X_{ES} variable (Panel A) defined in Eq. (VI-10) and the corrected version (Panel B) given in Eq. (VI-11) in combination with the *tc*-PR Eos for the case of Krypton

VI-E-2) Comparison between the use of the total specific heat capacity at constant volume and its contribution due to vibrational and rotational internal degrees of freedom in the definition of the reference thermal conductivity

Figure VI-17 reports a comparison between the entropy scaling curves obtained by considering $c_{\mathrm{v}}^{\mathrm{real}}$ (Panel A) and in Panel B, $c_{\mathrm{v,int}} = c_{\mathrm{v}}^{\mathrm{real}} - c_{\mathrm{v,tr}}$ (with $c_{\mathrm{v,tr}} = 3R/2$) for the definition of the reference thermal conductivity reported in Eq. (VI-12) of Table VI-1. As pointed out in section II.C, this figure shows that a more universal behaviour is achieved by considering the total specific heat capacity $c_{\mathrm{v}}^{\mathrm{real}}$ of the real fluid while the qualitative aspect of the curves is only slightly influenced by this choice. In Panel B, it can be observed that simple molecules like Argon for which $c_{\mathrm{v}}^{\mathrm{real}} \to c_{\mathrm{v,tr}} = 3R/2$ and thus $c_{\mathrm{v,int}} \to 0$, enhance higher reduced thermal conductivities (y-coordinates) at low densities ($X_{\mathrm{ES}} \geq 0$) than other molecules, such like n-hexane, for which $c_{\mathrm{v,int}} > 0$. Therefore, considering $c_{\mathrm{v,int}}$ rather than $c_{\mathrm{v}}^{\mathrm{real}}$ will induce the up-

shifting of entropy scaling curves for molecules with negligible degrees of freedom like monoatomic and simple gases.

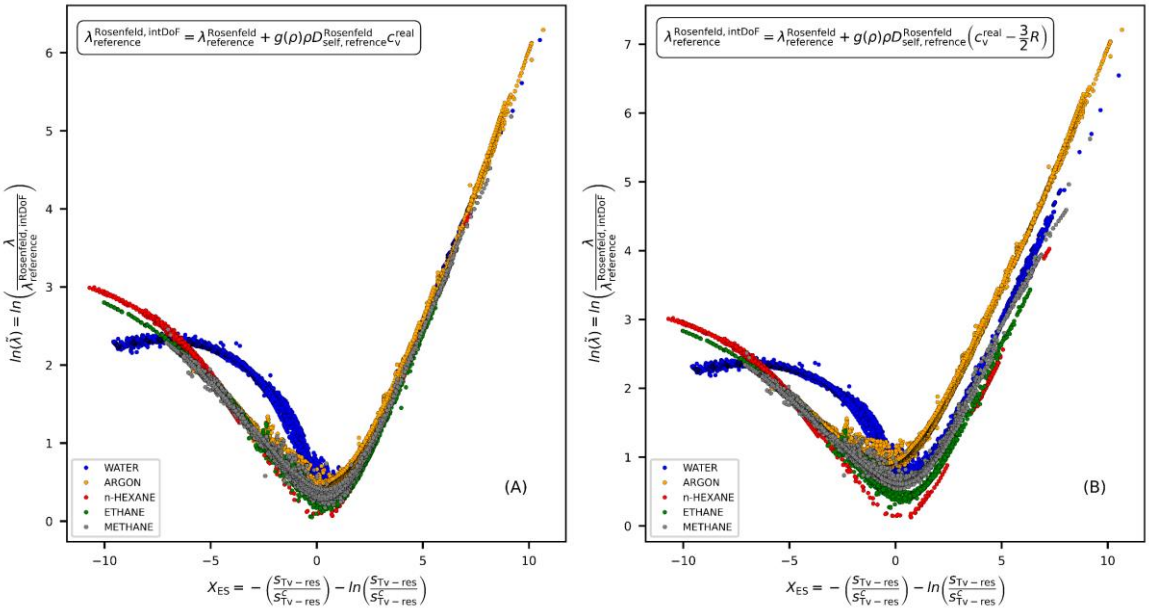

Figure VI-17 – Comparison between consideration of the total specific heat capacity at constant volume (Panel A) and its contribution due to vibrational and rotational degrees of freedom (Panel B) in the definition of the reference thermal conductivity reported in Eq. (VI-12) of Table VI-1. The thermodynamic quantities are generated by the *I*-PC-SAFT EoS.

VI-E-3) Optimisation strategy for the model's parameters:

In order to ensure the most meaningful parameters values, especially at low density states where a quasi-universal behaviour is observed (see Figure VI-5), the optimization procedure is as follows:

- Universal parameters were obtained considering the many components reported in figures VI-14 and VI-15.
- Chemical-family specific parameters were optimized considering each family as a whole. b_1, b_2, c and d parameters were fixed to the universal values when the number of the available experimental data points at the low-density states ($X_{ES}>0$) is less than 3 for the entire family.
- Finally, component-specific parameters are optimized according to Table VI-2

Table VI-2 - Strategy of fitting component-specific parameters depending on the availability of experimental data

Number of experimental data points at dense state	**Number of experimental data points at dilute state**	**Values of the a_1 and a_2 parameters**	**Values of the b_1, b_2, c and d parameters**
$\boldsymbol{Nb_{data}(X_{ES} < 0) \geq 5}$	$Nb_{data}(X_{ES} \geq 0) > 3$	Specific to the chemical component	Specific to the chemical component
	$Nb_{data}(X_{ES} \geq 0) < 3$		Fixed to the chemical-family values (fixed to the universal values when non-available)
$\boldsymbol{Nb_{data}(X_{ES} < 0) < 5}$	Component-specific parameters not ascertained.		

VII- Complément d'information du chapitre 3

Supporting information:

Thermal conductivities of pure fluids by combining the entropy-scaling concept with cubic- and SAFT-type equations of state

Aghilas Dehlouz[1,2], Jean-Noël Jaubert[1(*)], Guillaume Galliero[3], Marc Bonnissel[2], Romain Privat[1(*)]

[1] *Université de Lorraine, École Nationale Supérieure des Industries Chimiques, Laboratoire Réactions et Génie des Procédés (UMR CNRS 7274), 1 rue Grandville, 54000 Nancy, France*

[2] *Gaztransport & Technigaz (GTT), 1 route de Versailles, 78470 Saint-Rémy-lès-Chevreuse, France*

[3] *Université de Pau et des Pays de l'Adour, E2S UPPA, CNRS TotalEnergies, LFCR UMR 5150, Pau, France*

VII-A) *I*-PC-SAFT based model

VII-A-1) Equation of state parameters and viscosity experimental data informations

PC-SAFT is a well-known equation of state, extensively described in the literature. For more information, the reader is referred to the original publication by Gross and Sadowski[82]. The difference between the PC-SAFT and the *I*-PC-SAFT model lies in (1) the way used to estimate the 3 molecular input parameters for a given non-associating compound (m, σ, ε), (2) the application of a Peneloux volume translation to the EoS.

More precisely, the 3 molecular parameters are constrained to exactly reproduce the experimental critical temperature and pressure and the vapor-pressure datum at a reduced temperature equal to 0.7. To do so, the following correlations were used:

$$\begin{cases} \mathrm{m}_i \approx 0.5959\,\omega_{i,exp}^2 + 7.5437\omega_{i,exp} + 0.9729 \\ \varepsilon_i/\mathrm{k_b} \approx T_{\mathrm{c},i,\mathrm{exp}}/(4.7968\cdot 10^{-6}\mathrm{m}_i^5 - 3.0895\cdot 10^{-4}\mathrm{m}_i^4 + 7.8649\cdot 10^{-3}\mathrm{m}_i^3 - 0.10215\mathrm{m}_i^2 + 0.75358\mathrm{m}_i + 0.63659) \\ \sigma_i \approx \left[\varepsilon_i/\mathrm{k_b}\cdot\frac{\mathrm{k_b}}{P_{\mathrm{c},i,\mathrm{exp}}}10^{(1.6345\cdot 10^{-7}\mathrm{m}_i^6 - 1.1346\cdot 10^{-5}\mathrm{m}_i^5 + 3.1389\cdot 10^{-4}\mathrm{m}_i^4 - 4.4618\cdot 10^{-3}\mathrm{m}_i^3 + 3.6282\cdot 10^{-2}\mathrm{m}_i^2 - 022498\mathrm{m}_i + 0.77655)}\right]^{1/3} \end{cases} \quad (\mathrm{VII}-1)$$

The application of a volume translation requires the knowledge of a component-dependent *c* parameter. It was determined in order to exactly reproduce the experimental saturated liquid molar volume at a reduced temperature of 0.8:

$$c = v_{\mathrm{liq}}^{\mathrm{sat,u-EoS}}(T_{\mathrm{r}} = 0.8) - v_{\mathrm{liq,exp}}^{\mathrm{sat}}(T_{\mathrm{r}} = 0.8) \quad (\mathrm{VII}-2)$$

Where $v_{\mathrm{liq}}^{\mathrm{sat,u-EoS}}(T_{\mathrm{r}} = 0.8)$ is the molar volume calculated with the original (untranslated) EoS at $T_{\mathrm{r}} = 0.8$.

More details are available in the original paper introducing the *I*-PC-SAFT model[48]. The *I*-PC-SAFT parameters used in this study are reported in Table VII-1.

Table VII-1 - *I*-PC-SAFT EoS parameters and experimental thermal conductivity data informations

		EoS parameters				Experimental data informations					
Name	CAS	m -	σ $\AA$	$/k_b$ K	$c * 10^3$ m^3/mol	$T_{min}\,K$	$T_{max}\,K$	P_{min} MPa	P_{max} MPa	λ_{min} $W.m^{-1}.K^{-1}$	λ_{max} $W.m^{-1}.K^{-1}$
n-alkanes											
METHANE	74-82-8	1.0577	3.6335	145.557	0.0001	98.9	773.1	0.0025	95.9000	0.0121	0.2875
ETHANE	74-84-0	1.74901	3.47261	181.204	0.0032	111.7	800.6	0.0500	99.0000	0.0084	0.2687
n-BUTANE	106-97-8	2.51623	3.72001	211.407	0.0125	135.8	768.1	0.0010	70.1000	0.0122	0.1889
n-PENTANE	109-66-0	2.9127	3.80047	218.694	0.0195	146.3	623.6	0.0500	98.0660	0.0166	0.1725
n-HEXANE	110-54-3	3.30037	3.86477	224.08	0.0270	183.2	728.8	0.0030	99.2000	0.0157	0.1639
n-HEPTANE	142-82-5	3.67922	3.91767	228.209	0.0342	183.2	700.0	0.0025	98.0000	0.0124	0.1634
n-OCTANE	111-65-9	4.0762	3.95828	230.949	0.0422	223.2	640.0	0.0027	96.0000	0.0124	0.1617
n-NONANE	111-84-2	4.4271	4.00172	234.238	0.0493	223.2	700.0	0.0002	98.0000	0.0097	0.1655
n-DECANE	124-18-5	4.82084	4.02795	236.136	0.0568	243.2	680.0	0.0002	74.9100	0.0104	0.1581
n-UNDECANE	1120-21-4	5.12925	4.07999	239.194	0.0660	284.6	680.0	0.0980	98.0665	0.0228	0.1595
n-DODECANE	112-40-3	5.50599	4.09659	240.655	0.0729	273.1	680.0	0.0980	96.0000	0.0248	0.1722
n-TRIDECANE	629-50-5	5.84391	4.14076	242.269	0.0841	290.0	677.6	0.0980	98.0665	0.0253	0.1606
n-TETRADECANE	629-59-4	6.0562	4.20981	246.012	0.0971	280.0	677.7	0.0915	50.0000	0.0256	0.1532
n-PENTADECANE	629-62-9	6.41709	4.2206	247.01	0.1037	286.1	677.7	0.0980	49.0330	0.0266	0.1608
n-HEXADECANE	544-76-3	6.67775	4.25727	249.329	0.1107	294.8	693.1	0.0972	49.0333	0.0279	0.1555
n-HEPTADECANE	629-78-7	7.11917	4.22813	249.246	0.1128	302.1	693.1	0.0980	49.0333	0.0258	0.1582
n-OCTADECANE	593-45-3	7.47364	4.23565	249.618	0.1194	301.2	693.1	0.0980	49.0333	0.0282	0.1700
n-NONADECANE	629-92-5	7.82356	4.2398	250.213	0.1247	313.1	693.1	0.0981	49.0333	0.0960	0.1625
n-EICOSANE	112-95-8	8.29483	4.20835	249.693	0.1213	315.0	610.0	0.1000	50.0000	0.0930	0.1623
n-HENEICOSANE	629-94-7	8.5998	4.22042	250.647	0.1292	333.1	473.1	0.1000	49.1010	0.1150	0.1623
n-DOCOSANE	629-97-0	8.86315	4.24425	251.658	0.1371	333.1	473.1	0.1000	49.1010	0.1177	0.1649
n-TRICOSANE	638-67-5	9.33691	4.21456	251.347	0.1356	353.1	473.1	0.1000	49.1010	0.1195	0.1627
n-TETRACOSANE	646-31-1	9.73329	4.20453	251.398	0.1366	335.4	473.1	0.1000	49.1010	0.1258	0.1651
branched alkanes											
ISOBUTANE	75-28-5	2.38849	3.78831	207.777	0.0115	115.6	630.8	0.0070	99.0000	0.0090	0.1885
ISOPENTANE	78-78-4	2.72976	3.85923	220.615	0.0165	250.0	700.0	0.1000	80.8000	0.0168	0.1334
2,2-DIMETHYLBUTANE	75-83-2	2.77755	4.02794	232.508	0.0171	257.5	320.3	0.1000	0.1013	0.0871	0.1055
2,3-DIMETHYLBUTANE	79-29-8	2.89521	3.97732	233.416	0.0198	256.8	361.1	0.1000	97.5000	0.0940	0.1336
2-METHYLPENTANE	107-83-5	3.12767	3.90878	224.726	0.0221	256.6	329.1	0.1000	0.1013	0.0956	0.1182
3-METHYLPENTANE	96-14-0	3.05811	3.92458	230.038	0.0231	256.7	329.3	0.1000	0.1013	0.0970	0.1196
3-ETHYLPENTANE	617-78-7	3.3614	3.98054	236.849	0.0271	257.3	331.9	0.1000	0.1013	0.1029	0.1253
2,4-DIMETHYLPENTANE	108-08-7	3.30809	4.0227	229.245	0.0286	256.6	355.1	0.0500	0.1013	0.0186	0.1138
2,2,4-TRIMETHYLPENTANE	540-84-1	3.31755	4.16748	239.547	0.0292	190.0	620.0	0.0500	97.6000	0.0177	0.1495
2,3,4-TRIMETHYLPENTANE	565-75-3	3.41042	4.09852	246.683	0.0303	259.1	332.4	0.1013	0.1013	0.0955	0.1127
cycloalkanes											

Continued on next page

Table VII-1 – continued from previous page

Name	CAS	m -	σ Å	$/k_b$ K	$c * 10^3$ m^3/mol	T_{min} K	T_{max} K	P_{min} MPa	P_{max} MPa	λ_{min} $W.m^{-1}.K^{-1}$	λ_{max} $W.m^{-1}.K^{-1}$
CYCLOPENTANE	287-92-3	2.47558	3.75741	256.389	0.0139	223.2	454.4	0.0500	99.5000	0.0146	0.1628
CYCLOHEXANE	110-82-7	2.57692	3.93344	272.395	0.0152	280.8	633.1	0.0103	99.1000	0.0120	0.1446
CYCLOOCTANE	292-64-8	2.91927	4.14912	301.043	0.0233	288.7	398.1	0.1000	0.1013	0.1069	0.1205
alkenes											
ETHYLENE	74-85-1	1.6482	3.41383	172.685	0.0026	112.2	750.0	0.0340	97.0000	0.0097	0.2537
PROPYLENE	115-07-1	2.03793	3.56538	200.642	0.0063	180.0	639.9	0.0500	60.0000	0.0120	0.2017
1-BUTENE	106-98-9	2.39595	3.69567	213.423	0.0111	223.2	297.1	0.1000	0.1013	0.0159	0.1536
1-PENTENE	109-67-1	2.80199	3.77011	220.139	0.0167	257.4	370.6	0.0330	0.1013	0.0142	0.1284
1-HEXENE	592-41-6	3.17425	3.83408	226.151	0.0222	143.2	623.1	0.0123	98.0000	0.0130	0.1660
1-HEPTENE	592-76-7	3.62973	3.84822	228.247	0.0273	163.2	677.6	0.0024	98.0000	0.0116	0.1610
1-OCTENE	111-66-0	4.0173	3.88808	231.485	0.0328	200.0	573.1	0.0010	97.6800	0.0107	0.1677
1-NONENE	124-11-8	4.37319	3.93983	234.685	0.0402	209.2	677.6	0.0005	98.0000	0.0098	0.1596
1-DECENE	872-05-9	4.72488	3.98774	237.365	0.0484	218.7	677.6	0.0001	98.0000	0.0091	0.1596
1-DODECENE	112-41-4	5.3878	4.08086	242.017	0.0673	278.8	677.6	0.0980	98.0000	0.0785	0.1722
1-TRIDECENE	2437-56-1	5.76092	4.10936	243.281	0.0767	307.8	677.6	0.0980	49.0000	0.0834	0.1445
1-TETRADECENE	1120-36-1	6.11674	4.13887	244.562	0.0870	273.1	677.6	0.0980	98.0000	0.0868	0.1580
1-PENTADECENE	13360-61-7	6.37683	4.14935	247.471	0.0836	307.8	677.6	0.0980	49.0000	0.0902	0.1498
1-HEXADECENE	629-73-2	6.73512	4.16202	248.371	0.0902	307.8	677.6	0.0980	49.0000	0.0920	0.1520
aromatics											
BENZENE	71-43-2	2.59421	3.71133	275.605	0.0151	248.2	681.5	0.0248	99.0000	0.0157	0.1758
m-XYLENE	108-38-3	3.4982	3.83078	265.958	0.0326	258.2	698.9	0.0980	98.0665	0.0210	0.1583
p-XYLENE	106-42-3	3.4617	3.85493	266.746	0.0332	287.3	701.4	0.0980	98.0665	0.0638	0.1488
ETHYLBENZENE	100-41-4	3.31766	3.88181	271.854	0.0292	193.2	683.4	0.0980	99.4000	0.0209	0.1552
MESITYLENE	108-67-8	4.0682	3.81367	258.999	0.0394	233.2	453.1	0.0980	99.7000	0.1056	0.1587
esters											
VINYL ACETATE	108-05-4	3.69372	3.41496	218.966	0.0307	296.2	340.1	0.1000	0.1013	0.1365	0.1549
n-BUTYL ACETATE	123-86-4	4.39448	3.59226	227.28	0.0322	273.0	624.0	0.0010	96.0000	0.0097	0.1670
ISOPENTYL ACETATE	123-92-2	4.79042	3.62822	224.546	0.0356	273.0	624.5	0.0980	49.0000	0.0583	0.1440
n-PENTYL ACETATE	628-63-7	4.46172	3.75548	235.665	0.0408	273.0	621.5	0.0980	96.0000	0.0647	0.1638
n-HEPTYL ACETATE	112-06-1	5.65343	3.69206	231.019	0.0414	300.2	621.8	0.0980	98.0000	0.0875	0.1682
ethers											
DIMETHYL ETHER	115-10-6	2.51666	3.24729	198.949	0.0083	234.0	387.7	0.1446	30.6000	0.0135	0.1709
DI-n-PROPYL ETHER	111-43-3	3.83168	3.70975	220.622	0.0239	293.0	653.0	0.0980	49.0000	0.0200	0.1540
DI-n-BUTYL ETHER	142-96-1	4.4607	3.87277	229.477	0.0384	223.2	677.1	0.0980	96.0000	0.0233	0.1590
DI-n-PENTYL ETHER	693-65-2	5.70995	3.78253	224.872	0.0451	223.2	668.2	0.0980	49.0000	0.0780	0.1521
aldehydes											
ACETALDEHYDE	75-07-0	2.99801	3.17297	214.263	0.0206	273.1	399.1	0.0119	0.1010	0.0105	0.2005
BUTANAL	123-72-8	3.15421	3.53111	241.692	0.0230	273.1	628.1	0.1000	50.0810	0.0370	0.1640

Continued on next page

Table VII-1 – continued from previous page

Name	CAS	m -	σ Å	$/k_b$ K	$c * 10^3$ m^3/mol	T_{min} K	T_{max} K	P_{min} MPa	P_{max} MPa	λ_{min} $W.m^{-1}.K^{-1}$	λ_{max} $W.m^{-1}.K^{-1}$
2-METHYLPROPANAL	78-84-2	3.77964	3.31985	211.932	0.0237	305.2	625.1	0.1000	50.0810	0.0310	0.1550
3-METHYLBUTYRALDEHYDE	590-86-3	3.93688	3.4223	223.52	0.0201	301.6	557.6	0.1010	50.0810	0.0310	0.1490
HEPTANAL	111-71-7	4.12557	3.74553	250.649	0.0326	279.1	406.1	0.1000	0.1000	0.1137	0.1435
alcohols											
ETHANOL	64-17-5	6.06069	2.41836	182.427	0.0171	190.8	678.5	0.0035	98.0661	0.0171	0.2198
1-PROPANOL	71-23-8	5.87288	2.63227	192.371	0.0171	200.0	675.8	0.0025	60.0000	0.0171	0.1829
1-BUTANOL	71-36-3	5.60376	2.87407	204.791	0.0194	193.2	718.9	0.0980	98.0000	0.0244	0.1881
1-PENTANOL	71-41-0	5.49323	3.06448	215.25	0.0224	201.7	560.0	0.1000	60.0000	0.1173	0.1691
1-HEXANOL	111-27-3	5.36018	3.26659	225.525	0.0288	235.6	602.0	0.1000	60.0000	0.0271	0.1809
1-HEPTANOL	111-70-6	5.38889	3.42028	232.867	0.0244	246.8	675.5	0.0980	98.0000	0.0257	0.1873
1-OCTANOL	111-87-5	5.45109	3.56005	239.341	0.0367	257.2	628.1	0.1000	50.0000	0.0250	0.1814
1-NONANOL	143-08-8	5.56917	3.67874	244.479	0.0491	273.1	623.5	0.1000	49.0500	0.0290	0.1893
1-DECANOL	112-30-1	5.7579	3.77158	248.081	0.0531	273.1	623.0	0.0980	98.0000	0.0243	0.1900
1-UNDECANOL	112-42-5	5.8954	3.87226	251.955	0.0603	301.6	621.1	0.1013	49.0500	0.0960	0.1926
1-DODECANOL	112-53-8	6.16047	3.93338	253.817	0.0702	308.6	624.4	0.1000	50.0000	0.0883	0.1854
1-TETRADECANOL	112-72-1	6.67277	4.0467	257.074	0.0850	290.0	452.6	0.1000	0.1013	0.1472	0.1696
1-OCTADECANOL	112-92-5	7.65199	4.24227	262.084	0.1255	337.1	473.1	0.1000	0.1013	0.1497	0.1826
amines											
METHYLAMINE	74-89-5	3.14535	2.75453	193.715	0.0110	293.1	403.1	2.0000	50.0000	0.1400	0.2720
n-BUTYLAMINE	109-73-9	3.51929	3.43663	228.722	0.0184	273.1	323.1	0.1013	0.1013	0.1541	0.1659
DIETHYLAMINE	109-89-7	3.32069	3.57629	218.67	0.0234	273.1	422.1	0.1000	0.1013	0.0250	0.1754
n-PENTYLAMINE	110-58-7	4.13555	3.45949	224.169	0.0245	223.2	323.1	0.1013	0.1013	0.1522	0.1716
DI-n-PROPYLAMINE	142-84-7	4.47707	3.49432	215.796	0.0182	223.2	323.1	0.1013	0.1013	0.1224	0.1538
n-HEXYLAMINE	111-26-2	4.54125	3.53019	227.974	0.0303	273.1	373.1	0.1013	0.1013	0.1428	0.1570
n-OCTYLAMINE	111-86-4	5.44828	3.604	230.096	0.0376	298.1	423.1	0.1013	0.1013	0.1342	0.1503
n-DECYLAMINE	2016-57-1	6.2505	3.66948	233.126	0.0494	298.1	448.1	0.1013	0.1013	0.1347	0.1503
HFC-CFC											
DIFLUOROMETHANE	75-10-5	3.11199	2.81359	158.941	0.0149	153.2	465.6	0.0960	50.0000	0.0096	0.2436
1,1-DIFLUOROETHANE	75-37-6	3.09574	3.15939	175.251	0.0189	163.2	463.0	0.0309	55.0000	0.0107	0.1712
TRIFLUOROMETHANE	75-46-7	3.01086	2.86827	137.23	0.0124	118.7	473.1	0.1000	60.0000	0.0103	0.1947
1,1,1-TRIFLUOROETHANE	420-46-2	2.98968	3.27705	159.225	0.0189	233.2	499.0	0.1013	50.0000	0.0096	0.1121
CHLORODIFLUOROMETHANE	75-45-6	2.66318	3.18061	178.941	0.0107	114.0	514.3	0.0098	60.0000	0.0066	0.1750
1-CHLORO-1,1-DIFLUOROETHANE	75-68-3	2.75137	3.48938	195.907	0.0151	193.2	504.6	0.0156	69.5827	0.0109	0.1264
1,1,1,2-TETRAFLUOROETHANE	811-97-2	3.50128	3.09804	161.233	0.0168	169.9	533.0	0.0048	70.0060	0.0081	0.1456
DICHLORODIFLUOROMETHANE	75-71-8	2.35936	3.57957	197.271	0.0086	124.4	600.0	0.0300	60.0000	0.0084	0.1347
CHLOROTRIFLUOROMETHANE	75-72-9	2.29771	3.40327	156.714	0.0067	92.5	451.9	0.0980	60.0000	0.0095	0.1401
PENTAFLUOROETHANE	354-33-6	3.33167	3.17152	149.142	0.0132	187.4	513.2	0.0310	69.8630	0.0085	0.1236
DICHLOROFLUOROMETHANE	75-43-4	2.55216	3.40426	223.099	0.0107	148.2	473.1	0.1000	60.0000	0.0082	0.1594

Continued on next page

Table VII-1 – continued from previous page

Name	CAS	m -	σ $\AA$	$/k_b$ K	$c * 10^3$ m^3/mol	T_{min} K	T_{max} K	P_{min} MPa	P_{max} MPa	λ_{min} $W.m^{-1}.K^{-1}$	λ_{max} $W.m^{-1}.K^{-1}$
TRICHLOROFLUOROMETHANE	75-69-4	2.4333	3.7056	237.998	0.0101	168.2	523.1	0.0041	60.0000	0.0070	0.1304
BROMOTRIFLUOROMETHANE	75-63-8	2.28781	3.51621	176.876	0.0079	105.2	435.8	0.0029	58.9400	0.0083	0.1173
1,1,1,3,3,3-HEXAFLUOROPROPANE	690-39-1	4.00387	3.24822	162.751	0.0170	252.6	374.6	0.0310	30.0000	0.0110	0.0973
1,1,1,2,3,3-HEXAFLUOROPROPANE	431-63-0	3.83209	3.27771	171.46	0.0171	281.2	333.8	0.0480	0.5150	0.0132	0.0171
CHLOROPENTAFLUOROETHANE	76-15-3	2.91198	3.53216	164.446	0.0106	173.2	443.0	0.1000	60.0000	0.0096	0.1047
1,1,1,2,3,3,3-HEPTAFLUOROPROPANE	431-89-0	3.72471	3.38323	157.584	0.0185	259.3	344.2	0.0360	2.9380	0.0103	0.0609
1,2-DICHLOROTETRAFLUOROETHANE	76-14-2	2.91691	3.69685	194.896	0.0144	183.2	423.1	0.1000	75.0500	0.0099	0.0962
noble gases											
NEON	7440-01-9	0.666762	3.43647	39.3203	0.0025	25.0	2800.0	0.0012	99.1759	0.0078	0.2110
ARGON	7440-37-1	0.952492	3.44081	120.823	-0.0003	86.6	3600.0	0.0013	98.6000	0.0059	0.1532
KRYPTON	7439-90-9	0.952492	3.69199	167.668	0.0003	116.0	1300.0	0.0002	95.0000	0.0044	0.1094
others											
AMMONIA	7664-41-7	2.92125	2.41696	188.631	0.0089	199.0	723.5	0.0240	80.1000	0.0188	0.6699
WATER	7732-18-5	3.64287	2.08351	274.442	0.0071	273.1	1190.2	0.0026	98.6000	0.0218	0.7770
CARBON MONOXIDE	630-08-0	1.3574	3.21074	89.7577	-0.0002	78.2	429.1	0.0667	12.5100	0.0226	0.1486
NITROGEN	7727-37-9	1.27492	3.25959	87.9687	-0.0004	68.7	2073.2	0.0093	98.3900	0.0074	0.1888
OXYGEN	7782-44-7	1.14932	3.1795	113.452	-0.0001	66.0	1400.0	0.0048	68.4110	0.0064	0.2021
CARBON DIOXIDE	124-38-9	2.69691	2.60169	146.566	0.0049	196.8	1300.0	0.0003	98.6000	0.0084	0.2004
CHLOROFORM	67-66-3	2.68365	3.4792	259.011	0.0094	213.2	422.1	0.1000	0.1013	0.0093	0.1536

VII-A-2) Component-specific parameters

Component-specific parameters (a_1, a_2, b_1, b_2, c and d) to be used in the below equation for the viscosity estimation are reported in Table VII-2.

$$\begin{cases} \ln\left(\dfrac{\lambda}{\lambda_{\mathrm{ref}}^{\mathrm{Rosenfeld,intDoF}}}\right)_{\mathrm{calc}} = \left[\left(\dfrac{a_1 + a_2 X_{\mathrm{ES}}^{1/3}}{1 + e^{cX_{\mathrm{ES}}}}\right) + \left(\dfrac{b_1 + b_2 X_{\mathrm{ES}}^{1/3}}{1 + e^{-cX_{\mathrm{ES}}}}\right)\right] X_{\mathrm{ES}} + d \\ X_{\mathrm{ES}} = -\left(\dfrac{s_{\mathrm{Tv-res}}}{s_{\mathrm{Tv-res}}^{c}}\right) - \ln\left(\dfrac{s_{\mathrm{Tv-res}}}{s_{\mathrm{Tv-res}}^{c}}\right) \\ \lambda_{\mathrm{ref}}^{\mathrm{Rosenfeld,intDoF}} = \rho_{\mathrm{N}}^{2/3}\sqrt{\mathrm{k_b}T/\mathrm{m_0}}\left[1 + \left(\dfrac{C_{\mathrm{v}}^{\mathrm{real}}}{R}\right) e^{\left(-\rho/\rho_c\right)}\right] \\ \tilde{s}_{\mathrm{Tv-res}} = \dfrac{s_{Tv-res}}{R} \end{cases} \quad \text{(VII– 3)}$$

The Tv-residual entropy ($s_{\mathrm{Tv-res}}$), the molecular density (ρ_N) and ($C_{\mathrm{v}}^{\mathrm{real}}$) were estimated using the *I*-PC-SAFT EoS.

Table VII-2 - Component-specific parameters suitable for the *I*-PC-SAFT based model with the corresponding number of experimental data points and MAPE

Name	a_1	a_2	b_1	b_2	c	d	nb data	MAPE
n-alkanes							22665	3.00
METHANE	-0.441956	-0.084452	0.180301	0.170900	0.622347	0.312667	4348	3.22
ETHANE	-0.580478	-0.148403	0.260574	0.125791	0.666081	0.248458	2232	3.24
n-BUTANE	-0.663039	-0.185974	0.460326	0.038181	0.644839	0.172154	3429	2.76
n-PENTANE	-0.645260	-0.170220	0.491263	0.010000	0.677724	0.145049	920	2.90
n-HEXANE	-0.671582	-0.177580	0.474212	0.010000	0.743269	0.122180	951	3.46
n-HEPTANE	-0.737338	-0.204100	0.531388	0.010000	0.615336	0.110182	1658	3.68
n-OCTANE	-0.750917	-0.208521	0.491447	0.010000	0.720500	0.100000	684	3.28
n-NONANE	-0.714130	-0.189686	0.489349	0.043800	0.552071	0.189903	806	2.93
n-DECANE	-0.823336	-0.238372	0.587314	0.010011	0.533540	0.171609	1222	2.92
n-UNDECANE	-0.804601	-0.225606	0.563184	0.013427	0.591800	0.121328	621	3.32
n-DODECANE	-0.758690	-0.210059	0.561732	0.010000	0.500049	0.349417	655	3.18
n-TRIDECANE	-0.886691	-0.264559	0.628597	0.010000	0.500912	0.278754	699	2.80
n-TETRADECANE	-0.849235	-0.247124	0.607777	0.010000	0.500000	0.332143	693	2.31
n-PENTADECANE	-0.842142	-0.242183	0.601416	0.010272	0.500458	0.346964	561	2.24
n-HEXADECANE	-0.881257	-0.249894	0.579007	0.039533	0.585491	0.128525	684	2.67
n-HEPTADECANE	-0.877971	-0.254021	0.599574	0.010985	0.500874	0.323496	762	2.49
n-OCTADECANE	-0.950932	-0.276637	0.636839	0.048893	0.557616	0.106313	602	2.31
n-NONADECANE	-0.834453	-0.222814	0.363276	0.094278	0.620061	0.131054	544	3.33
n-EICOSANE	-0.811078	-0.212622	0.363276	0.094278	0.620061	0.131054	214	2.24
n-HENEICOSANE	-0.829695	-0.219308	0.363276	0.094278	0.620061	0.131054	96	1.97
n-DOCOSANE	-0.856687	-0.229770	0.363276	0.094278	0.620061	0.131054	102	1.84
n-TRICOSANE	-0.830769	-0.216797	0.363276	0.094278	0.620061	0.131054	84	1.96
n-TETRACOSANE	-0.853093	-0.226298	0.363276	0.094278	0.620061	0.131054	98	1.75
branched alkanes							2974	3.63
ISOBUTANE	-0.685962	-0.200212	0.513167	0.010000	0.634065	0.161137	2354	3.91
ISOPENTANE	-0.487660	-0.104911	0.027569	0.279744	0.568965	0.279323	55	2.00
2,2-DIMETHYLBUTANE	-0.547226	-0.127228	0.363276	0.094278	0.620061	0.131054	17	1.72
2,3-DIMETHYLBUTANE	-0.474862	-0.085863	0.363276	0.094278	0.620061	0.131054	33	2.50
2-METHYLPENTANE	-0.543270	-0.118160	0.363276	0.094278	0.620061	0.131054	18	1.07
3-METHYLPENTANE	-0.463094	-0.075769	0.363276	0.094278	0.620061	0.131054	20	2.01
3-ETHYLPENTANE	-0.686432	-0.191896	0.363276	0.094278	0.620061	0.131054	16	2.51
2,4-DIMETHYLPENTANE	-0.439932	-0.065725	0.363276	0.094278	0.620061	0.131054	18	2.39
2,2,4-TRIMETHYLPENTANE	-0.675521	-0.178329	0.560313	0.010000	0.500000	0.100000	428	2.85
2,3,4-TRIMETHYLPENTANE	-0.470748	-0.085330	0.363276	0.094278	0.620061	0.131054	15	0.81
cycloalkanes							921	2.57
CYCLOPENTANE	-0.785518	-0.239204	0.592558	0.010231	0.500058	0.207881	143	0.76
CYCLOHEXANE	-0.683181	-0.198621	0.507874	0.010000	0.612282	0.213481	762	2.94

Continued on next page

Table VII-2 – continued from previous page

Name	a_1	a_2	b_1	b_2	c	d	nb data	MAPE
CYCLOOCTANE	-0.566056	-0.139585	0.526750	0.000000	0.608467	0.212953	16	0.73
alkenes							5078	2.94
ETHYLENE	-0.464141	-0.083623	0.080987	0.218454	0.703031	0.286594	1113	2.76
PROPYLENE	-0.564541	-0.137676	0.226816	0.140634	0.715944	0.240203	821	2.92
1-PENTENE	-0.548871	-0.118936	0.272324	0.132430	0.748358	0.117811	32	0.44
1-HEXENE	-0.676252	-0.182491	0.478717	0.010000	0.746368	0.117538	297	2.54
1-HEPTENE	-0.747619	-0.213677	0.512989	0.014749	0.639444	0.124438	457	2.48
1-OCTENE	-0.741700	-0.213307	0.524941	0.010001	0.573452	0.236282	465	3.25
1-NONENE	-0.788867	-0.230670	0.539818	0.013964	0.500000	0.202046	302	3.06
1-DECENE	-0.872165	-0.261110	0.560435	0.010000	0.501619	0.100000	285	2.73
1-DODECENE	-0.668607	-0.159045	0.477984	0.035729	0.617414	0.133521	287	3.71
1-TRIDECENE	-0.743277	-0.194381	0.477984	0.035729	0.617414	0.133521	246	3.01
1-TETRADECENE	-0.781234	-0.210700	0.477984	0.035729	0.617414	0.133521	275	3.32
1-PENTADECENE	-0.720174	-0.179494	0.477984	0.035729	0.617414	0.133521	249	3.50
1-HEXADECENE	-0.794784	-0.214622	0.477984	0.035729	0.617414	0.133521	249	3.12
aromatics							3101	1.98
BENZENE	-0.625074	-0.161253	0.475227	0.010002	0.727629	0.160114	973	2.34
m-XYLENE	-0.601295	-0.148963	0.473916	0.020405	0.685072	0.188472	656	1.75
p-XYLENE	-0.636429	-0.166660	0.456001	0.030915	0.661361	0.194941	641	2.23
ETHYLBENZENE	-0.599610	-0.148574	0.495287	0.010000	0.691270	0.173892	692	1.60
MESITYLENE	-0.731678	-0.208379	0.456001	0.030915	0.661361	0.194941	139	1.20
esters							781	5.78
VINYL ACETATE	-0.872398	-0.274173	0.405924	0.072584	0.713075	0.132813	6	1.23
n-BUTYL ACETATE	-0.607153	-0.166020	0.499844	0.011196	0.500000	0.533205	269	2.72
ISOPENTYL ACETATE	-0.410539	-0.047236	0.405924	0.072584	0.713075	0.132813	148	8.93
n-PENTYL ACETATE	-0.383663	-0.033055	0.405924	0.072584	0.713075	0.132813	151	9.06
n-HEPTYL ACETATE	-0.656652	-0.158272	0.405924	0.072584	0.713075	0.132813	207	5.25
ethers							883	2.68
DIMETHYL ETHER	-0.626888	-0.178497	0.352067	0.075314	0.725702	0.264337	332	1.10
DI-n-PROPYL ETHER	-0.561889	-0.123292	0.453150	0.010000	0.626680	0.313996	115	2.27
DI-n-BUTYL ETHER	-0.743302	-0.210985	0.488902	0.010000	0.676934	0.189858	257	3.38
DI-n-PENTYL ETHER	-0.686145	-0.177996	0.495594	0.000000	0.670729	0.240063	179	4.88
aldehydes							434	3.31
ACETALDEHYDE	-0.861628	-0.324077	0.425000	0.029328	0.554846	0.702808	93	1.27
BUTANAL	-0.737831	-0.223532	0.557674	0.010000	0.584360	0.275439	137	3.83
2-METHYLPROPANAL	-0.719313	-0.218042	0.532769	0.010000	0.552157	0.394112	139	5.16
3-METHYLBUTYRALDEHYDE	-0.800958	-0.253601	0.634730	0.010871	0.500114	0.315249	53	1.27
HEPTANAL	-0.635608	-0.166674	0.496971	0.010202	0.654056	0.248883	12	0.89
alcohols							3273	3.62

Continued on next page

Table VII-2 – continued from previous page

Name	a_1	a_2	b_1	b_2	c	d	nb data	MAPE
ETHANOL	-0.557133	-0.169698	0.010002	0.267054	0.970234	0.409888	914	4.13
1-PROPANOL	-0.619886	-0.186592	0.169373	0.172682	0.924584	0.326725	391	3.50
1-BUTANOL	-0.672222	-0.205082	0.288755	0.103355	0.797215	0.329920	342	3.58
1-PENTANOL	-0.667390	-0.187849	0.183567	0.172621	0.745579	0.204669	145	3.22
1-HEXANOL	-0.880058	-0.277234	0.544046	0.036573	0.578100	0.100279	269	2.41
1-HEPTANOL	-0.866675	-0.265951	0.599943	0.010000	0.561573	0.101312	280	3.08
1-OCTANOL	-0.793838	-0.226701	0.531849	0.010000	0.693366	0.100000	222	3.09
1-NONANOL	-0.730166	-0.191128	0.516796	0.010000	0.700000	0.100000	188	3.63
1-DECANOL	-0.944445	-0.286116	0.701867	0.010000	0.500000	0.100000	306	4.20
1-UNDECANOL	-0.559131	-0.107614	0.183567	0.172621	0.745579	0.204669	92	3.84
1-DODECANOL	-0.490914	-0.071672	0.183567	0.172621	0.745579	0.204669	94	4.79
1-TETRADECANOL	-0.815077	-0.221495	0.183567	0.172621	0.745579	0.204669	14	1.66
1-OCTADECANOL	-0.882642	-0.242158	0.183567	0.172621	0.745579	0.204669	16	1.15
amines							138	3.24
METHYLAMINE	-0.547214	-0.118783	0.183567	0.172621	0.745579	0.204669	125	2.71
DIETHYLAMINE	-0.525809	-0.108555	0.183567	0.172621	0.745579	0.204669	13	8.42
HFC-CFC							20857	2.70
DIFLUOROMETHANE	-0.763311	-0.241821	0.142506	0.171134	0.887121	0.349111	1136	2.32
1,1-DIFLUOROETHANE	-0.658691	-0.188374	0.266955	0.118382	0.842166	0.245447	769	2.08
TRIFLUOROMETHANE	-0.715126	-0.216736	0.128685	0.171004	0.836955	0.297844	614	2.93
1,1,1-TRIFLUOROETHANE	-0.582821	-0.141972	0.202532	0.154859	0.799045	0.232527	695	2.18
CHLORODIFLUOROMETHANE	-0.691308	-0.203350	0.220558	0.140693	0.758910	0.250605	2081	2.78
1-CHLORO-1,1-DIFLUOROETHANE	-0.536319	-0.115202	0.231324	0.152213	0.742025	0.158526	469	2.51
1,1,1,2-TETRAFLUOROETHANE	-0.620796	-0.156676	0.266743	0.125407	0.795380	0.192500	7077	2.96
DICHLORODIFLUOROMETHANE	-0.635558	-0.166229	0.279882	0.111206	0.743211	0.169999	1385	2.61
CHLOROTRIFLUOROMETHANE	-0.647466	-0.176904	0.190737	0.156393	0.746821	0.225317	711	3.33
PENTAFLUOROETHANE	-0.645492	-0.164635	0.313322	0.098902	0.778788	0.164446	2266	2.07
DICHLOROFLUOROMETHANE	-0.613705	-0.166380	0.208431	0.145216	0.796690	0.280743	480	1.81
TRICHLOROFLUOROMETHANE	-0.669297	-0.187288	0.236491	0.141958	0.793673	0.201453	909	3.09
BROMOTRIFLUOROMETHANE	-0.592261	-0.155408	0.083576	0.212277	0.745244	0.298378	724	2.56
1,1,1,3,3,3-HEXAFLUOROPROPANE	-0.711169	-0.201683	0.487796	0.010086	0.695298	0.200982	265	0.94
CHLOROPENTAFLUOROETHANE	-0.616270	-0.158453	0.226847	0.204985	0.500000	0.232582	546	6.06
1,1,1,2,3,3,3-HEPTAFLUOROPROPANE	-0.589328	-0.130346	0.400424	0.064923	0.744394	0.100000	580	1.39
1,2-DICHLOROTETRAFLUOROETHANE	-0.627994	-0.179652	0.439812	0.028539	0.500000	0.496155	150	2.41
noble gases							12136	3.60
NEON	-0.366463	-0.020269	0.224914	0.159782	0.554979	0.431492	2419	5.89
ARGON	-0.449601	-0.089117	0.232271	0.147786	0.542430	0.437680	7742	3.06
KRYPTON	-0.429540	-0.077970	0.246066	0.135414	0.572239	0.438128	1975	2.91
others							15151	3.43

Continued on next page

Table VII-2 – continued from previous page

Name	a_1	a_2	b_1	b_2	c	d	nb data	MAPE
AMMONIA	-0.754255	-0.237091	0.010000	0.242447	0.874164	0.469462	1039	4.42
WATER	-0.940775	-0.367052	0.010000	0.235519	0.842079	0.648909	5644	3.74
NITROGEN	-0.439236	-0.082568	0.134122	0.192453	0.593359	0.392854	3167	3.13
OXYGEN	-0.465259	-0.100636	0.162451	0.176255	0.644211	0.359342	2062	2.42
CARBON DIOXIDE	-0.597549	-0.147296	0.139993	0.186027	0.719063	0.293621	3124	3.55
CHLOROFORM	-0.798648	-0.247619	0.450281	0.014723	0.941327	0.100000	115	2.77

VII-A-3) Chemical-family specific parameters

VII-A-3.1) Paraffins

Table VII-3 – Chemical-family specific parameters for paraffins to be used with the *I*-PC-SAFT based model

Variable	Value
nb component	31
nb data	19059
MAPE	15.48
a_1	-0.529149
a_2	-0.095298
b_1	0.363276
b_2	0.094278
c	0.620061
d	0.131054

Table VII-4 - Prediction of the thermal conductivity data of paraffins using chemical-family specific parameters for the *I*-PC-SAFT based model: data number and corresponding MAPE (Mean Absolute Percentage Error).

Name	nb data	MAPE
n-BUTANE	3429	13.66
n-PENTANE	920	10.09
n-HEXANE	951	7.18
n-HEPTANE	1658	6.46
n-OCTANE	684	6.78
n-NONANE	806	4.83
n-DECANE	1222	7.26
n-UNDECANE	621	9.50
n-DODECANE	655	11.94
n-TRIDECANE	699	16.42
n-TETRADECANE	693	19.17
n-PENTADECANE	561	21.28
n-HEXADECANE	684	24.19
n-HEPTADECANE	762	25.97
n-OCTADECANE	602	29.31
n-NONADECANE	544	31.99
n-EICOSANE	214	28.25
n-HENEICOSANE	96	30.89
n-DOCOSANE	102	33.33
n-TRICOSANE	84	34.51
n-TETRACOSANE	98	35.50
ISOBUTANE	2354	19.93
ISOPENTANE	55	6.51
2,2-DIMETHYLBUTANE	17	30.34
2,3-DIMETHYLBUTANE	33	24.57
2-METHYLPENTANE	18	19.31
3-METHYLPENTANE	20	20.71
3-ETHYLPENTANE	16	21.27
2,4-DIMETHYLPENTANE	18	21.63
2,2,4-TRIMETHYLPENTANE	428	29.67
2,3,4-TRIMETHYLPENTANE	15	34.47

VII-A-3.2) Cycloalkanes

Table VII-5 - Chemical-family specific parameters for cycloalkanes to be used with the *I*-PC-SAFT based model

Variable	Value
nb component	3
nb data	921
MAPE	3.09
a_1	-0.690741
a_2	-0.200921
b_1	0.526750
b_2	0.000000
c	0.608467
d	0.212953

Table VII-6 - Prediction of the thermal conductivity data of cycloalkanes using chemical-family specific parameters for the *I*-PC-SAFT based model: data number and corresponding MAPE (Mean Absolute Percentage Error).

Name	nb data	MAPE
CYCLOPENTANE	143	3.43
CYCLOHEXANE	762	3.05
CYCLOOCTANE	16	1.57

VII-A-3.3) Alkenes

Table VII-7 - Chemical-family specific parameters for alkenes to be used with the *I*-PC-SAFT based model

Variable	Value
nb component	12
nb data	3147
MAPE	9.83
a_1	-0.699686
a_2	-0.182824
b_1	0.477984
b_2	0.035729
c	0.617414
d	0.133521

Table VII-8 - Prediction of the thermal conductivity data of alkenes using chemical-family specific parameters for the *I*-PC-SAFT based model: data number and corresponding MAPE (Mean Absolute Percentage Error).

Name	nb data	MAPE
1-BUTENE	3	11.16
1-PENTENE	32	7.21
1-HEXENE	297	7.61
1-HEPTENE	457	5.80
1-OCTENE	465	5.98
1-NONENE	302	7.05
1-DECENE	285	4.15
1-DODECENE	287	8.97
1-TRIDECENE	246	12.81
1-TETRADECENE	275	17.51
1-PENTADECENE	249	16.74
1-HEXADECENE	249	19.92

VII-A-3.4) Aromatics

Table VII-9 - Chemical-family specific parameters for aromatics to be used with the *I*-PC-SAFT based model

Variable	Value
nb component	5
nb data	3101
MAPE	2.69
a_1	-0.606794
a_2	-0.152327
b_1	0.456001
b_2	0.030915
c	0.661361
d	0.194941

Table VII-10 - Prediction of the thermal conductivity data of aromatics using chemical-family specific parameters for the *I*-PC-SAFT based model: data number and corresponding MAPE (Mean Absolute Percentage Error).

Name	nb data	MAPE
BENZENE	973	2.65
m-XYLENE	656	1.90
p-XYLENE	641	2.61
ETHYLBENZENE	692	2.27
MESITYLENE	139	9.20

VII-A-3.5) Esters

Table VII-11 - Chemical-family specific parameters for esters to be used with the *I*-PC-SAFT based model

Variable	Value
nb component	5
nb data	781
MAPE	9.57
a_1	-0.574144
a_2	-0.123818
b_1	0.405924
b_2	0.072584
c	0.713075
d	0.132813

Table VII-12 - Prediction of the thermal conductivity data of esters using chemical-family specific parameters for the *I*-PC-SAFT based model: data number and corresponding MAPE (Mean Absolute Percentage Error).

Name	nb data	MAPE
VINYL ACETATE	6	10.99
n-BUTYL ACETATE	269	5.02
ISOPENTYL ACETATE	148	10.66
n-PENTYL ACETATE	151	14.20
n-HEPTYL ACETATE	207	11.29

VII-A-3.6) Ethers

Table VII-13 - Chemical-family specific parameters for ethers to be used with the *I*-PC-SAFT based model

Variable	Value
nb component	4
nb data	883
MAPE	5.29
a_1	-0.654687
a_2	-0.169273
b_1	0.495594
b_2	0.000000
c	0.670729
d	0.240063

Table VII-14 - Prediction of the thermal conductivity data of ethers using chemical-family specific parameters for the *I*-PC-SAFT based model: data number and corresponding MAPE (Mean Absolute Percentage Error).

Name	nb data	MAPE
DIMETHYL ETHER	332	5.15
DI-n-PROPYL ETHER	115	2.85
DI-n-BUTYL ETHER	257	4.11
DI-n-PENTYL ETHER	179	8.82

VII-A-3.7) Aldehydes

Table VII-15 - Chemical-family specific parameters for aldehydes to be used with the *I*-PC-SAFT based model

Variable	Value
nb component	5
nb data	434
MAPE	5.00
a_1	-0.655162
a_2	-0.180497
b_1	0.496971
b_2	0.010202
c	0.654056
d	0.248883

Table VII-16 - Prediction of the thermal conductivity data of aldehydes using chemical-family specific parameters for the *I*-PC-SAFT based model: data number and corresponding MAPE (Mean Absolute Percentage Error).

Name	nb data	MAPE
ACETALDEHYDE	93	1.74
BUTANAL	137	4.78
2-METHYLPROPANAL	139	6.93
3-METHYLBUTYRALDEHYDE	53	6.18
HEPTANAL	12	5.20

VII-A-3.8) Alcohols

Table VII-17 - Chemical-family specific parameters for alcohols to be used with the *I*-PC-SAFT based model

Variable	Value
nb component	13
nb data	3273
MAPE	17.02
a_1	-0.490613
a_2	-0.109465
b_1	0.188682
b_2	0.172209
c	0.761700
d	0.369608

Table VII-18 - Prediction of the thermal conductivity data of alcohols using chemical-family specific parameters for the *I*-PC-SAFT based model: data number and corresponding MAPE (Mean Absolute Percentage Error).

Name	nb data	MAPE
ETHANOL	914	19.96
1-PROPANOL	391	12.47
1-BUTANOL	342	8.51
1-PENTANOL	145	4.23
1-HEXANOL	269	8.54
1-HEPTANOL	280	12.50
1-OCTANOL	222	18.91
1-NONANOL	188	22.50
1-DECANOL	306	26.61
1-UNDECANOL	92	26.31
1-DODECANOL	94	28.55
1-TETRADECANOL	14	46.64
1-OCTADECANOL	16	58.21

VII-A-3.9) Amines

Table VII-19 - Chemical-family specific amines for paraffins to be used with the *I*-PC-SAFT based model

Variable	Value
nb component	8
nb data	158
MAPE	4.19
a_1	-0.558381
a_2	-0.125633
b_1	0.183567
b_2	0.172621
c	0.745579
d	0.204669

Table VII-20 - Prediction of the thermal conductivity data of amines using chemical-family specific parameters for the *I*-PC-SAFT based model: data number and corresponding MAPE (Mean Absolute Percentage Error).

Name	nb data	MAPE
METHYLAMINE	125	2.69
n-BUTYLAMINE	3	3.76
DIETHYLAMINE	13	8.50
n-PENTYLAMINE	3	8.85
DI-n-PROPYLAMINE	3	10.87
n-HEXYLAMINE	4	6.63
n-OCTYLAMINE	4	13.93
n-DECYLAMINE	3	20.91

VII-A-3.10) HFC-CFC

Table VII-21 - Chemical-family specific parameters for HFC-CFCs to be used with the *I*-PC-SAFT based model

Variable	Value
nb component	18
nb data	21058
MAPE	4.94
a_1	-0.681148
a_2	-0.192439
b_1	0.307295
b_2	0.098746
c	0.794172
d	0.205190

Table VII-22 - Prediction of the thermal conductivity data of HFC-CFCs using chemical-family specific parameters for the *I*-PC-SAFT based model: data number and corresponding MAPE (Mean Absolute Percentage Error).

Name	nb data	MAPE
DIFLUOROMETHANE	1136	16.07
1,1-DIFLUOROETHANE	769	3.47
TRIFLUOROMETHANE	614	9.69
1,1,1-TRIFLUOROETHANE	695	3.13
CHLORODIFLUOROMETHANE	2081	5.21
1-CHLORO-1,1-DIFLUOROETHANE	469	6.24
1,1,1,2-TETRAFLUOROETHANE	7077	3.24
DICHLORODIFLUOROMETHANE	1385	5.39
CHLOROTRIFLUOROMETHANE	711	5.41
PENTAFLUOROETHANE	2266	3.56
DICHLOROFLUOROMETHANE	480	3.61
TRICHLOROFLUOROMETHANE	909	3.53
BROMOTRIFLUOROMETHANE	724	5.26
1,1,1,3,3,3-HEXAFLUOROPROPANE	265	2.86
1,1,1,2,3,3-HEXAFLUOROPROPANE	201	11.11
CHLOROPENTAFLUOROETHANE	546	7.54
1,1,1,2,3,3,3-HEPTAFLUOROPROPANE	580	3.36
1,2-DICHLOROTETRAFLUOROETHANE	150	6.85

VII-A-4) Universal parameters

Table VII-23 - Universal parameters to be used with the *I*-PC-SAFT based model

Variable	Value
nb component	109
nb data	61331
MAPE	11.17
a_1	-0.528486
a_2	-0.110335
b_1	0.183567
b_2	0.172621
c	0.745579
d	0.204669

Table VII-24 - Prediction of thermal conductivity data using universal parameters for the *I*-PC-SAFT based model: data number and corresponding MAPE (Mean Absolute Percentage Error).

Name	nb data	MAPE
n-alkanes	22665	14.76
METHANE	4348	7.87
ETHANE	2232	5.50
n-BUTANE	3429	13.17
n-PENTANE	920	11.52
n-HEXANE	951	5.11
n-HEPTANE	1658	5.91
n-OCTANE	684	9.12
n-NONANE	806	10.17
n-DECANE	1222	12.64
n-UNDECANE	621	14.75
n-DODECANE	655	17.88
n-TRIDECANE	699	22.49
n-TETRADECANE	693	25.73
n-PENTADECANE	561	28.76
n-HEXADECANE	684	32.10
n-HEPTADECANE	762	33.59
n-OCTADECANE	602	37.21
n-NONADECANE	544	38.58
n-EICOSANE	214	40.70
n-HENEICOSANE	96	43.72
n-DOCOSANE	102	46.06
n-TRICOSANE	84	46.85
n-TETRACOSANE	98	48.04
branched alkanes	2974	17.50
ISOBUTANE	2354	17.14
ISOPENTANE	55	5.02
2,2-DIMETHYLBUTANE	17	22.79
2,3-DIMETHYLBUTANE	33	15.82
2-METHYLPENTANE	18	12.40
3-METHYLPENTANE	20	13.14
3-ETHYLPENTANE	16	9.67
2,4-DIMETHYLPENTANE	18	12.84
2,2,4-TRIMETHYLPENTANE	428	21.87
2,3,4-TRIMETHYLPENTANE	15	19.36
cycloalkanes	921	14.49
CYCLOPENTANE	143	11.54
CYCLOHEXANE	762	14.87
CYCLOOCTANE	16	22.65
alkenes	5081	9.46
ETHYLENE	1113	6.17
PROPYLENE	821	4.69
1-BUTENE	3	4.29
1-PENTENE	32	3.29
1-HEXENE	297	7.28
1-HEPTENE	457	4.82
1-OCTENE	465	5.72
1-NONENE	302	8.05
1-DECENE	285	8.29
1-DODECENE	287	14.28
1-TRIDECENE	246	16.74
1-TETRADECENE	275	21.51
1-PENTADECENE	249	20.94
1-HEXADECENE	249	24.33
aromatics	3103	8.06
ACETYLENE	2	6.56
BENZENE	973	7.59
m-XYLENE	656	8.05

Continued on next page

Table VII-24 – continued from previous page

Name	nb data	MAPE
p-XYLENE	641	6.91
ETHYLBENZENE	692	10.58
MESITYLENE	139	4.14
esters	781	11.22
VINYL ACETATE	6	13.67
n-BUTYL ACETATE	269	5.03
ISOPENTYL ACETATE	148	12.45
n-PENTYL ACETATE	151	16.62
n-HEPTYL ACETATE	207	14.36
ethers	883	7.97
DIMETHYL ETHER	332	6.24
DI-n-PROPYL ETHER	115	6.77
DI-n-BUTYL ETHER	257	7.40
DI-n-PENTYL ETHER	179	12.77
aldehydes	434	8.92
ACETALDEHYDE	93	6.06
BUTANAL	137	11.14
2-METHYLPROPANAL	139	7.66
3-METHYLBUTYRALDEHYDE	53	12.98
HEPTANAL	12	2.51
alcohols	3273	19.42
ETHANOL	914	31.37
1-PROPANOL	391	21.04
1-BUTANOL	342	16.93
1-PENTANOL	145	11.55
1-HEXANOL	269	5.25
1-HEPTANOL	280	5.40
1-OCTANOL	222	11.27
1-NONANOL	188	14.79
1-DECANOL	306	18.63
1-UNDECANOL	92	20.04
1-DODECANOL	94	22.34
1-TETRADECANOL	14	38.39
1-OCTADECANOL	16	51.07
amines	158	4.56
METHYLAMINE	125	3.09
n-BUTYLAMINE	3	3.98
DIETHYLAMINE	13	8.42
n-PENTYLAMINE	3	10.38
DI-n-PROPYLAMINE	3	11.92
n-HEXYLAMINE	4	7.07
n-OCTYLAMINE	4	13.93
n-DECYLAMINE	3	20.67
HFC-CFC	21058	6.09
DIFLUOROMETHANE	1136	18.03
1,1-DIFLUOROETHANE	769	5.19
TRIFLUOROMETHANE	614	12.79
1,1,1-TRIFLUOROETHANE	695	4.30
CHLORODIFLUOROMETHANE	2081	8.11
1-CHLORO-1,1-DIFLUOROETHANE	469	4.91
1,1,1,2-TETRAFLUOROETHANE	7077	3.90
DICHLORODIFLUOROMETHANE	1385	5.59
CHLOROTRIFLUOROMETHANE	711	7.28
PENTAFLUOROETHANE	2266	3.87
DICHLOROFLUOROMETHANE	480	5.35
TRICHLOROFLUOROMETHANE	909	5.51
BROMOTRIFLUOROMETHANE	724	9.28
1,1,1,3,3,3-HEXAFLUOROPROPANE	265	3.19
1,1,1,2,3,3-HEXAFLUOROPROPANE	201	12.55
CHLOROPENTAFLUOROETHANE	546	6.70

Continued on next page

Table VII-24 – continued from previous page

Name	nb data	MAPE
1,1,1,2,3,3,3-HEPTAFLUOROPROPANE	580	3.70
1,2-DICHLOROTETRAFLUOROETHANE	150	6.38

VII-B) *tc*-PR based model

VII-B-1) Equation of state parameters

The *translated-consistent* version of the Peng-Robinson (PR) EoS, denoted *tc*-PR[75,83] relies on consistent L, M and N parameters of the Twu 91 α-function (*consistent* means that these parameters passed a consistency test[83] ensuring safe calculations in the supercritical region). In this model, the volume translation parameter c was selected in order to exactly reproduce the experimental saturated liquid molar volume at a reduced temperature of 0.8:

$$c = v_{\text{liq}}^{\text{sat,u-EoS}}(T_r = 0.8) - v_{\text{liq,exp}}^{\text{sat}}(T_r = 0.8) \qquad \text{(VII-4)}$$

Where $v_{liq}^{sat,u-EoS}(T_r = 0.8)$ is the molar volume calculated with the original (untranslated) EoS at $T_r = 0.8$.

The final *tc*-PR EoS expression is:

$$P(T,v) = \frac{RT}{v-b} - \frac{a_c \cdot \alpha(T_r)}{(v+c)(v+b+2c)+(b+c)(v-b)}$$

$$\begin{cases} \alpha(T_r) = T_r^{N(M-1)} exp[L(1-T_r^{MN})] \\ c = v_{\text{liq}}^{\text{sat,u-EoS}}(T_r = 0.8) - v_{\text{liq,exp}}^{\text{sat}}(T_r = 0.8) \\ \eta_c = \left[1 + \sqrt[3]{4-2\sqrt{2}} + \sqrt[3]{4+2\sqrt{2}}\right] \approx 0.25308 \\ a_c = \dfrac{40\eta_c + 8}{49 - 37\eta_c} \dfrac{R^2 T_{\text{c,exp}}^2}{P_{\text{c,exp}}} \approx 0.45724 \dfrac{R^2 T_{\text{c,exp}}^2}{P_{\text{c,exp}}} \\ b = \dfrac{\eta_c}{\eta_c + 3} \dfrac{RT_{\text{c,exp}}}{P_{\text{c,exp}}} - c \approx 0.07780 \dfrac{RT_{\text{c,exp}}}{P_{\text{c,exp}}} - c \end{cases} \qquad \text{(VII-5)}$$

The *tc*-PR parameters used in this study are reported in Table VII-25.

Table VII-25 - *tc-PR* EoS parameters and experimental thermal conductivity data informations

		EoS parameters				Experimental data informations					
Name	CAS	L -	M -	N -	$c * 10^6$ m^3/mol	T_{min} K	T_{max} K	P_{min} MPa	P_{max} MPa	λ_{min} $W.m^{-1}.K^{-1}$	λ_{max} $W.m^{-1}.K^{-1}$
n-alkanes											
METHANE	74-82-8	0.14738	0.90748	1.82411	-3.56049	98.9	726.5	0.0980	95.9000	0.0121	0.2875
ETHANE	74-84-0	0.30533	0.86927	1.32966	-3.67453	111.7	800.6	0.1000	99.0000	0.0084	0.2687
n-BUTANE	106-97-8	0.41536	0.84901	1.32049	-3.43648	135.8	675.0	0.0920	70.1000	0.0143	0.1889
n-PENTANE	109-66-0	0.29330	0.83662	1.82462	-1.59871	146.3	623.6	0.0980	98.0660	0.0166	0.1725
n-HEXANE	110-54-3	0.28726	0.83405	2.01991	0.81628	183.2	728.8	0.0980	99.2000	0.0180	0.1639
n-HEPTANE	142-82-5	0.36295	0.82017	1.83664	3.10863	183.2	700.0	0.0933	98.0000	0.0187	0.1634
n-OCTANE	111-65-9	0.35700	0.81717	1.99996	6.42842	223.2	640.0	0.0980	96.0000	0.0200	0.1617
n-NONANE	111-84-2	0.41649	0.80811	1.89355	9.34517	223.2	700.0	0.0980	98.0000	0.0221	0.1655
n-DECANE	124-18-5	0.37696	0.81080	2.17809	12.82743	243.2	680.0	0.0980	74.9100	0.0222	0.1581
n-UNDECANE	1120-21-4	0.48046	0.80007	1.90454	18.32929	284.6	680.0	0.0980	98.0665	0.0228	0.1595
n-DODECANE	112-40-3	0.45843	0.80098	2.08729	22.22725	273.1	680.0	0.0980	96.0000	0.0248	0.1722
n-TRIDECANE	629-50-5	0.47740	0.79897	2.11999	30.13814	290.0	677.6	0.0980	98.0665	0.0253	0.1606
n-TETRADECANE	629-59-4	0.57041	0.78895	1.88879	39.90980	280.0	677.7	0.0915	50.0000	0.0256	0.1532
n-PENTADECANE	629-62-9	0.57955	0.78769	1.94902	45.35005	286.1	677.7	0.0980	49.0330	0.0266	0.1608
n-HEXADECANE	544-76-3	0.60685	0.78674	1.94340	52.13839	294.8	693.1	0.0972	49.0333	0.0279	0.1555
n-HEPTADECANE	629-78-7	0.56074	0.79245	2.18728	52.58577	302.1	693.1	0.0980	49.0333	0.0258	0.1582
n-OCTADECANE	593-45-3	0.58016	0.79247	2.21665	59.16994	301.2	693.1	0.0980	49.0333	0.0282	0.1700
n-NONADECANE	629-92-5	0.59247	0.79325	2.27181	64.88646	313.1	693.1	0.0981	49.0333	0.0960	0.1625
n-EICOSANE	112-95-8	0.56936	0.80387	2.50049	64.11107	315.0	610.0	0.1000	50.0000	0.0930	0.1623
n-HENEICOSANE	629-94-7	0.46937	0.81153	3.01913	72.69091	333.1	473.1	0.1000	49.1010	0.1150	0.1623
n-TRICOSANE	638-67-5	0.47273	0.81012	3.20180	84.63427	353.1	473.1	0.1000	49.1010	0.1195	0.1627
n-TETRACOSANE	646-31-1	0.46905	0.81025	3.33744	89.64608	335.4	473.1	0.1000	49.1010	0.1258	0.1651
branched alkanes											
ISOBUTANE	75-28-5	1.07723	0.99213	0.57426	-3.80262	115.6	630.8	0.0940	99.0000	0.0118	0.1885
ISOPENTANE	78-78-4	0.24029	0.83746	1.95199	-3.60373	250.0	700.0	0.1000	80.8000	0.0168	0.1334
2,2-DIMETHYLBUTANE	75-83-2	0.22181	0.83374	2.03473	-6.28035	257.5	320.3	0.1013	0.1013	0.0871	0.1055
2,3-DIMETHYLBUTANE	79-29-8	0.18994	0.84369	2.36194	-4.22445	256.8	361.1	0.1013	97.5000	0.0940	0.1336
2-METHYLPENTANE	107-83-5	0.34965	0.82087	1.65903	-3.09737	256.6	329.1	0.1013	0.1013	0.0956	0.1182
3-METHYLPENTANE	96-14-0	0.30612	0.82268	1.77981	-1.66760	256.7	329.3	0.1013	0.1013	0.0970	0.1196
3-ETHYLPENTANE	617-78-7	0.38602	0.82159	1.64786	-2.12401	257.3	331.9	0.1013	0.1013	0.1029	0.1253
2,4-DIMETHYLPENTANE	108-08-7	0.33004	0.81906	1.79014	-0.96763	256.6	334.8	0.1013	0.1013	0.0920	0.1138
2,2,4-TRIMETHYLPENTANE	540-84-1	0.28256	0.83661	2.07206	-4.01104	190.0	620.0	0.0980	97.6000	0.0182	0.1495
2,3,4-TRIMETHYLPENTANE	565-75-3	0.27375	0.83040	2.11222	-2.27854	259.1	332.4	0.1013	0.1013	0.0955	0.1127
cycloalkanes											
CYCLOPENTANE	287-92-3	0.39596	0.82692	1.29392	-1.98829	223.2	454.4	0.1000	99.5000	0.0146	0.1628

Continued on next page

Table VII-25 – continued from previous page

Name	CAS	L -	M -	N -	$c * 10^6$ m^3/mol	T_{min} K	T_{max} K	P_{min} MPa	P_{max} MPa	λ_{min} $W.m^{-1}.K^{-1}$	λ_{max} $W.m^{-1}.K^{-1}$
CYCLOHEXANE	110-82-7	0.37295	0.81214	1.35210	-4.22316	280.8	633.1	0.1000	99.1000	0.0181	0.1446
CYCLOOCTANE	292-64-8	0.13238	0.83720	2.69425	-4.11952	288.7	398.1	0.1013	0.1013	0.1069	0.1205
alkenes											
ETHYLENE	74-85-1	0.25059	0.85349	1.38986	-3.29106	112.2	750.0	0.0981	97.0000	0.0097	0.2537
PROPYLENE	115-07-1	0.49144	0.84580	1.00415	-3.54614	180.0	639.9	0.0991	60.0000	0.0120	0.2017
1-BUTENE	106-98-9	0.16900	0.86165	2.37074	-3.51399	223.2	297.1	0.1013	0.1013	0.0159	0.1536
1-PENTENE	109-67-1	0.93092	1.00000	0.77055	-2.77104	257.4	301.7	0.1013	0.1013	0.1111	0.1284
1-HEXENE	592-41-6	1.07672	1.00000	0.72580	-2.19294	143.2	623.1	0.0980	98.0000	0.0174	0.1660
1-HEPTENE	592-76-7	0.56499	0.84233	1.35286	-1.50579	163.2	677.6	0.0980	98.0000	0.0186	0.1610
1-OCTENE	111-66-0	0.27542	0.84919	2.56229	-1.08424	200.0	573.1	0.0980	97.6800	0.0195	0.1677
1-NONENE	124-11-8	0.30523	0.83019	2.41586	2.25852	209.2	677.6	0.0980	98.0000	0.0623	0.1596
1-DECENE	872-05-9	0.33273	0.82463	2.40215	6.30277	218.7	677.6	0.0980	98.0000	0.0745	0.1596
1-DODECENE	112-41-4	0.47130	0.80552	2.02825	17.84439	278.8	677.6	0.0980	98.0000	0.0785	0.1722
1-TRIDECENE	2437-56-1	0.43221	0.80688	2.28050	24.19833	307.8	677.6	0.0980	49.0000	0.0834	0.1445
1-TETRADECENE	1120-36-1	0.48019	0.80161	2.20438	31.87092	273.1	677.6	0.0980	98.0000	0.0868	0.1580
1-PENTADECENE	13360-61-7	0.41834	0.80837	2.54360	27.08880	307.8	677.6	0.0980	49.0000	0.0902	0.1498
1-HEXADECENE	629-73-2	0.41849	0.80946	2.66470	32.32805	307.8	677.6	0.0980	49.0000	0.0920	0.1520
aromatics											
BENZENE	71-43-2	0.13487	0.84816	2.57900	-1.43896	248.2	681.5	0.0980	99.0000	0.0157	0.1758
m-XYLENE	108-38-3	0.41847	0.82958	1.62883	4.13384	258.2	698.9	0.0980	98.0665	0.0210	0.1583
p-XYLENE	106-42-3	0.22490	0.84934	2.55991	4.28703	287.3	701.4	0.0980	98.0665	0.0638	0.1488
ETHYLBENZENE	100-41-4	0.49914	0.82220	1.35401	2.70311	193.2	683.4	0.0980	99.4000	0.0209	0.1552
MESITYLENE	108-67-8	0.42214	0.83883	1.86363	7.29428	233.2	453.1	0.0980	99.7000	0.1056	0.1587
esters											
VINYL ACETATE	108-05-4	0.50644	0.76962	1.35637	10.25022	296.2	340.1	0.1013	0.1013	0.1365	0.1549
n-BUTYL ACETATE	123-86-4	0.22830	0.83168	2.87088	3.29714	273.0	624.0	0.0980	96.0000	0.0204	0.1670
ISOPENTYL ACETATE	123-92-2	0.27716	0.83598	2.78979	3.52813	273.0	624.5	0.0980	49.0000	0.0583	0.1440
n-PENTYL ACETATE	628-63-7	0.22449	0.82964	2.91053	7.29250	273.0	621.5	0.0980	96.0000	0.0647	0.1638
n-HEPTYL ACETATE	112-06-1	0.34941	0.82031	2.66490	3.47608	300.2	621.8	0.0980	98.0000	0.0875	0.1682
ethers											
DIMETHYL ETHER	115-10-6	0.61030	0.84979	0.96628	-2.19464	234.0	387.7	0.1446	30.6000	0.0135	0.1709
DI-n-PROPYL ETHER	111-43-3	0.27948	0.84272	2.37935	-3.93257	293.0	653.0	0.0980	49.0000	0.0200	0.1540
DI-n-BUTYL ETHER	142-96-1	0.45325	0.81484	1.82231	1.89035	223.2	677.1	0.0980	96.0000	0.0233	0.1590
DI-n-PENTYL ETHER	693-65-2	0.32305	0.83002	2.90319	3.99768	223.2	668.2	0.0980	49.0000	0.0780	0.1521
aldehydes											
ACETALDEHYDE	75-07-0	1.00471	1.00000	0.74345	13.77891	273.1	399.1	0.1010	0.1013	0.0201	0.2005
BUTANAL	123-72-8	0.98654	0.99999	0.79134	4.15781	273.1	628.1	0.1010	50.0810	0.0370	0.1640
2-METHYLPROPANAL	78-84-2	0.15543	0.84033	2.71150	5.34491	305.2	625.1	0.1010	50.0810	0.0310	0.1550

Continued on next page

Table VII-25 – continued from previous page

Name	CAS	L -	M -	N -	$C * 10^6$ m^3/mol	T_{min} K	T_{max} K	P_{min} MPa	P_{max} MPa	λ_{min} $W.m^{-1}.K^{-1}$	λ_{max} $W.m^{-1}.K^{-1}$
3-METHYLBUTYRALDEHYDE	590-86-3	1.09811	0.99269	0.83049	-2.16276	301.6	557.6	0.1010	50.0810	0.0310	0.1490
HEPTANAL	111-71-7	0.39590	0.85967	2.08077	1.54762	279.1	406.1	0.1013	0.1013	0.1137	0.1435
alcohols											
ETHANOL	64-17-5	1.11945	0.97724	1.14643	6.08287	190.8	678.5	0.0908	98.0661	0.0226	0.2198
1-PROPANOL	71-23-8	1.10666	0.93817	1.13228	3.07305	200.0	675.8	0.0975	60.0000	0.0240	0.1829
1-BUTANOL	71-36-3	1.38509	1.00000	0.85377	1.58248	193.2	718.9	0.0980	98.0000	0.0244	0.1881
1-PENTANOL	71-41-0	1.45953	1.00000	0.78797	1.17104	201.7	560.0	0.1000	60.0000	0.1173	0.1691
1-HEXANOL	111-27-3	1.58034	1.00000	0.70297	3.69615	235.6	602.0	0.1000	60.0000	0.0271	0.1809
1-HEPTANOL	111-70-6	1.78291	1.00000	0.61750	-4.37783	246.8	675.5	0.0980	98.0000	0.0257	0.1873
1-OCTANOL	111-87-5	2.25536	0.99996	0.48078	4.23212	257.2	628.1	0.1000	50.0000	0.0250	0.1814
1-NONANOL	143-08-8	2.30846	0.75926	0.53701	13.25322	273.1	623.5	0.1000	49.0500	0.0290	0.1893
1-DECANOL	112-30-1	2.43051	0.99998	0.45843	13.67306	273.1	623.0	0.0980	98.0000	0.0243	0.1900
1-UNDECANOL	112-42-5	1.87042	0.75624	0.68029	17.23437	301.6	621.1	0.1013	49.0500	0.0960	0.1926
1-DODECANOL	112-53-8	0.18171	0.79723	3.68542	23.01208	308.6	624.4	0.1000	50.0000	0.0883	0.1854
1-OCTADECANOL	112-92-5	0.25776	0.79520	3.74512	66.66800	337.1	473.1	0.1013	0.1013	0.1497	0.1826
amines											
METHYLAMINE	74-89-5	1.30335	1.00000	0.57812	2.17260	293.1	403.1	2.0000	50.0000	0.1400	0.2720
n-BUTYLAMINE	109-73-9	0.17659	0.81642	2.56447	-1.45129	273.1	323.1	0.1013	0.1013	0.1541	0.1659
DIETHYLAMINE	109-89-7	1.18755	0.94265	0.65976	2.69022	273.1	422.1	0.1010	0.1013	0.0250	0.1754
n-PENTYLAMINE	110-58-7	0.17435	0.82501	3.00408	0.35495	223.2	323.1	0.1013	0.1013	0.1522	0.1716
DI-n-PROPYLAMINE	142-84-7	0.26764	0.83903	2.73460	-8.89796	223.2	323.1	0.1013	0.1013	0.1224	0.1538
n-HEXYLAMINE	111-26-2	0.19688	0.82294	3.04755	2.25658	273.1	373.1	0.1013	0.1013	0.1428	0.1570
n-OCTYLAMINE	111-86-4	0.26825	0.82301	3.04611	3.13253	298.1	423.1	0.1013	0.1013	0.1342	0.1503
n-DECYLAMINE	2016-57-1	0.31961	0.82156	3.07705	10.34059	298.1	448.1	0.1013	0.1013	0.1347	0.1503
HFC-CFC											
DIFLUOROMETHANE	75-10-5	0.28640	0.85516	2.05370	7.24952	153.2	465.6	0.0960	50.0000	0.0096	0.2436
1,1-DIFLUOROETHANE	75-37-6	0.29530	0.84627	1.95800	5.68966	163.2	463.0	0.0940	55.0000	0.0109	0.1712
TRIFLUOROMETHANE	75-46-7	0.38687	0.84268	1.57513	2.94268	118.7	473.1	0.1000	60.0000	0.0103	0.1947
1,1,1-TRIFLUOROETHANE	420-46-2	0.28849	0.84321	1.91206	4.85288	233.2	499.0	0.1013	50.0000	0.0096	0.1121
CHLORODIFLUOROMETHANE	75-45-6	0.52400	0.82812	1.11421	-0.09471	114.0	514.3	0.1000	60.0000	0.0066	0.1750
1-CHLORO-1,1-DIFLUOROETHANE	75-68-3	0.36281	0.82781	1.49017	0.11017	193.2	504.6	0.1000	69.5827	0.0109	0.1264
1,1,1,2-TETRAFLUOROETHANE	811-97-2	0.28510	0.83200	2.11744	2.26973	169.9	533.0	0.0900	70.0060	0.0083	0.1456
DICHLORODIFLUOROMETHANE	75-71-8	0.14934	0.85868	2.41594	-4.21947	124.4	600.0	0.0980	60.0000	0.0084	0.1347
CHLOROTRIFLUOROMETHANE	75-72-9	0.14133	0.85841	2.41981	-3.89034	92.5	451.9	0.0980	60.0000	0.0095	0.1401
PENTAFLUOROETHANE	354-33-6	0.25689	0.84291	2.24835	-1.53555	187.4	513.2	0.0910	69.8630	0.0092	0.1236
DICHLOROFLUOROMETHANE	75-43-4	0.15072	0.84821	2.44409	-1.78708	148.2	473.1	0.1000	60.0000	0.0082	0.1594
TRICHLOROFLUOROMETHANE	75-69-4	0.35915	0.82967	1.36748	-4.73846	168.2	523.1	0.0900	60.0000	0.0077	0.1304
BROMOTRIFLUOROMETHANE	75-63-8	1.32456	0.89300	0.44573	-3.27621	105.2	435.8	0.0900	58.9400	0.0084	0.1173

Continued on next page

Table VII-25 – continued from previous page

Name	CAS	L -	M -	N -	$c * 10^6$ m^3/mol	T_{min} K	T_{max} K	P_{min} MPa	P_{max} MPa	λ_{min} $W.m^{-1}.K^{-1}$	λ_{max} $W.m^{-1}.K^{-1}$
1,1,1,3,3,3-HEXAFLUOROPROPANE	690-39-1	0.87288	0.85453	1.01805	-2.31167	252.6	374.6	0.0900	30.0000	0.0111	0.0973
1,1,1,2,3,3-HEXAFLUOROPROPANE	431-63-0	0.22531	0.82242	2.51089	-1.95011	286.5	333.8	0.0900	0.5150	0.0135	0.0171
CHLOROPENTAFLUOROETHANE	76-15-3	0.71852	0.87018	0.95712	-6.22075	173.2	443.0	0.1000	60.0000	0.0096	0.1047
1,1,1,2,3,3,3-HEPTAFLUOROPROPANE	431-89-0	1.18998	0.99998	0.72595	-1.70550	259.3	344.2	0.0915	2.9380	0.0105	0.0609
1,2-DICHLOROTETRAFLUOROETHANE	76-14-2	0.15228	0.84461	2.63850	-5.05369	183.2	423.1	0.1000	75.0500	0.0099	0.0962
noble gases											
NEON	7440-01-9	0.18850	0.94691	1.47057	-2.35725	25.0	350.0	0.0933	99.1759	0.0078	0.1999
ARGON	7440-37-1	0.12268	0.90452	1.85408	-3.29332	86.6	1200.0	0.0930	98.6000	0.0059	0.1532
KRYPTON	7439-90-9	0.10130	0.89545	1.95004	-3.33250	116.0	1300.0	0.0933	95.0000	0.0044	0.1094
others											
AMMONIA	7664-41-7	0.22737	0.86452	2.33201	4.03062	199.0	723.5	0.1000	80.1000	0.0188	0.6699
WATER	7732-18-5	0.38720	0.87198	1.96692	5.27106	273.1	1190.2	0.0980	98.6000	0.0244	0.7770
CARBON MONOXIDE	630-08-0	0.09967	0.87823	2.15086	-3.67664	78.2	429.1	0.1013	12.5100	0.0251	0.1486
NITROGEN	7727-37-9	0.12427	0.88981	2.01285	-3.64285	68.7	1000.0	0.0980	98.3900	0.0074	0.1888
OXYGEN	7782-44-7	0.23391	0.88957	1.30528	-2.76205	66.0	1200.0	0.0980	68.4110	0.0084	0.2021
CARBON DIOXIDE	124-38-9	0.17800	0.85903	2.41074	-1.13352	196.8	1300.0	0.0906	98.6000	0.0093	0.2004
CHLOROFORM	67-66-3	0.22533	0.83791	1.98744	-4.91516	213.2	422.1	0.1010	0.1013	0.0093	0.1536

VII-B-2) Component-specific parameters

Component-specific parameters (a_1, a_2, b_1, b_2, c and d) to be used in the below equation for the viscosity estimation are reported in Table VII-2.

$$\begin{cases} \ln\left(\dfrac{\lambda}{\lambda_{\mathrm{ref}}^{\mathrm{Rosenfeld,intDoF}}}\right)_{\mathrm{calc}} = \left[\left(\dfrac{a_1 + a_2 X_{\mathrm{ES}}^{1/3}}{1 + e^{cX_{\mathrm{ES}}}}\right) + \left(\dfrac{b_1 + b_2 X_{\mathrm{ES}}^{1/3}}{1 + e^{-cX_{\mathrm{ES}}}}\right)\right] X_{\mathrm{ES}} + d \\ X_{\mathrm{ES}} = -\left(\dfrac{s_{\mathrm{Tv-res}}}{s_{\mathrm{Tv-res}}^{c}}\right) - \ln\left(\dfrac{s_{\mathrm{Tv-res}}}{s_{\mathrm{Tv-res}}^{c}} \times f_{\mathrm{corr}}(T)\right) \\ f_{\mathrm{corr}}(T) = 1 + \left(\dfrac{T - T_{\mathrm{c}}}{T_{\mathrm{c}}}\right)^3 \\ \lambda_{\mathrm{ref}}^{\mathrm{Rosenfeld,intDoF}} = \rho_{\mathrm{N}}^{2/3} \sqrt{\mathrm{k_b} T / \mathrm{m_0}} \left[1 + \left(\dfrac{C_v^{real}}{R}\right) e^{\left(-\rho/\rho_c\right)}\right] \\ \tilde{s}_{\mathrm{Tv-res}} = \dfrac{s_{Tv-res}}{R} \end{cases} \quad \text{(VII– 3)}$$

The Tv-residual entropy ($s_{\mathrm{Tv-res}}$), the molecular density (ρ_{N}) and ($C_{\mathrm{v}}^{\mathrm{real}}$) were estimated using the *I*-PC-SAFT EoS.

Table VII-26 - Component-specific parameters suitable for the *tc-PR* based model with the corresponding number of experimental data points and MAPE

Name	a_1	a_2	b_1	b_2	c	d	α	nb data	MAPE
n-alkanes								22045	3.47
METHANE	-0.485782	-0.064751	0.255949	0.135421	0.635269	0.328202	0.000000	4318	4.22
ETHANE	-0.622135	-0.152013	0.266964	0.119855	0.670439	0.278311	0.000000	2231	4.37
n-BUTANE	-0.705180	-0.199375	0.480998	0.010000	0.600247	0.219821	0.000000	2999	2.89
n-PENTANE	-0.655994	-0.172043	0.468309	0.010000	0.638085	0.191709	0.000000	918	2.84
n-HEXANE	-0.674448	-0.176807	0.468381	0.010000	0.669276	0.160953	0.000000	943	3.43
n-HEPTANE	-0.774167	-0.222808	0.528282	0.027597	0.500521	0.174107	0.000000	1624	3.34
n-OCTANE	-0.695488	-0.185462	0.453267	0.010000	0.693134	0.138799	0.000000	681	3.05
n-NONANE	-0.583211	-0.130691	0.324088	0.134288	0.500000	0.164922	0.000000	800	3.12
n-DECANE	-0.723041	-0.195784	0.480504	0.050457	0.500000	0.166928	0.000000	1218	3.61
n-UNDECANE	-0.642880	-0.158878	0.341901	0.129080	0.500000	0.147118	0.000000	621	3.72
n-DODECANE	-0.538783	-0.117759	0.311124	0.100845	0.500000	0.326925	0.000000	655	2.91
n-TRIDECANE	-0.587685	-0.144181	0.430818	0.010093	0.500000	0.435898	0.000000	699	3.42
n-TETRADECANE	-0.607743	-0.140614	0.192881	0.232548	0.500299	0.100021	0.000000	693	2.02
n-PENTADECANE	-0.623462	-0.147422	0.192496	0.234520	0.500303	0.100607	0.000000	561	2.08
n-HEXADECANE	-0.605168	-0.137930	0.143934	0.263459	0.502342	0.100003	0.000000	684	2.51
n-HEPTADECANE	-0.625406	-0.147424	0.185115	0.208814	0.502283	0.145098	0.000000	762	2.90
n-OCTADECANE	-0.643496	-0.152698	0.183353	0.225006	0.548238	0.100000	0.000000	602	3.34
n-NONADECANE	-0.688573	-0.173405	0.353918	0.078056	0.628911	0.164517	0.000000	544	4.48
n-EICOSANE	-0.696096	-0.176391	0.353918	0.078056	0.628911	0.164517	0.000000	214	4.43
n-HENEICOSANE	-0.777503	-0.211486	0.353918	0.078056	0.628911	0.164517	0.000000	96	4.38
n-TRICOSANE	-0.729546	-0.190247	0.353918	0.078056	0.628911	0.164517	0.000000	84	2.55
n-TETRACOSANE	-0.833943	-0.234757	0.353918	0.078056	0.628911	0.164517	0.000000	98	4.50
branched alkanes								2813	3.46
ISOBUTANE	-0.677281	-0.191580	0.481946	0.010000	0.631984	0.176305	0.000000	2195	3.66
ISOPENTANE	-0.667857	-0.185902	0.018686	0.339089	0.500032	0.100000	0.000000	55	1.56
2,2-DIMETHYLBUTANE	-0.419412	-0.058706	0.353918	0.078056	0.628911	0.164517	0.000000	17	1.80
2,3-DIMETHYLBUTANE	-0.509732	-0.102349	0.353918	0.078056	0.628911	0.164517	0.000000	33	1.75
2-METHYLPENTANE	-0.603723	-0.149205	0.353918	0.078056	0.628911	0.164517	0.000000	18	2.55
3-METHYLPENTANE	-0.476528	-0.083439	0.353918	0.078056	0.628911	0.164517	0.000000	20	1.84
3-ETHYLPENTANE	-0.544600	-0.120813	0.353918	0.078056	0.628911	0.164517	0.000000	16	1.85
2,4-DIMETHYLPENTANE	-0.448869	-0.072141	0.353918	0.078056	0.628911	0.164517	0.000000	17	1.24
2,2,4-TRIMETHYLPENTANE	-0.578698	-0.129905	0.504739	0.010000	0.500000	0.100000	0.000000	427	3.24
2,3,4-TRIMETHYLPENTANE	-0.493818	-0.099556	0.353918	0.078056	0.628911	0.164517	0.000000	15	0.43
cycloalkanes								906	2.61
CYCLOPENTANE	-0.868930	-0.271379	0.593795	0.010000	0.500000	0.100000	0.000000	142	0.56
CYCLOHEXANE	-0.712369	-0.214580	0.499206	0.010000	0.566180	0.248283	0.000000	748	3.01
CYCLOOCTANE	-0.671010	-0.196581	0.531572	0.000000	0.547104	0.249851	0.000000	16	2.12

Continued on next page

Table VII-26 – continued from previous page

Name	a_1	a_2	b_1	b_2	c	d	α	nb data	MAPE
alkenes								4974	3.10
ETHYLENE	-0.593046	-0.137074	0.177500	0.162149	0.713914	0.326708	0.000000	1106	3.38
PROPYLENE	-0.588828	-0.144802	0.195007	0.154658	0.736098	0.263961	0.000000	820	3.69
1-PENTENE	-0.663657	-0.168057	0.411030	0.042540	0.661050	0.135467	0.000000	12	1.20
1-HEXENE	-0.629119	-0.156379	0.440534	0.017701	0.722647	0.140302	0.000000	285	2.33
1-HEPTENE	-0.621718	-0.148224	0.455950	0.010001	0.729585	0.100000	0.000000	434	2.54
1-OCTENE	-0.781822	-0.226836	0.530154	0.010025	0.500007	0.256978	0.000000	452	3.50
1-NONENE	-0.626759	-0.154574	0.411030	0.042540	0.661050	0.135467	0.000000	285	4.43
1-DECENE	-0.561302	-0.121182	0.411030	0.042540	0.661050	0.135467	0.000000	274	2.94
1-DODECENE	-0.572728	-0.126664	0.411030	0.042540	0.661050	0.135467	0.000000	287	1.82
1-TRIDECENE	-0.581679	-0.127260	0.411030	0.042540	0.661050	0.135467	0.000000	246	2.06
1-TETRADECENE	-0.574973	-0.123836	0.411030	0.042540	0.661050	0.135467	0.000000	275	3.05
1-PENTADECENE	-0.605834	-0.139404	0.411030	0.042540	0.661050	0.135467	0.000000	249	1.59
1-HEXADECENE	-0.569896	-0.123040	0.411030	0.042540	0.661050	0.135467	0.000000	249	3.85
aromatics								3095	2.40
BENZENE	-0.655572	-0.179205	0.462339	0.010000	0.663685	0.222050	0.000000	967	2.68
m-XYLENE	-0.519691	-0.109418	0.351288	0.087854	0.596067	0.219710	0.000000	656	2.44
p-XYLENE	-0.550570	-0.122244	0.382933	0.059714	0.617596	0.227395	0.000000	641	2.13
ETHYLBENZENE	-0.488843	-0.095821	0.320883	0.099043	0.653439	0.175687	0.000000	692	2.12
MESITYLENE	-0.625362	-0.158486	0.382933	0.059714	0.617596	0.227395	0.000000	139	2.95
esters								772	5.54
VINYL ACETATE	-1.055675	-0.357313	0.498663	0.307117	0.259044	0.159318	0.000000	6	1.37
n-BUTYL ACETATE	-0.627431	-0.176432	0.450417	0.024920	0.500000	0.518202	0.000000	260	3.10
ISOPENTYL ACETATE	-0.572525	-0.111243	0.498663	0.307117	0.259044	0.159318	0.000000	148	9.44
n-PENTYL ACETATE	-0.699678	-0.186167	0.498663	0.307117	0.259044	0.159318	0.000000	151	9.66
n-HEPTYL ACETATE	-0.795562	-0.219969	0.498663	0.307117	0.259044	0.159318	0.000000	207	2.95
ethers								882	2.51
DIMETHYL ETHER	-0.688332	-0.206693	0.377805	0.053697	0.696871	0.308523	0.000000	331	1.85
DI-n-PROPYL ETHER	-0.767419	-0.217028	0.525700	0.010000	0.500000	0.309249	0.000000	115	1.60
DI-n-BUTYL ETHER	-0.723048	-0.210596	0.497192	0.010048	0.500062	0.399522	0.000000	257	2.62
DI-n-PENTYL ETHER	-0.673023	-0.177431	0.472293	0.000000	0.506818	0.383230	0.000000	179	4.13
aldehydes								354	3.56
ACETALDEHYDE	-0.908523	-0.311769	0.495242	0.000279	0.791391	0.240294	0.000000	13	2.20
BUTANAL	-0.462859	-0.084596	0.471176	0.010000	0.665829	0.397458	0.000000	137	3.22
2-METHYLPROPANAL	-0.800169	-0.258354	0.551834	0.010000	0.500000	0.443416	0.000000	139	5.13
3-METHYLBUTYRALDEHYDE	-0.640956	-0.159079	0.338070	0.182450	0.500003	0.100001	0.000000	53	1.06
HEPTANAL	-0.494256	-0.086047	0.495242	0.000279	0.791391	0.240294	0.000000	12	1.68
alcohols								3136	3.65
ETHANOL	-0.467792	-0.111322	0.010000	0.249273	0.840976	0.442210	0.000000	798	3.93

Continued on next page

Table VII-26 – continued from previous page

Name	a_1	a_2	b_1	b_2	c	d	α	nb data	MAPE
1-PROPANOL	-0.600654	-0.172319	0.161048	0.167074	0.835477	0.367949	0.000000	384	3.61
1-BUTANOL	-0.512877	-0.131457	0.012772	0.245232	0.719255	0.443549	0.000000	342	3.89
1-PENTANOL	-0.492323	-0.113641	-0.145196	0.338303	1.234875	0.358142	0.000000	145	3.28
1-HEXANOL	-0.706448	-0.201204	0.465847	0.011817	0.726735	0.114733	0.000000	269	2.58
1-HEPTANOL	-0.726776	-0.210166	0.442898	0.059445	0.588354	0.101358	0.000000	280	3.05
1-OCTANOL	-0.686731	-0.195009	0.374523	0.057452	0.723492	0.151134	0.000000	222	3.49
1-NONANOL	-0.699817	-0.199449	0.469951	0.010000	0.700000	0.100000	0.000000	188	2.82
1-DECANOL	-0.741862	-0.211931	0.528258	0.045835	0.504402	0.104403	0.000000	306	4.17
1-UNDECANOL	-0.448828	-0.088632	-0.145196	0.338303	1.234875	0.358142	0.000000	92	3.79
1-DODECANOL	-0.386374	-0.055979	-0.145196	0.338303	1.234875	0.358142	0.000000	94	6.24
1-OCTADECANOL	-0.693065	-0.182397	-0.145196	0.338303	1.234875	0.358142	0.000000	16	2.94
amines								138	4.19
METHYLAMINE	-0.481831	-0.080904	0.063082	0.229388	0.749849	0.240294	0.000000	125	3.76
DIETHYLAMINE	-0.597587	-0.152681	0.063082	0.229388	0.749849	0.240294	0.000000	13	8.33
HFC-CFC								20121	3.17
DIFLUOROMETHANE	-0.877853	-0.286920	0.250254	0.095587	0.900315	0.375587	0.000000	1136	2.80
1,1-DIFLUOROETHANE	-0.755097	-0.227931	0.350068	0.062577	0.765587	0.305816	0.000000	765	2.55
TRIFLUOROMETHANE	-0.790195	-0.242489	0.165986	0.148228	0.834559	0.330864	0.000000	614	3.50
1,1,1-TRIFLUOROETHANE	-0.613254	-0.139912	0.230229	0.131502	0.800519	0.262013	0.000000	695	3.27
CHLORODIFLUOROMETHANE	-0.731046	-0.220116	0.213838	0.134163	0.777854	0.285063	0.000000	2039	3.09
1-CHLORO-1,1-DIFLUOROETHANE	-0.568846	-0.124940	0.249549	0.133546	0.697234	0.189912	0.000000	467	2.51
1,1,1,2-TETRAFLUOROETHANE	-0.701133	-0.186125	0.332582	0.076868	0.746731	0.239442	0.000000	6868	3.38
DICHLORODIFLUOROMETHANE	-0.786825	-0.239047	0.442594	0.010000	0.743488	0.218007	0.000000	1384	2.93
CHLOROTRIFLUOROMETHANE	-0.837011	-0.268991	0.389099	0.035583	0.776844	0.273183	0.000000	711	3.95
PENTAFLUOROETHANE	-0.641058	-0.138610	0.283233	0.101407	0.744443	0.200116	0.000000	2205	2.97
DICHLOROFLUOROMETHANE	-0.720492	-0.220784	0.304210	0.082509	0.722469	0.345395	0.000000	480	2.09
TRICHLOROFLUOROMETHANE	-0.669276	-0.186808	0.195628	0.150017	0.699966	0.258994	0.000000	749	3.13
BROMOTRIFLUOROMETHANE	-0.650546	-0.190438	0.104915	0.190440	0.784555	0.320286	0.000000	552	3.42
1,1,1,3,3,3-HEXAFLUOROPROPANE	-0.741696	-0.218054	0.470278	0.010127	0.663966	0.244502	0.000000	230	1.79
CHLOROPENTAFLUOROETHANE	-0.659270	-0.174016	0.264784	0.171657	0.509458	0.268517	0.000000	543	5.92
1,1,1,2,3,3,3-HEPTAFLUOROPROPANE	-0.448088	-0.043976	0.199658	0.174476	0.703318	0.100000	0.000000	533	1.51
1,2-DICHLOROTETRAFLUOROETHANE	-0.848153	-0.281699	0.510205	0.010724	0.500788	0.409110	0.000000	150	2.31
noble gases								10725	2.45
NEON	-0.610694	-0.104448	0.358217	0.082128	0.630364	0.454304	0.016202	1336	2.93
ARGON	-0.465794	-0.058629	0.243301	0.143182	0.627379	0.435157	0.013208	7464	2.43
KRYPTON	-0.504315	-0.094379	0.266584	0.130009	0.628214	0.433764	0.008935	1925	2.21
others								14636	3.89
AMMONIA	-0.764113	-0.212525	0.010000	0.235494	0.909176	0.492831	0.000000	1020	5.48
WATER	-1.206945	-0.513449	0.238543	0.091827	0.892984	0.678279	0.000000	5503	4.38

Continued on next page

Table VII-26 – continued from previous page

Name	a_1	a_2	b_1	b_2	c	d	α	nb data	MAPE
NITROGEN	-0.486028	-0.070347	0.132362	0.195417	0.690793	0.393988	0.022338	2900	3.12
OXYGEN	-0.522939	-0.111537	0.116244	0.198844	0.703804	0.384135	0.011675	2012	3.82
CARBON DIOXIDE	-0.546972	-0.076171	0.110569	0.202159	0.695068	0.311639	0.075661	3086	3.31
CHLOROFORM	-0.875317	-0.291121	0.373876	0.073848	0.614146	0.253961	0.000000	115	2.78

VII-B-3) Chemical-family specific parameters

VII-B-3.1) Paraffins

Table VII-27 – Chemical-family specific parameters for paraffins to be used with the *tc*-PR based model

Variable	Value
nb component	30
nb data	18309
MAPE	5.88
a_1	-0.566063
a_2	-0.122197
b_1	0.353918
b_2	0.078056
c	0.628911
d	0.164517

Table VII-28 - Prediction of the thermal conductivity data of paraffins using chemical-family specific parameters for the *tc*-PR based model: data number and corresponding MAPE (Mean Absolute Percentage Error).

Name	nb data	MAPE
n-BUTANE	2999	4.47
n-PENTANE	918	3.20
n-HEXANE	943	4.69
n-HEPTANE	1624	4.05
n-OCTANE	681	5.03
n-NONANE	800	4.08
n-DECANE	1218	4.28
n-UNDECANE	621	4.69
n-DODECANE	655	3.44
n-TRIDECANE	699	4.24
n-TETRADECANE	693	3.16
n-PENTADECANE	561	3.58
n-HEXADECANE	684	3.99
n-HEPTADECANE	762	5.82
n-OCTADECANE	602	7.60
n-NONADECANE	544	9.57
n-EICOSANE	214	7.73
n-HENEICOSANE	96	11.20
n-TRICOSANE	84	12.92
n-TETRACOSANE	98	14.66
ISOBUTANE	2195	9.94
ISOPENTANE	55	7.66
2,2-DIMETHYLBUTANE	17	19.28
2,3-DIMETHYLBUTANE	33	12.74
2-METHYLPENTANE	18	10.95
3-METHYLPENTANE	20	11.94
3-ETHYLPENTANE	16	12.43
2,4-DIMETHYLPENTANE	17	16.00
2,2,4-TRIMETHYLPENTANE	427	22.67
2,3,4-TRIMETHYLPENTANE	15	23.52

VII-B-3.2) Cycloalkanes

Table VII-29 - Chemical-family specific parameters for cycloalkanes to be used with the *tc*-PR based model

Variable	Value
nb component	3
nb data	906
MAPE	3.70
a_1	-0.762471
a_2	-0.238550
b_1	0.531572
b_2	0.000000
c	0.547104
d	0.249851

Table VII-30 - Prediction of the thermal conductivity data of cycloalkanes using chemical-family specific parameters for the *tc*-PR based model: data number and corresponding MAPE (Mean Absolute Percentage Error).

Name	nb data	MAPE
CYCLOPENTANE	142	6.91
CYCLOHEXANE	748	3.02
CYCLOOCTANE	16	7.12

VII-B-3.3) Alkenes

Table VII-31 - Chemical-family specific parameters for alkenes to be used with the *tc*-PR-SAFT based model

Variable	Value
nb component	12
nb data	3051
MAPE	3.68
a_1	-0.600875
a_2	-0.138294
b_1	0.411030
b_2	0.042540
c	0.661050
d	0.135467

Table VII-32 - Prediction of the thermal conductivity data of alkenes using chemical-family specific parameters for the *I*-PC-SAFT based model: data number and corresponding MAPE (Mean Absolute Percentage Error).

Name	nb data	MAPE
1-BUTENE	3	6.72
1-PENTENE	12	3.74
1-HEXENE	285	3.41
1-HEPTENE	434	2.68
1-OCTENE	452	6.06
1-NONENE	285	6.07
1-DECENE	274	5.21
1-DODECENE	287	3.26
1-TRIDECENE	246	1.09
1-TETRADECENE	275	2.40
1-PENTADECENE	249	1.67
1-HEXADECENE	249	3.39

VII-B-3.4) Aromatics

Table VII-33 - Chemical-family specific parameters for aromatics to be used with the *tc*-PR based model

Variable	Value
nb component	5
nb data	3095
MAPE	4.33
a_1	-0.564848
a_2	-0.132489
b_1	0.382933
b_2	0.059714
c	0.617596
d	0.227395

Table VII-34 - Prediction of the thermal conductivity data of aromatics using chemical-family specific parameters for the *tc*-PR based model: data number and corresponding MAPE (Mean Absolute Percentage Error).

Name	nb data	MAPE
BENZENE	967	3.62
m-XYLENE	656	2.92
p-XYLENE	641	3.70
ETHYLBENZENE	692	6.37
MESITYLENE	139	8.67

VII-B-3.5) Esters

Table VII-35 - Chemical-family specific parameters for esters to be used with the *tc*-PR based model

Variable	Value
nb component	5
nb data	772
MAPE	7.83
a_1	-0.880283
a_2	-0.267208
b_1	0.498663
b_2	0.307117
c	0.259044
d	0.159318

Table VII-36 - Prediction of the thermal conductivity data of esters using chemical-family specific parameters for the *tc*-PR based model: data number and corresponding MAPE (Mean Absolute Percentage Error).

Name	nb data	MAPE
VINYL ACETATE	6	2.84
n-BUTYL ACETATE	260	5.44
ISOPENTYL ACETATE	148	9.76
n-PENTYL ACETATE	151	15.99
n-HEPTYL ACETATE	207	3.66

VII-B-3.6) Ethers

Table VII-37 - Chemical-family specific parameters for ethers to be used with the *tc*-PR based model

Variable	Value
nb component	4
nb data	882
MAPE	4.32
a_1	-0.660280
a_2	-0.175985
b_1	0.472293
b_2	0.000000
c	0.663869
d	0.269014

Table VII-38 - Prediction of the thermal conductivity data of ethers using chemical-family specific parameters for the *tc*-PR based model: data number and corresponding MAPE (Mean Absolute Percentage Error).

Name	nb data	MAPE
DIMETHYL ETHER	331	3.19
DI-n-PROPYL ETHER	115	5.28
DI-n-BUTYL ETHER	257	3.37
DI-n-PENTYL ETHER	179	7.16

VII-B-3.7) Aldehydes

Table VII-39 - Chemical-family specific parameters for aldehydes to be used with the *tc*-PR based model

Variable	Value
nb component	5
nb data	354
MAPE	5.39
a_1	-0.533845
a_2	-0.112440
b_1	0.495242
b_2	0.000279
c	0.791391
d	0.240294

Table VII-40 - Prediction of the thermal conductivity data of aldehydes using chemical-family specific parameters for the *tc*-PR based model: data number and corresponding MAPE (Mean Absolute Percentage Error).

Name	nb data	MAPE
ACETALDEHYDE	13	7.43
BUTANAL	137	3.45
2-METHYLPROPANAL	139	6.27
3-METHYLBUTYRALDEHYDE	53	7.16
HEPTANAL	12	7.34

VII-B-3.8) Alcohols

Table VII-41 - Chemical-family specific parameters for alcohols to be used with the *tc*-PR based model

Variable	Value
nb component	12
nb data	3136
MAPE	5.78
a_1	-0.473494
a_2	-0.104158
b_1	-0.145196
b_2	0.338303
c	1.234875
d	0.358142

Table VII-42 - Prediction of the thermal conductivity data of alcohols using chemical-family specific parameters for the *tc*-PR based model: data number and corresponding MAPE (Mean Absolute Percentage Error).

Name	nb data	MAPE
ETHANOL	798	4.73
1-PROPANOL	384	4.61
1-BUTANOL	342	5.16
1-PENTANOL	145	3.56
1-HEXANOL	269	5.21
1-HEPTANOL	280	5.45
1-OCTANOL	222	6.27
1-NONANOL	188	8.65
1-DECANOL	306	6.49
1-UNDECANOL	92	4.83
1-DODECANOL	94	13.59
1-OCTADECANOL	16	41.07

VII-B-3.9) Amines

Table VII-43 - Chemical-family specific amines for paraffins to be used with the *tc*-PR based model

Variable	Value
nb component	8
nb data	158
MAPE	5.50
a_1	-0.552544
a_2	-0.123667
b_1	0.063082
b_2	0.229388
c	0.749849
d	0.240294

Table VII-44 - Prediction of the thermal conductivity data of amines using chemical-family specific parameters for the *tc*-PR based model: data number and corresponding MAPE (Mean Absolute Percentage Error).

Name	nb data	MAPE
METHYLAMINE	125	4.21
n-BUTYLAMINE	3	10.20
DIETHYLAMINE	13	10.40
n-PENTYLAMINE	3	20.48
DI-n-PROPYLAMINE	3	5.56
n-HEXYLAMINE	4	8.23
n-OCTYLAMINE	4	7.08
n-DECYLAMINE	3	12.57

VII-B-3.10) HFC-CFC

Table VII-45 - Chemical-family specific parameters for HFC-CFCs to be used with the *tc*-PR based model

Variable	Value
nb component	18
nb data	20289
MAPE	5.78
a_1	-0.817787
a_2	-0.259761
b_1	0.415651
b_2	0.020498
c	0.768905
d	0.266016

Table VII-46 - Prediction of the thermal conductivity data of HFC-CFCs using chemical-family specific parameters for the *tc*-PR based model: data number and corresponding MAPE (Mean Absolute Percentage Error).

Name	nb data	MAPE
DIFLUOROMETHANE	1136	18.96
1,1-DIFLUOROETHANE	765	3.59
TRIFLUOROMETHANE	614	10.81
1,1,1-TRIFLUOROETHANE	695	4.13
CHLORODIFLUOROMETHANE	2039	4.45
1-CHLORO-1,1-DIFLUOROETHANE	467	9.02
1,1,1,2-TETRAFLUOROETHANE	6868	4.05
DICHLORODIFLUOROMETHANE	1384	4.33
CHLOROTRIFLUOROMETHANE	711	4.52
PENTAFLUOROETHANE	2205	4.84
DICHLOROFLUOROMETHANE	480	4.98
TRICHLOROFLUOROMETHANE	749	6.29
BROMOTRIFLUOROMETHANE	552	8.56
1,1,1,3,3,3-HEXAFLUOROPROPANE	230	5.91
1,1,1,2,3,3-HEXAFLUOROPROPANE	168	4.86
CHLOROPENTAFLUOROETHANE	543	8.46
1,1,1,2,3,3,3-HEPTAFLUOROPROPANE	533	4.26
1,2-DICHLOROTETRAFLUOROETHANE	150	11.59

VII-B-4) Universal parameters

Table VII-47 - Universal parameters to be used with the *tc*-PR based model

Variable	Value
nb component	106
nb data	59427
MAPE	9.19
a_1	-0.489129
a_2	-0.092260
b_1	0.063082
b_2	0.229388
c	0.749849
d	0.240294

Table VII-48 - Prediction of thermal conductivity data using universal parameters for the *tc*-PR based model: data number and corresponding MAPE (Mean Absolute Percentage Error).

Name	nb data	MAPE
n-alkanes	22045	7.47
METHANE	4318	8.95
ETHANE	2231	5.53
n-BUTANE	2999	10.07
n-PENTANE	918	8.37
n-HEXANE	943	5.90
n-HEPTANE	1624	5.90
n-OCTANE	681	5.88
n-NONANE	800	6.64
n-DECANE	1218	6.48
n-UNDECANE	621	5.89
n-DODECANE	655	4.57
n-TRIDECANE	699	5.12
n-TETRADECANE	693	3.11
n-PENTADECANE	561	3.93
n-HEXADECANE	684	5.45
n-HEPTADECANE	762	7.87
n-OCTADECANE	602	10.03
n-NONADECANE	544	11.82
n-EICOSANE	214	10.67
n-HENEICOSANE	96	14.00
n-TRICOSANE	84	15.55
n-TETRACOSANE	98	17.11
branched alkanes	2813	16.46
ISOBUTANE	2195	15.36
ISOPENTANE	55	6.90
2,2-DIMETHYLBUTANE	17	19.51
2,3-DIMETHYLBUTANE	33	12.29
2-METHYLPENTANE	18	10.95
3-METHYLPENTANE	20	11.67
3-ETHYLPENTANE	16	10.34
2,4-DIMETHYLPENTANE	17	14.73
2,2,4-TRIMETHYLPENTANE	427	24.13
2,3,4-TRIMETHYLPENTANE	15	20.54
cycloalkanes	906	16.80
CYCLOPENTANE	142	8.90
CYCLOHEXANE	748	17.79
CYCLOOCTANE	16	40.65
alkenes	4977	6.38
ETHYLENE	1106	8.27
PROPYLENE	820	4.47
1-BUTENE	3	7.78
1-PENTENE	12	2.57
1-HEXENE	285	7.80
1-HEPTENE	434	6.26
1-OCTENE	452	7.79
1-NONENE	285	10.85
1-DECENE	274	8.57
1-DODECENE	287	5.30
1-TRIDECENE	246	3.05
1-TETRADECENE	275	3.54
1-PENTADECENE	249	2.85
1-HEXADECENE	249	4.17
aromatics	3095	9.92
BENZENE	967	7.18
m-XYLENE	656	11.32
p-XYLENE	641	7.06
ETHYLBENZENE	692	16.60

Continued on next page

Table 2.24 – continued from previous page

Name	nb data	MAPE
MESITYLENE	139	2.37
esters	772	9.50
VINYL ACETATE	6	5.58
n-BUTYL ACETATE	260	5.24
ISOPENTYL ACETATE	148	13.02
n-PENTYL ACETATE	151	18.03
n-HEPTYL ACETATE	207	6.23
ethers	882	6.15
DIMETHYL ETHER	331	4.48
DI-n-PROPYL ETHER	115	9.52
DI-n-BUTYL ETHER	257	4.55
DI-n-PENTYL ETHER	179	9.37
aldehydes	354	9.30
ACETALDEHYDE	13	6.48
BUTANAL	137	9.16
2-METHYLPROPANAL	139	8.90
3-METHYLBUTYRALDEHYDE	53	11.51
HEPTANAL	12	8.65
alcohols	3136	18.73
ETHANOL	798	14.29
1-PROPANOL	384	12.82
1-BUTANOL	342	16.90
1-PENTANOL	145	18.29
1-HEXANOL	269	15.28
1-HEPTANOL	280	21.14
1-OCTANOL	222	26.20
1-NONANOL	188	37.69
1-DECANOL	306	25.64
1-UNDECANOL	92	21.85
1-DODECANOL	94	9.73
1-OCTADECANOL	16	16.99
amines	158	7.14
METHYLAMINE	125	6.24
n-BUTYLAMINE	3	8.13
DIETHYLAMINE	13	9.37
n-PENTYLAMINE	3	23.93
DI-n-PROPYLAMINE	3	6.91
n-HEXYLAMINE	4	9.31
n-OCTYLAMINE	4	8.67
n-DECYLAMINE	3	12.66
HFC-CFC	20289	8.95
DIFLUOROMETHANE	1136	22.98
1,1-DIFLUOROETHANE	765	11.44
TRIFLUOROMETHANE	614	14.13
1,1,1-TRIFLUOROETHANE	695	8.19
CHLORODIFLUOROMETHANE	2039	9.00
1-CHLORO-1,1-DIFLUOROETHANE	467	4.36
1,1,1,2-TETRAFLUOROETHANE	6868	7.51
DICHLORODIFLUOROMETHANE	1384	6.79
CHLOROTRIFLUOROMETHANE	711	8.27
PENTAFLUOROETHANE	2205	9.36
DICHLOROFLUOROMETHANE	480	6.57
TRICHLOROFLUOROMETHANE	749	6.51
BROMOTRIFLUOROMETHANE	552	15.23
1,1,1,3,3,3-HEXAFLUOROPROPANE	230	3.27
1,1,1,2,3,3-HEXAFLUOROPROPANE	168	6.90
CHLOROPENTAFLUOROETHANE	543	7.32
1,1,1,2,3,3,3-HEPTAFLUOROPROPANE	533	3.00
1,2-DICHLOROTETRAFLUOROETHANE	150	3.85

VIII- Perspectives et conclusion

VIII-A) Perspectives :

VIII-A.1) Application du concept d'Entropy Scaling aux mélanges : exemple de la viscosité

Dans cette section, on se propose de prospecter l'extension des modèles présentés dans les chapitres précédents et notamment le chapitre 1, qui concerne la viscosité dynamique, au cas des mélanges binaires.

Considérant les modèles développés ci-dessus et notamment les variables introduites dans leurs formes fonctionnelles, la première difficulté rencontrée lors de l'étude des mélanges réside dans l'estimation de l'entropie résiduelle du mélange au point critique. Si cette variable est accessible pour des substances pures, son estimation est une tâche délicate pour des mélanges (pour une composition donnée, certains mélanges possèdent plusieurs points critiques). Comme mentionné lors de l'introduction de la variable X_{ES}, la normalisation de la valeur de s_{Tv-res} par sa valeur au point critique permet d'approcher un comportement universel des courbes d'entropy scaling c'est-à-dire indépendantes des composés chimiques et de l'EoS choisie. Afin de préserver cette normalisation sans pour autant complexifier les modèles pour des mélanges, on se propose d'avoir recours à une entropie critique moyenne issue des valeurs de l'entropie résiduelle critique des corps purs pondérées par la fraction molaire de chaque constituant comme reporté dans l'équation (VIII-1).

$$s_{\mathrm{Tv-res}}^{\mathrm{c,mix}} = \sum_{i=1}^{nc} x_i s_{\mathrm{Tv-res}}^{\mathrm{c},i} \qquad \text{(VIII– 1)}$$

Où nc est le nombre de constituants dans le mélange et x_i la fraction molaire du constituant i. Pour l'exemple de la viscosité, on utilise là aussi la réduction macroscopique proposée par Rosenfeld, où la viscosité de référence est définie comme :

$$\eta_{\mathrm{ref}}^{\mathrm{mix}} = \left(\rho_{\mathrm{N}}^{\mathrm{mix}}\right)^{\frac{2}{3}} \sqrt{\mathrm{m}_{0,\mathrm{mix}} \mathrm{k_b} T} \;\; avec \;\; \mathrm{m}_{0,\mathrm{mix}} = \sum_{i=1}^{nc} x_i \frac{M_i}{N_a} \qquad \text{(VIII– 2)}$$

Dans l'équation (VIII-2), ρ_N^{mix} est la densité moléculaire calculée par l'équation d'état, N_a est le nombre d'Avogadro, M_i est la masse molaire en kg.mol^{-1} et $m_{0,\mathrm{mix}}$ est la masse moléculaire moyenne du mélange en kg. Il est utile de noter que tous les résultats relatifs aux cas des mélanges et reportés dans les figures suivantes sont obtenues avec l'équation d'état *I*-PC-SAFT en fixant les paramètres d'interactions binaires k_{ij} à 0.

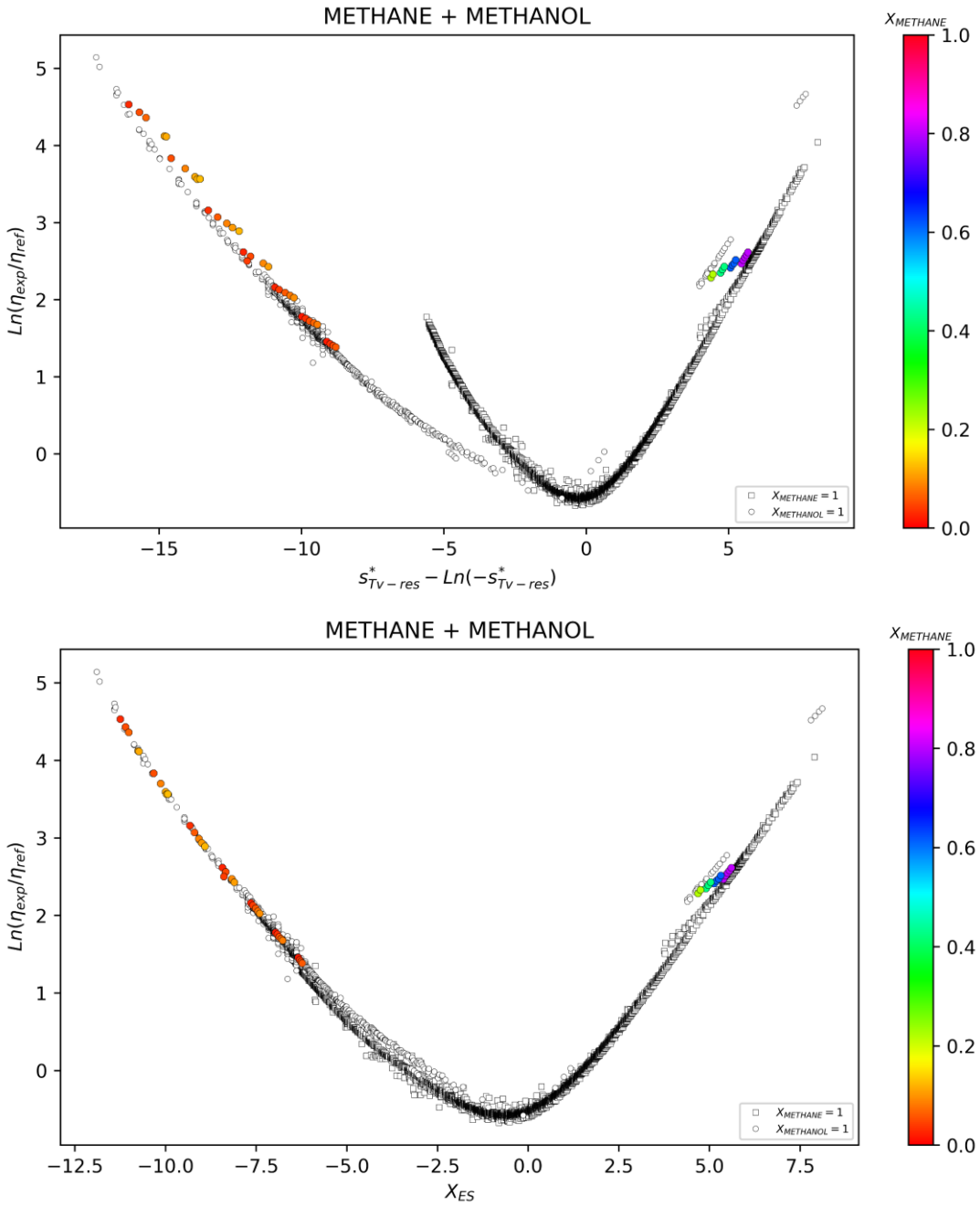

Figure VIII-1- Comparaison entre l'utilisation de l'entropie résiduelle réduite avec la constante de Boltzmann (en haut) et réduite avec sa valeur au point critique moyenne en fonction de la fraction massique lorsqu'il s'agit d'un mélange (en bas), lors de l'application du concept de l'Entropy Scaling à la viscosité du mélange méthane + méthanol. Les points sans couleur représentent les valeurs des viscosité réduites des corps purs. Chaque point coloré représente un mélange et sa couleur est définie selon la fraction massique du méthane.

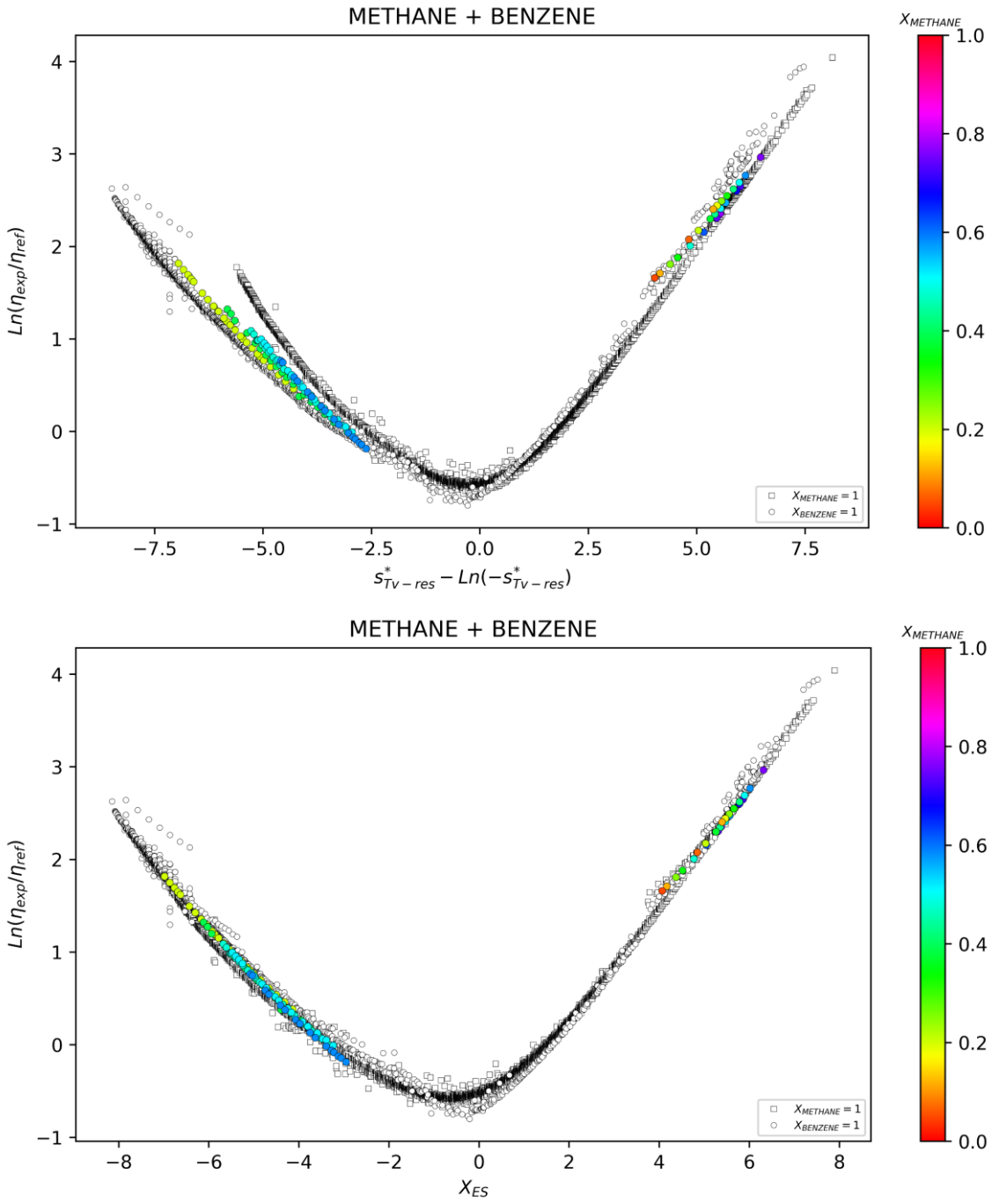

Figure VIII-2- Comparaison entre l'utilisation de l'entropie résiduelle réduite avec la constante de Boltzmann (en haut) et réduite avec sa valeur au point critique moyenne en fonction de la fraction massique lorsqu'il s'agit d'un mélange (en bas), lors de l'application du concept de l'Entropy Scaling à la viscosité du mélange méthane + benzène. Les points sans couleur représentent les valeurs des viscosité réduites des corps purs. Chaque point coloré représente un mélange et sa couleur est définie selon la fraction massique du méthane.

Comme on peut le constater sur les figures VIII-1 et VIII-2, l'impact de la normalisation des valeurs de l'entropie résiduelle par sa valeur au point critique permet un comportement beaucoup plus régulier mais aussi plus proche de l'universalité notamment à haute densité.

Afin d'avoir une idée du potentiel ainsi que de la précision que peut avoir le formalisme présenté ci-dessus à corréler des viscosités de mélange, plusieurs mélanges binaires ont été considérés. Leur viscosité a été calculée grâce aux coefficients optimisés pour les corps purs, moyennés par les fractions massiques de chaque constituant (voir l'équation (VIII-3)). Faisant cela, on évite ainsi un réajustement des coefficients pour chaque composition spécifiée.

$$\begin{cases} \ln\left(\dfrac{\eta_{\text{exp}}}{\eta_{\text{ref}}^{\text{mix}}}\right) = f_{\text{dense}} \times g_{\text{dense}} + f_{\text{gas}} \times g_{\text{gas}} + k \\ f_{\text{dense}}(\tilde{s}_{\text{Tv-res}}) = \left(\sum_{i=1}^{nc} x_i a_{1,i} + \sum_{i=1}^{nc} x_i a_{2,i} \tilde{s}_{\text{Tv-res}}\right) X_{\text{ES}} \\ f_{\text{gas}}(\tilde{s}_{\text{Tv-res}}) = \left(\sum_{i=1}^{nc} x_i b_{1,i} + \sum_{i=1}^{nc} x_i b_{2,i} \tilde{s}_{\text{Tv-res}}\right) X_{\text{ES}} \\ g_{\text{dense}} = \dfrac{1}{1 + e^{\sum_{i=1}^{nc} x_i c_i X_{\text{ES}}}} \\ g_{\text{gaz}} = \dfrac{1}{1 + e^{-\sum_{i=1}^{nc} x_i c_i X_{\text{ES}}}} \\ k = \dfrac{\sum_{i=1}^{nc} x_i d_i}{\tilde{s}_{\text{Tv-res}}^{\text{c,mix}}} \end{cases} \qquad \text{(VIII– 3)}$$

Dans l'équation (VIII-3), présentée pour les substances pures dans le chapitre 1, les paramètres $a_{1,i}$, $a_{2,i}$, $b_{1,i}$, $b_{2,i}$, c_i et d_i sont les coefficients ajustés pour les corps purs. $\tilde{s}_{\text{Tv-res}}^{\text{c,mix}}$ représente la valeur moyenne des entropies résiduelles au point critique obtenues avec l'équation (VIII-1). Les figures de VIII-3 à VIII-8 mettent en évidence les résultats obtenus avec cette approche pour différents mélanges.

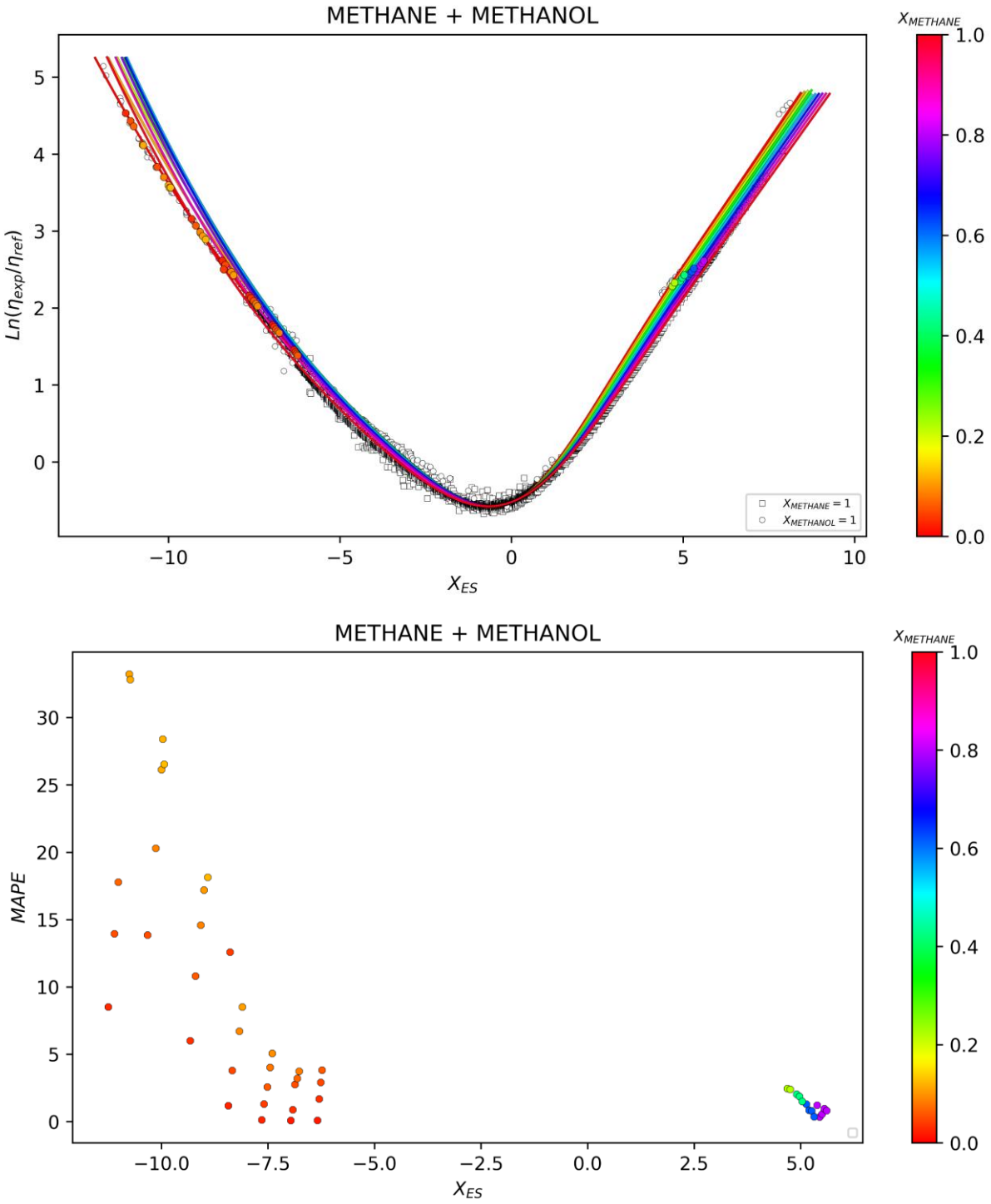

Figure VIII-3- En haut, viscosités réduites du mélange méthane + méthanol ainsi que les courbes prédictives correspondant aux fractions de méthane allant de 0.1 à 0.9 avec un pas de 0.1 ; En bas, les erreurs (en pourcentages) entre viscosités prédites et viscosités expérimentales en fonction de l'abscisse X_{ES}.

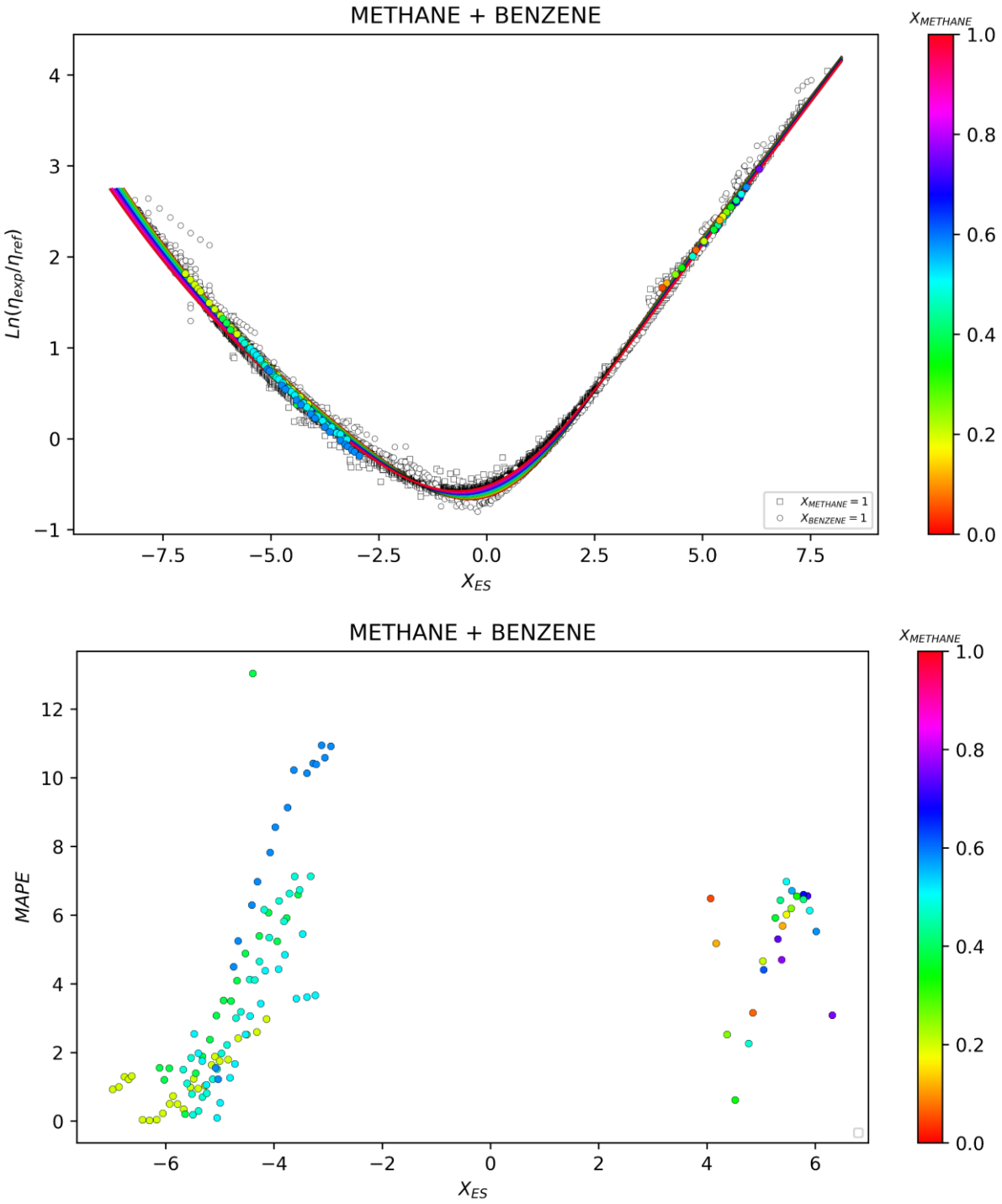

Figure VIII-4- En haut, viscosités réduites du mélange méthane + benzène ainsi que les courbes prédictives correspondant aux fractions de méthane allant de 0.1 à 0.9 avec un pas de 0.1 ; En bas, les erreurs (en pourcentages) entre viscosités prédites et viscosités expérimentales en fonction de l'abscisse X_{ES}.

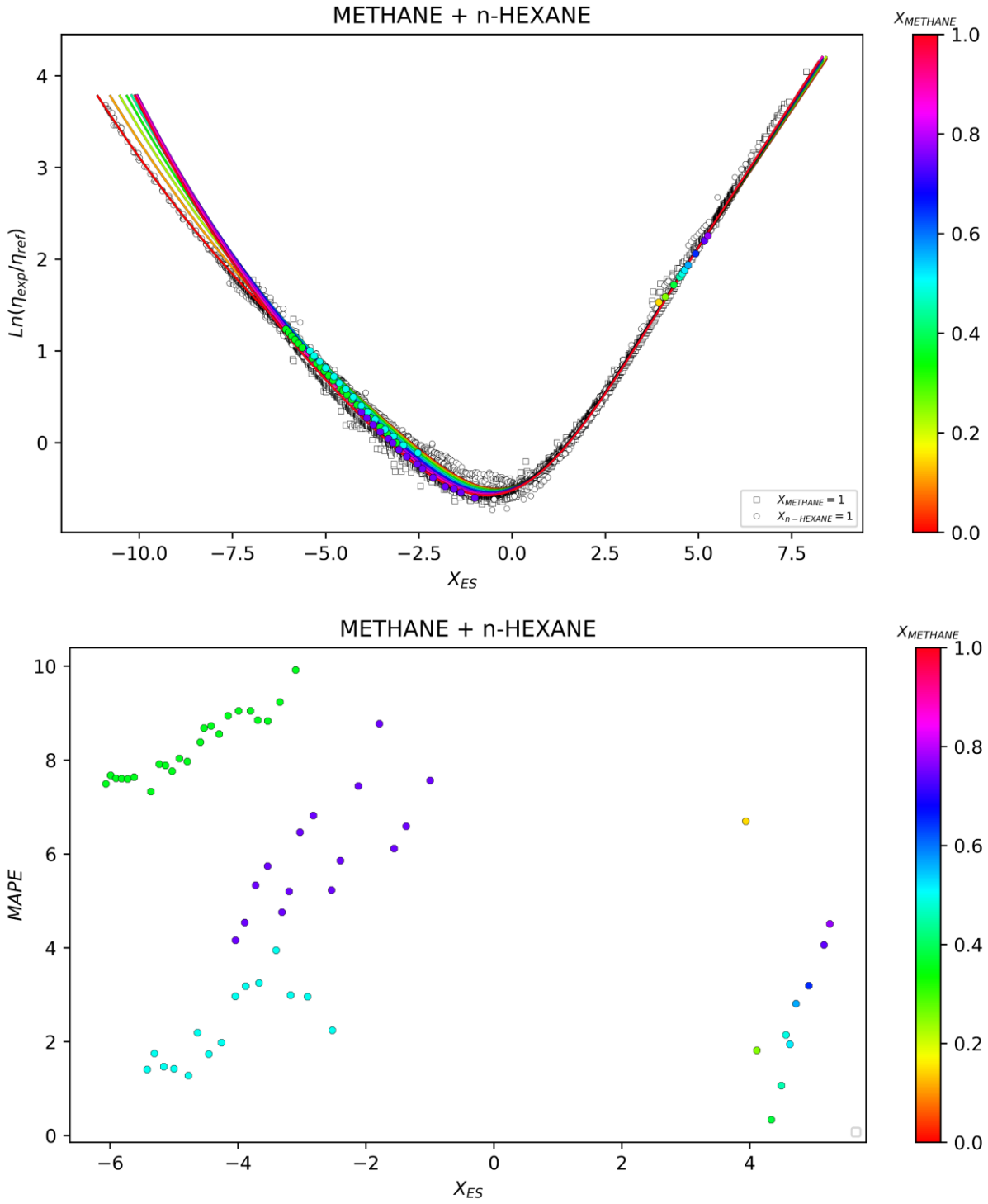

Figure VIII-5- En haut, viscosités réduites du mélange méthane + n-hexane ainsi que les courbes prédictives correspondant aux fractions de méthane allant de 0.1 à 0.9 avec un pas de 0.1 ; En bas, les erreurs (en pourcentages) entre viscosités prédites et viscosités expérimentales en fonction de l'abscisse X_{ES}.

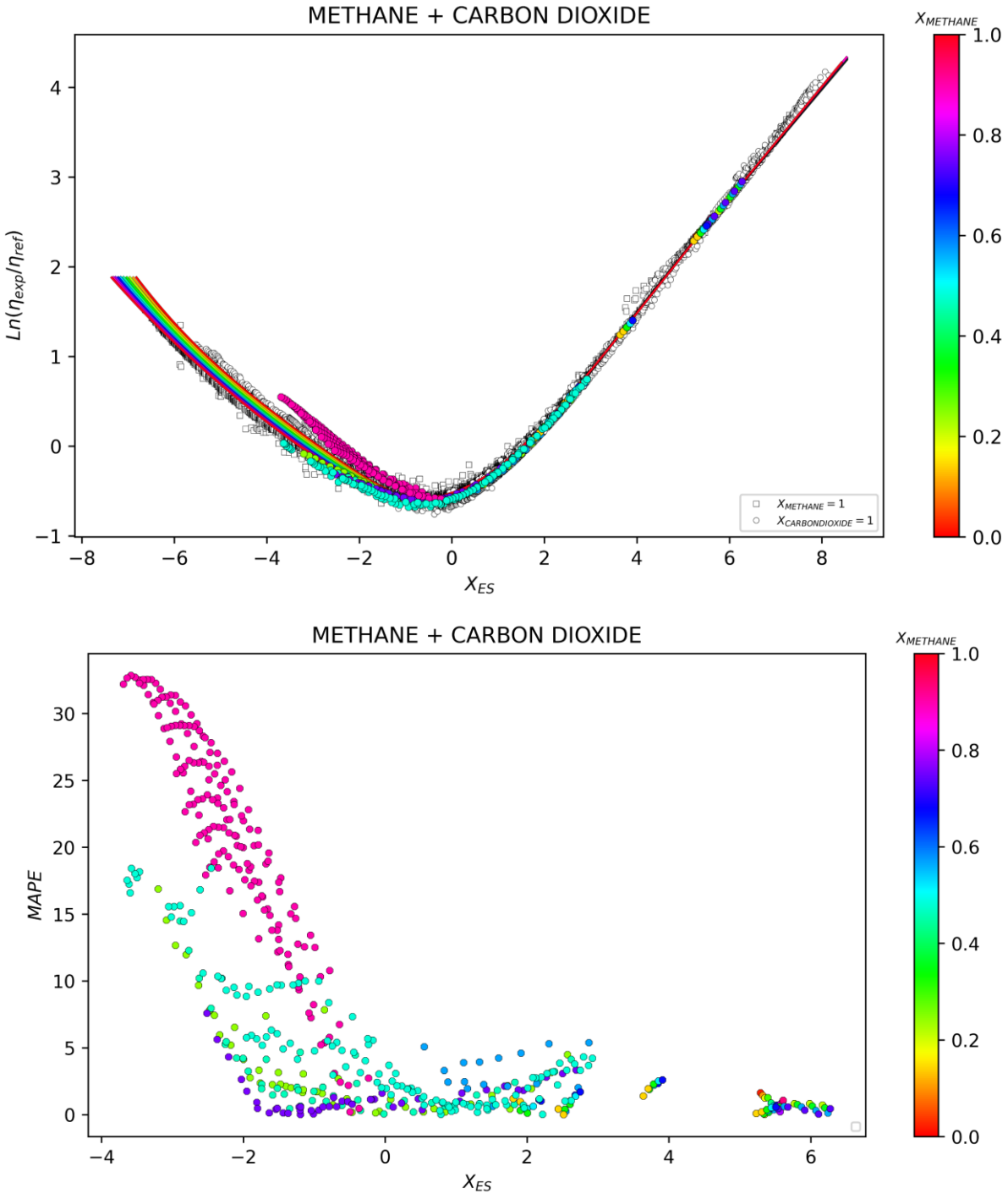

Figure VIII-6- En haut, viscosités réduites du mélange méthane + CO_2 ainsi que les courbes prédictives correspondant aux fractions de méthane allant de 0.1 à 0.9 avec un pas de 0.1 ; En bas, les erreurs (en pourcentages) entre viscosités prédites et viscosités expérimentales en fonction de l'abscisse X_{ES}.

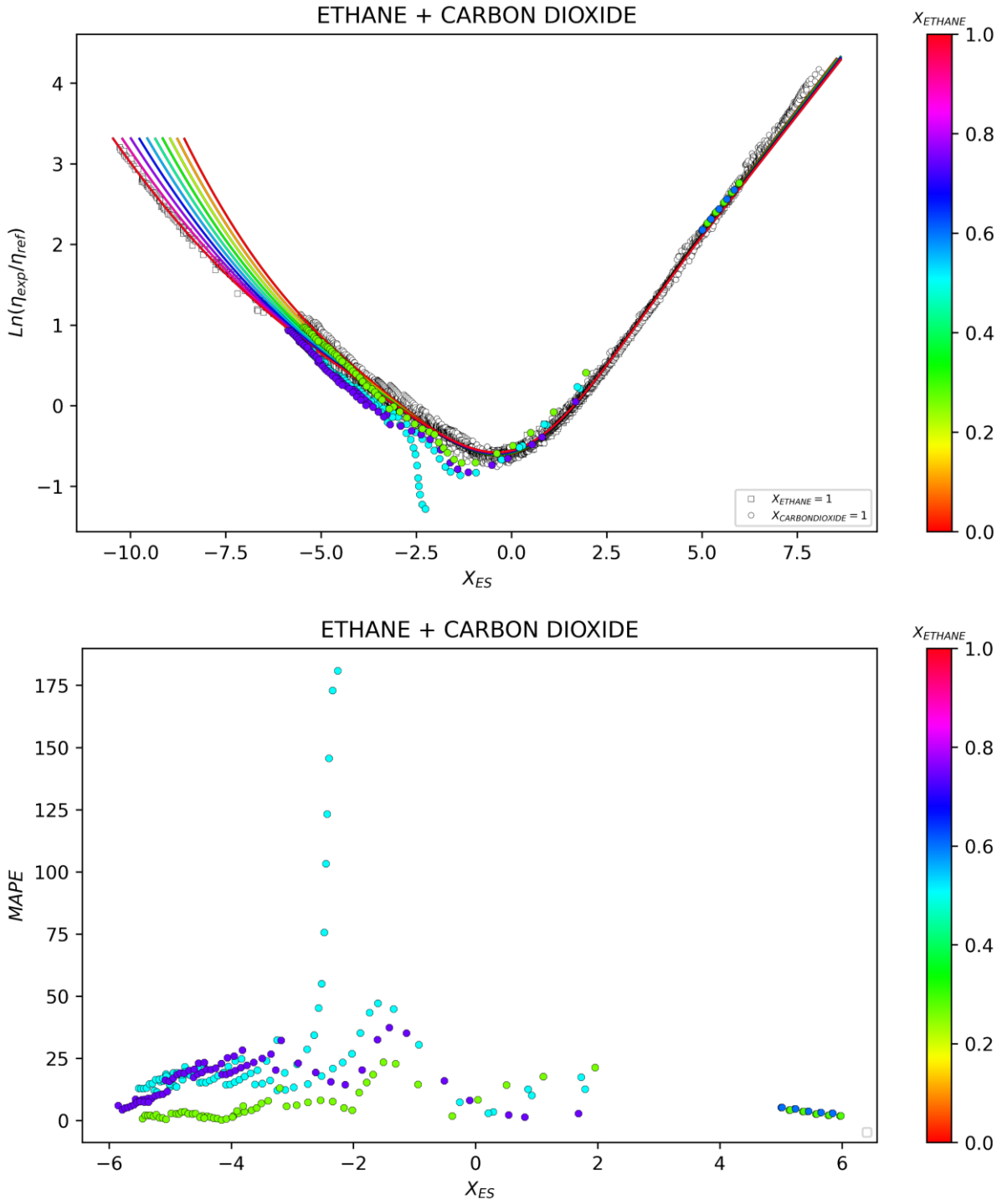

Figure VIII-7- En haut, viscosités réduites du mélange éthane + CO_2 ainsi que les courbes prédictives correspondant aux fractions de méthane allant de 0.1 à 0.9 avec un pas de 0.1 ; En bas, les erreurs (en pourcentages) entre viscosités prédites et viscosités expérimentales en fonction de l'abscisse X_{ES}.

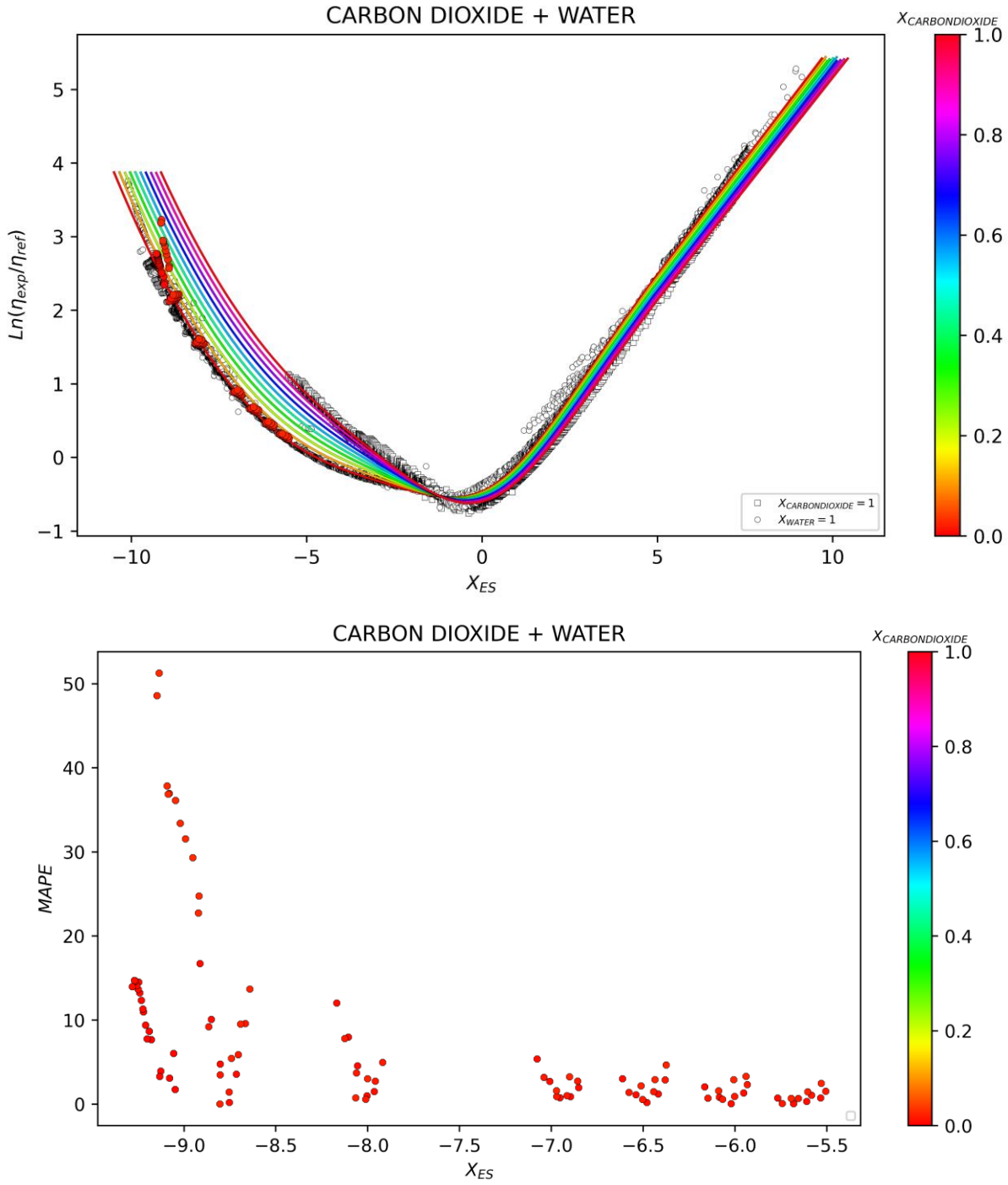

Figure VIII-8- En haut, viscosités réduites du mélange CO_2 + eau ainsi que les courbes prédictives correspondant aux fractions de méthane allant de 0.1 à 0.9 avec un pas de 0.1 ; En bas, les erreurs (en pourcentages) entre viscosités prédites et viscosités expérimentales en fonction de l'abscisse X_{ES}.

Comme le montrent les figures VIII-3 à 8, l'approche proposée permet d'obtenir des résultats satisfaisants et très prometteurs en ce qui concerne l'extension des modèles proposés pour les viscosités des corps purs aux mélanges. De façon plus globale, les précisions obtenues pour les

mélanges étudiés (comme reportées dans le tableau VIII-1) montrent des pourcentages d'erreurs ne dépassant pas les 22% pour les systèmes étudiés.

Tableau VIII-1 - Récapitulatif des erreurs moyennes et du nombre de données expérimentales considérées pour quelques mélanges binaires

Mélange considéré	Nombre de points expérimentaux	Erreur relative moyenne
METHANE + ETHANE	687	2.83
METHANE + PROPANE	1003	7.22
METHANE + n-BUTANE	366	15.79
METHANE + n-HEPTANE	111	6.18
METHANE + n-HEXANE	63	5.47
METHANE + n-OCTANE	41	21.05
METHANE + n-PENTANE	8	2.87
METHANE + n-DECANE	201	14.02
ETHANE + n-BUTANE	15	1.7
ETHANE + n-HEPTANE	77	17.37
ETHANE + n-HEXANE	12	3.31
ETHANE + n-OCTANE	12	5.42
n-BUTANE + n-HEXANE	7	3.86
n-BUTANE + PROPANE	19	3.05
n-BUTANE + n-OCTANE	8	6.95
n-HE¨PTANE + PROPANE	114	14.42
n-HEXANE + n-OCTANE	85	16.79
n-HEXANE + n-HEPTANE	119	0.93
n-OCTANE + PROPANE	9	9.84
n-PENTANE + n-HEPTANE	53	7.56
n-PENTANE + n-HEXANE	9	1.47
n-PENTANE + n-OCTANE	304	4.61
METHANE + CARBON MONOXIDE	5	1.98
METHANE + CARBON DIOXIDE	533	8.87
METHANE + NITROGEN	1004	7.35
METHANE + AMMONIA	36	3.47
ETHANE + CARBON DIOXIDE	226	16.72
ETHANE + NITROGEN	20	1.84
n-BUTANE + CARBON DIOXIDE	24	5.34
n-BUTANE + NITROGEN	18	0.83
n-PENTANE + NITROGEN	16	16.77
PROPANE + CARBON DIOXIDE	52	3.03
PROPANE + NITROGEN	20	1.92
CARBON MONOXIDE + NITROGEN	47	6.09
CARBON DIOXIDE + CARBON MONOXIDE	10	5.83
CARBON DIOXIDE + WATER	130	10.49
CARBON DIOXIDE + NITROGEN	199	1.53
METHANE + METHANOL	48	7.72
METHANE + BENZENE	126	3.85

Une des voies d'amélioration de ces résultats réside dans la considération des interactions binaires qui prennent effet entre des constituants différents. Dans les équations d'état cubiques ou de type SAFT, ces interactions sont traduites par les coefficients k_{ij} qui rentrent en jeu lors du calcul des propriétés thermodynamiques. De ce fait, ces coefficients qui sont spécifiques à chaque couple de constituants et qui peuvent varier selon les conditions du fluide (e.g. sa température) impactent systématiquement le calcul de la densité, de l'entropie résiduelle et des capacités calorifiques à volume constant. Ces quantités thermodynamiques, rentrent directement en jeu dans les modèles d'Entropy Scaling proposés dans ce travail. Les figures VIII-9 à 11 illustrent l'impact que peut avoir ce coefficient pour certains mélanges lorsqu'il s'agit de corréler leur propriété de transport en général et leur viscosité en particulier.

Ainsi, si dans certains cas, admettre une valeur nulle pour le coefficient d'interaction binaire peut aboutir à des résultats satisfaisants pour le calcul des propriétés thermodynamiques, il peut s'avérer nécessaire de le calibrer et de lui affecter une valeur non-nulle dans d'autres cas. On peut observer dans les figures VIII-9 à 11 où les coefficients d'interactions binaires sont fixés à une valeur donnée, qu'un k_{ij} adéquat peut sensiblement améliorer la capacité qu'à une EoS à modéliser la viscosité d'un mélange grâce au concept de l'Entropy Scaling.

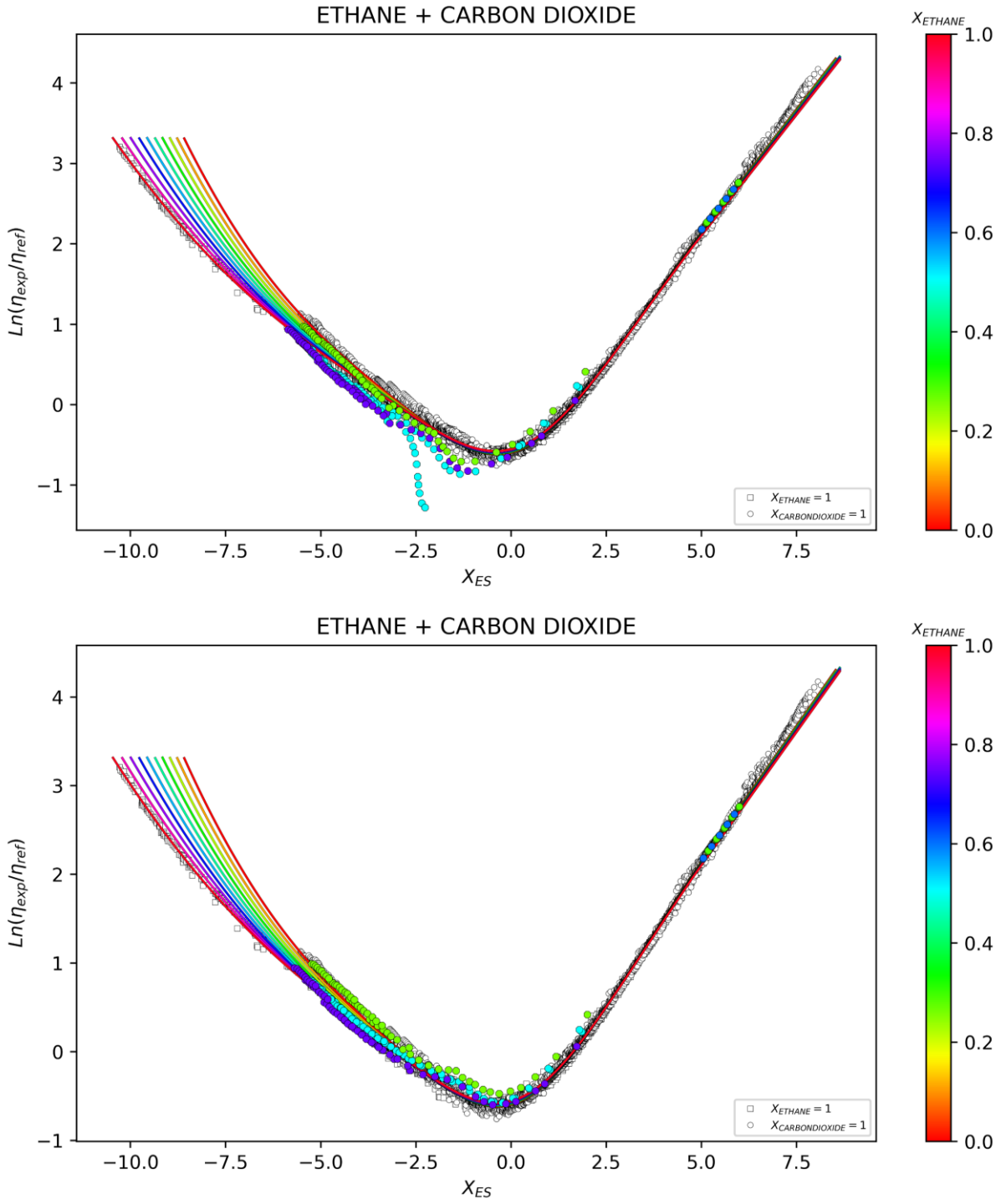

Figure VIII-9- Comparaison entre les viscosités expérimentales réduites en fonction de la fonction X_{ES} obtenues en fixant le k_{ij} = 0 (en haut) et k_{ij} = 0.1 (en bas) pour le mélange éthane + dioxyde de carbone.

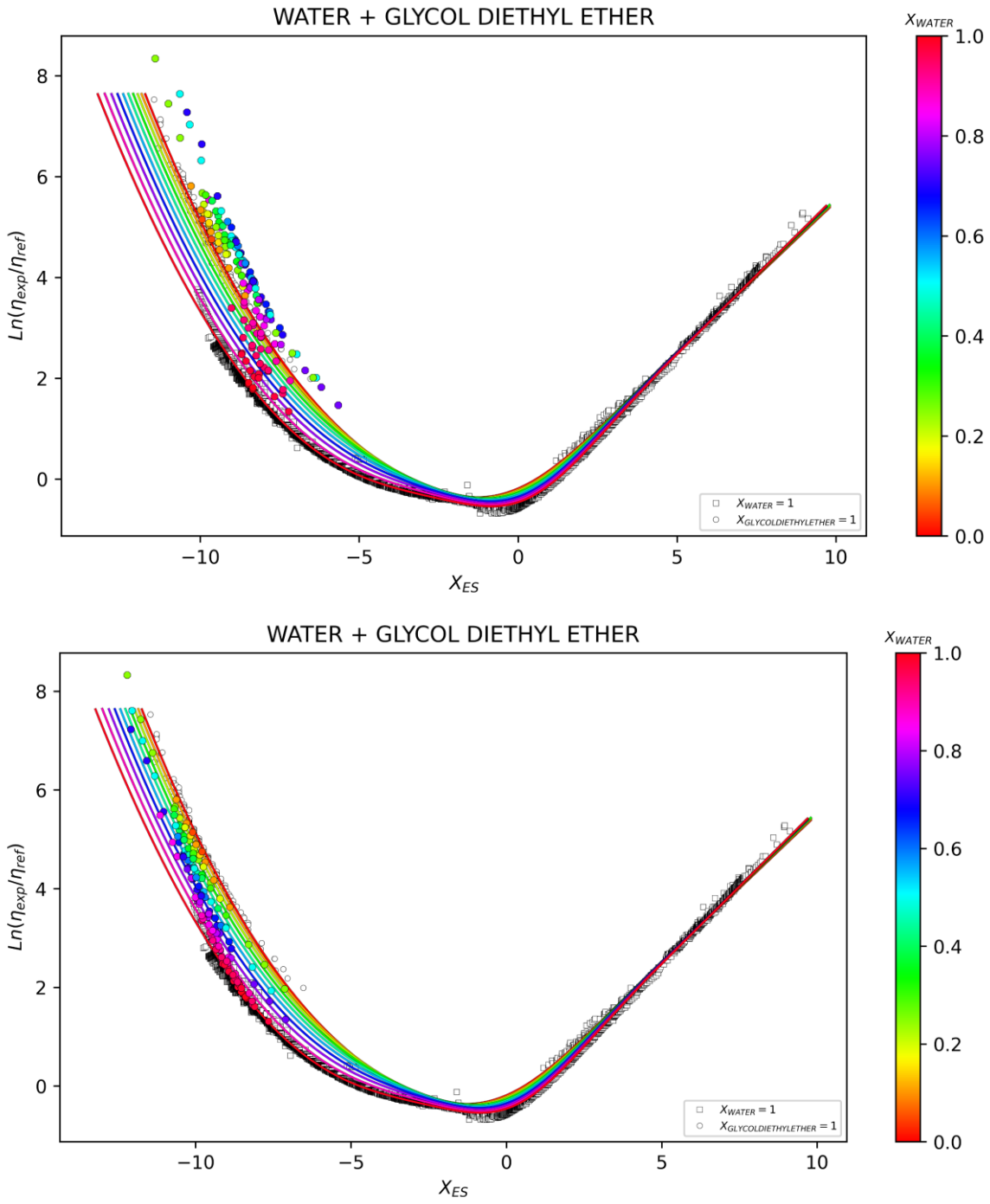

Figure VIII-10- Comparaison entre les viscosités expérimentales réduites en fonction de la fonction X_{ES} obtenues en fixant le k_{ij} = 0 (en haut) et k_{ij} = -0.5 (en bas) pour le mélange eau + glycol diméthyle éther.

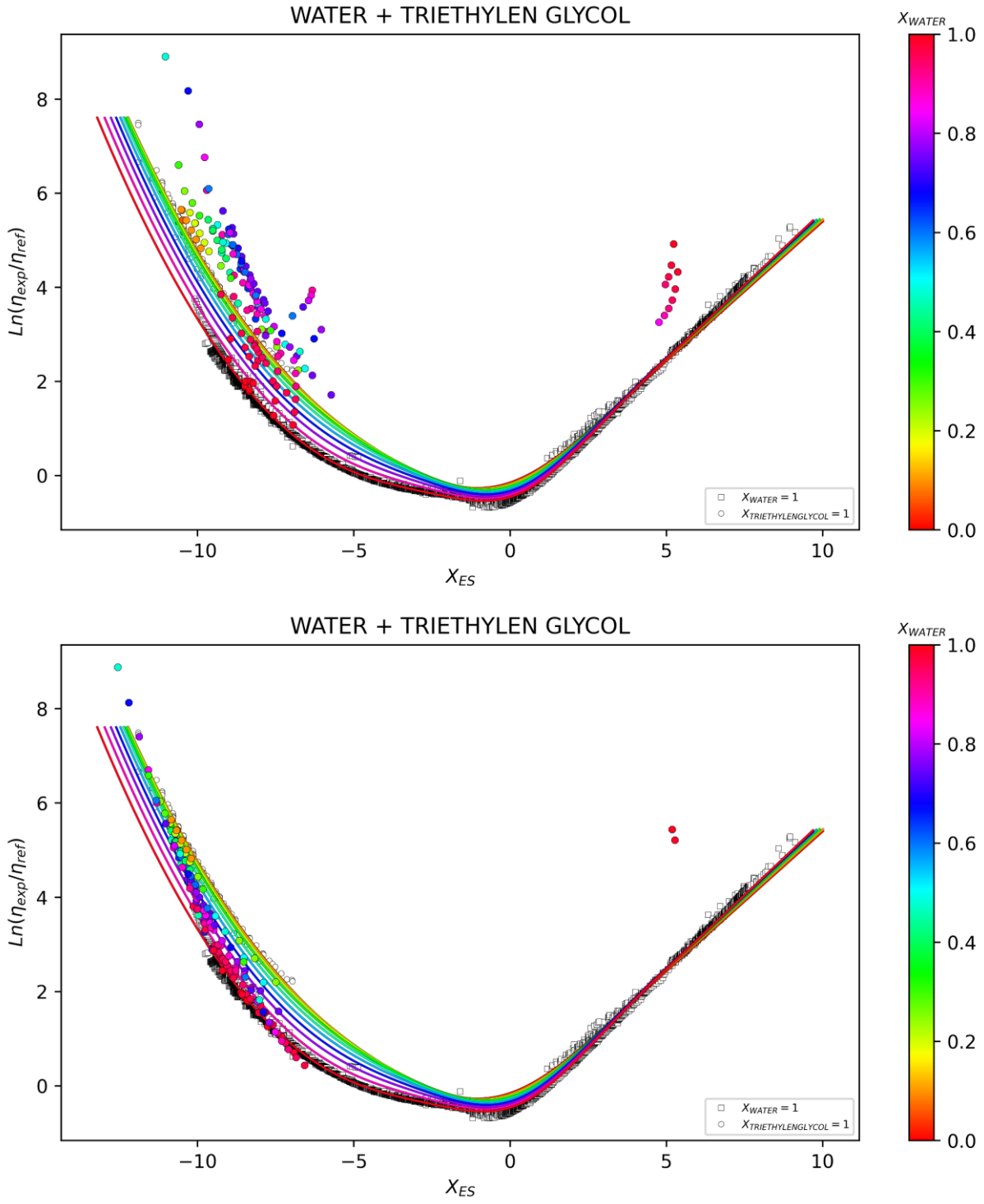

Figure VIII-11- Comparaison entre les viscosités expérimentales réduites en fonction de la fonction X_{ES} obtenues en fixant le k_{ij} = 0 (en haut) et k_{ij} = -0.6 (en bas) pour le mélange eau + tri-éthylène glycol.

VIII-A.2) Définition d'un nombre restreint de données expérimentales judicieusement choisies permettant de prédire avec précision les propriétés de transport à l'aide du concept d'Entropy Scaling

La réponse à cette question est d'une importance majeure. En effet, si de tels points (définis par un couple température et pression) existent et que leur nombre peut être limité à quelques-uns, une méthodologie – à moindre coût et temps- peut être définie pour la caractérisation des propriétés de transport d'une substance sur tout le domaine fluide. Cette idée découle du caractère quasi-universel obtenu grâce au formalisme de l'Entropy-Scaling proposé dans ce travail.

Ainsi, après avoir étudié les trois propriétés de transport des corps purs, il a été trouvé qu'en se restreignant à 6 conditions expérimentales bien sélectionnées (c-à-d en prenant uniquement en compte 6 mesures expérimentales de la propriété de transport voulue) lors de l'optimisation des coefficients des modèles, il est possible de reproduire la même courbe prédictive que dans le cas où la totalité des mesures expérimentales disponibles pour un composé ont été prises en compte, c'est-à-dire d'obtenir les mêmes coefficients des corrélations. Ces points sont représentés sur la figure VIII-12 et leur valeur pour le cas de la viscosité dynamique dans la figure VIII-13.

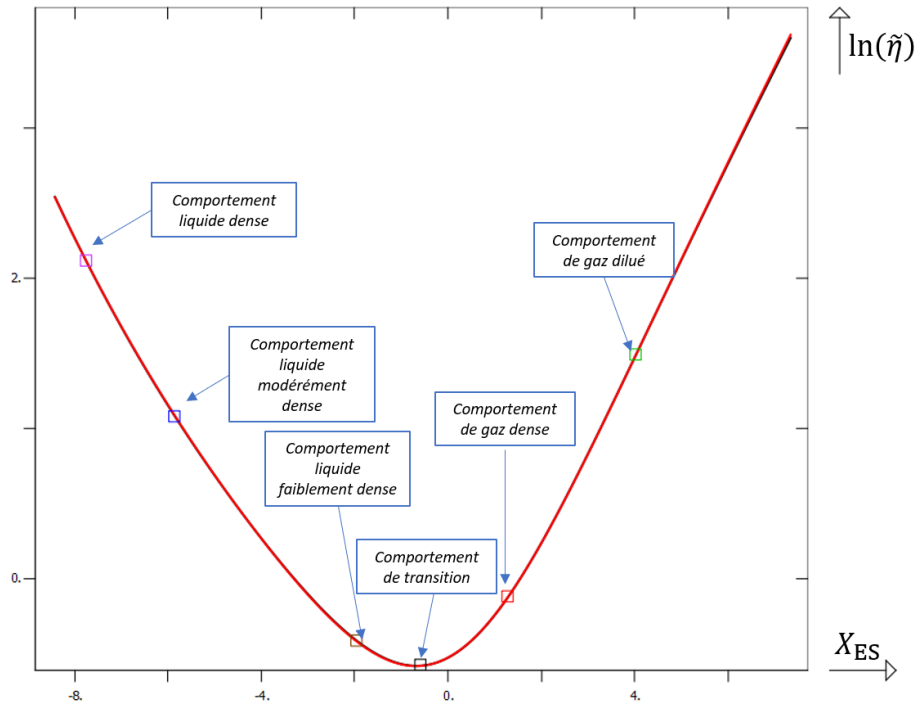

Figure VIII-12 - position schématique des points expérimentaux stratégiques sur une courbe d'Entropy Scaling relative aux viscosités des corps purs

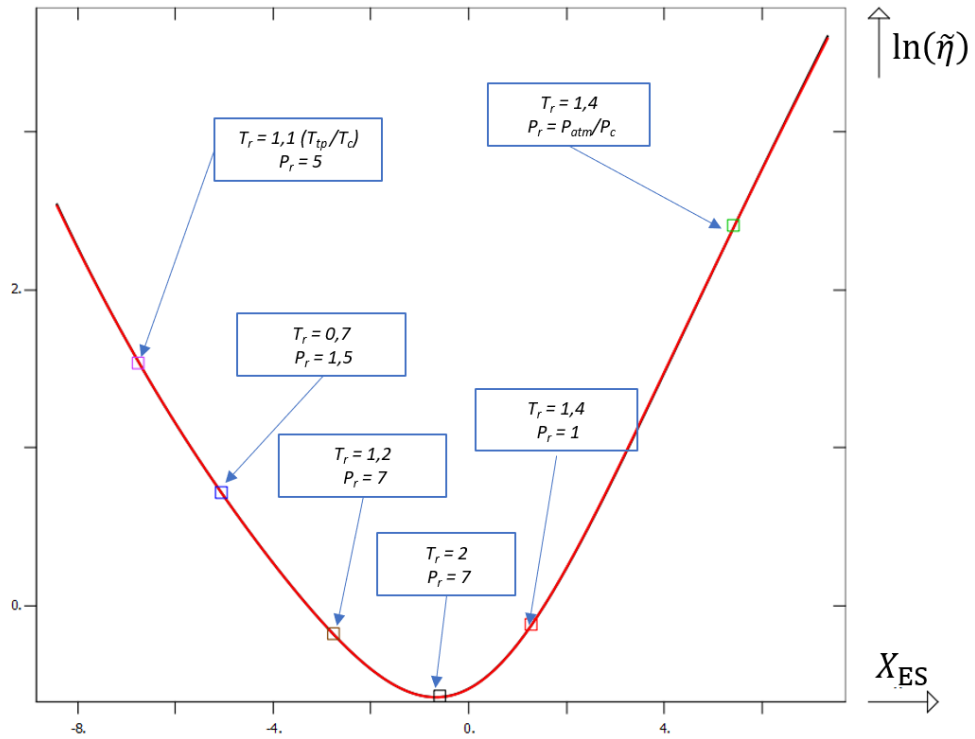

Figure VIII-13 – Valeurs des températures et des pressions réduites des points expérimentaux stratégiques sur une courbe d'Entropy Scaling relative aux viscosités des corps purs (exemple du méthane)

Il est à noter que ces valeurs de températures et des pressions réduites adéquates sont indépendantes du composé chimique et elles permettent de retrouver l'allure/l'évolution des données expérimentales des propriétés de transport (voir figures VIII-14 et VIII-15) tout en étant accessibles expérimentalement pour la majorité des fluides réels. Par ailleurs, le tableau VIII-2 montre que les prédictions obtenues avec 6 points expérimentaux définies par les valeurs reportées sur la Figure VIII-13 induisent des taux d'erreur très similaires à ceux obtenus en considérant la totalité des points expérimentaux.

Tableau VIII-2 - Exemples des taux d'erreur obtenus en considérant la totalité des points expérimentaux disponibles pour une substance, comparés au cas de la prise en compte des six points expérimentaux mis en évidence dans la Figure VIII-13

Substance	Optimisation avec tous les points expérimentaux Erreur moyenne sur la prédiction des viscosité (MAPE)	Optimisation avec six points stratégiques Erreur moyenne sur la prédiction des viscosité (MAPE)
Méthane	2.56	2.59
Ethane	2.62	2.68
Benzène	2.58	2.59
Propane	2.75	3.04
Isobutane	2.87	2.88
n-butane	2.26	2.26
n-pentane	3.81	3.88
n-hexane	2.84	2.89
n-octane	2.61	4.75
Néon	5.47	5.48
Argon	3.08	3.35
Xénon	2.21	2.22
Eau	3.87	3.96

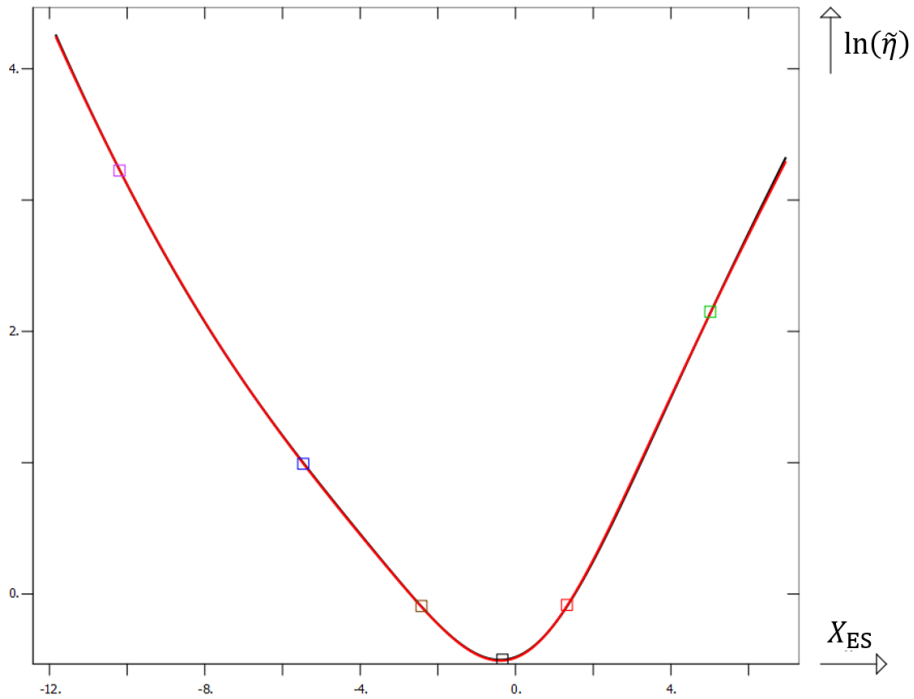

Figure VIII-14 – Représentation de la courbe prédictive obtenue en considérant la totalité des point expérimentaux (courbe en noir) comparée à celle obtenue en considérant les six points expérimentaux (courbe en rouge) définis dans la figure VIII-13 pour le cas du n-hexane

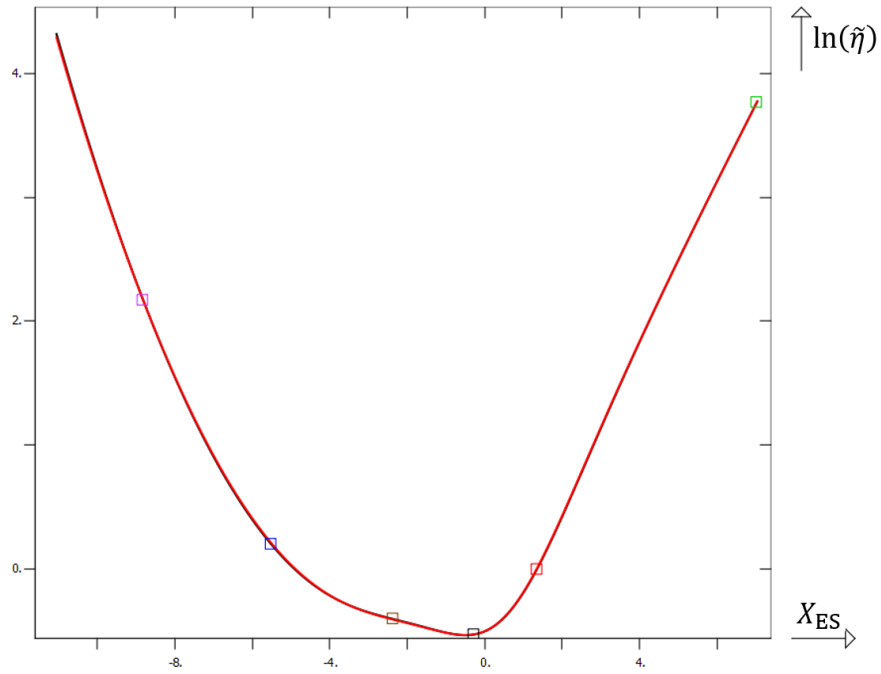

Figure VIII-15 – Représentation de la courbe prédictive obtenue en considérant la totalité des point expérimentaux (courbe en noir) comparée à celle obtenue en considérant les six points expérimentaux (courbe en rouge) définis dans la figure VIII-13 pour le cas de l'eau

Il est à noter que la prospection de la même méthodologie pour le cas des conductivités thermiques et des coefficients d'auto-diffusion a mené à des résultats similaires et ce, en fixant les six points expérimentaux à des valeurs de températures et de pressions réduites très proches de celles reportées sur la figure VIII-13 pour les viscosités. Finalement, à l'aide du concept d'Entropy Scaling reformulé comme proposé dans cette étude, il serait possible de retrouver l'évolution d'une propriété de transport d'une substance pure sur tout le domaine fluide à l'aide d'un nombre restreint – ici fixé à six- de mesures expérimentales bien localisées en termes de température et de pression ou en d'autres termes selon l'état thermodynamique du fluide (voir la figure VIII-12).

VIII-B) Conclusion :

Dans cette thèse ayant eu comme point de départ une problématique de mécanique des fluides, le souci d'une modélisation rigoureuse nous a conduits à focaliser notre attention sur la question de la prédiction des propriétés de transport. Ces dernières, caractérisant le comportement dynamique d'un fluide, sont d'une importance primordiale dans la majorité des procédés industriels. Dans la recherche d'un modèle pouvant satisfaire les besoins des logiciels de simulation actuels, on s'est intéressé ici au concept de l'Entropy Scaling. Ce dernier exploite le lien existant entre l'entropie résiduelle d'un fluide et ses propriétés de transport. Alliant simplicité (en ayant recours à des quantités thermodynamiques accessibles pour des fluides réels par des équations d'état) et polyvalence (car applicable aux viscosités, aux coefficients de diffusion de la matière et aux conductivités thermiques et regroupant les états gaz, liquide et supercritique), cette technique s'est avérée être un outil puissant pour aboutir à des modèles performants et précis.

Le concept de base ayant mis en évidence différentes défaillances lors de son application aux substances réelles, il a été ici revisité et reformulé pour son application aux corps purs. Pour valider les différents modèles proposés dans ce travail, de grosses bases de données expérimentales ont été utilisées pour comparer les valeurs prédites aux valeurs mesurées.

Au terme de l'étude de chacune des propriétés de transport (viscosité, coefficient de diffusion de la matière et conductivité thermique), ces travaux ont permis :

- La proposition d'une nouvelle fonction dépendant de l'entropie résiduelle, laquelle permet d'aboutir à un comportement quasi-universel à faible densité pour les fluides purs et leurs mélanges
- Dans le cas de la conductivité thermique, de proposer une réduction commune pour les fluides monoatomiques et polyatomiques tenant compte des degrés de liberté vibrationnels et rotationnels spécifiques à ces derniers
- Pour chacune des propriétés de transport, de proposer un seul formalisme applicable pour les équations d'état cubiques et de type SAFT, faisant intervenir selon le besoin des paramètres spécifiques aux composés, spécifiques à une famille chimique et universels (sauf dans le cas des coefficients d'auto diffusion)
- Globalement, de proposer une méthode simple et efficace pour l'obtention de fonctions continues sur tout le domaine fluide (liquide, gaz et états supercritiques) décrivant le comportement complexe des propriétés de transport en fonction des conditions de pression et température

Enfin, ce travail met la lumière sur certaines perspectives, notamment :

- L'extension de l'approche aux propriétés de transport des mélanges comme brièvement discuté dans la section précédente

- Sa possible implémentation dans le modèle numérique de mécanique des fluides développé en prémices de cette thèse
- La possibilité de rendre cette approche prédictive en y combinant une méthode de contributions de groupes ou un algorithme d'intelligence artificielle
- La possibilité de simplifier la caractérisation expérimentale des propriétés de transport d'un fluide donné en minimisant le nombre de mesures à effectuer
- Enfin, la possibilité de considérer les propriétés de transport comme un élément central dans le paramétrage des équations d'état c'est-à-dire dans l'estimation des coefficients qui y jouent un rôle clé (comme les coefficients d'interactions binaires)

IX- Bibliographie

(1) Rosenfeld, Y. Relation between the Transport Coefficients and the Internal Entropy of Simple Systems. *Phys. Rev. A* **1977**, *15* (6), 2545–2549. https://doi.org/10.1103/PhysRevA.15.2545.
(2) Rosenfeld, Y. A Quasi-Universal Scaling Law for Atomic Transport in Simple Fluids. *J. Phys.: Condens. Matter* **1999**, *11* (28), 5415–5427. https://doi.org/10.1088/0953-8984/11/28/303.
(3) Dzugutov, M. A Universal Scaling Law for Atomic Diffusion in Condensed Matter. *Nature* **1996**, *381* (6578), 137–139. https://doi.org/10.1038/381137a0.
(4) McLaughlin, E. The Thermal Conductivity of Liquids and Dense Gases. *Chem. Rev.* **1964**, *64* (4), 389–428. https://doi.org/10.1021/cr60230a003.
(5) Le Guennec, Y.; Privat, R.; Jaubert, J.-N. Development of the Translated-Consistent *tc*-PR and *tc*-RK Cubic Equations of State for a Safe and Accurate Prediction of Volumetric, Energetic and Saturation Properties of Pure Compounds in the Sub- and Super-Critical Domains. *Fluid Phase Equilibria* **2016**, *429*, 301–312. https://doi.org/10.1016/j.fluid.2016.09.003.
(6) Poling, B. E.; Prausnitz, J. M.; O'Connell, J. P. *The Properties of Gases and Liquids*, 5th ed.; McGraw-Hill: New York, 2001.
(7) *Viscosity of Liquids*; Springer Netherlands: Dordrecht, 2007. https://doi.org/10.1007/978-1-4020-5482-2.
(8) Wu, X.; Li, C.; Jia, W. An Improved Viscosity Model Based on Peng–Robinson Equation of State for Light Hydrocarbon Liquids and Gases. *Fluid Phase Equilibria* **2014**, *380*, 147–151. https://doi.org/10.1016/j.fluid.2014.08.001.
(9) Mishra, A. K.; Kumar, A. P-μ-T Cubic Equation of Viscosity for Hydrocarbons. *Fluid Phase Equilibria* **2020**, *505*, 112359. https://doi.org/10.1016/j.fluid.2019.112359.
(10) Chapman, S.; Cowling, T. G. *The Mathematical Theory of Non-Uniform Gases: An Account of the Kinetic Theory of Viscosity, Thermal Conduction, and Diffusion in Gases*, 3rd ed.; Cambridge mathematical library; Cambridge University Press: Cambridge ; New York, 1990.
(11) Dymond, J. H. Corrections to the Enskog Theory for Viscosity and Thermal Conductivity. *Physica B+C* **1987**, *144* (3), 267–276. https://doi.org/10.1016/0378-4363(87)90009-X.
(12) Assael, M. J.; Dymond, J. H.; Papadaki, M.; Patterson, P. M. Correlation and Prediction of Dense Fluid Transport Coefficients. I. n-Alkanes. *Int J Thermophys* **1992**, *13* (2), 269–281. https://doi.org/10.1007/BF00504436.
(13) Chung, T. H.; Ajlan, M.; Lee, L. L.; Starling, K. E. Generalized Multiparameter Correlation for Nonpolar and Polar Fluid Transport Properties. *Ind. Eng. Chem. Res.* **1988**, *27* (4), 671–679. https://doi.org/10.1021/ie00076a024.
(14) Vesovic, V.; Wakeham, W. A. The Prediction of the Viscosity of Dense Gas Mixtures. *Int J Thermophys* **1989**, *10* (1), 125–132. https://doi.org/10.1007/BF00500713.
(15) Vesovic, V.; Wakeham, W. A. Prediction of the Viscosity of Fluid Mixtures over Wide Ranges of Temperature and Pressure. *Chemical Engineering Science* **1989**, *44* (10), 2181–2189. https://doi.org/10.1016/0009-2509(89)85152-8.

(16) Ely, J. F.; Hanley, H. J. M. Prediction of Transport Properties. 1. Viscosity of Fluids and Mixtures. *Ind. Eng. Chem. Fund.* **1981**, *20* (4), 323–332. https://doi.org/10.1021/i100004a004.
(17) Teja, A. S.; Rice, P. Generalized Corresponding States Method for the Viscosities of Liquid Mixtures. *Ind. Eng. Chem. Fund.* **1981**, *20* (1), 77–81. https://doi.org/10.1021/i100001a015.
(18) Aasberg-Petersen, K.; Knudsen, K.; Fredenslund, A. Prediction of Viscosities of Hydrocarbon Mixtures. *Fluid Phase Equilibria* **1991**, *70* (2–3), 293–308. https://doi.org/10.1016/0378-3812(91)85041-R.
(19) Pedersen, K. S.; Fredenslund, A.; Christensen, P. L.; Thomassen, P. Viscosity of Crude Oils. *Chemical Engineering Science* **1984**, *39* (6), 1011–1016. https://doi.org/10.1016/0009-2509(84)87009-8.
(20) Llovell, F.; Marcos, R. M.; Vega, L. F. Free-Volume Theory Coupled with Soft-SAFT for Viscosity Calculations: Comparison with Molecular Simulation and Experimental Data. *J. Phys. Chem. B* **2013**, *117* (27), 8159–8171. https://doi.org/10.1021/jp401307t.
(21) Polishuk, I.; Yitzhak, A. Modeling Viscosities of Pure Compounds and Their Binary Mixtures Using the Modified Yarranton–Satyro Correlation and Free Volume Theory Coupled with SAFT+Cubic EoS. *Ind. Eng. Chem. Res.* **2014**, *53* (2), 959–971. https://doi.org/10.1021/ie4030352.
(22) Quiñones-Cisneros, S. E.; Zéberg-Mikkelsen, C. K.; Stenby, E. H. One Parameter Friction Theory Models for Viscosity. *Fluid Phase Equilibria* **2001**, *178* (1–2), 1–16. https://doi.org/10.1016/S0378-3812(00)00474-X.
(23) Quiñones-Cisneros, S. E.; Zéberg-Mikkelsen, C. K.; Stenby, E. H. The Friction Theory (f-Theory) for Viscosity Modeling. *Fluid Phase Equilibria* **2000**, *169* (2), 249–276. https://doi.org/10.1016/S0378-3812(00)00310-1.
(24) Yarranton, H. W.; Satyro, M. A. Expanded Fluid-Based Viscosity Correlation for Hydrocarbons. *Ind. Eng. Chem. Res.* **2009**, *48* (7), 3640–3648. https://doi.org/10.1021/ie801698h.
(25) Loria, H.; Motahhari, H.; Satyro, M. A.; Yarranton, H. W. Process Simulation Using the Expanded Fluid Model for Viscosity Calculations. *Chemical Engineering Research and Design* **2014**, *92* (12), 3083–3095. https://doi.org/10.1016/j.cherd.2014.06.019.
(26) Delage-Santacreu, S.; Galliero, G.; Hoang, H.; Bazile, J.-P.; Boned, C.; Fernandez, J. Thermodynamic Scaling of the Shear Viscosity of Mie *n* -6 Fluids and Their Binary Mixtures. *The Journal of Chemical Physics* **2015**, *142* (17), 174501. https://doi.org/10.1063/1.4919296.
(27) Macías-Salinas, R.; Flores-Granados, M. A.; Díaz-Cruz, M.; García-Sánchez, F. Modeling the Dynamic Viscosity of Associating and Polar Fluids via the Use of Density Scaling. *Fluid Phase Equilibria* **2018**, *458*, 16–29. https://doi.org/10.1016/j.fluid.2017.10.032.
(28) Rosenfeld, Y. Quasi-Universal Scaling Law for Atomic Transport in Simple Fluids. *J. Phys. IV France* **2000**, *10* (PR5), Pr5-129-Pr5-134. https://doi.org/10.1051/jp4:2000517.

(29) Baled, H. O.; Gamwo, I. K.; Enick, R. M.; McHugh, M. A. Viscosity Models for Pure Hydrocarbons at Extreme Conditions: A Review and Comparative Study. *Fuel* **2018**, *218*, 89–111. https://doi.org/10.1016/j.fuel.2018.01.002.

(30) Hopp, M.; Mele, J.; Gross, J. Self-Diffusion Coefficients from Entropy Scaling Using the PCP-SAFT Equation of State. *Ind. Eng. Chem. Res.* **2018**, *57* (38), 12942–12950. https://doi.org/10.1021/acs.iecr.8b02406.

(31) Hopp, M.; Mele, J.; Hellmann, R.; Gross, J. Thermal Conductivity via Entropy Scaling: An Approach That Captures the Effect of Intramolecular Degrees of Freedom. *Ind. Eng. Chem. Res.* **2019**, *58* (39), 18432–18438. https://doi.org/10.1021/acs.iecr.9b03998.

(32) Hopp, M.; Gross, J. Thermal Conductivity of Real Substances from Excess Entropy Scaling Using PCP-SAFT. *Ind. Eng. Chem. Res.* **2017**, *56* (15), 4527–4538. https://doi.org/10.1021/acs.iecr.6b04289.

(33) Novak, L. T. Fluid Viscosity-Residual Entropy Correlation. *International Journal of Chemical Reactor Engineering* **2011**, *9* (1). https://doi.org/10.2202/1542-6580.2839.

(34) Novak, L. Self-Diffusion Coefficient and Viscosity in Fluids. *International Journal of Chemical Reactor Engineering* **2011**, *9* (1). https://doi.org/10.1515/1542-6580.2640.

(35) Novak, L. T. Predictive Corresponding-States Viscosity Model for the Entire Fluid Region: *N* -Alkanes. *Ind. Eng. Chem. Res.* **2013**, *52* (20), 6841–6847. https://doi.org/10.1021/ie400654p.

(36) Novak, L. T. Predicting Fluid Viscosity of Nonassociating Molecules. *Ind. Eng. Chem. Res.* **2015**, *54* (21), 5830–5835. https://doi.org/10.1021/acs.iecr.5b01526.

(37) Galliero, G.; Boned, C.; Fernández, J. Scaling of the Viscosity of the Lennard-Jones Chain Fluid Model, Argon, and Some Normal Alkanes. *The Journal of Chemical Physics* **2011**, *134* (6), 064505. https://doi.org/10.1063/1.3553262.

(38) Lötgering-Lin, O.; Gross, J. Group Contribution Method for Viscosities Based on Entropy Scaling Using the Perturbed-Chain Polar Statistical Associating Fluid Theory. *Ind. Eng. Chem. Res.* **2015**, *54* (32), 7942–7952. https://doi.org/10.1021/acs.iecr.5b01698.

(39) Lötgering-Lin, O.; Fischer, M.; Hopp, M.; Gross, J. Pure Substance and Mixture Viscosities Based on Entropy Scaling and an Analytic Equation of State. *Ind. Eng. Chem. Res.* **2018**, *57* (11), 4095–4114. https://doi.org/10.1021/acs.iecr.7b04871.

(40) Bell, I. H.; Messerly, R.; Thol, M.; Costigliola, L.; Dyre, J. C. Modified Entropy Scaling of the Transport Properties of the Lennard-Jones Fluid. *J. Phys. Chem. B* **2019**, *123* (29), 6345–6363. https://doi.org/10.1021/acs.jpcb.9b05808.

(41) Bell, I. H. Entropy Scaling of Viscosity—I: A Case Study of Propane. *J. Chem. Eng. Data* **2020**, *65* (6), 3203–3215. https://doi.org/10.1021/acs.jced.0c00209.

(42) Rokni, H. B.; Moore, J. D.; Gupta, A.; McHugh, M. A.; Mallepally, R. R.; Gavaises, M. General Method for Prediction of Thermal Conductivity for Well-Characterized Hydrocarbon Mixtures and Fuels up to Extreme Conditions Using Entropy Scaling. *Fuel* **2019**, *245*, 594–604. https://doi.org/10.1016/j.fuel.2019.02.044.

(43) Rokni, H. B.; Moore, J. D.; Gupta, A.; McHugh, M. A.; Gavaises, M. Entropy Scaling Based Viscosity Predictions for Hydrocarbon Mixtures and Diesel Fuels up to Extreme Conditions. *Fuel* **2019**, *241*, 1203–1213. https://doi.org/10.1016/j.fuel.2018.12.043.

(44) Liu, H.; Yang, F.; Yang, Z.; Duan, Y. Modeling the Viscosity of Hydrofluorocarbons, Hydrofluoroolefins and Their Binary Mixtures Using Residual Entropy Scaling and Cubic-plus-Association Equation of State. *Journal of Molecular Liquids* **2020**, *308*, 113027. https://doi.org/10.1016/j.molliq.2020.113027.

(45) Binti Mohd Taib, M.; Trusler, J. P. M. Residual Entropy Model for Predicting the Viscosities of Dense Fluid Mixtures. *J. Chem. Phys.* **2020**, *152* (16), 164104. https://doi.org/10.1063/5.0002242.

(46) Fouad, W. A.; Vega, L. F. Transport Properties of HFC and HFO Based Refrigerants Using an Excess Entropy Scaling Approach. *The Journal of Supercritical Fluids* **2018**, *131*, 106–116. https://doi.org/10.1016/j.supflu.2017.09.006.

(47) Bell, I. H. Probing the Link between Residual Entropy and Viscosity of Molecular Fluids and Model Potentials. *Proc Natl Acad Sci USA* **2019**, *116* (10), 4070–4079. https://doi.org/10.1073/pnas.1815943116.

(48) Moine, E.; Piña-Martinez, A.; Jaubert, J.-N.; Sirjean, B.; Privat, R. *I* -PC-SAFT: An Industrialized Version of the Volume-Translated PC-SAFT Equation of State for Pure Components, Resulting from Experience Acquired All through the Years on the Parameterization of SAFT-Type and Cubic Models. *Ind. Eng. Chem. Res.* **2019**, *58* (45), 20815–20827. https://doi.org/10.1021/acs.iecr.9b04660.

(49) Jaubert, J.-N.; Privat, R.; Le Guennec, Y.; Coniglio, L. Note on the Properties Altered by Application of a Péneloux-Type Volume Translation to an Equation of State. *Fluid Phase Equilibria* **2016**, *419*, 88–95. https://doi.org/10.1016/j.fluid.2016.03.012.

(50) Privat, R.; Jaubert, J.-N.; Le Guennec, Y. Incorporation of a Volume Translation in an Equation of State for Fluid Mixtures: Which Combining Rule? Which Effect on Properties of Mixing? *Fluid Phase Equilibria* **2016**, *427*, 414–420. https://doi.org/10.1016/j.fluid.2016.07.035.

(51) Le Guennec, Y.; Lasala, S.; Privat, R.; Jaubert, J.-N. A Consistency Test for α-Functions of Cubic Equations of State. *Fluid Phase Equilibria* **2016**, *427*, 513–538. https://doi.org/10.1016/j.fluid.2016.07.026.

(52) Le Guennec, Y.; Privat, R.; Lasala, S.; Jaubert, J.-N. On the Imperative Need to Use a Consistent α-Function for the Prediction of Pure-Compound Supercritical Properties with a Cubic Equation of State. *Fluid Phase Equilibria* **2017**, *445*, 45–53. https://doi.org/10.1016/j.fluid.2017.04.015.

(53) Le Guennec, Y.; Privat, R.; Jaubert, J.-N. Development of the Translated-Consistent *tc*-PR and *tc*-RK Cubic Equations of State for a Safe and Accurate Prediction of Volumetric, Energetic and Saturation Properties of Pure Compounds in the Sub- and Super-Critical Domains. *Fluid Phase Equilibria* **2016**, *429*, 301–312. https://doi.org/10.1016/j.fluid.2016.09.003.

(54) Krekelberg, W. P.; Kumar, T.; Mittal, J.; Errington, J. R.; Truskett, T. M. Anomalous Structure and Dynamics of the Gaussian-Core Fluid. *Phys. Rev. E* **2009**, *79* (3), 031203. https://doi.org/10.1103/PhysRevE.79.031203.

(55) Johnson, M. E.; Head-Gordon, T. Assessing Thermodynamic-Dynamic Relationships for Waterlike Liquids. *The Journal of Chemical Physics* **2009**, *130* (21), 214510. https://doi.org/10.1063/1.3140608.

(56) Chopra, R.; Truskett, T. M.; Errington, J. R. Excess Entropy Scaling of Dynamic Quantities for Fluids of Dumbbell-Shaped Particles. *The Journal of Chemical Physics* **2010**, *133* (10), 104506. https://doi.org/10.1063/1.3477767.
(57) Errington, J. R.; Truskett, T. M.; Mittal, J. Excess-Entropy-Based Anomalies for a Waterlike Fluid. *The Journal of Chemical Physics* **2006**, *125* (24), 244502. https://doi.org/10.1063/1.2409932.
(58) Chopra, R.; Truskett, T. M.; Errington, J. R. On the Use of Excess Entropy Scaling To Describe Single-Molecule and Collective Dynamic Properties of Hydrocarbon Isomer Fluids. *J. Phys. Chem. B* **2010**, *114* (49), 16487–16493. https://doi.org/10.1021/jp107878u.
(59) Agarwal, M.; Singh, M.; Sharma, R.; Parvez Alam, M.; Chakravarty, C. Relationship between Structure, Entropy, and Diffusivity in Water and Water-Like Liquids. *J. Phys. Chem. B* **2010**, *114* (20), 6995–7001. https://doi.org/10.1021/jp101956u.
(60) Gerek, Z. N.; Elliott, J. R. Self-Diffusivity Estimation by Molecular Dynamics. *Ind. Eng. Chem. Res.* **2010**, *49* (7), 3411–3423. https://doi.org/10.1021/ie901247k.
(61) Galliero, G.; Boned, C. Thermal Conductivity of the Lennard-Jones Chain Fluid Model. *Phys. Rev. E* **2009**, *80* (6), 061202. https://doi.org/10.1103/PhysRevE.80.061202.
(62) Mausbach, P.; May, H.-O. Transport Anomalies in the Gaussian Core Model Fluid. *Zeitschrift für Physikalische Chemie* **2009**, *223* (9), 1035–1046. https://doi.org/10.1524/zpch.2009.6056.
(63) Bell, I. H.; Galliero, G.; Delage-Santacreu, S.; Costigliola, L. An Entropy Scaling Demarcation of Gas- and Liquid-like Fluid Behaviors. *J. Chem. Phys.* **2020**, *152* (19), 191102. https://doi.org/10.1063/1.5143854.
(64) Galliero, G.; Boned, C. Shear Viscosity of the Lennard-Jones Chain Fluid in Its Gaseous, Supercritical, and Liquid States. *Phys. Rev. E* **2009**, *79* (2), 021201. https://doi.org/10.1103/PhysRevE.79.021201.
(65) Perkins, R. A.; Sengers, J. V.; Abdulagatov, I. M.; Huber, M. L. Simplified Model for the Critical Thermal-Conductivity Enhancement in Molecular Fluids. *Int J Thermophys* **2013**, *34* (2), 191–212. https://doi.org/10.1007/s10765-013-1409-z.
(66) Vogel, E.; Span, R.; Herrmann, S. Reference Correlation for the Viscosity of Ethane. *Journal of Physical and Chemical Reference Data* **2015**, *44* (4), 043101. https://doi.org/10.1063/1.4930838.
(67) Perkins, R. A.; Huber, M. L.; Assael, M. J.; Mihailidou, E. K.; Mylona, S. K.; Sykioti, E. A. Reference Correlations for the Viscosity and Thermal Conductivity of Fluids over an Extended Range of Conditions: Hexane in the Vapor, Liquid, and Supercritical Regions (IUPAC Technical Report). *Pure and Applied Chemistry* **2015**, *87* (3), 321–337. https://doi.org/10.1515/pac-2014-0104.
(68) *Transport Properties of Fluids: Their Correlation, Prediction and Estimation*; Millat, J., Dymond, J. H., Castro, C. A. N. de, International Union of Pure and Applied Chemistry, Eds.; IUPAC : Cambridge University Press: Cambridge ; New York, 1996.
(69) Dyre, J. C. Perspective: Excess-Entropy Scaling. *J. Chem. Phys.* **2018**, *149* (21), 210901. https://doi.org/10.1063/1.5055064.

(70) Hirschfelder, J. O.; Curtiss, C. F.; Bird, R. B. *Molecular Theory of Gases and Liquids*, Corr. print. with notes added.; Structure of matter series; Wiley: New York,NY, 1964.
(71) Najafi, B.; Ghayeb, Y.; Rainwater, J. C.; Alavi, S.; Snider, R. F. Improved Initial Density Dependence of the Viscosity and a Corresponding States Function for High Pressures. *Physica A: Statistical Mechanics and its Applications* **1998**, *260* (1–2), 31–48. https://doi.org/10.1016/S0378-4371(98)00287-8.
(72) Bell, I. H. Entropy Scaling of Viscosity—II: Predictive Scheme for Normal Alkanes. *J. Chem. Eng. Data* **2020**, *65* (11), 5606–5616. https://doi.org/10.1021/acs.jced.0c00749.
(73) Neufeld, P. D.; Janzen, A. R.; Aziz, R. A. Empirical Equations to Calculate 16 of the Transport Collision Integrals $\Omega^{(l,s)^*}$ for the Lennard-Jones (12–6) Potential. *The Journal of Chemical Physics* **1972**, *57* (3), 1100–1102. https://doi.org/10.1063/1.1678363.
(74) Smoot, L. D.; Pratt, D. T. Pulverized-Coal Combustion and Gasification: Theory and Applications for Continuous Flow Processes.
(75) Pina-Martinez, A.; Le Guennec, Y.; Privat, R.; Jaubert, J.-N.; Mathias, P. M. Analysis of the Combinations of Property Data That Are Suitable for a Safe Estimation of Consistent Twu α-Function Parameters: Updated Parameter Values for the Translated-Consistent *Tc* -PR and *Tc* -RK Cubic Equations of State. *J. Chem. Eng. Data* **2018**, *63* (10), 3980–3988. https://doi.org/10.1021/acs.jced.8b00640.
(76) Tegeler, Ch.; Span, R.; Wagner, W. A New Equation of State for Argon Covering the Fluid Region for Temperatures From the Melting Line to 700 K at Pressures up to 1000 MPa. *Journal of Physical and Chemical Reference Data* **1999**, *28* (3), 779–850. https://doi.org/10.1063/1.556037.
(77) Huber, M.; Harvey, A.; Lemmon, E.; Hardin, G.; Bell, I.; McLinden, M. NIST Reference Fluid Thermodynamic and Transport Properties Database (REFPROP) Version 10 - SRD 23, 2018. https://doi.org/10.18434/T4/1502528.
(78) Dyre, J. C. Hidden Scale Invariance in Condensed Matter. *J. Phys. Chem. B* **2014**, *118* (34), 10007–10024. https://doi.org/10.1021/jp501852b.
(79) Dyre, J. C. Simple Liquids' Quasiuniversality and the Hard-Sphere Paradigm. *J. Phys.: Condens. Matter* **2016**, *28* (32), 323001. https://doi.org/10.1088/0953-8984/28/32/323001.
(80) Lötgering-Lin, O.; Fischer, M.; Hopp, M.; Gross, J. Pure Substance and Mixture Viscosities Based on Entropy Scaling and an Analytic Equation of State. *Ind. Eng. Chem. Res.* **2018**, *57* (11), 4095–4114. https://doi.org/10.1021/acs.iecr.7b04871.
(81) Bell, I. H.; Hellmann, R.; Harvey, A. H. Zero-Density Limit of the Residual Entropy Scaling of Transport Properties. *J. Chem. Eng. Data* **2020**, *65* (3), 1038–1050. https://doi.org/10.1021/acs.jced.9b00455.
(82) Gross, J.; Sadowski, G. Perturbed-Chain SAFT: An Equation of State Based on a Perturbation Theory for Chain Molecules. *Ind. Eng. Chem. Res.* **2001**, *40* (4), 1244–1260. https://doi.org/10.1021/ie0003887.
(83) Le Guennec, Y.; Privat, R.; Jaubert, J.-N. Development of the Translated-Consistent Tc-PR and Tc-RK Cubic Equations of State for a Safe and Accurate Prediction of Volumetric, Energetic and Saturation Properties of Pure Compounds in the Sub- and

Super-Critical Domains. *Fluid Phase Equilibria* **2016**, *429*, 301–312. https://doi.org/10.1016/j.fluid.2016.09.003.

(84) Collell, J.; Galliero, G.; Vermorel, R.; Ungerer, P.; Yiannourakou, M.; Montel, F.; Pujol, M. Transport of Multicomponent Hydrocarbon Mixtures in Shale Organic Matter by Molecular Simulations. *J. Phys. Chem. C* **2015**, *119* (39), 22587–22595. https://doi.org/10.1021/acs.jpcc.5b07242.

(85) Tian, Y.; Xu, X.; Wu, J. Thermodynamic Route to Efficient Prediction of Gas Diffusivity in Nanoporous Materials. *Langmuir* **2017**, *33* (42), 11797–11803. https://doi.org/10.1021/acs.langmuir.7b02428.

(86) Tian, Y.; Fei, W.; Wu, J. Separation of Carbon Isotopes in Methane with Nanoporous Materials. *Ind. Eng. Chem. Res.* **2018**, *57* (14), 5151–5160. https://doi.org/10.1021/acs.iecr.8b00364.

(87) Dahanayake, J. N.; Mitchell-Koch, K. R. Entropy Connects Water Structure and Dynamics in Protein Hydration Layer. *Phys. Chem. Chem. Phys.* **2018**, *20* (21), 14765–14777. https://doi.org/10.1039/C8CP01674G.

(88) *Electrochemical Aspects of Ionic Liquids*, 2. ed.; Ohno, H., Ed.; Wiley: Hoboken, NJ, 2011.

(89) Katsumata, R.; Dulaney, A. R.; Kim, C. B.; Ellison, C. J. Glass Transition and Self-Diffusion of Unentangled Polymer Melts Nanoconfined by Different Interfaces. *Macromolecules* **2018**, *51* (19), 7509–7517. https://doi.org/10.1021/acs.macromol.8b00475.

(90) Guo, C. J.; de Kee, D. Effect of Molecular Size and Free Volume on Diffusion in Liquids. *Chemical Engineering Science* **1991**, *46* (8), 2133–2141. https://doi.org/10.1016/0009-2509(91)80171-T.

(91) Reis, R. A.; Nobrega, R.; Oliveira, J. V.; Tavares, F. W. Self- and Mutual Diffusion Coefficient Equation for Pure Fluids, Liquid Mixtures and Polymeric Solutions. *Chemical Engineering Science* **2005**, *60* (16), 4581–4592. https://doi.org/10.1016/j.ces.2005.03.018.

(92) Ricci, F. P.; Ricci, M. A.; Rocca, D. The Free Volume Theory and the Macedo-Litovitz Hybrid Equation for Diffusion in Liquids. *J. Phys. Chem.* **1977**, *81* (2), 171–177. https://doi.org/10.1021/j100517a015.

(93) Wanner, P.; Hunkeler, D. Isotope Fractionation Due to Aqueous Phase Diffusion – What Do Diffusion Models and Experiments Tell? – A Review. *Chemosphere* **2019**, *219*, 1032–1043. https://doi.org/10.1016/j.chemosphere.2018.12.038.

(94) Hoang, H.; Ho, K. H.; Battani, A.; Pujol, M.; Galliero, G. On Elemental and Isotopic Fractionation of Noble Gases in Geological Fluids by Molecular Diffusion. *Geochimica et Cosmochimica Acta* **2021**, *315*, 172–184. https://doi.org/10.1016/j.gca.2021.09.002.

(95) Suárez-Iglesias, O.; Medina, I.; Sanz, M. de los Á.; Pizarro, C.; Bueno, J. L. Self-Diffusion in Molecular Fluids and Noble Gases: Available Data. *J. Chem. Eng. Data* **2015**, *60* (10), 2757–2817. https://doi.org/10.1021/acs.jced.5b00323.

(96) Dehlouz, A.; Privat, R.; Galliero, G.; Bonnissel, M.; Jaubert, J.-N. Revisiting the Entropy-Scaling Concept for Shear-Viscosity Estimation from Cubic and SAFT Equations of State: Application to Pure Fluids in Gas, Liquid and Supercritical States.

Ind. Eng. Chem. Res. **2021**, *60* (34), 12719–12739. https://doi.org/10.1021/acs.iecr.1c01386.

(97) Bretonnet, J.-L. Self-Diffusion Coefficient of Dense Fluids from the Pair Correlation Function. *The Journal of Chemical Physics* **2002**, *117* (20), 9370–9373. https://doi.org/10.1063/1.1516594.

(98) Krekelberg, W. P.; Pond, M. J.; Goel, G.; Shen, V. K.; Errington, J. R.; Truskett, T. M. Generalized Rosenfeld Scalings for Tracer Diffusivities in Not-so-Simple Fluids: Mixtures and Soft Particles. *Phys. Rev. E* **2009**, *80* (6), 061205. https://doi.org/10.1103/PhysRevE.80.061205.

(99) Zmpitas, J.; Gross, J. Modified Stokes–Einstein Equation for Molecular Self-Diffusion Based on Entropy Scaling. *Ind. Eng. Chem. Res.* **2021**, *60* (11), 4453–4459. https://doi.org/10.1021/acs.iecr.0c06090.

(100) Moine, E.; Piña-Martinez, A.; Jaubert, J.-N.; Sirjean, B.; Privat, R. *I* -PC-SAFT: An Industrialized Version of the Volume-Translated PC-SAFT Equation of State for Pure Components, Resulting from Experience Acquired All through the Years on the Parameterization of SAFT-Type and Cubic Models. *Ind. Eng. Chem. Res.* **2019**, *58* (45), 20815–20827. https://doi.org/10.1021/acs.iecr.9b04660.

(101) Jaubert, J.-N.; Privat, R.; Le Guennec, Y.; Coniglio, L. Note on the Properties Altered by Application of a Péneloux-Type Volume Translation to an Equation of State. *Fluid Phase Equilibria* **2016**, *419*, 88–95. https://doi.org/10.1016/j.fluid.2016.03.012.

(102) Privat, R.; Jaubert, J.-N.; Le Guennec, Y. Incorporation of a Volume Translation in an Equation of State for Fluid Mixtures: Which Combining Rule? Which Effect on Properties of Mixing? *Fluid Phase Equilibria* **2016**, *427*, 414–420. https://doi.org/10.1016/j.fluid.2016.07.035.

(103) Piña-Martinez, A.; Privat, R.; Jaubert, J. Use of 300,000 Pseudo-experimental Data over 1800 Pure Fluids to Assess the Performance of Four Cubic Equations of State: SRK, PR, *Tc*-RK, and *Tc*-PR. *AIChE Journal* **2022**, *68* (2), e17518. https://doi.org/10.1002/aic.17518.

(104) Kontogeorgis, G. M.; Dohrn, R.; Economou, I. G.; de Hemptinne, J.-C.; ten Kate, A.; Kuitunen, S.; Mooijer, M.; Žilnik, L. F.; Vesovic, V. Industrial Requirements for Thermodynamic and Transport Properties: 2020. *Ind. Eng. Chem. Res.* **2021**, *60* (13), 4987–5013. https://doi.org/10.1021/acs.iecr.0c05356.

(105) Cardona, L. F.; Forero, L. A.; Velásquez, J. A. Correlation and Prediction of Thermal Conductivity Using the Redlich–Kwong Cubic Equation of State and the Geometric Similitude Concept for Pure Substances and Mixtures. *Ind. Eng. Chem. Res.* **2019**, *58* (51), 23417–23437. https://doi.org/10.1021/acs.iecr.9b04974.

(106) Roy, D.; Thodos, G. Thermal Conductivity of Gases. Organic Compounds at Atmospheric Pressure. *Ind. Eng. Chem. Fund.* **1970**, *9* (1), 71–79. https://doi.org/10.1021/i160033a011.

(107) Ely, J. F.; Hanley, H. J. M. Prediction of Transport Properties. 2. Thermal Conductivity of Pure Fluids and Mixtures. *Ind. Eng. Chem. Fund.* **1983**, *22* (1), 90–97. https://doi.org/10.1021/i100009a016.

(108) Quiñones-Cisneros, S. E.; Pollak, S.; Schmidt, K. A. G. Friction Theory Model for Thermal Conductivity. *J. Chem. Eng. Data* **2021**, *66* (11), 4215–4227. https://doi.org/10.1021/acs.jced.1c00400.
(109) Hopp, M.; Gross, J. Thermal Conductivity from Entropy Scaling: A Group-Contribution Method. *Ind. Eng. Chem. Res.* **2019**, *58* (44), 20441–20449. https://doi.org/10.1021/acs.iecr.9b04289.
(110) Rokni, H. B.; Moore, J. D.; Gavaises, M. Entropy-Scaling Based Pseudo-Component Viscosity and Thermal Conductivity Models for Hydrocarbon Mixtures and Fuels Containing Iso-Alkanes and Two-Ring Saturates. *Fuel* **2021**, *283*, 118877. https://doi.org/10.1016/j.fuel.2020.118877.
(111) Fouad, W. A. Thermal Conductivity of Pure Fluids and Multicomponent Mixtures Using Residual Entropy Scaling with PC-SAFT—Application to Refrigerant Blends. *J. Chem. Eng. Data* **2020**, *65* (12), 5688–5697. https://doi.org/10.1021/acs.jced.0c00682.
(112) Liu, H.; Yang, F.; Yang, X.; Yang, Z.; Duan, Y. Modeling the Thermal Conductivity of Hydrofluorocarbons, Hydrofluoroolefins and Their Binary Mixtures Using Residual Entropy Scaling and Cubic-plus-Association Equation of State. *Journal of Molecular Liquids* **2021**, *330*, 115612. https://doi.org/10.1016/j.molliq.2021.115612.
(113) Yang, X.; Kim, D.; May, E. F.; Bell, I. H. Entropy Scaling of Thermal Conductivity: Application to Refrigerants and Their Mixtures. *Ind. Eng. Chem. Res.* **2021**, *60* (35), 13052–13070. https://doi.org/10.1021/acs.iecr.1c02154.
(114) Malatesta, W. A.; Yang, B. Aviation Turbine Fuel Thermal Conductivity: A Predictive Approach Using Entropy Scaling-Guided Machine Learning with Experimental Validation. *ACS Omega* **2021**, *6* (43), 28579–28586. https://doi.org/10.1021/acsomega.1c02934.
(115) Mylona, S. K.; Assael, M. J.; Wakeham, W. A. Transport Properties of Fluids. In *Reference Module in Chemistry, Molecular Sciences and Chemical Engineering*; Elsevier, 2014; p B9780124095472110000. https://doi.org/10.1016/B978-0-12-409547-2.11001-7.
(116) *Experimental Thermodynamics Volume IX: Advances in Transport Properties of Fluids*; Assael, M. J., Goodwin, A. R. H., Vesovic, V., Wakeham, W. A., Eds.; Royal Society of Chemistry: Cambridge, 2014. https://doi.org/10.1039/9781782625254.
(117) Olchowy, G. A.; Sengers, J. V. A Simplified Representation for the Thermal Conductivity of Fluids in the Critical Region. *Int J Thermophys* **1989**, *10* (2), 417–426. https://doi.org/10.1007/BF01133538.
(118) Kiselev, S. B.; Kulikov, V. D. Crossover Behavior of the Transport Coefficients of Critical Binary Mixtures. *Int J Thermophys* **1994**, *15* (2), 283–308. https://doi.org/10.1007/BF01441587.
(119) Ferrell, R. A. Decoupled-Mode Dynamical Scaling Theory of the Binary-Liquid Phase Transition. *Phys. Rev. Lett.* **1970**, *24* (21), 1169–1172. https://doi.org/10.1103/PhysRevLett.24.1169.
(120) Eucken, A. Allgemeine Gesetzmäßigkeiten für das Wärmeleitvermögen verschiedener Stoffarten und Aggregatzustände. *Forsch Ing-Wes* **1940**, *11* (1), 6–20. https://doi.org/10.1007/BF02584103.

(121) Bell, I. H.; Delage-Santacreu, S.; Hoang, H.; Galliero, G. Dynamic Crossover in Fluids: From Hard Spheres to Molecules. *J. Phys. Chem. Lett.* **2021**, *12* (27), 6411–6417. https://doi.org/10.1021/acs.jpclett.1c01594.